Clinical, biochemical and radiological insights in X-linked adrenoleukodystrophy

van de Stadt, S.I.W.

Publication date
2022
Document Version
Final published version

Clinical, biochemical and radiological insights in X-linked adrenoleukodystrophy

STEPHANIE I.W. VAN DE STADT

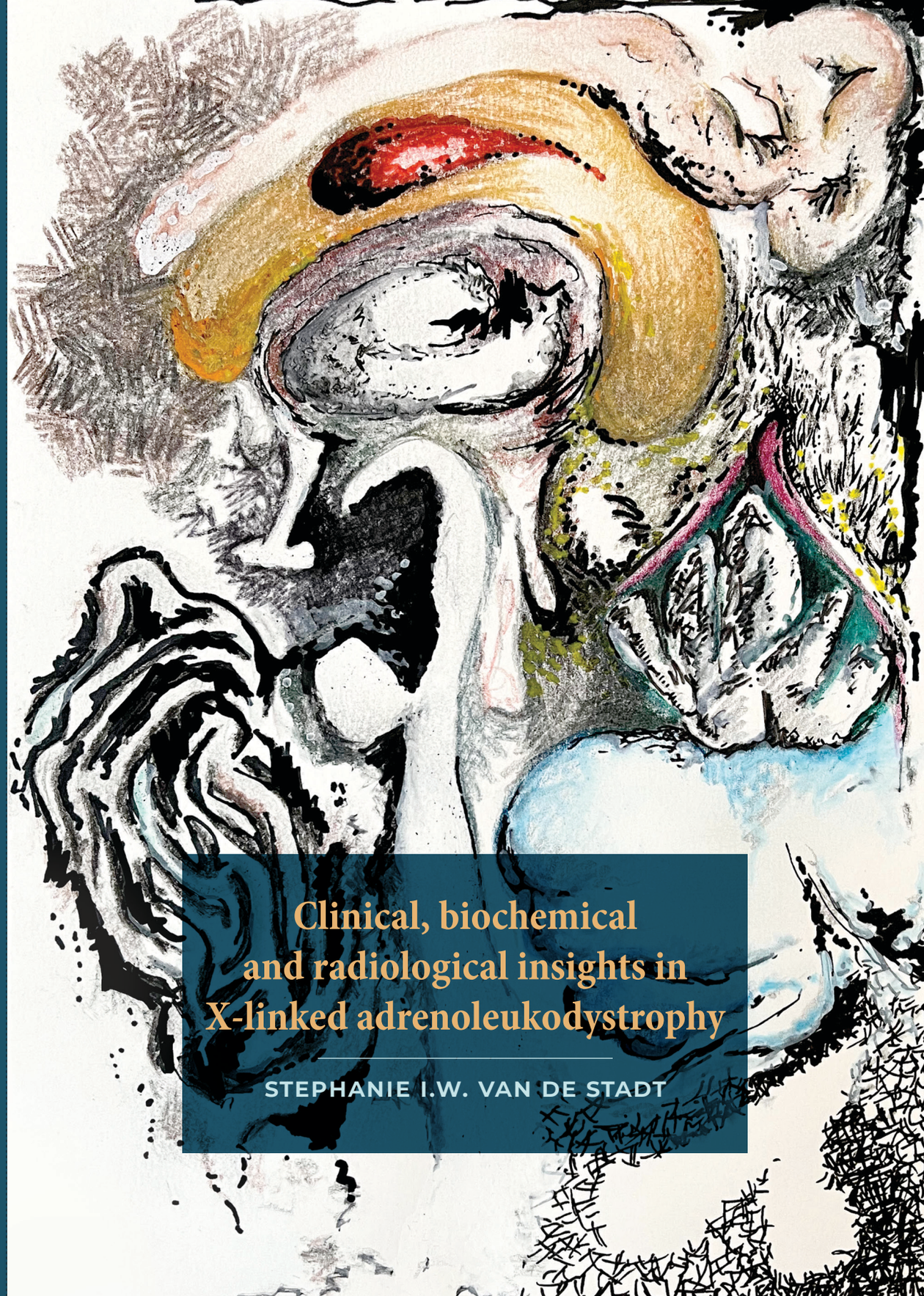

Clinical, biochemical and radiological insights in X-linked adrenoleukodystrophy

STEPHANIE I.W. VAN DE STADT

Clinical, biochemical and radiological insights in X-linked adrenoleukodystrophy

Stephanie I.W. van de Stadt

Clinical, biochemical and radiological insights in X-linked adrenoleukodystrophy

ISBN: 978-94-6361-745-1
Cover design | Vivian Mac Gillavry
Layout and print | Optima Grafische Communicatie

Clinical, biochemical and radiological insights in X-linked adrenoleukodystrophy

ACADEMISCH PROEFSCHRIFT

ter verkrijging van de graad van doctor
aan de Universiteit van Amsterdam
op gezag van de Rector Magnificus
prof. dr. ir. P.P.C.C. Verbeek
ten overstaan van een door het College voor Promoties ingestelde commissie,
in het openbaar te verdedigen in de Aula der Universiteit
op vrijdag 21 oktober 2022, te 11.00 uur

door Stephanie Ingrid Wilhelmina van de Stadt
geboren te Blaricum

PROMOTIECOMMISSIE

Promotores:	prof. dr. J.B. van Goudoever	AMC-UvA
	prof. dr. M.S. van der Knaap	Vrije Universiteit Amsterdam
Copromotores:	dr. M. Engelen	AMC-UvA
	dr. S. Kemp	AMC-UvA
Overige leden:	prof. dr. I.N. van Schaik	AMC-UvA
	dr. J.J.F.M. Smolders	Erasmus MC
	prof. dr. A.M. Bosch	AMC-UvA
	dr. S.D. Roosendaal	AMC-UvA
	dr. F.M. Vaz	AMC-UvA
	prof. dr. N.I. Wolf	Vrije Universiteit Amsterdam
	prof. dr. C.E.M. Hollak	AMC-UvA

Faculteit der Geneeskunde

TABLE OF CONTENTS

I Introduction

1 General introduction & thesis outline

A diagnosis of X-linked adrenoleukodystrophy (ALD) means a lifetime of uncertainty. Even with the myriad of new insights that have been obtained since the initial descriptions of the first cases in the early 20th century[1,2], many aspects of the disease remain enigmatic. Patients with ALD are at risk of developing several neurologic and endocrine symptoms, of which some are life-threatening.[3–8] The lack of genotype-phenotype correlation means even brothers and monozygotic twins can have completely different symptomatology.[9,10] Previous work has outlined the core symptoms, but age of symptom onset and rate of disease progression remain unpredictable.

Male patients can develop a progressive leukodystrophy (cerebral ALD), with onset before the age of 18 years (an estimated 40% of male patients) or in adulthood (an additional 20% of patients).[5,11,12] The leukodystrophy can be halted by hematopoietic stem cell transplantation[13,14] and therefore yearly and lifelong MRI screening for cerebral disease is recommended for all male patients.[11] However, a large proportion of patients will never develop cerebral ALD, and at this time it is impossible to predict which patients will be affected, or at what age, as multiple genetic modifiers and environmental factors are involved.[8,15–17] Predicting disease course would make life – of some patients – a little less unexpected.

Adult patients (male and female) can, furthermore, develop a slowly progressive myelopathy in adulthood, characterized by a gait disorder and bowel- and bladder dysfunction.[4,18,19] As with the leukodystrophy, the age of onset and rate of progression are highly variable. Treatment is purely symptomatic, there is currently no disease modifying treatment, but many potential new treatments (small compounds and AAV9 gene therapy) are in different stages of development (https://clinicaltrials.gov)[20]. In order to determine efficacy of potential new treatments in clinical trials, it is necessary to adequately quantify disease severity. However, current outcome measures are not sensitive to small changes in disease severity and therefore not valuable in patients with very slow disease progression such as female patients. In addition, some outcome measures are affected by floor- and ceiling effects and therefore only useful in symptomatic but ambulant patients. And finally, some are influenced by non-disease specific factors. For example, a recent study showed that the "6 minute walk test" can be used to detect progression of myelopathy over a period of 2 years[4], but only with a very large number of patients (>200), which is difficult in a rare disease like ALD and hampered by the fact that many patients are not eligible to participate.

For answers to (among others) the abovementioned concerns, the 'Dutch ALD cohort' – a large cohort of men and women with ALD – was set up at the Amsterdam University Medical Centers. This makes it possible to extensively and systematically investigate the disease by performing clinical, laboratory and imaging examinations over the course of several years. We used this valuable information and established a twofold aim for this thesis:

1) To gain more insight in the natural history of ALD, with the aim of predicting disease course for individual patients.
2) To develop sensitive (surrogate) outcome measures, able to monitor severity of myelopathy, making clinical trials in ALD more feasible.

We introduce the history, pathophysiology and clinical features of ALD in **chapter 2**, followed by the radiologic (MRI) characteristics of the disease and quantitative imaging possibilities for future research purposes.

In the following part (**Part II**) of this thesis we continue to describe the dynamic aspects of the clinical spectrum of ALD. In **chapter 3** we focus on the natural history of patients whose cerebral lesions spontaneously stopped progressing (arrested cerebral ALD) by quantifying the clinical symptoms and MRI scores over time. **Chapter 4** describes the frequent occurrence of sexual dysfunction in ALD and the relationship with hypogonadism and myelopathy. In **chapter 5** we evaluate postural body sway (a measure for balance – one of the most invalidating symptoms in ALD) as a surrogate outcome measure for the myelopathy in ALD.

Part III delineates several biochemical characteristics of ALD. First, in **chapter 6,** we describe an array of functional tests in fibroblast which aids in diagnosing ALD in patients with a variant of unknown significance (VUS) in the *ABCD1* gene. Second, we evaluate the value of Neurofilament light (NfL) and Glial Fibrillary Acidic Protein (GFAP) as biomarkers for the myelopathy in ALD in **chapter 7.**

Part IV focusses on magnetic resonance (MR) imaging biomarkers as surrogate outcome measures for progression and/or severity of myelopathy. We firstly evaluate spinal cord atrophy measured with structural MRI in **chapter 8** and secondly, magnetic resonance spectroscopy as quantitative imaging biomarker for neurodegeneration in **chapter 9.**

The research in this thesis contributes to understanding the disease course of ALD and the development of new surrogate outcome measures to improve the clinical trials of the future.

REFERENCES

1. Schilder PF. Zur Kenntnis der sogenannten diffusen Sklerose (über Encephalitis periaxialis diffusa). *Z Gesamte Neurol Psychiatr*. 1912;10:1-60.
2. Haberfeld W, Spieler F. Zur diffusen Hirn-Rückenmarksklerose im Kindesalter. *Dtsch Z Nervenheilkd*. 1910;40(5):436-463. doi:10.1007/BF01629013
3. Huffnagel IC, Laheji FK, Aziz-Bose R, et al. The natural history of adrenal insufficiency in X-linked adrenoleukodystrophy: an international collaboration. *J Clin Endocrinol Metab*. 2019;104(1). doi:10.1210/jc.2018-01307
4. Huffnagel IC, van Ballegoij WJ, Van Geel BM, MBW Vos J, Kemp S, Engelen M. Progression of myelopathy in males with adrenoleukodystrophy: towards clinical trial readiness. *Brain*. 2019;142(2):334-343. doi:10.1093/brain/awy299
5. De Beer M, Engelen M, Van Geel BM. Frequent occurrence of cerebral demyelination in adrenomyeloneuropathy. *Neurology*. 2014;83(24):2227-2231. doi:10.1212/WNL.0000000000001074
6. Van Geel BM, Bezman L, Loes DJ, Moser HW, Raymond G V. Evolution of phenotypes in adult male patients with X-linked adrenoleukodystrophy. *Ann Neurol*. 2001;49(2):186-194. doi:10.1002/1531-8249(20010201)49:2<186::AID-ANA38>3.0.CO;2-R
7. Assies J, Gooren LJG, Van Geel B, Barth PG. Signs of testicular insufficiency in andrenomyeloneuropathy and neurologically asymptomatic X-linked adrenoleukodystrophy: A retrospective study. *Int J Androl*. 1997;20(5):315-321. doi:10.1046/j.1365-2605.1997.00066.x
8. Kemp S, Huffnagel IC, Linthorst GE, Wanders RJA, Engelen M. Adrenoleukodystrophy - Neuroendocrine pathogenesis and redefinition of natural history. *Nat Rev Endocrinol*. 2016;12. doi:10.1038/nrendo.2016.90
9. Berger J, Molzer B, Fae I, Bernheimer H. X-Linked Adrenoleukodystrophy (ALD): A Novel Mutation of the ALD Gene in 6 Members of a Family Presenting with 5 Different Phenotypes. *Biochem Biophys Res Commun*. 1994;205(3):1638-1643. doi:https://doi.org/10.1006/bbrc.1994.2855
10. Korenke GC, Fuchs S, Krasemann E, et al. Cerebral Adrenoleukodystrophy (ALD) in only one of monozygotic twins with an identical ALD genotype. *Ann Neurol*. 1996;(40):254-257.
11. Engelen M, Kemp S, De Visser M, et al. X-linked adrenoleukodystrophy (X-ALD): clinical presentation and guidelines for diagnosis, follow-up and management. *Orphanet J Rare Dis*. 2012;7(51). http://www.ojrd.com/content/7/1/51.
12. Moser HW, Loes DJ, Melhem ER, et al. X-Linked Adrenoleukodystrophy: Overview and Prognosis as a Function of Age and Brain Magnetic Resonance Imaging Abnormality. A Study Involving 372 Patients. *Neuropediatrics*. 2000;31(5):227-239. doi:10.1055/s-2000-9236
13. Shapiro E, Krivit W, Lockman L, et al. Long-term effect of bone-marrow transplantation for childhood-onset cerebral X-linked adrenoleukodystrophy. *Lancet*. 2000;356(9231):713-718. doi:10.1016/S0140-6736(00)02629-5
14. Peters C, Charnas LR, Tan Y, et al. Cerebral X-linked adrenoleukodystrophy: the international hematopoietic cell transplantation experience from 1982 to 1999. *Blood*. 2004;104(3):881-888. doi:10.1182/blood-2003-10-3402

15. Richmond PA, van der Kloet F, Vaz FM, et al. Multi-Omic Approach to Identify Phenotypic Modifiers Underlying Cerebral Demyelination in X-Linked Adrenoleukodystrophy. *Front cell Dev Biol*. 2020;8:520. doi:10.3389/fcell.2020.00520
16. Raymond G V, Seidman R, Monteith TS, et al. Head trauma can initiate the onset of adrenoleukodystrophy. *J Neurol Sci*. 2010;290(1-2):70-74. doi:10.1016/j.jns.2009.11.005
17. Bouquet F, Dehais C, Sanson M, Lubetzki C, Louapre C. Dramatic worsening of adult-onset X-linked adrenoleukodystrophy after head trauma. *Neurology*. 2015;85(22):1991-1993. doi:10.1212/WNL.0000000000002173
18. Huffnagel IC, Dijkgraaf MGW, Janssens GE, et al. Disease progression in women with X-linked adrenoleukodystrophy is slow. *Orphanet J Rare Dis*. 2019;14(30). doi:10.1186/s13023-019-1008-6
19. Powers JM, DeCiero DP, Cox C, et al. The Dorsal Root Ganglia in Adrenomyeloneuropathy: Neuronal Atrophy and Abnormal Mitochondria. *J Neuropathol Exp Neurol*. 2001;60(5):493-501. doi:10.1093/jnen/60.5.493
20. Gong Y, Mu D, Prabhakar S, et al. Adenoassociated virus serotype 9-mediated gene therapy for x-linked adrenoleukodystrophy. *Mol Ther*. 2015;23(5):824-834. doi:10.1038/mt.2015.6

2 Imaging in X-linked adrenoleukodystrophy

Stephanie I.W. van de Stadt
Irene C. Huffnagel
Bela R. Turk
Marjo S. van der Knaap
Marc Engelen

Neuropediatrics 2021;52:252-260

ABSTRACT

Magnetic Resonance Imaging (MRI) is the gold standard for detection of cerebral lesions in X-linked adrenoleukodystrophy (ALD). ALD is one of the most common peroxisomal disorders and is characterized by a defect in degradation of very long chain fatty acids (VLCFA), resulting in accumulation of VLCFA in plasma and tissues. The clinical spectrum of ALD is wide and includes adrenocortical insufficiency, a slowly progressive myelopathy in adulthood, and cerebral demyelination in a subset of male patients. Cerebral demyelination (cerebral ALD) can be treated with hematopoietic cell transplantation (HCT) but only in an early (pre- or early symptomatic) stage and therefore active MRI surveillance is recommended for male patients, both pediatric and adult. Although structural MRI of the brain can detect the presence and extent of cerebral lesions, it does not predict if and when cerebral demyelination will occur. There is a great need for imaging techniques that predict onset of cerebral ALD before lesions appear. Also, imaging markers for severity of myelopathy as surrogate outcome measure in clinical trials would facilitate drug development. New quantitative MRI techniques are promising in that respect. This review focuses on structural and quantitative imaging techniques - including magnetic resonance spectroscopy (MRS), diffusion tensor imaging (DTI), MR perfusion imaging, magnetization transfer (MT) imaging, neurite orientation dispersion and density imaging (NODDI) and myelin water fraction (MWF) imaging - used in ALD and their role in clinical practice and research opportunities for the future.

INTRODUCTION

About 60% of boys and men with adrenoleukodystrophy (ALD) develop progressive and fatal cerebral demyelination.[1] Pre-symptomatic demyelinating lesions can be detected with Magnetic Resonance Imaging (MRI) and early detection improves therapeutic outcomes.[2] This is why neuroimaging is indispensable in the monitoring of ALD patients. ALD is a relatively common (1: 15 000 birth incidence) peroxisomal disorder, caused by mutations in the *ABCD1* gene.[3,4] Pathogenic variants result in defective ALD protein, a transmembrane protein that transports very long chain fatty acid (VLCFA)-CoA esters into the peroxisome.[5] Consequently, VLCFA accumulate in tissues and plasma.[6] Besides the brain white matter, other clinically affected tissues are the spinal cord and adrenal glands.[1,7,8] Although all boys and men with ALD have a genetic defect in the *ABCD1* gene and accumulate VLCFA, onset and severity of symptoms is highly variable for individual patients. Peak onset of cerebral demyelination (cerebral ALD) is between the ages of 4-8 years, but cerebral ALD also occurs in adolescence or adulthood.[1,9] When diagnosed early, hematopoietic cell transplantation (HCT) halts progression of cerebral disease.[10] By contrast, untreated cerebral ALD causes severe disability and death approximately two years after symptom onset.[11,12] Besides being at risk for cerebral ALD, adult men with ALD invariably develop a slowly progressive myelopathy, even after HCT in childhood.[13–16] Typically, age of onset is in the 3rd decade of life and progression occurs over years.[4,15] Treatment of the myelopathy is solely symptomatic. Extra-neurological manifestations include adrenal insufficiency, which develops in approximately 80% of boys and men and can be the presenting symptom of ALD.[4,7] Treatment with adrenal steroid replacement therapy is necessary and can be lifesaving. Although, adrenal insufficiency can occur at all ages, men who have normal adrenal function at the age of 45 years are at low risk of developing adrenal failure later in life.[17] Female heterozygotes also develop myelopathy but the rate of progression is much slower than in men and occurs over decades instead of years.[18] Cerebral ALD and adrenal insufficiency are extremely rare.[19]

Although neuroimaging has been part of standard clinical practice in ALD management for years, there are still many unresolved issues. Open questions are, for instance, if quantitative MRI can predict onset of cerebral ALD before structural MRI and if imaging techniques could be developed into new outcome measures for clinical trials. In this review we outline the neuroimaging possibilities for ALD in both routine clinical care and research.

Historical overview

Computed tomography (CT) in the 1970s provided the first i*n vivo* images of the brain in patients with leukodystrophies. Large symmetric hypodense lesions, located in the parieto-temporo-occipital white matter of a 9-year old boy with progressive neurologic deterioration and adrenal insufficiency were detected with CT, and brain biopsy confirmed

cellular inclusions typical for ALD.[20] In the late 1980s MRI became available and was clearly superior to CT; thereafter imaging of leukodystrophies improved dramatically.[21] Systematic MRI pattern recognition improved classification and eventually diagnosis.[22] The increasing use of MRI as a diagnostic and potentially prognostic tool called for methods to quantify MR findings. In 1994, Loes et al. developed a scoring method for brain MR lesions in male ALD patients.[23] This severity score, ranging from 0 (no abnormalities) to 34 (severe abnormalities) is based on a point system derived from location and extent of lesions and atrophy. To date, the Loes score is still widely used to quantify disease severity and monitor disease progression in cerebral ALD.

Neuropathology

Cerebral ALD is characterized by large, confluent areas of demyelination and inflammation of the white matter.[24] Histopathologically, white matter lesions can be divided into three concentric zones.[25] The first and innermost zone (zone A) is characterized by an almost complete loss of axons, myelin sheaths and oligodendrocytes. No active disease process is visible; only a dense mesh of glial fibrils and scattered astrocytes is present. Moving outward, to the edge of the lesion, numerous perivascular mononuclear cells indicate a zone of active inflammation. This zone (zone B) is responsible for gadolinium enhancement of the lesions seen on MRI. Like in zone A, myelin sheaths are grossly absent. The outermost zone (zone C) shows active myelin destruction by macrophages, without perivascular inflammatory cells, and axons are still preserved. The zonal gradation as described here can be visualized on MRI.[24–29] (**figure 1**) The pathology of the myelopathy of ALD is characterized by axonal degeneration of mainly the corticospinal tracts and dorsal columns of the spinal cord, with a "dying-back" pattern towards the brain. There are no signs of inflammation. In the peripheral nerves a distal, combined, axonopathy and myelinopathy is found.[13,14,27]

STRUCTURAL MRI

Brain

White matter lesions in cerebral ALD are seen on T2-weighted and Fluid-Attenuated Inversion Recovery (FLAIR) images as hyperintense confluent lesions. Distribution is usually symmetrical and demyelination begins in the corpus callosum in almost all patients.[22,30] On T1-weighted imaging lesions are hypointense and less clearly visible. This sequence is primarily used for post-contrast imaging where a clear enhancing rim is visible after gadolinium administration in case of active inflammation.[31]

Multiple MRI patterns, based on neuroanatomic location of the lesions, are described in boys and men with cerebral ALD. In most boys the splenium of corpus callosum and

parieto-occipital white matter is predominantly affected (~80%) (**figure 1**). Involvement of the genu of corpus callosum and frontal white matter occurs in approximately 20% of boys. Less common is involvement of the frontal and occipital white matter simultaneously (2,5%) or involvement of the cerebellar white matter (1%) or capsula interna.[29,32,33] During adulthood 75% of patients with MRI abnormalities show lesions primarily in the frontopontine and corticospinal projection fibers, without affecting the periventricular white matter.[33] In all patterns the entire cerebral white matter is eventually affected.[22] ALD patients without cerebral disease, such as female heterozygotes and men with myelopathy often have subtle abnormalities on brain MRI. Usually, these are seen in the posterior limb of the capsula interna and not in the frontal, temporal, parietal or occipital white matter.[22] Moderate increased signal intensities of the pyramidal tracts on T2-weighted and FLAIR sequences are considered to reflect Wallerian degeneration and are not a manifestation of cerebral ALD.[12,34]

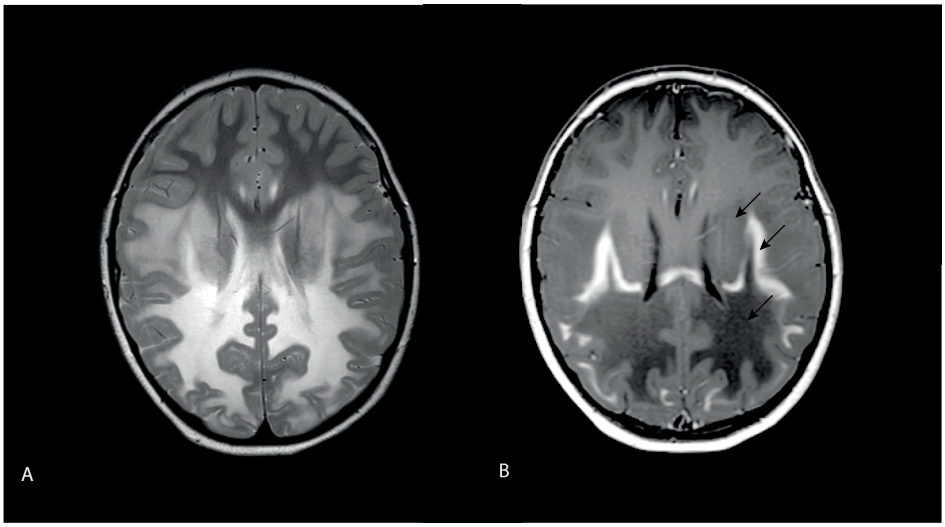

Figure 1: Structural MRI in a boy with cerebral ALD

A. T2-weighted image shows extensive, confluent white matter lesions in the splenium of the corpus callosum and parieto-occipital white matter, extending towards the frontal white matter in a 7 year old boy with cerebral ALD.

B. T1-weighted image in the same patient shows contrast enhancement of the white matter lesions after gadolinium administration. Note that the three pathological zones are visible (indicated with arrows) and the disease has progressed beyond the enhancing edge.

Lesion load on T1- and T2-weighted sequences, as quantified with the Loes score, strongly correlates with prognosis of cerebral ALD. In a study involving 372 patients, Moser et al showed that 70-80% of patients with a Loes score ≥ 3 worsened over time, irrespective of age. Boys with a Loes score ≤ 1 had a better prognosis, their neurological and MRI scores remained stable in 80-100%, depending on age.[11] Moreover, contrast enhancement on MRI is strongly associated with disease progression and neurological deterioration.[31] The rate

of lesion progression is nonlinear and depends on Loes score and age. Rapid progression is seen in early stage lesions (e.g. when Loes score is still <1) and young patients, whereas in adults lesion progression is much slower.[35,36] In a minority of patients (12.4%) clinical and radiological deterioration arrests spontaneously (arrested cerebral ALD).[37] Why disease progression halts in these patients is not understood, but continued follow-up is advised as re-activation of these lesions may occur up to many years later.[37]

The hallmark of structural MRI is the ability to detect cerebral ALD lesions before clinical symptoms become apparent. Therefore, the current recommendation is to repeat brain MRI every 6 months up until the age of 12 years and yearly after that[12,38], which is a great burden for patients. Another concern is the safety of repeated gadolinium use, which is crucial for demonstrating active disease. Although gadolinium administration is considered safe, long-term retention of gadolinium in human tissues has recently been demonstrated.[39] If and how this retention affects the health of individual patients is unknown. Therefore, administration of gadolinium should be restricted to patients between the age of 3 and 12 years (due to the higher risk of developing cerebral ALD) and patients with white matter lesions on structural imaging. Furthermore, post contrast images should not be obtained immediately after gadolinium injection but after a delay of at least 5 minutes.[40] In our personal experience, lesion enhancement may otherwise be missed **(figure 2)**.

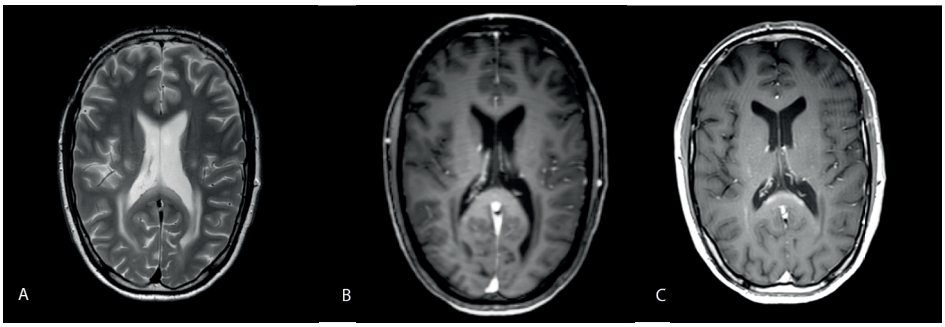

Figure 2: Late lesion enhancement after gadolinium administration

A. T2-weighted image of a 35 year old male with cerebral ALD. Lesions are visible in the splenium of the corpus callosum, capsula interna and optic radiations.
B. T1-weighted post-contrast image, acquired directly after gadolinium administration. No lesion enhancement is visible.
C. T1-weighted post-contrast image, acquired 5 minutes after gadolinium administration. Lesion enhancement is now visible in the splenium of corpus callosum, optic radiation (right) and capsula interna (right).

Spinal Cord

Spinal cord imaging is not used in routine follow-up care in ALD as it has no therapeutic or prognostic consequences. Before ALD is diagnosed, a spinal cord MRI will, however, often be made in patients presenting with spastic paraparesis, to exclude other causes of myelopathy. T1-weighted imaging of the spinal cord of ALD men and women shows diffuse atrophy

on thoracic and cervical levels of up to 40% in comparison to healthy controls, depending on the level measured.[41–44] In a study assessing morphology of the spinal cord, reduction of anteroposterior diameters was more pronounced than reduction of right-left diameters, making the spinal cord look flattened **(figure 3)**. This is probably due to degeneration of the dorsal columns and corticospinal tracts. The degree of atrophy correlated with the severity of myelopathy and has therefore been suggested as a surrogate outcome measure for severity of myelopathy in clinical trials.[44]

Unfortunately, because the spinal cord is small, mobile and surrounded by cerebrospinal fluid, (quantitative) spinal cord imaging can be challenging.

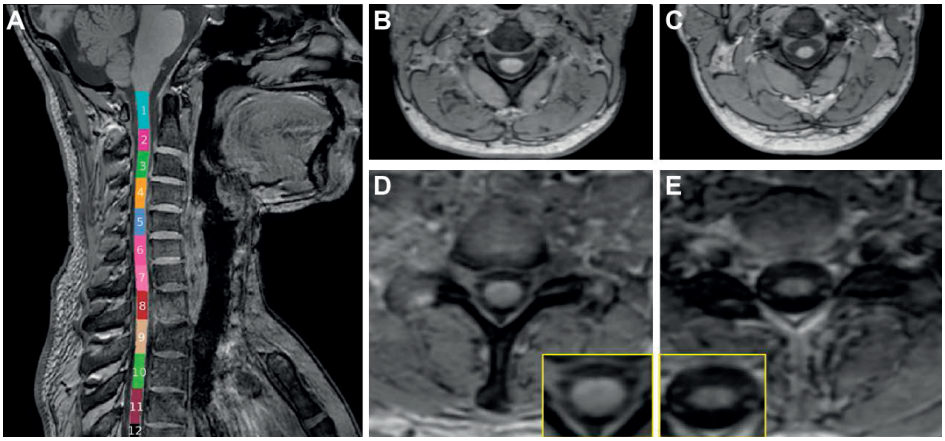

Figure 3: Structural MRI of the spinal cord

A. Spinal cord segmentation and labeling of the vertebrae for assessment of spinal cord morphology
B. Healthy control subject without spinal cord atrophy
C. Visible spinal cord atrophy in a severely affected ALD male with myelopathy
D. Healthy control subject with normal spinal cord morphology
E. Visible spinal cord flattening in the same severely affected ALD male

Original image was previously published (S.I.W. van de Stadt et al, Spinal cord atrophy as a measure of severity of myelopathy in adrenoleukodystrophy, JIMD 2020). Approval for secondary use has been retrieved from publisher.

QUANTITATIVE MRI

Although structural MRI of the brain and spinal cord is an excellent tool for diagnosis, quantitative MRI techniques are being studied to provide insight in pathogenesis, to explore their function as surrogate outcome measure for monitoring treatment effects in clinical trials and to determine if it is possible to predict lesion onset or progression at an earlier stage.

Spectroscopy

MR spectroscopy (MRS) measures cerebral metabolite levels using the chemical shift phenomenon. If an external magnetic field is applied, precession is induced in the atomic nucleus as well as the surrounding electron cloud, resulting in a small local magnetic field. The small magnetic field of the surrounding electron cloud influences the atomic nucleus and modifies the effect of the external magnetic field. Because of this slight change in magnetic field the nucleus resonates at a slightly different frequency. The precise chemical shift is characteristic of a particular atomic nucleus in a particular compound.[29]

In ALD different metabolic disturbances are present, corresponding to the underlying pathological mechanisms. In patients with active cerebral ALD, choline containing compounds (Cho) and myo-inositol (MI) are increased in the affected white matter.[45–47] Elevated Cho/creatine (Cr) ratios, MI/Cr ratios and lactate levels are believed to reflect active demyelination, gliosis and inflammation.[48] A decrease in N-acetylaspartate (NAA) levels is a result of neuroaxonal loss.[46] In all types of patients, including cerebral ALD, female heterozygotes and asymptomatic patients, NAA concentrations and corresponding NAA/Cho and NAA/Cr ratios are decreased in the white matter, also in the normal appearing white matter (NAWM) (**figure 4**).[34,45,47,49,50] The latter suggests that primary axonal damage is not confined to the spinal cord and peripheral nerves.[49]

Besides pathophysiological associations, in the future some metabolic ratios may be used to monitor disease severity or even predict onset of cerebral ALD. Two studies showed that brain NAA/Cr, MI/Cr and glutamate (Glu)/Cr correlated strongly with measures for clinical disability, such as the Expanded Disability Status Scale (EDSS).[47,49] These metabolite ratios may be suitable as biomarkers for severity of myelopathy. However, the correlations are indirect and markers measured directly (e.g. in the spinal cord) may be more suitable in this context. Furthermore, in the NAWM of 25 ALD patients a NAA/Cho ratio of <5.0 was strongly predictive of subsequent lesion progression on MRI. In patients with normal NAA/Cho ratio (>5.0), no MRI evidence of lesion progression was found during a follow-up period of 3.5 years, irrespective of initial abnormal MRI findings.[51]

The main limitation of MRS, in our own personal experience, is the non-sensitivity and corresponding low spatial resolution of this technique, causing difficulties in acquiring an appropriate and clinically interpretable spectrum.

Diffusion weighted imaging

Diffusion tensor imaging (DTI) evaluates white matter microstructural properties. The diffusion process in the white matter is dependent on the orientation of the axons and the integrity of the myelin sheath. With different parameters, such as fractional anisotropy (FA -

a measure of the degree of diffusion anisotropy) and apparent diffusion coefficient (ADC - a measure of the freedom of water movement) it is possible to map the diffusivity of free water molecules.[52] This diffusivity may be used to quantify disease progression.

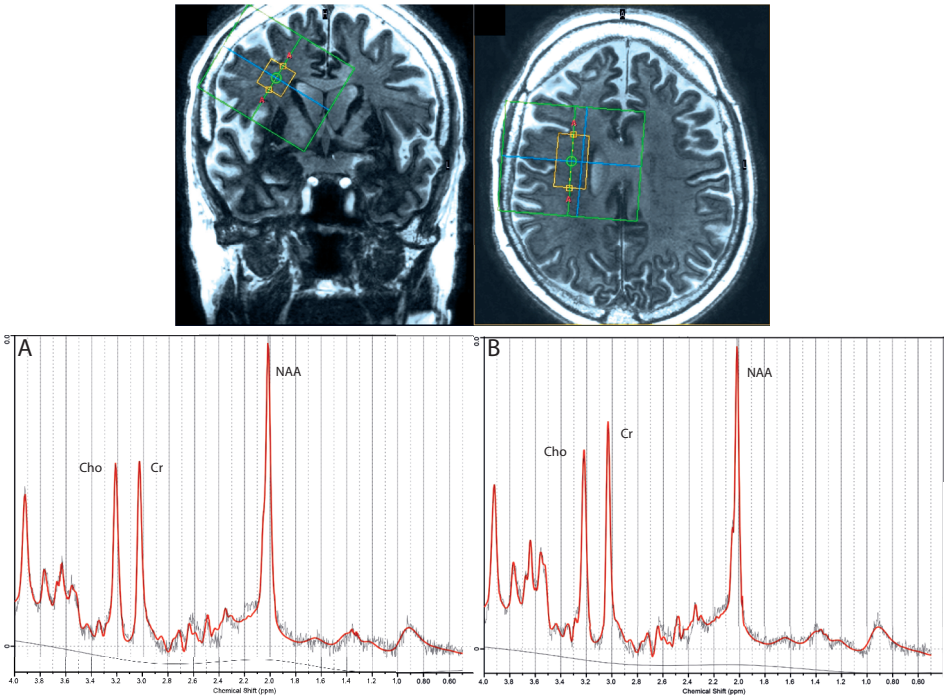

Figure 4: 7T single voxel magnetic resonance spectroscopy

A. Healthy control subject with similar Cho and Cr peaks and an almost twice as high NAA peak: NAA/Cr = 1.94.

B. ALD male with myelopathy shows a lower NAA peak and NAA/Cr ratio (1.45), when compared to A.

Abbreviations: Cho: choline-containing compounds. Cr: creatine. NAA: *N*-acetyl-aspartate.

In active cerebral ALD, a zonal gradation of decreasing FA and increasing ADC from periphery to core of the lesion indicates tissue damage, in correspondence to the three aforementioned histopathological zones.[53] ALD patients with myelopathy usually do not have abnormalities of their brain white matter on structural MRI, in DTI studies, however, abnormalities are detected. In the brain, FA was lower in the entire corticospinal tract (brainstem to corona radiata) with more pronounced reduction at the lower corticospinal segments.[43,54] (**figure 5)** Moreover, several other white matter tracts were affected, such as the optic radiations, splenium and genu of corpus callosum and the superior cerebellar peduncles.[43,55] In addition, brain FA, mean diffusivity and radial diffusivity differed between asymptomatic patients and controls.[54] These alterations in DTI parameters imply that the pathological process in the (pre-symptomatic) myelopathy of ALD is not restricted to axonopathy of the spinal cord long tracts alone, but is more widespread and also involves

the brain. In the spinal cord, a decrease in FA and axial diffusivity – indicating axonal damage – and increase in radial diffusivity is found.[43] In a mouse model, such changes in radial diffusivity have been associated with demyelination.[56] This confirms that the myelopathy in ALD consist of combined axonal degeneration and myelin loss. Differences in FA and radial diffusivity between symptomatic patients and healthy controls were largest in the spinal cord and decrease towards the cortex of the brain, suggesting a spatiotemporal axonal degeneration. Differences in spinal cord DTI parameters between asymptomatic patients and controls have not yet been found but results suggest a trend.[54]

In the future, spinal cord DTI parameters may be used as surrogate outcome measure for severity of myelopathy in clinical trials. Moderate to strong correlations between clinical outcomes and spinal cord DTI parameters illustrate the potential of DTI as a surrogate outcome measure.[54] Moreover, longitudinal data suggest that brain DTI parameters are superior to clinical outcome measures for assessment of disease progression, as significant change in brain DTI parameters is detectable over time, also in asymptomatic patients where clinical measures are unable to detect progression.[54] A limitation of DTI is that the analysis process is still time consuming and therefore not yet useable in clinic.

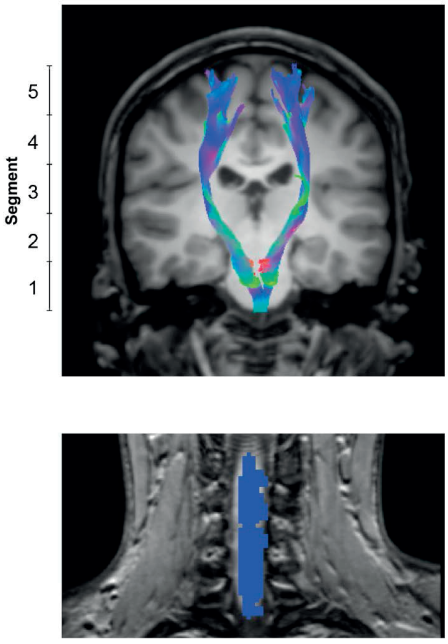

Figure 5: Diffusion Tensor Imaging of the corticospinal tracts in the brain and spinal cord
Tractography and segmentation of the corticospinal tracts in the brain and spinal cord of a healthy control subject, after processing of the diffusion tensor image. Colors indicate direction of the tracts: top-bottom (blue), front-back (green) and left-right (red).
Original image was previously published (I.C. Huffnagel et al, longitudinal diffusion tensor MRI as surrogate outcome measure for myelopathy in adrenoleukodystrophy, Neurology 2019). Approval for secondary use has been retrieved from authors and publisher.

Perfusion weighted imaging

Dynamic susceptibility perfusion MRI explores the hemodynamic changes of the brain white matter after administration of a contrast agent like gadolinium. The contrast agent causes a transient decrease in T1-signal intensity during initial transit through the vasculature. Subsequently, gadolinium can be tracked through tissue over time and its progress can be analyzed.[57]

Distinct MR perfusion changes are described in patients with cerebral ALD, corresponding to the aforementioned pathological zones. A significant decrease of 80% in normalized cerebral blood volume (perfusion) was found at the necrotic demyelinated core (zone A) of the lesions, while the contrast enhancing zone (zone B) demonstrated normal perfusion. Moreover, decreased perfusion beyond the enhancing edge (zone C) was indicative of early tissue injury and predictive of lesion progression at follow-up.[58] These findings were confirmed in another study, where CTH (capillary transit time heterogeneity - a different marker for perfusion) was significantly elevated in perilesional white matter later progressing to T2- weighted hyperintensities.[59] CTH was also elevated in NAWM of asymptomatic ALD males compared to healthy controls. This implies that *ABCD1* dysfunction in ALD patients alters white matter microvascular physiology.[59] However, these findings could not be reproduced in a recently performed study of our own group (data not published). Probably this is partly due to difficulties in determining absolute quantification of microvascular flow, the presence of susceptibility artefacts (blood product, calcification, air) and user dependency of the methods.[60]

Magnetization Transfer Imaging

Magnetization Transfer (MT) imaging measures the interaction between mobile, i.e. free, and macromolecule-bound water. The MT pulse, an offset radiofrequency pulse, targets macromolecules, depositing energy in lipid species. Following the magnetization transfer from the MT pulse, energy is transferred and dissipated towards the free water pool. The dissipation as a function of time is captured as a reduced signal of the free water.[61] Due to the large quantity of myelin present in the white matter, MT imaging has been shown to be useful in detection of early white matter changes, not otherwise detectable by structural imaging.[62]

In 1996, Melhem et al demonstrated that MT brain imaging in cerebral ALD showed two zones of signal abnormalities in the affected white matter; a peripheral zone with moderate decrease in MT and a central zone with a more pronounced decrease in MT. Here, the location of the peripheral zone corresponded to the enhancing part of the lesion as seen on structural imaging, whereas the location of the central zone corresponded to the necrotic center of the lesion. Although it has previously been hypothesized that MT imaging

should be able to detect white matter changes before such changes are visible in anatomic structural imaging, this was not confirmed in these ALD patients.[28] However, in ALD spinal cords, abnormal findings were visible on MT imaging, in the absence of abnormalities on structural imaging.[63] The cervical spinal cord of healthy subjects showed a sharp, high contrast delineation between grey and white matter, whereas in both male and female ALD patients the grey/white matter boundary was less distinct. Quantitative MT imaging (qMT) demonstrated tissue abnormalities in the dorsal and lateral columns of ALD patients with myelopathy, as well as atrophy of the spinal cord. Additionally, the qMT signal in the dorsal column was significantly higher in ALD males, compared to the (less symptomatic) female heterozygotes.[62,63]

In the future, MT imaging may be used as surrogate outcome measure for myelopathy in clinical trials, as MT abnormalities of the spinal cord have been associated with sensorimotor assessments such as postural sway performance and vibration sensation in the great toe of males and females.[63] However, longitudinal studies are still lacking.

NEW MRI TECHNIQUES

The aforementioned MRI techniques have been well studied, amongst others in ALD, over the past decades. However, new MRI techniques have been developed and are being examined in different neurodegenerative and demyelinating diseases. These techniques may provide an excellent tool for more specific imaging of axons and myelin, which can be of great value in ALD.

Neurite Orientation Dispersion and Density Imaging

Neurite Orientation Dispersion and Density Imaging (NODDI) is a diffusion MRI technique able to overcome some of the limitations of standard DTI, such as the low specificity for individual tissue microstructural features. NODDI facilitates the analysis of neurite morphology by separating the signal arising from three different tissue compartments: intraneurite water, extraneurite water and cerebrospinal fluid. This makes it possible to quantify axonal neurite orientation and density changes, possibly at an earlier stage than standard DTI.[64]

In normal ageing, white matter neurite orientation dispersion increases and neurite density decreases.[65,66] These results are, however, not conclusive and differ between studies, probably due to different age categories used in the studies. In patients with amyotrophic lateral sclerosis (ALS) a reduction of neurite density has been described in the corticospinal tracts and corpus callosum, suggesting loss of axonal density in these areas.[67] Similar changes in

microstructure have been found in other neurodegenerative diseases, such as Alzheimers' disease and Parkinsons' disease.[68,69]

Spinal cord NODDI in multiple sclerosis (MS) patients demonstrated increased orientation dispersion before changes were detected by structural MRI.[70] Furthermore, the aforementioned ALS study showed that NODDI could detect larger areas of neurodegeneration than FA measured with DTI.[67] These findings suggest that NODDI may have a higher sensitivity for detecting WM pathology than structural MRI and DTI.

Myelin water fraction imaging

Myelin Water fraction Imaging (MWI) provides quantitative measurements specific to myelin by separating the MRI signal from a voxel into contributions from different water pools. The different water pools generally correspond to: intra- and extra cellular water – with long T2 relaxation times – and water within the myelin bilayers – with short T2 relaxation times. The fraction of water corresponding to the myelin water (the myelin water fraction or MWF) correlates strongly with histopathological myelin staining and has thus been validated as corresponding to the amount of myelin present in the tissue.[71,72]

In normal healthy white matter MWF declines with age, starting approximately from the 4th decade of life.[73,74] A decline in MWF has also been reported in diseases affecting the cerebral white matter such as MS, neuromyelitis optica, schizophrenia and stroke.[72] Furthermore, MWF correlates with radial diffusivity (DTI measure for myelin content) and not with FA or mean diffusivity (DTI measures for axonal damage).[73] This shows indeed that MWF is specific to myelin content. In the future MWF may aid in the early recognition of lesion onset in cerebral ALD.

CONCLUSIONS

Structural MRI is indispensable in the clinical follow-up of ALD patients, especially for detection and prognosis of cerebral ALD. In combination with quantitative imaging techniques it provides us with important information on the pathological processes and disease evolution in ALD. Unfortunately, it is still not possible to predict onset of cerebral ALD before lesions appear on structural MRI. More advanced quantitative imaging techniques may contribute in predicting lesion onset and disease course for individual patients. This is of great importance, as ALD is being implemented in neonatal screening programs all over the world, and many new, pre-symptomatic, patients will be recognized. In addition, research focus should lay on finding (imaging) biomarkers for severity of myelopathy, in order to function as surrogate outcome measure for clinical trials, as potential new therapies

for ALD are emerging. For this, spinal cord DTI and spinal cord MT imaging have shown to be interesting candidates, while newer techniques, such as NODDI and MWF, are also highly promising.

REFERENCES

1. De Beer M, Engelen M, Van Geel BM. Frequent occurrence of cerebral demyelination in adrenomyeloneuropathy. *Neurology*. 2014;83(24):2227-2231. doi:10.1212/WNL.0000000000001074
2. Pierpont EI, Eisengart JB, Shanley R, et al. Neurocognitive trajectory of boys who received a hematopoietic stem cell transplant at an early stage of childhood cerebral adrenoleukodystrophy. *JAMA Neurol*. 2017;74(6):710-717. doi:10.1001/jamaneurol.2017.0013
3. Moser AB, Jones RO, Hubbard WC, et al. Newborn Screening for X-Linked Adrenoleukodystrophy. *Int J neonatal Screen*. 2016;2(4):15. doi:10.3390/ijns2040015
4. Kemp S, Huffnagel IC, Linthorst GE, Wanders RJA, Engelen M. Adrenoleukodystrophy - Neuroendocrine pathogenesis and redefinition of natural history. *Nat Rev Endocrinol*. 2016;12. doi:10.1038/nrendo.2016.90
5. Singh I, Moser AB, Moser HW, Kishimoto Y. Adrenoleukodystrophy: Impaired oxidation of very long chain fatty acids in white blood cells, cultured skin fibroblasts, and amniocytes. *Pediatr Res*. 1984;18(3):286-290. doi:10.1203/00006450-198403000-00016
6. Berger J, Forss-Petter S, Eichler FS. Pathophysiology of X-linked adrenoleukodystrophy. *Biochimie*. 2014;98(1):135-142. doi:10.1016/j.biochi.2013.11.023
7. Dubey P, Raymond G V., Moser AB, Kharkar S, Bezman L, Moser HW. Adrenal insufficiency in asymptomatic adrenoleukodystrophy patients identified by very long-chain fatty acid screening. *J Pediatr*. 2005;146(4):528-532. doi:10.1016/J.JPEDS.2004.10.067
8. Bezman L, Moser HW. Incidence of X-linked adrenoleukodystrophy and the relative frequency of its phenotypes. *Am J Med Genet*. 1998;76(5):415-419.
9. Van Geel BM, Bezman L, Loes DJ, Moser HW, Raymond G V. Evolution of phenotypes in adult male patients with X-linked adrenoleukodystrophy. *Ann Neurol*. 2001;49(2):186-194. doi:10.1002/1531-8249(20010201)49:2<186::AID-ANA38>3.0.CO;2-R
10. Miller WP, Rothman SM, Nascene D, et al. Outcomes after allogeneic hematopoietic cell transplantation for childhood cerebral adrenoleukodystrophy: the largest single-institution cohort report. *Blood*. 2011;118(7):1971 LP - 1978. doi:10.1182/blood-2011-01-329235
11. Moser HW, Loes DJ, Melhem ER, et al. X-Linked Adrenoleukodystrophy: Overview and Prognosis as a Function of Age and Brain Magnetic Resonance Imaging Abnormality. A Study Involving 372 Patients. *Neuropediatrics*. 2000;31(5):227-239. doi:10.1055/s-2000-9236
12. Engelen M, Kemp S, De Visser M, et al. X-linked adrenoleukodystrophy (X-ALD): clinical presentation and guidelines for diagnosis, follow-up and management. *Orphanet J Rare Dis*. 2012;7(51). http://www.ojrd.com/content/7/1/51.
13. Powers JM, DeCiero DP, Ito M, Moser AB, Moser HW. Adrenomyeloneuropathy: A neuropathologic review featuring its noninflammatory myelopathy. *J Neuropathol Exp Neurol*. 2000;59:89-102.
14. Powers JM, DeCiero DP, Cox C, et al. The Dorsal Root Ganglia in Adrenomyeloneuropathy: Neuronal Atrophy and Abnormal Mitochondria. *J Neuropathol Exp Neurol*. 2001;60(5):493-501. doi:10.1093/jnen/60.5.493
15. Huffnagel IC, van Ballegoij WJ, Van Geel BM, MBW Vos J, Kemp S, Engelen M. Progression of myelopathy in males with adrenoleukodystrophy: towards clinical trial readiness. *Brain*. 2019;142(2):334-343. doi:10.1093/brain/awy299

16. van Geel BM, Poll-The BT, Verrips A, Boelens JJ, Kemp S, Engelen M. Hematopoietic cell transplantation does not prevent myelopathy in X-linked adrenoleukodystrophy: a retrospective study. *J Inherit Metab Dis*. 2015;38(2):359-361. doi:10.1007/s10545-014-9797-1

17. Huffnagel IC, Laheji FK, Aziz-Bose R, et al. The natural history of adrenal insufficiency in X-linked adrenoleukodystrophy: an international collaboration. *J Clin Endocrinol Metab*. 2019;104(1). doi:10.1210/jc.2018-01307

18. Huffnagel IC, Dijkgraaf MGW, Janssens GE, et al. Disease progression in women with X-linked adrenoleukodystrophy is slow. *Orphanet J Rare Dis*. 2019;14(30). doi:10.1186/s13023-019-1008-6

19. Jung HH, Wimplinger I, Jung S, Landau K, Gal A, Heppner FL. Phenotypes of female adrenoleukodystrophy. *Neurology*. 2007;68(12):960 LP - 961. doi:10.1212/01.wnl.0000257129.51273.73

20. Duda E, Huttenlocher P. Computed tomography in adrenoleukodystrophy. *Radiology*. 1976;120:349-350.

21. Kumar AJ, Rosenbaum A, Naidu S, et al. Adrenoleukodystrophy: Correlating MR Imaging with CT. *Radiology*. 1987;165(2):497-504.

22. van der Knaap MS, Valk J, de Neeling N, Nauta JJP. Pattern recognition in magnetic resonance imaging of white matter disorders inchildren and young adults. *Neuroradiology*. 1991;33(6):478-493. doi:10.1007/BF00588038

23. Loes DJ, Hite S, Moser HW, et al. Adrenoleukodystrophy: A scoring method for brain MR observations. *Am J Neuroradiol*. 1994;15(9):1761-1766.

24. Engelen M, Kemp S, Poll-The BT. X-linked adrenoleukodystrophy: Pathogenesis and treatment. *Curr Neurol Neurosci Rep*. 2014;14(486). doi:10.1007/s11910-014-0486-0

25. Schaumburg HH, Powers JM, Raine CS, Suzuki K, Richardson Jr. EP. Adrenoleukodystrophy: A Clinical and Pathological Study of 17 Cases. *Arch Neurol*. 1975;32(9):577-591. doi:10.1001/archneur.1975.00490510033001

26. van der Voorn JP, Pouwels PJW, Powers JM, et al. Correlating Quantitative MR Imaging with Histopathology in X-Linked Adrenoleukodystrophy. *Am J Neuroradiol*. 2011;32(3):481-489. doi:10.3174/ajnr.a2327

27. Powers JM, Liu Y, Moser AB, Moser HW. The inflammatory myelinopathy of adreno-leukodystrophy: Cells, effector molecules, and pathogenetic implications. *J Neuropathol Exp Neurol*. 1992;51(6):630-643. doi:10.1097/00005072-199211000-00007

28. Melhem ER, Breiter SN, Ulug AM, Raymond G V., Moser HW. Improved Tissue Characterization in Adrenoleukodystrophy Using Magnetization Transfer Imaging. *AJR*. 1996;166.

29. Valk J, van der Knaap MS. *Magnetic Resonance of Myelin, Myelination and Myelin Disorders*. Springer, Berlin, Heidelberg; 1989. doi:10.1007/978-3-662-02568-0

30. Schiffmann R, Van Der Knaap MS. Invited Article: An MRI-based approach to the diagnosis of white matter disorders. *Neurology*. 2009;72(8):750-759. doi:10.1212/01.wnl.0000343049.00540.c8

31. Melhem ER, Loes DJ, Georgiades CS, Raymond G V., Moser HW. X-linked Adrenoleukodystrophy: The Role of Contrast-enhanced MR Imaging in Predicting Disease Progression. *Am J Neuroradiol*. 2000;15(9):1761-1766. http://www.ajnr.org/content/21/5/839. Accessed February 19, 2019.

32. Ji HK, Kim HJ. Childhood X-linked adrenoleukodystrophy: Clinical-pathologic overview and MR imaging manifestations at initial evaluation and follow-up. *Radiographics*. 2005;25(3):619-631. doi:10.1148/rg.253045118

33. Loes DJ, Fatemi A, Melhem ER, et al. Analysis of MRI patterns aids prediction of progression in X-linked adrenoleukodystrophy. *Neurology*. 2003;61:369-374. doi:10.1212/01.wnl.0000079050.91337.83

34. Fatemi A, Barker PB, Ulug AM, et al. MRI and proton MRSI in women heterozygous for X-linked adrenoleukodystrophy. *Neurology*. 2003;60(8):1301-1307. doi:10.1212/01.wnl.0000059546.15529.cb

35. Liberato AP, Mallack EJ, Aziz-Bose R, et al. MRI brain lesions in asymptomatic boys with X-linked adrenoleukodystrophy. *Neurology*. 2019;92(15):e1698-e1708. doi:10.1212/WNL.0000000000007294

36. Eichler F, Mahmood A, Loes D, et al. Magnetic resonance imaging detection of lesion progression in adult patients with X-linked adrenoleukodystrophy. *Arch Neurol*. 2007;64(5):659-664. doi:10.1001/archneur.64.5.659

37. Mallack EJ, van de Stadt SI, Caruso PA, et al. Clinical and radiographic course of arrested cerebral adrenoleukodystrophy. 2020;94(24):e2499-e2507.

38. Mallack EJ, Turk BR, Yan H, et al. MRI surveillance of boys with X-linked adrenoleukodystrophy identified by newborn screening: Meta-analysis and consensus guidelines. *J Inherit Metab Dis*. 2020;(December 2020):1-12. doi:10.1002/jimd.12356

39. McDonald RJ, Levine D, Weinreb J, et al. Gadolinium Retention: A Research Roadmap from the 2018 NIH/ACR/RSNA Workshop on Gadolinium Chelates. *Radiology*. 2018;289(2):517-534. doi:10.1148/radiol.2018181151

40. Uysal E, Erturk SM, Yildirim H, Seleker F, Basak M. Sensitivity of immediate and delayed gadolinium-enhanced MRI after injection of 0.5 M and 1.0 M gadolinium chelates for detecting multiple sclerosis lesions. *AJR Am J Roentgenol*. 2007;188(3):697-702. doi:10.2214/AJR.05.2212

41. Kumar AJ, Kohler W, Kruse B, et al. MR findings in adult-onset adrenoleukodystrophy. *Am J Neuroradiol*. 1995;16(6):1227-1237.

42. Israel H, Ostendorf F, Stiepani H, Ploner CJ. Spinal Cord Atrophy in Adrenomyeloneuropathy. *Arch Neurol*. 2005;62(7):1157. doi:10.1001/archneur.62.7.1157

43. Castellano A, Papinutto N, Cadioli M, et al. Quantitative MRI of the spinal cord and brain in adrenomyeloneuropathy: In vivo assessment of structural changes. *Brain*. 2016;139(6):1735-1746. doi:10.1093/brain/aww068

44. van de Stadt SIW, van Ballegoij WJC, Labounek R, et al. Spinal cord atrophy as a measure of severity of myelopathy in adrenoleukodystrophy. *J Inherit Metab Dis*. 2020;43(4):852-860. doi:10.1002/jimd.12226

45. Rajanayagam V, Grad J, Krivit W, et al. Proton MR spectroscopy of childhood adrenoleukodystrophy. *Am J Neuroradiol*. 1996;17(6):1013-1024.

46. Pouwels PJ, Kruse B, Korenke GC, Mao X, Hanefeld FA, Frahm J. Quantitative proton magnetic resonance spectroscopy of childhood adrenoleukodystrophy. *Neuropediatrics*. 1998;29(5):254-264. doi:10.1055/s-2007-973571

47. Ratai E, Kok T, Wiggins C, et al. Seven-tesla proton magnetic resonance spectroscopic imaging in adult X-linked adrenoleukodystrophy. *Arch Neurol*. 2008;65(11):1488-1494. doi:10.1001/archneur.65.11.1488

48. Van Der Voorn JP, Pouwels PJW, Hart AAM, et al. Childhood white matter disorders: Quantitative MR imaging and spectroscopy. *Radiology*. 2006;241(2):510-517. doi:10.1148/radiol.2412051345

49. Dubey P, Fatemi A, Barker PB, et al. Spectroscopic evidence of cerebral axonopathy in patients with "pure" adrenomyeloneuropathy. *Neurology*. 2005;64(2):304-310. doi:10.1212/01.WNL.0000149514.13580.84

50. Eichler FS, Itoh R, Barker PB, et al. Proton MR Spectroscopic and Diffusion Tensor Brain MR Imaging in X-linked Adrenoleukodystrophy: Initial Experience. *Radiology*. 2002;225(1):245-252. doi:10.1148/radiol.2251011040

51. Eichler FS, Barker PB, Cox C, et al. Proton MR spectroscopic imaging predicts lesion progression on MRI in X-linked adrenoleukodystrophy. *Neurology*. 2002;58(6):901-907. doi:10.1212/WNL.58.6.901

52. Pierpaoli C, Jezzard P, Basser PJ, Barnett A, Di Chiro G. Diffusion tensor MR imaging of the human brain. *Radiology*. 1996;201(3):637-648. doi:10.1148/radiology.201.3.8939209

53. Ito R, Melhem ER, Mori S, Eichler FS, Raymond G V., Moser HW. Diffusion tensor brain MR imaging in X-linked cerebral adrenoleukodystrophy. *Neurology*. 2001;56(4):544-547. doi:10.1212/WNL.56.4.544

54. Huffnagel IC, van Ballegoij WJ, Vos JM, Kemp S, Caan MW, Engelen M. Longitudinal diffusion MRI as surrogate outcome measure for myelopathy in adrenoleukodystrophy. *Neurology*. 2019;93:1-12. doi:10.1212/WNL.0000000000008572

55. Dubey P, Fatemi A, Huang H, et al. Diffusion tensor-based imaging reveals occult abnormalities in adrenomyeloneuropathy. *Ann Neurol*. 2005;58(5):758-766. doi:10.1002/ana.20643

56. Song S-K, Yoshino J, Le TQ, et al. Demyelination increases radial diffusivity in corpus callosum of mouse brain. *Neuroimage*. 2005;26(1):132-140. doi:10.1016/j.neuroimage.2005.01.028

57. McGehee BE, Pollock JM, Maldjian JA. Brain perfusion imaging: How does it work and what should i use? *J Magn Reson Imaging*. 2012;36(6):1257-1272. doi:10.1002/jmri.23645

58. Musolino PL, Rapalino O, Caruso P, Caviness VS, Eichler FS. Hypoperfusion predicts lesion progression in cerebral X-linked adrenoleukodystrophy. *Brain*. 2012;135(9):2676-2683. doi:10.1093/brain/aws206

59. Lauer A, Da X, Hansen MB, et al. ABCD1 dysfunction alters white matter microvascular perfusion. *Brain*. 2017;140(12):3139-3152. doi:10.1093/brain/awx262

60. Essig M, Shiroishi MS, Nguyen TB, et al. Perfusion MRI: the five most frequently asked technical questions. *AJR Am J Roentgenol*. 2013;200(1):24-34. doi:10.2214/AJR.12.9543

61. Henkelman RM, Stanisz GJ, Graham SJ. Magnetization transfer in MRI: A review. *NMR Biomed*. 2001;14(2):57-64. doi:10.1002/nbm.683

62. Smith SA, Golay X, Fatemi A, et al. Quantitative magnetization transfer characteristics of the human cervical spinal cord in vivo: Application to adrenomyeloneuropathy. *Magn Reson Med*. 2009;61(1):22-27. doi:10.1002/mrm.21827

63. Fatemi A, Smith SA, Dubey P, et al. Magnetization transfer MRI demonstrates spinal cord abnormalities in adrenomyeloneuropathy. *Neurology*. 2005;64(10):1739-1745. doi:10.1212/01.WNL.0000164458.02141.06

64. Zhang H, Schneider T, Wheeler-Kingshott CA, Alexander DC. NODDI: Practical in vivo neurite orientation dispersion and density imaging of the human brain. *Neuroimage*. 2012;61(4):1000-1016. doi:10.1016/j.neuroimage.2012.03.072

65. Merluzzi AP, Dean 3rd DC, Adluru N, et al. Age-dependent differences in brain tissue microstructure assessed with neurite orientation dispersion and density imaging. *Neurobiol Aging*. 2016;43:79-88. doi:10.1016/j.neurobiolaging.2016.03.026

66. Nazeri A, Chakravarty MM, Rotenberg DJ, et al. Functional consequences of neurite orientation dispersion and density in humans across the adult lifespan. *J Neurosci*. 2015;35(4):1753-1762. doi:10.1523/JNEUROSCI.3979-14.2015

67. Broad RJ, Gabel MC, Dowell NG, et al. Neurite orientation and dispersion density imaging (NODDI) detects cortical and corticospinal tract degeneration in ALS. *J Neurol Neurosurg Psychiatry*. 2019;90(4):404-411. doi:10.1136/jnnp-2018-318830

68. Kamagata K, Hatano T, Okuzumi A, et al. Neurite orientation dispersion and density imaging in the substantia nigra in idiopathic Parkinson disease. *Eur Radiol*. 2016;26(8):2567-2577. doi:10.1007/s00330-015-4066-8

69. Colgan N, Siow B, O'Callaghan JM, et al. Application of neurite orientation dispersion and density imaging (NODDI) to a tau pathology model of Alzheimer's disease. *Neuroimage*. 2016;125:739-744. doi:10.1016/j.neuroimage.2015.10.043

70. By S, Xu J, Box BA, Bagnato FR, Smith SA. Application and evaluation of NODDI in the cervical spinal cord of multiple sclerosis patients. *NeuroImage Clin*. 2017;15:333-342. doi:10.1016/j.nicl.2017.05.010

71. MacKay A, Laule C, Vavasour I, Bjarnason T, Kolind S, Mädler B. Insights into brain microstructure from the T2 distribution. *Magn Reson Imaging*. 2006;24(4):515-525. doi:10.1016/j.mri.2005.12.037

72. MacKay AL, Laule C. Magnetic Resonance of Myelin Water: An in vivo Marker for Myelin. *Brain Plast*. 2016;2(1):71-91. doi:10.3233/bpl-160033

73. Faizy TD, Kumar D, Broocks G, et al. Age-Related Measurements of the Myelin Water Fraction derived from 3D multi-echo GRASE reflect Myelin Content of the Cerebral White Matter. *Sci Rep*. 2018;8(1):1-8. doi:10.1038/s41598-018-33112-8

74. Faizy TD, Thaler C, Broocks G, et al. The Myelin Water Fraction Serves as a Marker for Age-Related Myelin Alterations in the Cerebral White Matter – A Multiparametric MRI Aging Study. *Front Neurosci*. 2020;14(February):1-14. doi:10.3389/fnins.2020.00136

II Clinical studies

3 Clinical and Radiographic Course of Arrested Cerebral Adrenoleukodystrophy

Eric J. Mallack
Stephanie van de Stadt
Paul A. Caruso
Patricia L. Musolino
Reza Sadjadi
Marc Engelen
Florian S. Eichler

Neurology 2020;94(24):e2499-e2507

ABSTRACT

Objective: To gain insight into the natural history of arrested cerebral adrenoleukodystrophy (CALD), we quantified the change in Neurologic Function Score (NFS) and Loes Score (LS) over time in patients whose cerebral lesions spontaneously stopped progressing.

Methods: We retrospectively reviewed a series of 22 patients with arrested CALD followed longitudinally over a median time of 2.4 years (0.7 – 17.0). Primary outcomes were change in radiographic disease burden (measured by LS) and clinical symptoms (measured by NFS) between patients who never developed a contrast-enhancing lesion (GdE- subgroup), and those who did (GdE+ subgroup). Secondary analyses comparing patterns of neuroanatomical involvement and lesion number, and prevalence estimates, were performed.

Results: Cerebral lesions were first detected at a median age of 23.3 years old (8.0 – 67.6), with an initial LS of 4 (0.5 – 9). NFS was 0.5 (0 – 6). Overall change in NFS or LS per year did not differ between subgroups. No patients who remained GdE- converted to a progressive CALD phenotype. The presence of contrast enhancement was associated with disease progression ($r_s = 0.559$, $p < 0.001$). Four patients (18.2%) underwent step-wise progression, followed by spontaneous resolution of contrast enhancement, and re-arrest of disease. Three patients (13.6%) converted to progressive CALD. Nineteen patients (86.4%) have arrested CALD at most recent follow-up. The prevalence of arrested CALD is 12.4%.

Conclusion: Arrested CALD lesions can begin in childhood, and patients are often asymptomatic early in disease. The majority of patients remain stable. However, clinical and MRI surveillance is recommended as a minority of patients undergo step-wise progression, or conversion to progressive CALD.

INTRODUCTION

X-linked Adrenoleukodystrophy (ALD) is caused by mutations in the *ABCD1* gene. Mutations lead to an accumulation of very long chain fatty acids (VLCFA) in plasma and tissues. Multiple phenotypes emerge as a consequence. However, no genotype-phenotype relationship has been established[1]. Thirty-five percent of boys develop cerebral ALD (CALD) in childhood, the most severe form of the disease[2]. Of the patients with childhood CALD, 85-90% will progress to inflammatory demyelination, followed by progressive neurological decline and death within 2-3 years[2,3].

Conversely, 10-15% of patients have spontaneous self-halting of disease, or "arrested CALD", without evidence of brain inflammation. Symptoms remain stable over the course of years[2,4,5]. However, the only study to date dedicated primarily to arrested CALD reviews the clinical and imaging characteristics of three patients, one 7 year old and two 11 year old boys[3]. All patients remained neurologically stable without hematopoietic stem cell transplant for 5 to 12 years after initial symptom onset. On imaging, lesions remained anatomically stable, no contrast enhancement was noted, and the metabolites detected by MR spectroscopy differed from patients with classical CALD[4]. Similar findings were found in the landmark study dedicated to understanding the role of contrast enhancement in CALD; eighteen of 22 patients with non-contrast-enhancing cerebral lesions showed no evidence of clinical or radiographic disease progression over an average of three follow-up evaluations, distributed over 22 months (range 2 – 46 months)[5]. A recent analysis included 6 patients who underwent self-halting of cerebral disease, accounting for 21% of patients with asymptomatic childhood CALD. They tended to be older than the patients with progressive childhood CALD (median age 14.4 years old vs 7.3 years old). Their lesions remained volumetrically stable across a median of 3.5 follow-up MRIs, distributed over 17.7 months[6]. To our knowledge, no other studies exist which aim to understand the evolution of disease in patients with arrested CALD.

Clinically, it is of paramount importance to differentiate between patients with arrested and progressive CALD early and accurately, when treatment with hematopoietic stem cell transplant (HSCT) is most effective[3,4,7–11]. Patients with arrested CALD should not receive HSCT due to the significant morbidity and mortality associated with the procedure, and its failure to modify the disease course[2,4,12,13]. Notably, early childhood CALD follows a protracted phase of minimal lesion change, which imposes potential difficulty in distinguishing arrested vs progressive phenotypes[6].

The primary objective of this study is to describe the clinical and radiographic evolution of patients with arrested CALD. We hypothesize that patients remain clinically stable after lesions undergo arrest, and therefore differ from patients who suffer the more common neurodegenerative course typical of CALD.

MATERIALS AND METHODS

Participants

We retrospectively reviewed medical records of 178 ALD patients across two institutions (Massachusetts General Hospital/MGH and Amsterdam University Medical Center/AUMC) from January 2001 to January 2019. The aim was to select patients diagnosed with arrested CALD.

Diagnosis of arrested CALD was defined by two or more consecutive MRIs spanning a minimum of six months with (1) no disease progression on MRI, (2) no contrast enhancement, and (3) no progression of cerebral symptoms. Clinical symptoms were defined by the Neurologic Function Score (NFS, range 0 – 25)[2]. Asymptomatic was defined as an NFS = 0. Symptom progression was defined as an increase in NFS $\geq$ 1 over consecutive clinical visits. Burden of cerebral disease was quantified by the Loes scoring (LS, range 0 – 34)[14]. Presence of a brain lesion was defined as a LS $\geq$ 0.5. Radiographic progression was defined as an increase in LS $\geq$ 0.5 between two MRI scans over a minimal period of 6 months.

Inclusion criteria were: (1) Biochemical or genetic confirmation of ALD (elevated VLCFAs or *ABCD1* mutation testing), (2) diagnosis of CALD on MRI defined by a characteristic T2 lesion, (3) Diagnosis of arrested CALD at any time point, (4) No history of hematopoietic stem cell or gene therapy, (5) $\geq$ 2 available MRIs with at least one axial T2-weighted (T2W) sequence and one axial pre- and post-contrast T1-weighted (T1W) sequence per MRI. MRI surveillance every 6 months from 3 – 10 years old and yearly thereafter was followed[15]. Otherwise, MRI follow-up was completed per clinical determination. NFS, LS, follow-up duration and interval were recorded for all time points. Treatment with Lorenzo's Oil (LO) did not exclude patients from participation in the study[1].

Due to the strong association between contrast enhancement and disease progression[3], participants were subdivided into two groups: those who never had a contrast-enhancing lesion (GdE-), and participants who had a contrast-enhancing scan (GdE+) at any time point[3,16]. Due to the importance of determining treatment eligibility in childhood, patients $\leq$ 10 years old at diagnosis of CALD were analyzed.

Imaging analysis

MR studies of the brain were performed on 1.5T/3.0T MR units (Siemens, Munich, Germany; General Electric Medical Systems, Milwaukee, USA; Philips Medical Systems, Cleveland, USA) using 8-12 channel head coils. Outside images were imported into the MGH imaging database. Parameters: frequency 350-400, phase 250-300, slice thickness 2-5 mm, gap 0-1 mm, NEX 2-3, FOV 22 x 22 to 24 x 24 cm.

Loes Scores were clinically assigned by neuroradiologists (PC, AL, KB) or neurologists (FE, PM, ME) with experience in cerebral ALD. Reviewers evaluated T2W sequences for abnormal signal hyperintensity or atrophy involving specific brain structures known to be involved in CALD. Pre- and post-contrast T1W images were analyzed for the presence (+) or absence (-) of lesional gadolinium enhancement (GdE). The lesions were subdivided into five patterns according to their primary neuroanatomic distribution[17]: 1) parieto-occipital lobe white matter or splenium of the corpus callosum; 2) frontal lobe white matter or genu of the corpus callosum; 3) frontopontine or corticospinal projection fibers; 4) cerebellar white matter and; 5) global involvement.

Statistical analysis

Continuous variables are reported as median and range. Binary variables and categorical variables are summarized as percentages. The phi correlation coefficient was used to calculate the correlation between the presence or absence of disease progression (radiographic and/or clinical) with presence or absence of contrast enhancement. The Mann-Whitney U Test was used to compare the difference in median values between skewed samples. An odds ratio was calculated to quantify the likelihood of an MRI with $\geq$ 2 neuroanatomical lesion distributions vs 1 to undergo contrast enhancement. Two-tailed *p*-values lower than 0.05 were considered statistically significant. IBM SPSS Statistics Version 25 was used for data analysis.

Standard Protocol Approvals, Registrations, and Patient Consents

Participant data was retrospectively reviewed, de-identified, and storage was encrypted and password protected. Due to anonymization, consent was waived. The Institutional/Ethics Review Boards from participating institutions approved this study. Protocol numbers: 2012P000132, METC 2014_347.

RESULTS

Participants

We identified 22 patients diagnosed with arrested CALD from a total cohort of 178 patients. 117 MRIs were available for analysis. There were a median of 4 MRIs per patient (range 2 – 14) over a follow-up duration of 2.4 years (0.7 – 17.0), at intervals of 0.9 years (0.02 – 10.8) between MRIs. Two patients received a course of LO (**Table 1**).

Clinical and Radiographic Evolution of Patients with Arrested CALD

Cerebral lesions were uncovered for the first time on brain MRI at a median age of 23.3 years old (8.0 – 67.6), with an initial LS of 4 (0.5 – 9). NFS at diagnosis was 0.5 (0 – 6), with an age of symptom onset of 29.3 years old (16.7 – 67.6).

11 patients (50.0%) were asymptomatic at diagnosis. They were a median age of 14.2 years old (8.0 – 34.8). Initial LS was 3 (0.5 – 7.5). At last follow-up, 6 patients (54.5%) have remained asymptomatic (median age 15.8 years old, 15.1 – 19.2). Four patients (36.4%) acquired myelopathic symptoms (i.e. hyperreflexia, spasticity, gait difficulty), most of whom were diagnosed with Adrenomyeloneuropathy (AMN), and have since remained stable (median age at last follow-up 33.3 years old, range 19.3 – 48.8).

After meeting a diagnosis of arrested CALD, 3 patients (13.6%) converted to progressive CALD. One patient developed lesional contrast enhancement in childhood (Patient 16). Two patients (Patients 17 and 18) demonstrated symptoms of progressive cerebral disease in adulthood (**Table 1**).

On most recent follow up, the remaining 19 patients (86.4%) continue to fulfill the diagnosis of arrested CALD (**Figure 1**). 6 patients (31.6%) have remained asymptomatic. 13 patients (68.4%) either presented with, or acquired over time, myelopathy with or without urinary incontinence, Of the 13 patients with data available, 7 (53.8%) had adrenal insufficiency diagnosed in childhood, 4 (30.8%) came to medical attention due to a family history of ALD, and 2 (15.4%) presented with spasticity in the lower extremities. Of the 19 patients with data available at last follow-up, 17 (89.5%) have adrenal insufficiency.

Overall, posterior lesions (pattern 1) were most common, appearing in 51 (44.3%) of the 115 abnormal MRIs. Frontal (pattern 2) and internal capsule lesions (pattern 3) had similar frequencies of 35.7% and 37.4%, respectively. Cerebellar white matter involvement (pattern 4) appeared in 24 MRIs (20.9%). No patients had global white matter disease (pattern 5). Interestingly, 36 MRIs (31.3%) had $\geq$ 2 distinct neuroanatomical lesions, occurring in 9 (40.9%) patients (**Table 1**).

Table 1. Patients with Arrested Cerebral Adrenoleukodystrophy

ID	Genotype	Age of First Abnormal MRI (y)	Loes Score on First MRI	Change in Loes Score per year*	Lesion Pattern[1]	Neurologic Phenotype on Presentation	Change in NFS per year*	Total Follow-Up Time (years)	Phenotype on Most Recent Follow-Up	GdE Subgroup
1	c.614C>A, p.A205E	14.5	1	0.0	2	asymptomatic	0.0	4.6	asymptomatic	-
2	c.1073C>G p.Ser358X	21.5	3	0.0	1	myelopathy°, urinary incontinence	0.0	0.7	myelopathy, urinary incontinence	-
3	Nt2252-10G>A	26.5	5	0.0	1	myelopathy, urinary incontinence	0.0	10.2	myelopathy, urinary incontinence	-
4	c.761C>T p.Thr254Met	14.9	7.5	0.0	1	asymptomatic	0.0	1.2	asymptomatic	-
5	c.1534 G>A	14.2	4	0.0	1	asymptomatic	0.0	0.9	asymptomatic	-
6	c.692_694 delGGGinsC	25.0	3	0.0	1	asymptomatic	0.1	17.0	myelopathy	-
7	c.143_155del13inAG p.Ala48GlufsX143	8.2	0.5	0.1	1	asymptomatic	0.5	11.1	myelopathy, urinary incontinence	-
8	c.852_855insACTC	12.9	4.5	0.0	3	asymptomatic	0.0	2.6	asymptomatic	-
9	c.1078delGGGinsC	34.8	1	0.3	4	asymptomatic	0.1	14.0	myelopathy	-
10	c.1866-2A>T	16.7	5	0.0	1	hyperreflexia only	0.0	2.0	hyperreflexia only	-
11	-	13.5	3	0.5	1, 3	asymptomatic	0.0	1.9	asymptomatic	-
12	c.1899delC p.Ser633Argfs*3	29.3	3	0.0	2	myelopathy, urinary incontinence	0.0	2.1	myelopathy, urinary incontinence	-
13	c.543C>A p.Tyr181	37.4	6	0.0	1, 3	myelopathy	0.0	1.8	myelopathy	-
14	-	67.6	9	0.0	1, 3	myelopathy	1.0	1.9	myelopathy, wheelchair bound, urinary incontinence	-
15	c.1899delC p.Ser633Argfs*3	29.3	2	0.0	3	myelopathy, urinary incontinence	0.0	1.2	myelopathy, urinary incontinence	-
16	c.454C>T p.Arg152Cys	8.1	4	0.0	1,2,3	asymptomatic	0.0	0.7	Progressive Childhood CALD	+
17	c.1992-2 A>G (splicing defect).	34.8	4	2.6	3, 4	myelopathy	7.7	1.2	Myelopathy, Progressive Adult-onset CALD	+

Table 1. Patients with Arrested Cerebral Adrenoleukodystrophy (*continued*)

ID	Genotype	Age of First Abnormal MRI (y)	Loes Score on First MRI	Change in Loes Score per year*	Lesion Pattern[ł]	Neurologic Phenotype on Presentation	Change in NFS per year*	Total Follow-Up Time (years)	Phenotype on Most Recent Follow-Up	GdE Subgroup
18	-	30.4	-	-	1, 3	myelopathy, urinary incontinence	0.4	5.1	myelopathy, urinary incontinence, dysarthria, Progressive Adult-onset CALD	+
19	-	51.5	0	1.2	3	hyperreflexia only	0.0	3.7	hyperreflexia only	+
20	c.1850G>A and c.1399G>A	8.0	0	0.5	2	asymptomatic	0.0	8.5	asymptomatic	+
21	c.874_876delGAG p.Glu292del	35.2	6	0.0	3,4	myeloneuropathy	0.4	2.8	myeloneuropathy, urinary incontinence	+
22	c.1609 C>T	15.5	2	0.1	2	asymptomatic	0.1	9.1	myelopathy	+

ł 1 = splenium, 2 = genu, 3 = corticospinal, 4 = cerebellar, 5 = global
* over total follow up
°myelopathy = hyperreflexia, spasticity, gait difficulty
GdE = Gadolinium

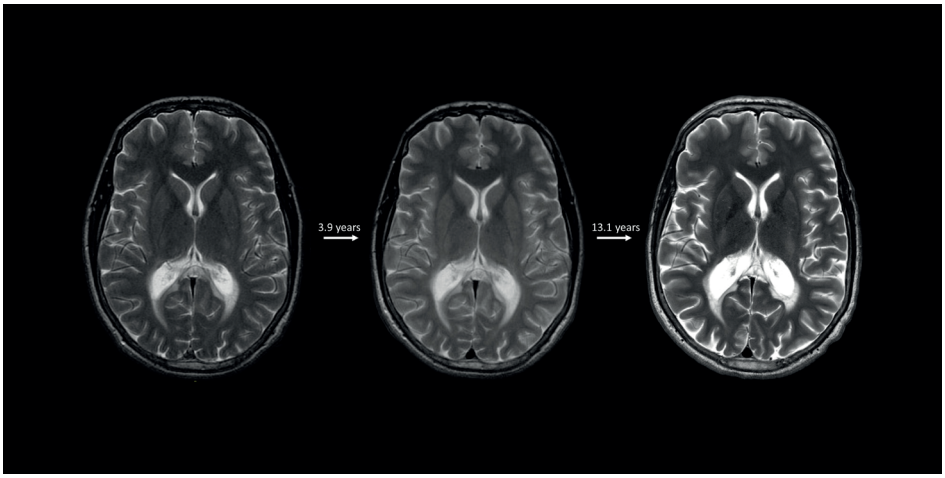

Figure 1. Arrested Cerebral Lesion.
Arrested Cerebral Lesion on T2-weighted MRI over a total follow up time of 17.0 years in Patient 6. Loes Score = 3 for all MRIs.

Childhood-Onset Arrested CALD

Importantly, three patients (7, 16, and 20) diagnosed with arrested CALD had evidence of a cerebral lesion at ≤ 10 years old (**Table 1**). Patient 16 subsequently converted to progressive childhood CALD, and was referred for HSCT. Patient 7 was diagnosed with ALD at 19.0 years old after presenting with lower extremity spasticity. Evidence of an early parieto-occipital T2 lesion (LS = 0.5) was uncovered on retrospective review of an MRI obtained at 8.2 years old for a childhood concussion[18]. Patient 20 developed CALD (LS = 1) at 8.0 years old following a previously normal MRI (LS = 0) 1.9 years earlier. His cerebral lesion remained arrested without evidence of contrast enhancement for 1.4 years. Despite the appearance, and subsequent resolution of contrast enhancement, he has remained asymptomatic for the last 8.5 years since the appearance of his cerebral lesion.

Role of Contrast Enhancement

Contrast enhancement was present in 20 of the 115 (17.4%) abnormal MRIs. Eleven of the contrast-enhancing MRIs (55.0%) occurred in scans with ≥ 2 affected anatomical areas. There was no statistical difference in age between the gadolinium negative (GdE-) and gadolinium positive (GdE+) subgroups: 27.5 vs 21.8 years old, $p = 0.26$.

GdE- Subgroup

Fifteen patients (68.2%) have never had contrast enhancement on MRI. Median age at last evaluation was 22.2 years old (15.1 – 69.5), after a follow-up time from diagnosis of 2.0 years (0.7 – 17.0). No patients in the GdE- subgroup underwent rapid clinical deterioration. At last evaluation, 5 patients were asymptomatic, the remaining 10 have myelopathic symptoms or a diagnosis of AMN.

GdE+ Subgroup

After a diagnosis of arrested CALD, 7 patients (31.8%) developed lesional contrast enhancement (GdE+) on MRI at some time point during follow-up imaging. Contrast enhancement occurred for the first time at a median age of 35.2 years old (8.8 – 51.5), 4.1 years (0.0 – 8.8) after the first abnormal MRI. GdE+ lesions correlated with a period of clinical and/or radiographic progression ($r_s = 0.559$, $p < 0.001$). Despite this, the overall median change in LS per year did not differ between the GdE+ vs GdE- subgroups: 0.3 (0.0 – 2.6) vs 0.0 (0.0 – 0.5), $p = 0.08$ (**Figure 2**). Similarly, the overall median change in NFS per year did not differ between subgroups: 0.1 (0.0 – 7.7) vs 0.0 (0.0 – 1.0), $p = 0.27$ (**Figure 2**).

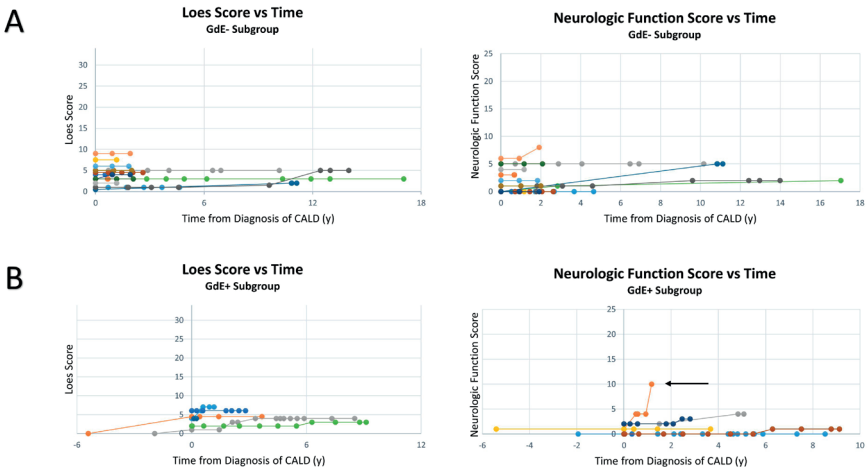

Figure 2. Change in Loes and Neurologic Function Scores from Diagnosis of CALD. Loes Scores and Neurologic Function Scores over time from diagnosis of CALD in (Row A) GdE- Subgroup and (Row B) GdE+ Subgroup. The median change in LS per year did not differ between the GdE+ vs GdE- subgroups: 0.3 (0.0 – 2.6) vs 0.0 (0.0 – 0.5) $p = 0.08$. The median change in NFS per year did not differ between subgroups: 0.1 (0.0 – 7.7) vs 0.0 (0.0 – 1.0), $p = 0.27$. The outlier is Patient 17 (black arrow) who converted to progressive CALD in adulthood: change in LS per year of 2.6, change in NFS per year of 7.7

Four patients (57.1%) had resolution of contrast enhancement between 0.3 and 3.0 years from their first GdE+ MRI, with re-stabilization of LS and NFS, thus meeting criteria again for arrested CALD. Age range is 16.5 – 55.2 years old at most recent follow-up.

3 of the 7 patients (42.9%) converted to progressive CALD. As described above, Patient 16 was diagnosed at 8.8 years old. Patient 17 showed lesion contrast enhancement and disease progression at 35.4 years old with a change in LS per year of 2.6, and change in NFS per year of 7.7. Cerebral symptoms included dysarthria, dysphagia, motor and cognitive deterioration (**Table 1**, **Figure 2B arrow**). Similarly, Patient 18 developed dysarthria and contrast enhancement on MRI at 35.3 years old (**Table 1**).

While not the most frequent, the neuroanatomical distributions with the highest proportion of GdE+ MRIs were lesions of the cerebellum (pattern 4) with 9 MRIs (37.5%) of 24. This was followed by 12 (27.9%) internal capsule (pattern 3) lesions. The proportion of GdE+ frontal white matter (pattern 2) and splenial (pattern 1) lesions were 19.5% and 9.8%, respectively.

Multiple vs Single Neuroanatomical Lesions

71.4% of patients (5/7) in the GdE+ subgroup had ≥ 2 affected anatomical areas on MRI. Conversely, only 26.7% of patients (4/15) in the GdE- subgroup had 2 or more affected areas.

30.6% of the MRIs with ≥ 2 lesions (11/36) showed contrast enhancement (**Figure 3**). Only 11.1% of MRIs with singular lesions (9/81) showed contrast enhancement. The odds of an MRI with ≥ 2 neuroanatomical lesions to have contrast enhancement is 3.52 times higher than an MRI with a singular lesion (OR = 3.52, 95%CI: 1.31 – 9.49, $p = 0.01$).

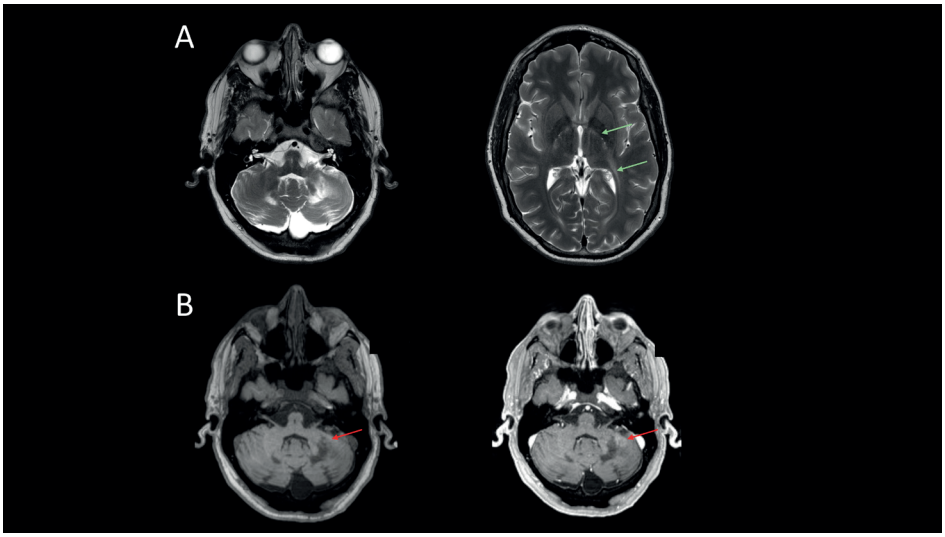

Figure 3. Multiple Cerebral Lesions and Contrast Enhancement in a Patient with Arrested CALD. Two different neuroanatomical lesions with evidence of inflammation in a single patient (Patient 21). Row A: T2-hyperintense lesions in the bilateral cerebellar hemispheres (Pattern 4), and T2-hyperintense lesions affecting the posterior limbs of the internal capsules bilaterally, with posterior extension to the left periventricular white matter (Pattern 3, green arrows). Row B: T1-pre and post contrast images demonstrating patchy contrast enhancement in the left cerebellar hemisphere (red arrows). Loes Score = 6.

Prevalence and Age-Distribution

22 of the total 178 combined cases of ALD (all phenotypes) between institutions (12 of 117 from MGH, 10 of 61 from AUMC) presented with arrested CALD. This translates to an overall prevalence of 12.4%. Only 3 of the 22 (13.6%) arrested cases were diagnosed in pa-

tients less than 10 years old. The majority of patients were diagnosed in late adolescence or adulthood. If the three patients who converted to progressive cerebral disease are excluded, the prevalence of patients with stable, arrested CALD in our cohort is 10.7% (19/178).

DISCUSSION

Here we provide the largest study to date dedicated to understanding the clinical and radiographic evolution of patients with arrested CALD. No formal definitions of arrested CALD have been reported previously in the literature. Korenke et. al. described arrested CALD as the lack of neurological deterioration in the absence of lesion progression or contrast enhancement on the patient's most recent MRI[4]. Melhem et. al. defined disease progression as an increase in both clinical and MRI scores on a minimum of one follow-up evaluation. For the eighteen patients who showed no enhancement on MRI and had no evidence of both clinical or radiographic progression, average follow-up between MRIs was 7.33 months[16]. Accordingly, we defined arrested CALD as two or more consecutive MRIs spanning a minimum of six months with no increase in LS, no contrast enhancement, and no progression of cerebral symptoms. Twenty-two patients initially met a diagnosis of arrested CALD. Nineteen (86.4%) retained a diagnosis of arrested disease at most recent follow-up. Median follow-up time in this study was 2.35 years, with a maximum of 17. We previously reported a 21% prevalence of arrested CALD patients in a cohort of asymptomatic boys with childhood CALD[6]. Proportionately, the prevalence of patients with arrested cerebral disease amongst all cases of ALD is 12.4%.

Patients who underwent self-halting of disease were initially asymptomatic in childhood and adolescence. Remarkably, brain lesions were often clinically silent, only to be uncovered at an older age when patients came to medical attention with adrenal insufficiency, or presented with myelopathic symptoms, and a diagnosis of ALD was made. Alternatively, after diagnosis by family screening, MRI monitoring enabled for early presymptomatic lesion detection. Overall, clinical and radiographic disease progressed slowly over years, most likely due to evolving AMN. This trajectory is in stark contrast to the presentation of progressive CALD, where patients undergo rapid neurological deterioration[2,3]. Here patients identified once symptomatic have invariably poor outcomes, even following treatment [2,7,10,19–21].

The earliest evidence of arrested CALD was present in three patients at 8 years old (Patients 7, 16, and 20), consistent with childhood-onset arrested CALD first reported by Korenke et. al.[4]. Our data demonstrate that new lesions destined to arrest can develop in the same age range of new lesions destined to undergo progressive demyelination[2]. The overwhelming majority of children with cerebral lesions will undergo progression after a protracted phase

of minimal lesion change, thus making it difficult to distinguish arrested versus progressive phenotypes in early childhood[6]. Therefore, patients with new cerebral lesions in childhood may, by default, initially fit the diagnosis of arrested CALD prior to conversion to progressive disease, as seen in Patient 16. Our study highlights the importance of early MRI monitoring of patients diagnosed with ALD, especially given the novel, presymptomatic approach to disease afforded by newborn screening[15]. It is of paramount importance to differentiate between phenotypes as early, and as accurately, in the disease course as possible to maximize treatment outcomes for children with progressive CALD, and avoid toxic treatments for those who will go on to self-halt[3,4,7–11].

The potential difficulties of early, accurate phenotypic diagnosis begins to address the larger diagnostic issue across an ALD patient's lifespan. Namely, the transient nature of diagnosing a patient with arrested, or progressive, CALD. Our data illustrate that the permanence of a diagnosis of arrested CALD is proportional to age. Younger children with cerebral disease are more likely to undergo inflammatory demyelination, followed by rapid disease progression[2,3]. Conversely, older patients with arrested CALD tend to remain stable, despite the presence or absence of contrast enhancement. The majority of patients with arrested CALD in this study had no evidence of contrast enhancement on MRI. No patients in the GdE- subgroup followed a progressive CALD phenotype. This is prognostically valuable for patients with a cerebral lesion that continues to show no signs of inflammation.

Notably, signs of inflammation can be transiently present after a patient is diagnosed with arrested CALD. Contrast enhancement appeared in 17.4% of the total abnormal MRIs in the study, distributed over one-third of patients. Importantly, the presence of contrast enhancement did not invariably lead to the rapid neurodegeneration. Rather, contrast enhancement correlated ($r_s = 0.559$) with a *temporary period* of disease progression. Overall clinical and radiographic progression was slow, and statistically the same as the GdE- subgroup. At most recent follow-up, 4 of the 7 patients had resolution of enhancement, and re-stabilized to a diagnosis of arrested CALD. This supports a *step-wise* disease trajectory.

Radiographically, enhancement was 3.5 times more likely to appear in MRIs with $\geq$2 distinct neuroanatomical lesions. It was detected most often in the cerebellum (pattern 4) followed by involvement of the internal capsules (pattern 3). This is seemingly distinct from its predilection for the splenium of the corpus callosum (pattern 1) as observed in progressive childhood CALD[6]. Lesion distribution may be important from a transplant perspective; adult patients who convert to progressive CALD with bilateral involvement of the internal capsules (pattern 3) have significantly worse post-transplant outcomes[22,23].

Three patients in the GdE+ subgroup (13.6% of the total series) converted to progressive CALD. One patient underwent inflammatory transformation at 8.8 years old. He was referred for treatment while asymptomatic due to the known natural history of childhood CALD[3]. Patients 17 and 18 converted at 35.4 and 35.3 years old, respectively. Both clinical and radiographic changes accelerated faster than the indolent trajectory of continued arrested disease. Cerebral symptoms included dysarthria, dysphagia, motor and cognitive deterioration. Clinical progression was observed in both patients prior to the onset of contrast enhancement. This is the inverse of events in presymptomatic childhood CALD: radiographic changes and contrast enhancement precede the onset of neurological symptoms[6,24].

The major clinical implications are (1) adults with cerebral ALD should also undergo MRI surveillance in addition to periodic neurological examinations, and (2) the presence of contrast enhancement, especially in the second and third decade of life, does not necessitate a reflexive, time-sensitive referral for transplant as it does in progressive childhood CALD. Rather, patients with arrested CALD in the setting of emerging, or established, AMN should be monitored closely for signs of radiographic or clinical progression of cerebral symptoms.

Several limitations apply to our study. The retrospective nature only allows us to analyze patient histories once they come to medical attention. Our data only includes lesion onset (i.e. first abnormal MRI following a previously normal MRI) for two of the 22 patients. Lesions were uncovered for the remaining nineteen upon diagnosis of ALD. While we have some insight into the onset of cerebral lesions in arrested CALD, only prospective, systematic MRI monitoring from birth, as now possible by the addition of ALD to Newborn Screening, will provide the true timing of lesion onset and natural history of disease. Additionally, while minimal, our series had some missing data that may have limited analysis and interpretation. As two major referral institutions, ascertainment bias may have influenced our results. In terms of symptom scoring, the NFS is relatively insensitive to subtle cognitive symptoms, and therefore the number of asymptomatic patients may have been overestimated. The LS is similarly insensitive to subtle changes in lesion size[6]. Heterogeneity in MR field strength may have led to differences in interpretation of onset and degree of cerebral involvement. Finally, as with many rare diseases, generalizable conclusions are limited due to the number of available cases.

Our findings document that cerebral ALD is not invariably progressive, and that an entity of arrested cerebral ALD exists. Arrested CALD lesions can begin in childhood, and patients are often asymptomatic early in disease. Despite developing AMN, patients remain cognitively intact, with brain lesions stabilizing in the absence of bone marrow transplantation or gene therapy. Overall, MRIs demonstrate an intact blood brain barrier, i.e. no contrast

enhancement. The finding of arrested CALD should not dissuade ongoing monitoring of patients with brain lesions as conversion to active progressive cerebral ALD can still occur at any age.

REFERENCES

1. Moser HW. Adrenoleukodystrophy : phenotype , genetics , pathogenesis and therapy * Dedicated to the memory of Peter Moser. 1997:1485-1508.
2. Moser HW, Loes DJ, Melhem ER, et al. X-linked adrenoleukodystrophy: Overview and prognosis as a function of age and brain magnetic resonance imaging abnormality. A study involving 372 patients. *Neuropediatrics*. 2000;31(5):227-239. doi:10.1055/s-2000-9236
3. Raymond G V, Aubourg P, Paker A, et al. Survival and Functional Outcomes in Boys with Cerebral Adrenoleukodystrophy with and without Hematopoietic Stem Cell Transplantation. *Biol Blood Marrow Transplant*. 2018. doi:10.1016/j.bbmt.2018.09.036
4. Korenke GC, Pouwels PJ, Frahm J, et al. Arrested cerebral adrenoleukodystrophy: a clinical and proton magnetic resonance spectroscopy study in three patients. *Pediatr Neurol*. 1996;15(2):103-107.
5. Melhem ER, Loes DJ, Georgiades CS, Raymond G V., Moser HW. X-linked adrenoleukodystrophy: The role of contrast-enhanced MR imaging in predicting disease progression. *Am J Neuroradiol*. 2000;21(5):839-844.
6. Liberato AP, Mallack EJ, Aziz-Bose R, et al. MRI brain lesions in asymptomatic boys with X-linked adrenoleukodystrophy. *Neurology*. 2019;92(15):e1698-e1708. doi:10.1212/WNL.0000000000007294
7. Peters C, Charnas LR, Tan Y, et al. Cerebral X-linked adrenoleukodystrophy : the international hematopoietic cell transplantation experience from 1982 to 1999. 2004;104(3):881-888. doi:10.1182/blood-2003-10-3402
8. Moser HW, Moser AB, Smith KD, et al. Adrenoleukodystrophy: Phenotypic variability and implications for therapy. *J Inherit Metab Dis*. 1992;15(4):645-664. doi:10.1007/BF01799621
9. Van Geel BM, Bezman L, Loes DJ, Moser HW, Raymond G V. Evolution of phenotypes in adult male patients with X-linked adrenoleukodystrophy. *Ann Neurol*. 2001;49(2):186-194. doi:10.1002/1531-8249(20010201)49:2<186::AID-ANA38>3.0.CO;2-R
10. Shapiro E, Krivit W, Lockman L, et al. Long-term effect of bone-marrow transplantation for childhood-onset cerebral X-linked adrenoleukodystrophy. *Lancet (London, England)*. 2000;356(9231):713-718. doi:10.1016/S0140-6736(00)02629-5
11. Pierpont EI, Eisengart JB, Shanley R, et al. Neurocognitive trajectory of boys who received a hematopoietic stem cell transplant at an early stage of childhood cerebral adrenoleukodystrophy. *JAMA Neurol*. 2017;74(6):710-717. doi:10.1001/jamaneurol.2017.0013
12. Henig I, Zuckerman T. Hematopoietic Stem Cell Transplantation—50 Years of Evolution and Future Perspectives. *Rambam Maimonides Med J*. 2014;5(4):e0028. doi:10.5041/rmmj.10162
13. van Geel BM, Poll-The BT, Verrips A, Boelens J-J, Kemp S, Engelen M. Hematopoietic cell transplantation does not prevent myelopathy in X-linked adrenoleukodystrophy: a retrospective study. *J Inherit Metab Dis*. 2015. doi:10.1007/s10545-014-9797-1
14. Loes DJ, Hite S, Moser H, et al. Adrenoleukodystrophy: A scoring method for brain MR observations. *Am J Neuroradiol*. 1994;15(9):1761-1766. doi:10.1016/j.rcl.2013.11.008
15. Vogel BH, Bradley SE, Adams DJ, et al. Newborn screening for X-linked adrenoleukodystrophy in New York State: Diagnostic protocol, surveillance protocol and treatment guidelines. *Mol Genet Metab*. 2015. doi:10.1016/j.ymgme.2015.02.002

16. Melhem ER, Loes DJ, Georgiades CS, Raymond G V, Moser HW. X-linked Adrenoleukodystrophy: The Role of Contrast-enhanced MR Imaging in Predicting Disease Progression. *AJNR Am J Neuroradiol*. 2000;21:839-844. http://www.ajnr.org.ezproxy.med.cornell.edu/content/ajnr/21/5/839.full.pdf. Accessed September 10, 2017.

17. Loes DJ, Fatemi a, Melhem ER, et al. Analysis of MRI patterns aids prediction of progression in X-linked adrenoleukodystrophy. *Neurology*. 2003;61(3):369-374. doi:10.1212/01.WNL.0000079050.91337.83

18. Lin JE, Armour EA, Heshmati A, et al. Pearls & Oy-sters: Adolescent-onset adrenomyeloneuropathy and arrested cerebral adrenoleukodystrophy. *Neurology*. 2019;93(2):81-84. doi:10.1212/WNL.0000000000007755

19. van den Broek BTA, Page K, Paviglianiti A, et al. Early and late outcomes after cord blood transplantation for pediatric patients with inherited leukodystrophies. *Blood Adv*. 2018. doi:10.1182/bloodadvances.2017010645

20. Mahmood A, Raymond G V., Dubey P, Peters C, Moser HW. Survival analysis of haematopoietic cell transplantation for childhood cerebral X-linked adrenoleukodystrophy: a comparison study. *Lancet Neurol*. 2007;6(8):687-692. doi:10.1016/S1474-4422(07)70177-1

21. Miller WP, Rothman SM, Nascene D, et al. Outcomes after allogeneic hematopoietic cell transplantation for childhood cerebral adrenoleukodystrophy: The largest single-institution cohort report. *Blood*. 2011;118(7):1971-1978. doi:10.1182/blood-2011-01-329235

22. Kühl JS, Suarez F, Gillett GT, et al. Long-term outcomes of allogeneic haematopoietic stem cell transplantation for adult cerebral X-linked adrenoleukodystrophy. *Brain*. 2017;140(4):953-966. doi:10.1093/brain/awx016

23. Waldhüter N, Köhler W, Hemmati PG, et al. Allogeneic hematopoietic stem cell transplantation with myeloablative conditioning for adult cerebral X-linked adrenoleukodystrophy. *J Inherit Metab Dis*. 2019;42(2):313-324. doi:10.1002/jimd.12044

24. Aubourg P, Sellier N, Chaussain JL, Kalifa G. MRI detects cerebral involvement in neurologically asymptomatic patients with adrenoleukodystrophy. *Neurology*. 1989;39(12):1619-1621. http://www.ncbi.nlm.nih.gov/pubmed/2586779. Accessed March 1, 2019.

4 The prevalence of sexual dysfunction and its relationship with hypogonadism and myelopathy in patients with X-linked adrenoleukodystrophy

Stephanie I.W. van de Stadt
Aimy M.A. Wessel
Mirjam Langeveld
Marc Engelen
Barbara Sjouke

Manuscript in preparation

ABSTRACT

Introduction X-linked adrenoleukodystrophy (ALD) is a genetic disorder with neurological and endocrine manifestations, amongst which a myelopathy, adrenal insufficiency and hypogonadism. Many patients with ALD experience sexual dysfunction but the underlying cause of these symptoms has not been clarified. The aim of this study was to assess the prevalence of sexual dysfunction and its relationship with the presence of hypogonadism and/or myelopathy.

Methods Male ALD patients from "the Dutch ALD cohort" at the Amsterdam University Medical Centers were questioned regarding sexual functioning (erectile dysfunction and/or diminished libido), and underwent neurological examination to assess myelopathy. Fasting blood samples were taken for analysis of testosterone, luteinizing hormone (LH) and follicle stimulating hormone (FSH) concentrations.

Results The prevalence of hypogonadism in the total cohort was 4/37 patients (11%), of whom 3 were diagnosed prior to initiation of this study. 19/34 patients (56%), of whom clinical data were collected, experienced sexual dysfunction. Of these patients 10 (53%) were eugonadal, 8 (42%) had subclinical hypogonadism and one was diagnosed with hypogonadism. Neurological function between patients with and without sexual dysfunction was significantly different, with more severe myelopathy in the patients with sexual dysfunction (Expanded Disability Status Scale: 5.0 (IQR 3-6) versus 0.0 (IQR 0-2); $p = <0.001$,).

Conclusions In this study, approximately half of all adult male ALD patients experienced sexual dysfunction and the majority of these patients had normal testosterone levels. Neurological impairment appears to play a more important role in these complaints then previously appreciated. We recommend to discuss sexual dysfunction in ALD regularly, in order to start early and adequate treatment.

INTRODUCTION

X-linked adrenoleukodystrophy (ALD, OMIM #300100) is a genetic metabolic disorder with a broad spectrum of neurological and endocrine manifestations. ALD is caused by pathologic variants in the *ABCD1* gene, located on the X-chromosome[1]. Impaired functioning of the peroxisomal membrane located ABC half-transporter (named ALDP) results in impaired β-oxidation of very long chain fatty acids (VLCFA) in peroxisomes and subsequent accumulation of VLCFA in plasma and tissues[2–4]. Symptoms of ALD and rate of progression are highly variable, even in individuals from the same family[5]. In some cases ALD presents with a progressive leukodystrophy, known as cerebral ALD. This affects mostly boys <12 years of age and is often fatal within two to four years when left without hematopoietic stem cell transplantation[6]. In addition, all males and most females with ALD will develop a slowly progressive myelopathy[7,8]. A common presenting endocrine symptom in boys and men with ALD is Addisonian crisis as a result of insufficient adrenocortical function, which eventually affects approximately 80% of males during the course of the disease[9]. The occurrence of hypergonadotropic hypogonadism in patients with ALD is less clarified but previous studies suggest there is an association.

Testicular lesions in patients with ALD were first observed in 1974[4]. In particular the interstitial Leydig cells are affected, as was found in a pathological study by Powers and Schaumburg, who showed the presence of intracytoplasmic lamellas and lamellar-lipid profiles in Leydig cells with the electron microscope. These lesions were identical as those described in adrenocortical, Schwann, endoneurial and microglial cells of ALD patients and pathognomonic for ALD[10]. Leydig cells are accountable for testosterone synthesis, therefore defects in Leydig cells may eventually result in deficient testosterone production. In previous clinical studies, more than half of the male ALD patients reported diminished libido and/or erectile dysfunction[11,12]. Diminished libido and erectile dysfunction might be attributed to testosterone deficiency, although these symptoms are also common symptoms of a myelopathy[13]. Damage to sympathetic or parasympathetic nerves in the spinal cord and peripheral ganglia can directly cause erectile dysfunction[14] and diminished libido could be a consequence of the erectile dysfunction and/or chronic disease in general[14,15]. Distinguishing the causes of sexual symptoms (i.e. ALD-induced myelopathy, hypogonadism and/or related to having a chronic disease) is relevant since treatment options differ depending on the cause. In addition, it is important to establish the prevalence of sexual dysfunction and hypogonadism, since both are associated with significant consequences when untreated. Firstly, sexual dysfunction has been associated with psychological complaints[16] and is an under-addressed problem since both doctors and patients are not likely to bring it up during routine outpatient visits[17]. Secondly, long-term testosterone deficiency can lead to osteoporosis[18].

The estimated prevalence of hypogonadism in ALD ranges from 0-12%[11,12,19]. However, one study focused on plasma testosterone and gonadotropin levels for the diagnosis of hypogonadism, while correlations with clinical symptoms are lacking[19]. Moreover, all three studies used different cut-off values for testosterone and gonadotropins and different diagnostic methods for the analysis of gonadotropins were used, which makes accurate comparison complicated.

The aim of this observational study was to assess the prevalence of sexual dysfunction and its relationship to hypogonadism and myelopathy in a large cohort of adult ALD males. This was done by interviewing and examining patients as well as measurement of serum testosterone, luteinizing hormone (LH) and follicle stimulating hormone (FSH) levels. Secondly, the origin of the sexual dysfunction in patients with ALD was described.

METHODS

Subjects

The current study was part of an ongoing prospective cohort study (The Dutch ALD cohort) at the Amsterdam University Medical Centers (location AMC, Amsterdam, The Netherlands) which serves as the national referral center for peroxisomal disorders and leukodystrophies. For the current study, all male ALD patients aged 18 years and over, under follow-up at this center, were included. Patients with a history of hematopoietic stem cell transplantation because of cerebral ALD were excluded. Patients were recruited at the outpatient neurology clinic between August 2020 and February 2021. Written informed consent was obtained from all participants and the project was approved by the local Institutional Review Board (IRB) (2018_310).

Clinical assessment and data collection

Participants visited the outpatient endocrine and neurology clinics of the AMC where they were interviewed regarding the presence of sexual dysfunction (erectile function and libido) and/or (potential) complaints of adrenocortical insufficiency. Medical history and medication use were also reported. Furthermore, participants underwent neurological examination. Severity of myelopathy was determined using the Expanded Disability Status Scale (EDSS) and the Severity Score System for Progressive Myelopathy (SSPROM). The EDSS, which was originally designed for multiple sclerosis, measures neurological disability on a scale of 0 (no disability) to 10 (death)[20]. SSPROM describes the severity of myelopathy and ranges from 0-100, with lower scores indicating more severe disease[21].

Patients who already used testosterone replacement therapy before start of this study were included, but were not interviewed by an endocrinologist and no blood samples were taken since hypogonadism was already established in these patients.

Laboratory tests

Morning blood samples were obtained after an overnight fast. For analysis of testosterone levels, serum was stored at 2 – 8 °C for a maximum of 7 days or at -18 – -22°C for a maximum of 2 months before analysis. LH and FSH were analyzed on the day of collection. Analyses of blood samples were performed at the Laboratory for Endocrinology, Amsterdam University Medical Centers (location AMC, Amsterdam, The Netherlands). Detection of testosterone was performed using tandem mass spectrometry. Concentrations of testosterone below 9 nmol/L were considered deficient[22]. Detection of LH and FSH concentrations were determined using non-competitive immunoassays. Reference values were based on the DELFIA® hLH Spec kit version 13903238-6 and DELFIA® hFSH kit version 13903806-3. LH values of 1.0 – 8.4 U/L and FSH values of 1.0 – 10.5 U/L were considered normal.

Based on the results of the endocrine tests, patients were divided into three groups: patients with 1) normal gonadal function (eugonadal) 2) subclinical hypogonadism and 3) hypogonadism. Normal gonadal function was defined as testosterone, LH and FSH levels within the normal range of the reference values. Subclinical hypogonadism applied to patients with normal testosterone levels but elevation of at least one of the gonadotropins. Hypogonadism was defined as testosterone levels below the lower limit of reference value combined with elevated gonadotropins (hypergonadotropic hypogonadism).

Statistical analysis

Descriptive statistics were used to illustrate the prevalence of sexual dysfunction and the three categories of gonadal function. Patients were first grouped based on the presence (yes/no) of sexual dysfunction (erectile dysfunction and/or diminished libido). Between these groups baseline characteristics (age, presence of adrenal insufficiency and use of medication that could possibly cause sexual dysfunction), neurological status (as measured by EDSS and SSPROM) and gonadal function were compared. To assess whether the variables (age, interfering medication, neurological function) were significant predictors for experiencing sexual dysfunction, multiple logistic regression analysis was used. In addition, the prevalence of normal gonadal function, subclinical hypogonadism and hypogonadism in the total cohort was described, based on the laboratory definitions as described above. Continues variables are expressed as means ± standard deviations or medians [interquartile ranges], were appropriate. Independent samples t-tests (parametrical data) and Mann-Whitney U tests (non-parametrical data) were used to analyze continuous data. Chi-squared tests were used to analyze categorical data. R-studio version 3.6.1 was used for analyses and a p-value < 0.05 (two-sided) was defined as statistically significant.

RESULTS

Clinical and endocrine characteristics of the cohort

The Dutch ALD cohort includes 62 male ALD patients. For this study, 14 patients were excluded (11 age <18 years and 3 with a history of hematopoietic stem cell transplantation). Furthermore, as a result of the COVID-19 pandemic, another 11 patients postponed their yearly visit. Therefore, 37 adult male ALD patients were included of whom three patients already received testosterone replacement therapy before start of the study. Of these three patients we were able to retrieve data from the time of diagnosis of hypogonadism for one patient, but not for the other two patients. Nevertheless, we assumed diagnosis was made correctly and classified all three patients as having hypogonadism.

Patients' characteristics are presented in **Table 1.** Patients had a mean age of 42.0 (± 15.5) years (ranging from 18-71 years). Adrenocortical insufficiency was present in 23 patients (62%). Median EDSS was 3.0 [IQR 0-6] and median SSPROM was 83.5 [IQR 78-100]. For the 34 patients without testosterone replacement therapy, mean testosterone level was 17.6 (± 6.4) nmol/L, median LH was 6.9 U/L (IQR 4.2-9.6) and median FSH 7.4 U/L (IQR 4.4-11.5). Thirteen patients (38%) used medication that could interfere with sexual function and/or endocrine laboratory measurements (**see supplement Table 1**).

Table 1: Clinical characteristics and prevalence of sexual dysfunction

			Sexual dysfunction		
	Total (n=37)	**Treated hypogonadism (n=3)**	**Yes (n=19)**	**No (n=15)**	***p*-value**
Age in years, mean ± SD	42.0 (± 15.5)	58.0 (± 17.0)	46.1 (± 12.5)	33.1 (± 14.0)	<0.01*
Adrenocortical insufficiency, n (%)	23 (62)	1 (33)	11 (58)	11 (73)	0.35
Interfering medication, n (%)	13 (38)[1]	NA	11 (58)	2 (13)	<0.01*
Severity of myelopathy					
EDSS, median [IQR]	3.0 [0-6]	6.5 [3.0-7.0][2]	5.0 [3-6]	0 [0-2]	<0.001*
SSPROM, median [IQR]	83.5 [78-100]	62.5 [62.0-85.0][2]	78.5 [72.0-83.5]	100 [90.3-100]	<0.001*

[1] As proportion of the 34 patients without treatment for hypogonadism
[2] Median with range (due to number of patients)
* Statistically significant difference between patients with and without sexual dysfunction
Abbreviations: SD (standard deviation); EDSS (Expanded Disability Status Scale); SSPROM (Severity score System for Progressive Myelopathy)

Sexual dysfunction and the relation to endocrine and neurological function

Complaints of sexual dysfunction were present in 19/34 (56%) of patients. Eighteen patients experienced erectile dysfunction and 10 diminished libido. Nine patients with diminished libido, also experienced erectile dysfunction. From the 19 males that experienced sexual dysfunction, 10 (53%) had normal gonadal function, eight (42%) had subclinical hypogo-

nadism and one (5%) was diagnosed with hypergonadotropic hypogonadism (**Table 2**). Age and medication use were significantly different between patients with and without sexual dysfunction (**Table 1**). Patients with complaints of sexual dysfunction were older compared to patients without complaints of sexual dysfunction (46.1 (± 12.5) versus 33.1 (± 14.0) years, respectively, p = <0.001) and more often used medication with sexual dysfunction as potential side-effect (58% versus 13%, p = <0.001). In addition, EDSS and SSPROM differed significantly between patients with and without sexual dysfunction. Patients with sexual symptoms had higher EDSS and lower SSPROM (i.e. higher grade of impairment) compared to patients without sexual symptoms (EDSS: 5.0 (IQR 3-6) versus 0.0 (IQR 0-2); p = <0.001, and SSPROM: 78.5 (IQR 78-100) versus 100 (IQR 90.3-100); p = <0.001). (**Table 1**)**.** The difference in neurological function remained significant after separating the sexual dysfunction into erectile dysfunction and diminished libido (**Figure 1**). In both logistic regression models (model 1: EDSS, interfering medication and age, model 2: SSPROM, interfering medication and age), neurological function was the only significant predictor for experiencing sexual symptoms (model 1: B = 0.821, p = 0.004; model 2: B = -0.24, p = 0.003), interfering medication and age were not (p = >0.05).

Table 2: Sexual functioning and gonadal function

	Sexual dysfunction	
	Yes (n = 19)	**No (n = 15)**
Eugonadal, n (%)	10 (53)	10 (67)
Subclinical hypogonadism, n (%)	8 (42)	5 (33)
Hypergonadotropic hypogonadism, n (%)	1 (5)	0

Estimated prevalence of (subclinical) hypogonadism

Following our laboratory definitions of groups, newly diagnosed hypogonadism was present in one 63 year old male (testosterone: 5 nmol/L, LH: 14 U/L, FSH: 11 U/L). Together with the three patients already using testosterone replacement therapy, this results in a total of four out of 37 patients (11%) with hypogonadism. Three of these four patients suffered from adrenal insufficiency and severe symptoms of myelopathy (EDSS 6-7), their age was between 34-69 years. One patient with hypogonadism had no adrenal insufficiency and only mild symptoms of a myelopathy (EDSS 3.5), at the age of 72. Subclinical hypogonadism was present in 13/37 males (35%). In eight of these patients both gonadotropins were elevated, three patients had elevated LH only and two patients had elevated FSH only. Five patients with subclinical hypogonadism had no symptoms of sexual dysfunction. The remaining 20 males (54%) were considered eugonadal. (**Figure 2**). Age between patients with normal gonadal function (41.0 ± 15.5 years) and subclinical hypogonadism (39.0 ± 12.3 years) did not differ significantly.

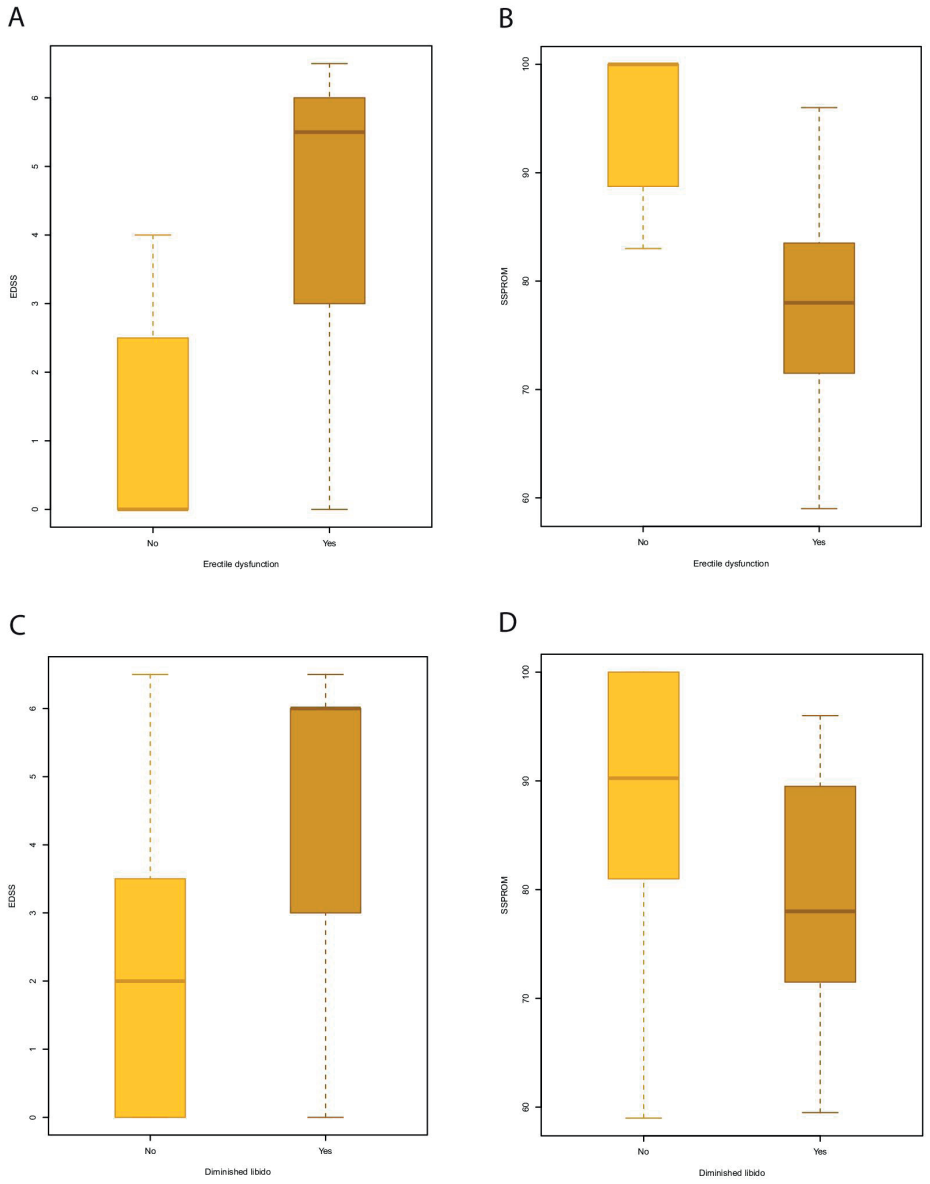

Figure 1: Presence of sexual dysfunction versus neurological function
(A) EDSS in patients with and without erectile dysfunction) and (B) SSPROM in patients with and without erectile dysfunction. (C) EDSS in patients with and without diminished libido and (D) SSPROM in patients with and without diminished libido. Bars represent ranges (min-max) and boxes represent median with interquartile ranges.
Abbreviations: EDSS (Expanded Disability Status Scale); SSPROM (Severity score System for Progressive Myelopathy)

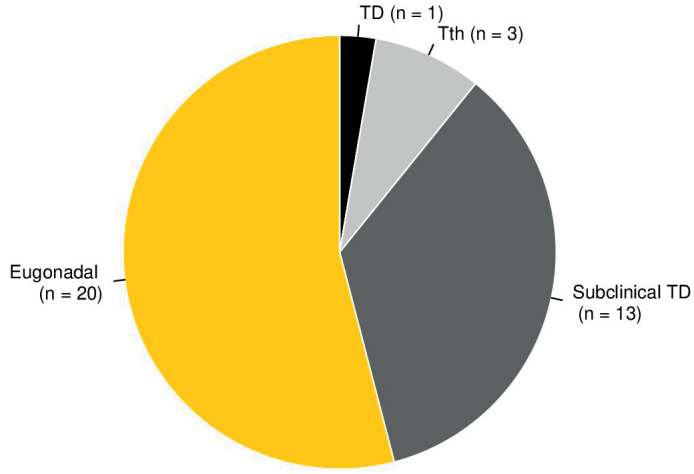

Figure 2: Gonadal function in patients with ALD
A pie chart showing the distribution of testicular function of the total cohort of ALD patients (n=37). Prevalence of hypogonadism was 11% (n=4), subclinical hypogonadism was present in 35% (n=13) and 54% (n=20) of patients were eugonadal.

DISCUSSION

This study shows that more than half (56%) of adult patients with ALD experience sexual dysfunction (ie erectile dysfunction and/or diminished libido). This is in accordance with previous studies by Brennemann et al. and Assies et al. who reported 53% and 58% respectively[11,12], and clearly illustrates this is a common problem in this population. It is important to recognize sexual dysfunction as it can be a major burden for patients and, depending on the cause, different forms of treatment are available.

We recognized three possible contributing factors to sexual dysfunction in this ALD patient population: neurological impairment caused by myelopathy, hypergonadotropic hypogonadism and medication use. Neurological impairment seems to be the main contributor to sexual dysfunction – especially erectile dysfunction – in patients with these complaints. Patients experiencing sexual dysfunction had significantly more severe neurological impairment compared to those without sexual functioning complaints. Especially for the occurrence of erectile dysfunction, the difference in neurological impairment was considerable; median EDSS for patients with erectile dysfunction was 5.5 and SSPROM 78.3 (severe symptoms of myelopathy) compared to EDSS 0 and SSPROM 100 (no signs or symptoms of myelopathy) for patients without erectile dysfunction. (**see Fig. 1**). For the occurrence of diminished libido, this difference was slightly smaller although still significant. Moreover, neurological function (EDSS and SSPROM individiually) remained a significant predictor for experiencing sexual dysfunction after adjusting for age and use of medication. Interest-

ingly, more than half (53%) of the patients with sexual dysfunction had normal gonadal function, indicating that in these patients hypogonadism is not the main cause of their sexual dysfunction.

The estimated prevalence of hypergonadotropic hypogonadism in this cohort was 11% (4/37; one newly diagnosed patient and three patients that already used testosterone replacement therapy prior to this study). This prevalence is close to the prevalence of 12% described by Assies et al.[11], but higher compared with the studies by Brennemann et al. and Stradomska et al., who both described a prevalence of 0%[12,19]. This difference could be caused by differences in methodology for endocrine analysis, as the methods used in the previous studies are more imprecise compared to the tandem mass spectrometry used in the current study[23]. Moreover, Stradomska et al. used lower cut-off values for testosterone deficiency, which might have resulted in an underestimation of patients with hypogonadism. Nevertheless, a prevalence of 11% in this cohort shows that hypogonadism should be recognized as part of the ALD spectrum, albeit in a minority of patients.

More than one third of males in this cohort (35%) had (slightly) abnormal gonadotropin levels but testosterone levels still within normal range, meeting the criteria for subclinical hypogonadism **(see Fig. 2)**. These results resemble other studies in the ALD field, in which (low) normal testosterone levels were found in combination with elevated LH or FSH (referred to as partial testicular insufficiency)[24,25]. In general, subclinical hypogonadism, despite the origin, is not associated with sexual signs and symptoms as gonadal dysfunction is still compensated by the positive feedback of gonadotropins. Subclinical hypogonadism affects 9.5% of males, according to epidemiological data from the European Male Ageing Study, and the prevalence increases with age, up to 20% in males between 70-79 years of age[26]. Accordingly, in our study, the proportion of patients with subclinical hypogonadism actually experiencing sexual dysfunction was 42%, which was similar to the eugonadal group (53%). Age between these groups did not significantly differ. This indicates that partially (sub- or preclinical) affected testicular function is common in ALD, despite patients' age, but does not necessarily results in increased sexual dysfunction. There are however no studies that show subclinical hypogonadism necessarily progresses into overt hypogonadism and testosterone therapy is therefore not recommended[26]. Prospective studies should be initiated to investigate whether and among which circumstances subclinical hypogonadism in ALD patients might progress into overt hypogonadism.

It should be noted that the number of patients using medication possibly interfering with sexual function was significantly higher in the group with sexual symptoms compared to the group without sexual symptoms. We could, however, not conclude whether the sexual dysfunction was caused by use of this medication as in most patients there was no temporal

relation between start of medication and occurrence of symptoms. Moreover, the use of medication was not a significant predictor for experiencing sexual dysfunction in our regression models. Nevertheless, use of medication should be taken into account when assessing sexual dysfunction, as discontinuation might improve or even resolve symptoms.

Based on our findings, it is advised to regularly discuss potential complaints of sexual dysfunction in all adult male ALD patients. When sexual dysfunction is present, testosterone and gonadotropin levels should be measured. In case of hypergonadotropic hypogonadism, patients should be further examined by an experienced endocrinologist to exclude other causes of hypogonadism and to consider testosterone supplementation in order to treat symptoms and to prevent future osteoporotic complications[29]. Phosphodiesterase-5 inhibitors (for example Sildenafil) might be considered in ALD patients with erectile dysfunction and normal testosterone levels. In case of subclinical hypogonadism it is recommended to provide follow-up to monitor whether or not patients develop overt hypogonadism, but treatment with testosterone replacement therapy is not (yet) recommended.

Some limitations should be taken into account when interpreting our results. As discussed before, hypogonadism was already diagnosed before start of this study in 3 out of 4 patients and we could not retrieve all information regarding diagnosis of hypogonadism. The prevalence of hypogonadism in this cohort (11%) could therefore be an overestimation, as we could not confirm if the diagnoses were made correctly. The one patient diagnosed with hypogonadism during the study suffered from other critical illnesses as well, which may worsen the experience of sexual symptoms and affect his testosterone level[30]. Moreover, other causes for primary hypogonadism could not be excluded as the patient was not able to visit the hospital for a follow-up visit due to his illness. Furthermore, blood sampling in our study was supposed to be in the morning, because of the morning peak in testosterone levels as a result of the circadian rhythm of testosterone synthesis. Yet three patients were tested in the afternoon due to traveling time and timing of appointment, including the patient that was diagnosed with hypogonadism. This might have resulted in an overestimation of the prevalence as reported in this study. A strength of this study is that for detection of testosterone levels we used tandem mass spectrometry, which is much more precise compared to immunoassays used in previous research[31] and we attributed cut-off values that are more strict compared to research estimating the prevalence of hypogonadism in the general population (<9 nmol/L compared to <10.4nmol/L by Araujo et al)[32]. Therefore, the reported prevalence (11%) in this study might be a more reliable estimate as compared to previous studies.

In conclusion, this study shows that over half of the male ALD patients experience sexual dysfunction and neurological impairment plays an important causal role in these com-

plaints. Overt hypogonadism does occur in ALD patients, though only in a minority. The prevalence of subclinical hypogonadism in this group of patients is high but it is unknown to which extent this results in overt hypogonadism. Therefore these patients should be monitored over time. As both erectile dysfunction due to myelopathy as well as sexual dysfunction due to hypogonadism are well treatable, clinicians should actively discuss these problems in the follow-up care for ALD patients.

REFERENCES

1. Moser HW, Smith KD, Watkins PA, Powers J, Moser AB. X-linked adrenoleukodysotrophy. In: *The Metabolic and Molecular Bases of Inherited Disease*. ; 2001:3257-3302.
2. Kemp S, Wanders RJ. X-linked adrenoleukodystrophy: very long-chain fatty acid metabolism, ABC half-transporters and the complicated route to treatment. *Mol Genet Metab*. 2007;90(3):268-276. doi:10.1016/j.ymgme.2006.10.001
3. Schaumburg HH, Powers JM, Raine CS, et al. Adrenomyeloneuropathy: a probable variant of adrenoleukodystrophy. II. General pathologic, neuropathologic, and biochemical aspects. *Neurology*. 1977;27(12):1114-1119. doi:10.1212/wnl.27.12.1114
4. Powers JM, Schaumburg HH. Adreno-leukodystrophy (sex-linked Schilder's disease). A pathogenetic hypothesis based on ultrastructural lesions in adrenal cortex, peripheral nerve and testis. *Am J Pathol*. 1974;76(3):481-491.
5. Engelen M, Kemp S, De Visser M, et al. X-linked adrenoleukodystrophy (X-ALD): clinical presentation and guidelines for diagnosis, follow-up and management. *Orphanet J Rare Dis*. 2012;7(51). http://www.ojrd.com/content/7/1/51.
6. Van Geel BM, Bezman L, Loes DJ, Moser HW, Raymond G V. Evolution of phenotypes in adult male patients with X-linked adrenoleukodystrophy. *Ann Neurol*. 2001;49(2):186-194. doi:10.1002/1531-8249(20010201)49:2<186::AID-ANA38>3.0.CO;2-R
7. Huffnagel IC, van Ballegoij WJ, Van Geel BM, MBW Vos J, Kemp S, Engelen M. Progression of myelopathy in males with adrenoleukodystrophy: towards clinical trial readiness. *Brain*. 2019;142(2):334-343. doi:10.1093/brain/awy299
8. Huffnagel IC, Dijkgraaf MGW, Janssens GE, et al. Disease progression in women with X-linked adrenoleukodystrophy is slow. *Orphanet J Rare Dis*. 2019;14(30). doi:10.1186/s13023-019-1008-6
9. Huffnagel IC, Laheji FK, Aziz-Bose R, et al. The natural history of adrenal insufficiency in X-linked adrenoleukodystrophy: an international collaboration. *J Clin Endocrinol Metab*. 2019;104(1). doi:10.1210/jc.2018-01307
10. Powers JM, Schaumburg HH. The testis in adreno-leukodystrophy. *Am J Pathol*. 1981;102(1):90-98.
11. Assies J, Gooren LJG, Van Geel B, Barth PG. Signs of testicular insufficiency in andrenomyeloneuropathy and neurologically asymptomatic X-linked adrenoleukodystrophy: A retrospective study. *Int J Androl*. 1997;20(5):315-321. doi:10.1046/j.1365-2605.1997.00066.x
12. Brennemann W, Köhler W, Zierz S, Klingmüller D. Testicular dysfunction in adrenomyeloneuropathy. *Eur J Endocrinol*. 1997;137(1):34-39. doi:10.1530/eje.0.1370034
13. Morgentaler A, Traish A, Hackett G, Jones TH, Ramasamy R. Diagnosis and Treatment of Testosterone Deficiency: Updated Recommendations From the Lisbon 2018 International Consultation for Sexual Medicine. *Sex Med Rev*. 2019;7(4):636-649. doi:10.1016/j.sxmr.2019.06.003
14. Dean RC, Lue TF. Physiology of penile erection and pathophysiology of erectile dysfunction. *Urol Clin North Am*. 2005;32(4):379-395. doi:10.1016/j.ucl.2005.08.007
15. Basson R, Rees P, Wang R, Montejo AL, Incrocci L. Sexual function in chronic illness. *J Sex Med*. 2010;7(1 Pt 2):374-388. doi:10.1111/j.1743-6109.2009.01621.x
16. Gao J, Zhang X, Su P, et al. Relationship between sexual dysfunction and psychological burden in men with infertility: a large observational study in China. *J Sex Med*. 2013;10(8):1935-1942. doi:10.1111/jsm.12207

17. Hoesl CE, Woll EM, Burkart M, Altwein JE. Erectile Dysfunction (ED) is Prevalent, Bothersome and Underdiagnosed in Patients Consulting Urologists for Benign Prostatic Syndrome (BPS). *Eur Urol*. 2005;47(4):511-517. doi:https://doi.org/10.1016/j.eururo.2004.10.029

18. Meier C, Nguyen T V, Handelsman DJ, et al. Endogenous Sex Hormones and Incident Fracture Risk in Older Men: The Dubbo Osteoporosis Epidemiology Study. *Arch Intern Med*. 2008;168(1):47-54. doi:10.1001/archinternmed.2007.2

19. Stradomska TJ, Kubalska J, Janas R, Tylki-Szymanska A. Reproductive function in men affected by X-linked adrenoleukodystrophy/adrenomyeloneuropathy. *Eur J Endocrinol*. 2012;166(2):291-294. doi:10.1530/EJE-11-0490

20. Kurtzke JF. Rating neurologic impairment in multiple sclerosis. *Neurology*. 1983;33(11):1444 LP - 1444. doi:10.1212/WNL.33.11.1444

21. Castilhos RM, Blank D, Netto CBO, et al. Severity score system for progressive myelopathy: development and validation of a new clinical scale. *Brazilian J Med Biol Res*. 2012;45(7):565-572. doi:10.1590/S0100-879X2012007500072

22. Travison TG, Vesper HW, Orwoll E, et al. Harmonized Reference Ranges for Circulating Testosterone Levels in Men of Four Cohort Studies in the United States and Europe. *J Clin Endocrinol Metab*. 2017;102(4):1161-1173. doi:10.1210/jc.2016-2935

23. Cawood ML, Field HP, Ford CG, et al. Testosterone measurement by isotope-dilution liquid chromatography-tandem mass spectrometry: validation of a method for routine clinical practice. *Clin Chem*. 2005;51(8):1472-1479. doi:10.1373/clinchem.2004.044503

24. Libber SM, Migeon CJ, Brown III FR, Moser HW. Adrenal and Testicular Function in 14 Patients with Adrenoleukodystrophy or Adrenomyeloneuropathy. *Hormones*. 1986;24(1):1-8. doi:10.1159/000180533

25. Moser HW, Bergin A, Naidu S, Ladenson PW. Adrenoleukodystrophy. *Endocrinol Metab Clin North Am*. 1991;20(2):297-318.

26. Giannetta E, Gianfrilli D, Barbagallo F, Isidori AM, Lenzi A. Subclinical male hypogonadism. *Best Pract Res Clin Endocrinol Metab*. 2012;26(4):539-550. doi:10.1016/j.beem.2011.12.005

27. Ahern T, Swiecicka A, Eendebak RJ, et al. Natural history, risk factors and clinical features of primary hypogonadism in ageing men: Longitudinal Data from the European Male Ageing Study. *Clin Endocrinol*. 2016;85(6):891-901. doi:10.1111/cen.13152

28. Krakowsky Y, Conners W, Morgentaler A. Serum Concentrations of Sex Hormone-binding Globulin Vary Widely in Younger and Older Men: Clinical Data from a Men's Health Practice. *Eur Urol Focus*. 2019;5(2):273-279. doi:10.1016/j.euf.2017.05.007

29. Mosekilde L, Vestergaard P, Rejnmark L. The Pathogenesis, Treatment and Prevention of Osteoporosis in Men. *Drugs*. 2013;73(1):15-29. doi:10.1007/s40265-012-0003-1

30. Dandona P, Rosenberg MT. A practical guide to male hypogonadism in the primary care setting. *Int J Clin Pract*. 2010;64(6):682-696. doi:10.1111/j.1742-1241.2010.02355.x

31. Carruthers M, Trinick TR, Wheeler MJ. The validity of androgen assays. *Aging Male*. 2007;10(3):165-172. doi:10.1080/13685530701483738

32. Araujo AB, Esche GR, Kupelian V, et al. Prevalence of symptomatic androgen deficiency in men. *J Clin Endocrinol Metab*. 2007;92(11):4241-4247. doi:10.1210/jc.2007-1245

Supplement Table 1. Usage of medication potentially interfering with sexual and gonadal functioning
Shown are all patients with their sexual symptoms and the combinations of medication used with corresponding potential side-effects.

Patient	Group	Sexual Symptoms	Medication	Relevant potential side-effect of medication
D	Eugonadal	ED	Amitriptyline	ED
E	Eugonadal	ED	Baclofen Carbamazepine Oxycodone	ED Sexual problems TD and ED
F	Eugonadal	ED	Ezetimibe Perindopril	ED ED
G	Eugonadal	-	Simvastatin	ED
H	Eugonadal	DL, ED	Ezetimibe Oxybutynin Rosuvastatin	ED ED ED
I	Subclinical hypogonadism	DL, ED	Clonazepam Fentanyl Gabapentin Gemfibrozil Nifedipine Oxycodone	DL and ED DL Sexual dysfunction NOS DL and ED ED TD and ED
J	Subclinical hypogonadism	DL, ED	Baclofen	ED
K	Subclinical hypogonadism	-	Carbamazepine	Sexual dysfunction NOS, abnormal spermatogenesis
L	Subclinical hypogonadism	ED	Fluvoxamine Tamsulosin[a]	Sexual dysfunction NOS ED
M	Subclinical hypogonadism	DL, ED	Clonazepam	DL and ED
N	Subclinical hypogonadism	ED	Metoprolol Rosuvastatin	Sexual dysfunction NOS and ED ED
O	Subclinical hypogonadism	DL, ED	Pregabalin Temazepam	ED DL
P	hypogonadism	DL, ED	Metoprolol	Sexual dysfunction NOS and ED

[a] Symptoms started after start therapy as reported by the patient.
Retrieved from Farmacotherapeutisch Kompas (Boomkamp et al. 2012);
Abbreviations: ED: erectile dysfunction; DL: diminished libido; TD: testicular dysfunction; NOS: not otherwise specified

5 Postural body sway as surrogate outcome for myelopathy in adrenoleukodystrophy

Wouter J.C. van Ballegoij
Stephanie I.W. van de Stadt
Irene C. Huffnagel
Stephan Kemp
Marjo S. van der Knaap
Marc Engelen

Frontiers in Physiology (2020) 11: 786

ABSTRACT

Background: Myelopathy is the core clinical manifestation of adrenoleukodystrophy (ALD), which is the most common peroxisomal disorder. Development of therapies requires sensitive and clinically relevant outcome measures. Together with spastic paraparesis, balance disturbance is the main cause of disability from myelopathy in ALD. In this cross-sectional study, we evaluated whether postural body sway – a measure of balance – could serve as a surrogate outcome in clinical trials.

Methods: Forty-eight male ALD patients and 49 age-matched healthy male controls were included in this study. We compared sway amplitude and sway path of ALD patients to controls. We then correlated the body sway parameters showing the largest between-group differences with clinical measures of severity of myelopathy. To correct for age, we performed multiple linear regression analysis with age and severity of myelopathy as independent variables.

Results: All body sway parameters were significantly higher in patients than controls, with medium to large effect sizes ($r = 0.43$-0.66, $p<0.001$). In the subgroup of asymptomatic patients, body sway amplitude was also higher, but the difference with controls was smaller than for symptomatic patients (effect size $r = 0.38$-0.46). We found moderate to strong correlations between body sway amplitude and clinical severity of myelopathy ($r=0.40$-0.79, $p<0.005$). After correction for age, severity of myelopathy was a significant predictor of body sway amplitude in all regression models.

Conclusions: These results indicate that postural body sway may serve as a surrogate outcome for myelopathy in ALD. Such outcomes are important to evaluate new therapies in clinical trials. Further longitudinal studies are needed and ongoing in this cohort.

INTRODUCTION

Progressive myelopathy affects almost all men with X-linked adrenoleukodystrophy (ALD) [1,2]. ALD is a genetic neurometabolic disorder with an estimated incidence of 1 in 17000 [3]. It is caused by mutations in the *ABCD1*-gene that encodes the peroxisomal transmembrane transporter (referred to as *ABCD1*-protein) for very long-chain fatty acids (VLCFA) [4,5]. A defect in the *ABCD1*-protein results in impaired peroxisomal β-oxidation of VLCFA, leading to their accumulation in plasma and tissues, including the spinal cord [6,7]. Symptoms of myelopathy typically start in the 3rd to 4th decade with a slowly progressive gait disorder [8]. Sphincter disturbance with both urinary and fecal incontinence is also frequently reported. On average, patients require a walking aid from the 6th decade and can eventually become wheelchair dependent [9], making myelopathy the main cause of disability in ALD.

Development of disease modifying therapies for myelopathy in ALD is hampered by a lack of reliable quantitative outcomes for clinical trials. Traditional clinical outcomes – such as the Expanded Disability Status Scale (EDSS), Severity Scoring system for Progressive Myelopathy (SSPROM), timed up-and-go and 6-minute walk test (6MWT) - are limited by their low sensitivity and high interrater and intrarater variability [2]. Studies on more sophisticated surrogate outcomes such as magnetization transfer (MT) imaging [10], diffusion tensor imaging (DTI) [11] and optical coherence tomography (OCT) [12] provide evidence that they could be more sensitive and rater-independent. However, they lack direct clinical relevance, meaning that they are not of direct importance to the patient in terms of functional impairment or quality of life, while that is usually a required for approval by regulatory agencies. Therefore, there is a need for surrogate outcomes that are both sensitive and clinically relevant.

The pathological hallmark of myelopathy in ALD is degeneration of the corticospinal tracts and dorsal columns of the spinal cord, causing spastic paraparesis and sensory ataxia [6]. Sensory ataxia leads to an impaired balance, a key feature of the gait disorder in ALD [13]. A measure of balance could, therefore, serve as a surrogate outcome in ALD. Indeed, Zackowski et al. showed that ALD patients with myelopathy have reduced balance compared to controls, as expressed by increased postural body sway amplitude measured with a force plate [14]. This measurement of body sway is fast, non-invasive and largely rater-independent, making it potentially suitable as surrogate outcome [15]. It is also clinically relevant, as reduced balance directly contributes to disability in ALD. However, the number of patients in the Zackowski study was quite small (n=20) and correlations with disease severity were not performed, leaving the value of body sway as surrogate outcome for myelopathy in ALD still largely undetermined.

In this cross-sectional study, we explored body sway as surrogate outcome for myelopathy in men with ALD. We compared body sway of ALD patients (symptomatic and asymptomatic) to a healthy age-matched control group. Moreover, we correlated body sway parameters with severity of myelopathy, measured by clinical and functional outcome measures.

METHODS

Study design and participants

This single-center cross-sectional study was part of an ongoing observational cohort study on the natural history of ALD (the Dutch ALD cohort). For this particular study, patients were recruited at the Amsterdam UMC (Amsterdam, the Netherlands) between January 2018 and December 2019. Male patients over 16 years of age with a confirmed diagnosis of ALD were eligible to participate. Exclusion criteria were: inability to stand unsupported, active cerebral ALD (defined as gadolinium-enhancing cerebral white matter lesions on MRI) and any comorbidity interfering with the assessment of myelopathy, such as diabetes mellitus, neurodegenerative diseases (other than ALD) and a history of vertigo/vestibular disorder.

Study participation for patients included one hospital visit with neurological assessments, body sway measurement and MR imaging. MRI scans to exclude active cerebral ALD were evaluated by an experienced neuroradiologist. Age-matched male controls without a history of diabetes, neurological or vestibular disease were recruited via public advertisement. All participant gave written informed consent prior to participation. The study protocol was approved by the local Institutional Review Board (METC 2014_302).

Neurological assessment

The protocol used to assess myelopathy in this cohort has been previously described [2,16]. In short, patients underwent a detailed neurological history and examination. They were scored as symptomatic if they had both signs and symptoms of myelopathy; otherwise they were scored as asymptomatic. We used clinical outcome measures to quantify myelopathy: the Expanded Disability Status Scale (EDSS), Severity Scoring system for Progressive Myelopathy (SSPROM) and 6-minute walk test. The EDSS, originally designed to assess disability in multiple sclerosis but also widely used in ALD, measures neurological disability ranging from 0 (no disability) to 10 (death) [2,14,17-19]. SSPROM measures severity of myelopathy ranging from 0 to 100, with lower scores indicating a higher degree of impairment [20,21]. The 6-minute walk test (6MWT) measures the maximum walking distance in 6 minutes and was performed on a 50-meter flat indoor trail [22]. Neurological assessments and body sway measurements were done on the same day.

Measurement of postural body sway

Postural body sway was measured in the outpatient clinic by three operators using a Kistler force plate type 9260AA (Kistler instrument AG, Winterthur, Switzerland) paired with Kistler's Measurement, Analysis and Reporting software (MARS). The force plate dimensions were 60x60x5cm, the sampling frequency was 1000Hz. The protocol consisted of two series of measurements in four conditions with a fixed sequence: eyes closed – feet apart, eyes open – feet apart, eyes closed - feet together, eye open – feet together. Each measurement lasted 20 seconds; the mean of the two recordings per condition was used for the analysis. Recordings were performed in an adequately lit, quiet room with a hard and flat floor. We instructed subjects to take off their shoes and stand upright with their hands passively hanging. They were standing with their feet on visual markers at approximately shoulder width (feet apart condition) or parallel immediately adjacent to each other (feet closed condition). In the eyes open condition, they were asked to keep focus on a visual marker placed on the wall approximately 2 meters in front of them. During the recordings, subjects were to stand as still as possible and avoid any movements such as head movements, coughing and talking. If the subject was not able to remain standing on the force plate in one of the conditions, this was recorded and the measurement in this condition was stopped. We used sway amplitude (total, antero-posterior and medio-lateral) and sway path (total, antero-posterior and medio-lateral) as parameters of postural sway (**Figure 1A**). Sway amplitude represents the average amount of the center of pressure (COP) sway in antero-posterior or medio-lateral direction and was calculated as the length of the trajectory of the COP sway in the antero-posterior or medio-lateral direction divided by the number of changes in this direction (i.e. from moving forward to backward or vice versa). Sway path represents the length of the trajectory of COP over the support base divided by the measurement time.[23]

Statistical analysis

We used IBM SPSS statistics version 25 (IBM Inc.) for all statistical analyses. Normality was assessed with visual inspection of QQ-plots and using the Shapiro-Wilk test [24]. Normally distributed data were presented as mean with standard deviation (SD), non-normally distributed data as median with interquartile range (IQR).

First, we assessed differences in body sway parameters between patients and controls with the Mann-Whitney U-test (non-normally distributed data). Second, we assessed differences in body sway parameters between asymptomatic patients and controls. As the prevalence of myelopathy in ALD increases with age, asymptomatic patients were significantly younger than the control group. Correction for the possible confounding effect of age through ANCOVA was not possible because the residuals of the asymptomatic group were not normally distributed. Therefore, we selected an equally sized sample of subjects from the control group, matched for age with the asymptomatic group. Subsequently, we compared body sway

parameters between these groups using unpaired t-test (normally distributed data) or Mann-Whitney U-test (non-normally distributed data). For both group comparisons, the effect size (r) was reported, which was calculated as the test statistic (*t*) divided by the square root of the number of patients for normally distributed data and as the test statistic (*z*) divided by square root of the number subjects for non-normally distributed data. An effect size <0.3 was considered a small effect, 0.3-0.5 a medium effect and >0.5 a large effect [25,26]. Third, in patients, we correlated clinical outcome measures of severity of myelopathy with the body sway parameters that showed the largest between-group differences using Spearman's rank-order correlation (non-normally distributed continuous data and ordinal data) with a Bonferroni correction for multiple comparisons. Finally, to control for a possible confounding effect of age, we performed multiple linear regression analyses with both age and clinical outcome measures of severity of myelopathy as independent variables and body sway parameters as dependent variables. Body sway parameters were not normally-distributed, but the residuals were, thereby not violating the assumptions of linear regression analysis.

For all statistical tests a significance level of α=0.05 (2-sided) was chosen. Significance levels after correction for multiple comparisons were reported separately.

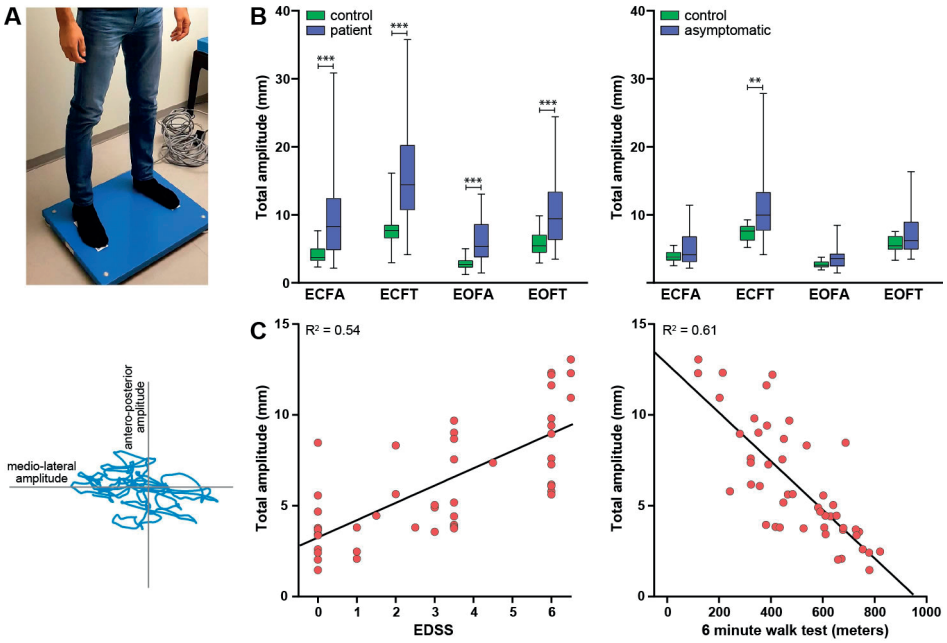

Figure 1. Study overview. (A): experimental setup. Upper panel: subject standing on the force plate in the feet-apart condition. Lower panel: body sway output. The body sway amplitude is the displacement of the center of gravity in the antero-posterior (y-axis) or medio-lateral (x-axis) direction, the sway path is the distance traveled by the blue line. **(B)**: differences in body sway amplitude between patients and controls (left) and asymptomatic patients and an age-matched selection of controls (right). **(C)**: two examples of the association between clinical severity of myelopathy and body sway: EDSS and total sway amplitude (left) and 6MWT and total sway amplitude (right). The lines represent simple linear regression lines.

RESULTS

Participant characteristics

Of 103 subjects screened, 97 were included in the analysis: 48 patients and 49 healthy controls. Six patients were excluded: 3 because they were unable to stand unsupported (all were wheelchair-dependent), 2 because of active cerebral ALD and 1 because of a technical problem during the measurement. None of the screened healthy controls were excluded. Mean age of the patient group was slightly higher than the control group (44.0 versus 41.4 years), but the difference was not statistically significant (p=0.41), nor was difference in weight (79.1 versus 82.4 kg, p=0.104). The healthy control group was significantly taller than the patient group (185 versus 180 cm, p=<0.001).

Details on the neurological assessments in our cohort have been previously described [2]. In short, for the patients included in this particular study, 32/48 (67%) were symptomatic, meaning that they had both signs and symptoms of myelopathy. Median score on the EDSS was 3.5 (IQR 0.25-6.0), on the SSPROM 87.3 (IQR 76.4-100) and mean distance walked on 6MWT was 509.0 (SD 176.7) meters.

Body sway analysis

First, we assessed differences in body sway parameters between patients and controls. Six patients were not able to remain standing on the force plate in the eyes closed – feet together condition, therefore 42 instead of 48 patients were included in this analysis. Patients had significantly higher sway amplitudes and longer sway paths in all four measured conditions (**Table 1**, **Figure 1B**). For most parameters, effect sizes were large and slightly higher for sway amplitude than sway path.

Second, we compared body sway parameters between asymptomatic patients and an equally sized age-matched selection of healthy controls. The body sway parameters were higher in the asymptomatic patient group, but only the sway amplitudes in the eyes closed – feet together condition reached statistical significance (**Table 2**, **Figure 1B**).

Third, we correlated the body sway parameters that showed the largest between-group differences (i.e. sway amplitudes and not sway paths) with clinical outcome measures of severity of myelopathy. All of these parameters correlated moderately to strongly with severity of myelopathy (Spearman's rho correlation coefficient >0.6, p=<0.001); correlations were strongest for the 6MWT compared to the other clinical outcome measures (**Table 3**, **Figure 1C**).

Table 1.
Differences in body sway parameters between patients and controls.

Eyes	Feet	Body sway parameter	Control (n=49)	Patient (n=48)	p-value	Effect size (r)
Closed	Apart	Amplitude - total	3.75 (3.24-5.04)	8.25 (4.81-12.45)	<0.001	0.56
		Amplitude - AP	2.99 (1.89-4.56)	10.48 (5.07-18.67)	<0.001	0.63
		Amplitude - ML	0.91 (0.52-1.25)	2.26 (1.34-5.33)	<0.001	0.58
		Path - total	258.0 (192.0-328.1)	514.8 (315.6-729.7)	<0.001	0.60
		Path - AP	217.4 (160.2-262.9)	437.3 (264.2-652.9)	<0.001	0.57
		Path - ML	102.6 (75.7-129.6)	172.5 (135.5-269.1)	<0.001	0.55
	Together[a]	Amplitude - total	7.70 (6.57-8.52)	14.40 (10.71-20.26)	<0.001	0.64
		Amplitude - AP	4.84 (3.36-6.51)	11.86 (7.63-18.79)	<0.001	0.60
		Amplitude - ML	6.41 (4.84-9.26)	17.66 (10.36-25.33)	<0.001	0.56
		Path - total	508.3 (386.6-653.1)	957.4 (611.0-1249.5)	<0.001	0.53
		Path - AP	290.1 (221.5-390.9)	558.1 (377.9-764.5)	<0.001	0.54
		Path - ML	329.7 (260.2-432.8)	617.0 (389.7-892.9)	<0.001	0.51
Open	Apart	Amplitude - total	2.71 (2.26-3.32)	5.37 (3.76-8.63)	<0.001	0.65
		Amplitude - AP	1.33 (1.02-1.84)	2.70 (2.07-4.37)	<0.001	0.66
		Amplitude - ML	0.56 (0.37-0.75)	0.96 (0.66-1.61)	<0.001	0.48
		Path - total	148.3 (129.2-187.4)	213.0 (189.5-307.3)	<0.001	0.58
		Path - AP	116.3 (97.1-141.6)	164.7 (153.0-238.6)	<0.001	0.60
		Path - ML	76.4 (58.2-95.6)	100.9 (80.7-190.5)	<0.001	0.43
	Together	Amplitude - total	5.43 (4.43-7.07)	9.44 (6.32-13.39)	<0.001	0.56
		Amplitude - AP	2.00 (1.43-2.46)	4.71 (2.81-6.58)	<0.001	0.58
		Amplitude - ML	2.69 (1.91-4.17)	6.82 (3.90-9.42)	<0.001	0.57
		Path - total	266.2 (212.8-318.0)	434.3 (336.2-585.4)	<0.001	0.57
		Path - AP	152.6 (126.5-198.5)	261.7 (171.7-350.5)	<0.001	0.53
		Path - ML	184.0 (142.4-225.9)	290.8 (218.4-357.3)	<0.001	0.56

Body sway amplitude (mm) and body sway path (mm) values are summarized as median (interquartile range). Mann-Whitney U-test was used to compare groups. [a] There were 42 measurements available for the patient group in the eyes closed – feet together condition, as 6 patients were not able to remain standing in this condition.

Finally, in exploratory scatter dot plots, we saw that there was an increase in most body sway parameters with age in both the patient and control group (**Figure 2**). Therefore, to be able to correct for age, we performed multiple linear regression analysis with body sway amplitudes as dependent variables and 1) age and EDSS; 2) age and SSPROM; and 3) age and 6MWT as predictors. As expected, age and clinical parameters of severity of myelopathy were correlated (correlation coefficient between 0.59-0.68), but the correlation was below the regularly used cutoff value for collinearity (correlation coefficient >0.8) – an important assumption for regression analysis [27]. In all three models, the clinical parameters

Table 2.
Differences in body sway parameters between asymptomatic patients and controls.

Eyes	Feet	Body sway parameter	Control (n=16)	Asymptomatic (n=16)	p-value	Effect size (r)
Closed	Apart	Amplitude - total	3.81 (3.29-4.53)	4.15 (3.08-6.83)	0.353	0.18
		Amplitude - AP	2.53 (1.84-3.77)	4.29 (2.32-5.68)	0.061	0.33
		Amplitude - ML	0.99 (0.75-1.26)	1.43 (1.14-1.64)	0.056	0.34
		Path - total	233.0 (198.9-376.4)	302.1 (253.8-442.0)	0.128	0.27
		Path - AP	188.9 (149.5-290.7)	242.7 (166.5-367.9)	0.361	0.17
		Path - ML	122.7 (45.7)	145.0 (52.3)	0.210	0.23
	Together[a]	Amplitude - total	7.64 (6.24-8.35)	9.95 (7.70-13.34)	**0.008**	**0.46**
		Amplitude - AP	4.92 (2.41)	7.93 (4.73)	**0.030**	**0.40**
		Amplitude - ML	6.49 (2.63)	10.15 (6.24)	**0.043**	**0.38**
		Path - total	512.7 (382.1-673.6)	606.8 (462.5-863.0)	0.184	0.24
		Path - AP	319.0 (123.2)	440.9 (247.4)	0.088	0.31
		Path - ML	352.9 (258.8-401.2)	386.3 (308.3-577.7)	0.341	0.17
Open	Apart	Amplitude - total	2.60 (2.29-3.12)	3.55 (2.43-4.29)	0.110	0.29
		Amplitude - AP	1.39 (0.46)	1.79 (0.81)	0.096	0.30
		Amplitude - ML	0.64 (0.51-0.75)	0.85 (0.66-1.10)	0.080	0.31
		Path - total	161.9 (141.2-212.7)	200.7 (162.5-250.7)	0.184	0.24
		Path - AP	122.5 (95.6-157.6)	145.2 (118.2-172.9)	0.381	0.16
		Path - ML	87.9 (76.6-108.0)	100.0 (86.2-135.8)	0.239	0.21
	Together	Amplitude - total	5.43 (4.91-6.87)	6.17 (4.92-8.97)	0.171	0.25
		Amplitude - AP	2.09 (0.75)	2.74 (1.68)	0.178	0.25
		Amplitude - ML	2.78 (1.05)	3.86 (2.55)	0.133	0.28
		Path - total	284.1 (61.5)	329.6 (128.7)	0.215	0.23
		Path - AP	174.7 (54.3)	197.2 (86.8)	0.387	0.16
		Path - ML	185.1 (38.1)	217.1 (89.9)	0.204	0.23

Body sway amplitude (mm) and body sway path (mm) values are summarized as median (interquartile range) or mean (standard deviation) depending on the distribution of data. Unpaired T-test (normally distributed data) or Mann-Whitney U-test (non-normally distributed data) was used to compare groups. Significant differences are displayed in bold text.

of severity of myelopathy (EDSS, SSPROM and 6MWT) were significant predictors of body sway amplitude (Online Resource 1). Conversely, age was a significant predictor for only three parameters: total and medio-lateral sway amplitude in the model with EDSS and eyes closed – feet together condition, and total sway amplitude in the model with SSPROM and eyes closed – feet apart condition.

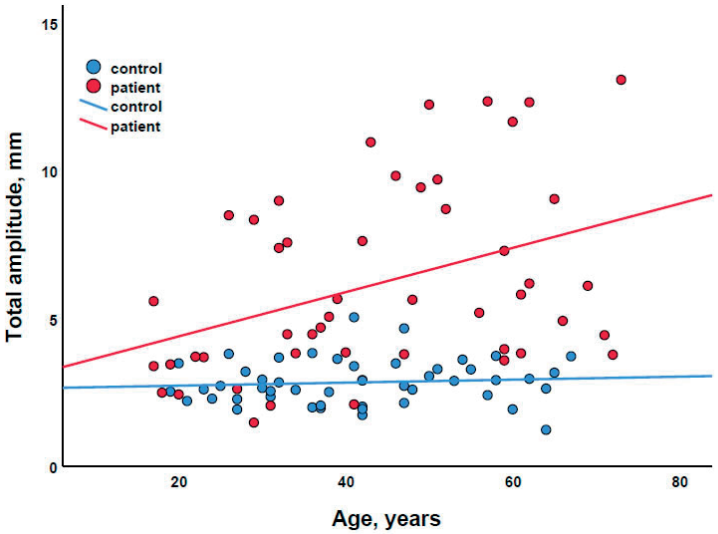

Figure 2. Scatter plot of the association between age and total sway amplitude for both patients (red) and controls (blue). The lines represent simple linear regression lines

DISCUSSION

In this cross-sectional study, we explore the potential of postural body sway as surrogate outcome for myelopathy in ALD. We provide evidence that male ALD patients have significantly higher postural body sway than healthy controls, and that body sway is also increased in clinically asymptomatic patients. Moreover, body sway parameters correlated strongly with clinical measures of severity of myelopathy.

Our results are in line with the study of Zackowski et al. [14], who demonstrated increased body sway amplitude in 20 ALD patients compared to healthy controls. Apart from this study, no studies on body sway as a measure of myelopathy in ALD are available. In hereditary spastic paraplegia, a myelopathy resembling that in ALD, postural body sway was significantly higher than in healthy controls and was correlated with muscle strength in the legs [28]. In cervical spondylotic myelopathy, the most common myelopathy, postural body sway was also increased [29,30] and improved after decompressive surgery [31]. Although these conditions do not have the same pathophysiology as ALD, they indicate that postural sway could be a useful way to measure myelopathy.

As the balance disturbance in ALD is primarily caused by degeneration of the dorsal columns of the spinal cord that relay the proprioceptive information from the legs [6], one would expect it to be most pronounced in the 'eyes closed' condition. In the 'eyes open' condition the patient can use his visual input to compensate for the lack of proprioceptive

Table 3. Correlations between severity of myelopathy and body sway amplitude in men with ALD.

Eyes	Feet	Body sway parameter		EDSS	SSPROM	6MWT
Closed	Apart	Amplitude - total	Spearman's rho	0.71	-0.76	-0.69
			p-value	<0.001	<0.001	<0.001
		Amplitude - AP	Spearman's rho	0.59	-0.56	-0.68
			p-value	<0.001	<0.001	<0.001
		Amplitude - ML	Spearman's rho	0.77	-0.76	-0.80
			p-value	<0.001	<0.001	<0.001
	Together	Amplitude - total	Spearman's rho	0.56	-0.56	-0.62
			p-value	<0.001	<0.001	<0.001
		Amplitude - AP	Spearman's rho	0.75	-0.75	-0.74
			p-value	<0.001	<0.001	<0.001
		Amplitude - ML	Spearman's rho	0.65	-0.59	-0.72
			p-value	<0.001	<0.001	<0.001
Open	Apart	Amplitude - total	Spearman's rho	0.73	-0.72	-0.71
			p-value	<0.001	<0.001	<0.001
		Amplitude - AP	Spearman's rho	0.74	-0.71	-0.76
			p-value	<0.001	<0.001	<0.001
		Amplitude - ML	Spearman's rho	0.67	-0.70	-0.67
			p-value	<0.001	<0.001	<0.001
	Together	Amplitude - total	Spearman's rho	0.62	-0.58	-0.67
			p-value	<0.001	<0.001	<0.001
		Amplitude - AP	Spearman's rho	0.36	-0.40	-0.41
			p-value	<0.001	0.005	0.004
		Amplitude - ML	Spearman's rho	0.62	-0.60	-0.66
			p-value	<0.001	<0.001	<0.001

All correlations were calculated with Spearman's rank order correlation test. After Bonferroni correction for multiple comparisons, correlations were considered significant if $p < 0.025$

information. Similarly, a bigger difference with the control group could be expected in the more difficult 'feet together' than the 'feet apart' condition. However, although the absolute body sway values were indeed higher in both the 'eyes closed' and 'feet together' conditions, the differences between patients and controls were very similar for all four conditions (effect sizes around 0.5-0.6, **Table 1**), indicating that balance is severely affected in all conditions for the total patient group. By contrast, for the asymptomatic group, only the 'eyes closed - feet together' condition showed significant between-group differences in sway amplitude (**Table 2**). Asymptomatic patients, although by definition not having any symptoms of myelopathy, frequently do have subtle signs of dorsal column dysfunction on neurological examination

such as decreased vibration sense in the legs [2]. This probably explains why their body sway amplitude is higher when tested in the most difficult condition. The fact that body sway is sensitive enough to detect changes in asymptomatic patients is important, because it could enable evaluation of disease modifying therapies in the presymptomatic state - before any disability appears.

Although sensitive, postural body sway is not specific for myelopathy. For example, most male ALD patients also develop peripheral neuropathy [32]. The signs and symptoms of myelopathy are usually more severe, masking this neuropathy. However, the neuropathy does contribute to the balance disturbance. When measuring the effect of a disease modifying therapy directed at the myelopathy (and not the peripheral neuropathy), one would not know if a change in postural body sway was caused by progression of the myelopathy or neuropathy. Similarly, body sway can be influenced by comorbidities such as cerebellar or vestibular disorders, but also by motor or sensory deficits from for example cerebrovascular disorders. It is important to take such conditions into account and exclude subjects if necessary. Finally, application of body sway as surrogate outcome is also limited by disability, as it cannot be used for more severely affected and wheelchair bound patients. This so called 'ceiling effect' is, however, also a problem for other outcome measures such as the 6MWT and DTI [11].

There are several potential sources of bias in our study. First, postural body sway is known to increase with age [33]. For the group comparisons, this should not be a problem as groups were matched for age. For the association with disease severity, we corrected for age through multiple linear regression analysis. However, age and disease severity were correlated, as both prevalence and severity of myelopathy in ALD increase with age. Although this correlation was below the commonly used threshold for collinearity in regression analysis [27], correcting for age could have caused an underestimation of the association we found between body sway and disease severity. Second, height and weight can influence body sway, although studies show conflicting results [33,34]. Patients and controls in our cohort did not differ significantly in weight, but the healthy controls were significantly taller. Because we did not find an association between either height or weight and postural body sway in our cohort (data not shown), we decided not to correct for these parameters.

Strengths of our study are the fairly large sample size for such a rare disease, the use of an age- and sex-matched control group and the comparisons with multiple, systematically collected clinical outcome measures. A limitation is that we did not evaluate test-retest reliability. In literature, however, it appears to be reasonable [35,36] and - although beyond the scope of the current study- it may be included in our future studies.

In conclusion, in this study we provide evidence that myelopathy in ALD is associated with increased postural body sway, correlating strongly with disease severity. Body sway measurement is fast, noninvasive, largely rater-independent and clinically relevant. It can be done in the outpatient clinic with automated analysis, enabling research in multicenter setting which is often needed in a rare disease like ALD. Therefore, postural body sway may serve as a new surrogate outcome for myelopathy in ALD. Further validation in a longitudinal design is needed and will

REFERENCES

1. Moser HW, Smith, K. D., Watkins, P. A., Powers, J. & Moser, A. B. The Metabolic and Molecular Bases of Inherited Disease. 2001.
2. Huffnagel IC, van Ballegoij WJC, van Geel BM, Vos J, Kemp S, Engelen M. Progression of myelopathy in males with adrenoleukodystrophy: towards clinical trial readiness. Brain. 2019;142(2):334-343.
3. Bezman L, Moser AB, Raymond GV, et al. Adrenoleukodystrophy: incidence, new mutation rate, and results of extended family screening. Ann Neurol. 2001;49(4):512-517.
4. Mosser J, Douar AM, Sarde CO, et al. Putative X-linked adrenoleukodystrophy gene shares unexpected homology with ABC transporters. Nature. 1993;361(6414):726-730.
5. van Roermund CW, Visser WF, Ijlst L, et al. The human peroxisomal ABC half transporter ALDP functions as a homodimer and accepts acyl-CoA esters. FASEB J. 2008;22(12):4201-4208.
6. Powers JM, DeCiero DP, Ito M, Moser AB, Moser HW. Adrenomyeloneuropathy: a neuropathologic review featuring its noninflammatory myelopathy. Journal of neuropathology and experimental neurology. 2000;59(2):89-102.
7. Igarashi M, Schaumburg HH, Powers J, Kishmoto Y, Kolodny E, Suzuki K. Fatty acid abnormality in adrenoleukodystrophy. J Neurochem. 1976;26(4):851-860.
8. Engelen M, Kemp S, de Visser M, et al. X-linked adrenoleukodystrophy (X-ALD): clinical presentation and guidelines for diagnosis, follow-up and management. Orphanet J Rare Dis. 2012;7:51.
9. van Geel BM, Bezman L, Loes DJ, Moser HW, Raymond GV. Evolution of phenotypes in adult male patients with X-linked adrenoleukodystrophy. Ann Neurol. 2001;49(2):186-194.
10. Fatemi A, Smith SA, Dubey P, et al. Magnetization transfer MRI demonstrates spinal cord abnormalities in adrenomyeloneuropathy. Neurology. 2005;64(10):1739-1745.
11. Huffnagel IC, van Ballegoij WJC, Vos J, Kemp S, Caan MWA, Engelen M. Longitudinal diffusion MRI as surrogate outcome measure for myelopathy in adrenoleukodystrophy. Neurology. 2019;93(23):e2133-e2143.
12. van Ballegoij WJC, Kuijpers SC, Huffnagel IC, et al. Optical coherence tomography shows neuroretinal thinning in myelopathy of adrenoleukodystrophy. J Neurol. 2020;267(3):679-687.
13. Moser HW, Mahmood A, Raymond GV. X-linked adrenoleukodystrophy. Nat Clin Pract Neurol. 2007;3(3):140-151.
14. Zackowski KM, Dubey P, Raymond GV, Mori S, Bastian AJ, Moser HW. Sensorimotor function and axonal integrity in adrenomyeloneuropathy. Arch Neurol. 2006;63(1):74-80.
15. Ruhe A, Fejer R, Walker B. The test-retest reliability of centre of pressure measures in bipedal static task conditions--a systematic review of the literature. Gait Posture. 2010;32(4):436-445.
16. Huffnagel IC, Dijkgraaf MGW, Janssens GE, et al. Disease progression in women with X-linked adrenoleukodystrophy is slow. Orphanet Journal of Rare Diseases. 2019;14(1):30.
17. Kurtzke JF. Rating neurologic impairment in multiple sclerosis: an expanded disability status scale (EDSS). Neurology. 1983;33(11):1444-1452.
18. Moser HW, Fatemi A, Zackowski K, et al. Evaluation of therapy of X-linked adrenoleukodystrophy. Neurochem Res. 2004;29(5):1003-1016.

19. Castellano A, Papinutto N, Cadioli M, et al. Quantitative MRI of the spinal cord and brain in adrenomyeloneuropathy: in vivo assessment of structural changes. Brain. 2016;139(Pt 6):1735-1746.
20. Castilhos RM, Blank D, Netto CB, et al. Severity score system for progressive myelopathy: development and validation of a new clinical scale. Brazilian journal of medical and biological research = Revista brasileira de pesquisas medicas e biologicas. 2012;45(7):565-572.
21. D'Souza M, Yaldizli O, John R, et al. Neurostatus e-Scoring improves consistency of Expanded Disability Status Scale assessments: A proof of concept study. Multiple sclerosis (Houndmills, Basingstoke, England). 2017;23(4):597-603.
22. van Hedel HJ, Wirz M, Dietz V. Assessing walking ability in subjects with spinal cord injury: validity and reliability of 3 walking tests. Archives of physical medicine and rehabilitation. 2005;86(2):190-196.
23. Baratto L, Morasso PG, Re C, Spada G. A new look at posturographic analysis in the clinical context: sway-density versus other parameterization techniques. Motor control. 2002;6(3):246-270.
24. Shapiro SS, Wilk MB. An Analysis of Variance Test for Normality (Complete Samples). Biometrika. 1965;52(3/4):591-611.
25. Lakens D. Calculating and reporting effect sizes to facilitate cumulative science: a practical primer for t-tests and ANOVAs. Frontiers in psychology. 2013;4:863.
26. Cohen J. Statistical power analysis for the behavioral sciences. Hillsdale, N.J.: L. Erlbaum Associates; 1988.
27. Vatcheva KP, Lee M, McCormick JB, Rahbar MH. Multicollinearity in Regression Analyses Conducted in Epidemiologic Studies. Epidemiology (Sunnyvale). 2016;6(2):227.
28. Marsden J, Stevenson V. Balance dysfunction in hereditary and spontaneous spastic paraparesis. Gait Posture. 2013;38(4):1048-1050.
29. Haddas R, Lieberman I, Boah A, Arakal R, Belanger T, Ju KL. Functional Balance Testing in Cervical Spondylotic Myelopathy Patients. Spine. 2019;44(2):103-109.
30. Yoshikawa M, Doita M, Okamoto K, Manabe M, Sha N, Kurosaka M. Impaired postural stability in patients with cervical myelopathy: evaluation by computerized static stabilometry. Spine (Phila Pa 1976). 2008;33(14):E460-464.
31. Haddas R, Ju KL, Boah A, Kosztowski T, Derman PB. The Effect of Surgical Decompression on Functional Balance Testing in Patients With Cervical Spondylotic Myelopathy. Clinical spine surgery. 2019;32(9):369-376.
32. Kemp S, Huffnagel IC, Linthorst GE, Wanders RJ, Engelen M. Adrenoleukodystrophy - neuroendocrine pathogenesis and redefinition of natural history. Nat Rev Endocrinol. 2016;12(10):606-615.
33. Yoon JJ, Yoon TS, Shin BM, Na EH. Factors affecting test results and standardized method in quiet standing balance evaluation. Ann Rehabil Med. 2012;36(1):112-118.
34. Hue O, Simoneau M, Marcotte J, et al. Body weight is a strong predictor of postural stability. Gait Posture. 2007;26(1):32-38.
35. Corriveau H, Hebert R, Prince F, Raiche M. Postural control in the elderly: an analysis of test-retest and interrater reliability of the COP-COM variable. Archives of physical medicine and rehabilitation. 2001;82(1):80-85.
36. Pinsault N, Vuillerme N. Test-retest reliability of centre of foot pressure measures to assess postural control during unperturbed stance. Medical engineering & physics. 2009;31(2):276-286.

III Biochemical studies

6 Biochemical studies in fibroblasts to interpret variants of unknown significance in the *ABCD1* gene

Stephanie I.W. van de Stadt
Petra A.W. Mooyer
Inge M.E. Dijkstra
Conny J.M. Dekker
Divya Vats
Moin Vera
Maura R. Z. Ruzhnikov
Keith van Haren
Nelson Tang
Klaas Koop
Michel A. Willemsen
Joannie Hui
Frédéric M. Vaz
Merel S. Ebberink
Marc Engelen
Stephan Kemp
Sacha Ferdinandusse

Genes 2021;12(12) 1930

ABSTRACT

Due to newborn screening for X-linked adrenoleukodystrophy (ALD), and the use of exome sequencing in clinical practice, the detection of variants of unknown significance (VUS) in the *ABCD1* gene is increasing. In these cases, functional tests in fibroblasts may help to classify a variant as (likely) benign or pathogenic. We sought to establish reference ranges for these tests in ALD patients and control subjects with the aim to help determine the pathogenicity of VUS in *ABCD1*. Fibroblasts from 36 male patients with confirmed ALD, 26 healthy control subjects and 17 individuals without a family history of ALD, an uncertain clinical diagnosis and a VUS identified in *ABCD1* were included. We performed a combination of tests: very long-chain fatty acids (VLCFA) levels, D_3-C22:0 loading test to study VLCFA metabolism and immunoblotting for ALD protein. All ALD patient fibroblasts had elevated VLCFA levels and reduced peroxisomal ß-oxidation capacity (as measured by D_3-C16:0/ D_3-C22:0 ratio in the D_3-C22:0 loading test) compared to control subjects. Of the VUS cases, VLCFA metabolism was not significantly impaired (most test results in the reference range) in 6/17, VLCFA metabolism was significantly impaired (most test results in/near the ALD range) in 9/17 and a definite conclusion could not be drawn in 2/17. Biochemical studies in fibroblasts provided clearly defined reference and disease ranges for VLCFA metabolism. In 15/17 (88%) VUS we were able to classify the variant as likely benign or pathogenic. This is of great clinical importance as new variants will be detected.

INTRODUCTION

The most common peroxisomal disorder, X-linked adrenoleukodystrophy (ALD), is characterized by mutations in the *ABCD1* gene [1,2]. Pathological mutations cause dysfunction of the ALD protein (ALDP) [3], resulting in impaired peroxisomal ß-oxidation of very long-chain fatty acids (VLCFA; ≥C22:0) [4]. As a consequence, VLCFA accumulate in plasma and tissues; primarily the adrenal cortex, brain white matter and spinal cord [2,5]. Established pathogenic variants have no prognostic value with respect to clinical outcome, and even monozygotic twins can have a vastly different disease course [6]. Clinically, all adult male patients and 80% of female patients develop symptoms of a slowly progressive myelopathy [7–9]. Furthermore, male patients – especially <12 years of age – are at risk of developing adrenal insufficiency and/or a progressive leukodystrophy (cerebral ALD) [10–13]. When diagnosed at an early stage, treatment of cerebral ALD is possible with hematopoietic stem-cell transplantation (HCT) [14]. Adrenal insufficiency can be treated with steroid replacement therapy. Due to these clinical implications frequent follow-up is advised for boys and men with ALD [10,15].

The availability of life-saving treatments and better prognosis with early diagnosis provided rational for including ALD in newborn screening (NBS) programs [16,17]. NBS is different from confirmatory diagnostic testing based on clinical suspicion. Due to the very low a priori probability of disease with NBS, even diagnostic tests with very high specificity and sensitivity will result in false-positives and false-negatives [18]. In practice, this means that if NBS is positive, but with a variant of unknown significance (VUS) in *ABCD1*, there is a heightened level of diagnostic uncertainty. Clinical evaluation (which should be normal in a newborn with ALD) and repeat plasma VLCFA or C26:0-lysophosphatidylcholine (C26:0-lysoPC) testing can be helpful, but some uncertainty may remain. Especially in patients without a family history of disease, and if plasma VLCFA levels are elevated between the upper limit of the reference range but below the lower limit of the disease range – here referred to as the "grey zone". In these cases, additional biochemical and functional testing in skin fibroblasts may help to determine the pathogenicity of a VUS. These tests include: 1) measurement of VLCFA levels, 2) D_3-C22:0 loading test (used to measure D_3-C26:0 de novo synthesis and D_3-C22:0 ß-oxidation) [19], and 3) immunoblotting for ALDP. The laboratory Genetic Metabolic Diseases (GMD) at the Amsterdam UMC is the only center worldwide that performs this combination of testing. With the increasing number of patients identified via newborn screening or exome/whole genome sequencing, we receive an increasing amount of skin fibroblasts of individuals with a VUS in *ABCD1*, potentially suffering from ALD, from all over the world. For these tests to have a better predictive value, a well-defined reference and ALD range is crucial, but not yet available.

The aim of this study was to establish the ranges for biochemical and functional tests in fibroblasts in ALD patients and healthy controls to help with the interpretation of results in patients with a VUS in *ABCD1*. To this end, we performed the aforementioned three tests in fibroblasts from control subjects and a large cohort of adult ALD patients. In addition, we included fibroblasts from 17 individuals without a family history of ALD, or with an otherwise uncertain diagnosis, in whom NBS or whole exome sequencing had identified a VUS in *ABCD1*. This study will contribute to a more clear and uniform laboratory diagnostic process for ALD.

MATERIALS AND METHODS

Study design and patient selection (AMC, the Netherlands)

The present study is part of an ongoing observational cohort study on the national history of ALD – called the "Dutch ALD cohort" – performed at the Amsterdam University Medical Centers, location AMC, the national referral center for ALD. Participants visit the hospital yearly for multiple assessments including blood tests and an extensive neurological examination. For this particular cross-sectional study, we included male patients over 16 years of age with confirmed ALD diagnosis (confirmed by elevated VLCFA (C26:0, C26:0/C22:0 and C26:0-lysoPC) and the presence of a pathogenic *ABCD1* mutation (**Table 1**)). Written informed consent was received from each patient. The study protocol was approved by the local Institutional Review Board (METC 2018-013). The fibroblasts of healthy controls subjects were collected for research purposes after informed consent and approval of the local Institutional Review Board.

Clinical assessments of the Dutch ALD cohort

Clinical assessments and skin biopsy took place on the same day. History and neurological examination were performed as described previously [7]. We used the following clinical outcome measures to quantify disease severity: Expanded Disability Status Scale (EDSS), Severity Score system for Progressive Myelopathy (SSPROM), and Timed Up-and-Go (TUG). The EDSS measures neurological disability and ranges from 0 (no disability) to 10 (death) [20]. The SSPROM scores symptoms of myelopathy and ranges from 0 to 100, with lower scores indicating a higher degree of impairment [21]. TUG measures the time to get up from a chair, walk 3m, walk back and sit down again [22].

Table 1. ABCD1 variants, the effect on ALDP expression and VLCFA levels in fibroblasts of the ALD patients included in the study.

ID	ABCD1 variant	Consequence	ALDP expression	C26:0	C26:0/C22:0
ALD022	c.1A>G	p.Met1Val	Not detectable	0.89	0.37
ALD030	c.1A>G	p.Met1Val	Not detectable	1.06	0.42
ALD043	c.1A>G	p.Met1Val	Not detectable	1.15	0.31
ALD062	c.1A>G	p.Met1Val	Not detectable	1.10	0.62
ALD063	c.1A>G	p.Met1Val	Not detectable	1.03	0.58
ALD064	c.1A>G	p.Met1Val	Not detectable	0.89	0.21
ALD031	c.220C>T	p.Arg74Trp	Not detectable	0.81	0.30
ALD056	c.411G>T	p.Trp137Cys	Not detectable	0.94	0.40
ALD034	c.446G>A	p.Ser149Asn	Detectable	1.08	0.37
ALD222	c.446G>A	p.Ser149Asn	Detectable	1.04	0.49
ALD003	c.529C>T	p.Gln177*	Not detectable	1.15	0.25
ALD055	c.543C>A	p.Tyr181*	Not detectable	1.01	0.39
ALD020	c.659T>C	p.Leu220Pro	Reduced	1.41	0.32
ALD045	c.734C>A	p.Ala245Asp	Detectable	1.02	0.49
ALD017	c.832G>T	p.Glu278*	Not detectable	2.00	0.34
ALD228	c.874_76del	p.Glu292del	Not detectable	1.07	0.50
ALD058	c.892G>A	p.Gly298Ser	Detectable	1.17	0.43
ALD059	c.892G>A	p.Gly298Ser	Detectable	1.11	0.26
ALD081	c.892G>A	p.Gly298Ser	Detectable	0.91	0.81
ALD001	c.901-5C>A	p.Val301fs*?	Not detectable	1.86	0.43
ALD024	c.1166G>A	p.Arg389His	Reduced	0.97	0.38
ALD202	c.1166G>A	p.Arg389His	Reduced	1.24	0.33
ALD006	c.1322insA	p.Asp442Glyfs*114	Not detectable	1.31	0.46
ALD011	c.1390C>T	p.Arg464*	Not detectable	1.44	0.25
ALD899	c.1390C>T	p.Arg464*	Not detectable	1.46	0.54
ALD009	c.1415_16delAG	p.Gln472Argfs*83	Not detectable	2.08	0.35
ALD068	c.1488+3A>G	p.Val497fs*?	Not detectable	1.01	0.39
ALD069	c.1488+3A>G	p.Val497fs*?	Not detectable	1.01	0.39
ALD079	c.1846G>A	p.Ala616Thr	Not detectable	1.46	0.42
ALD025	c.1866-10G>A	p.Pro623fs*?	Not detectable	1.02	0.32
ALD048	c.1866-2A>T	p.Pro623fs*?	Not detectable	2.05	0.47
ALD049	c.1866-2A>T	p.Pro623fs*?	Not detectable	1.69	0.50
ALD027	c.1899delC	p.Ser633Argfs*3	Not detectable	1.73	0.58
ALD008	c.1961T>C	p.Leu654Pro	Not detectable	1.76	0.51
ALD015	c.1961T>C	p.Leu654Pro	Not detectable	0.94	0.40
ALD019	c.1970delTCA	p.Ile657del	Not detectable	1.13	0.38

Reference ranges in fibroblasts for control subjects C26:0 (0.18 - 0.39 nmol/mg protein) and C26:0/C22:0 ratio (0.03 - 0.10).

ABCD1 VUS fibroblasts

Fibroblasts from 17 individuals without a family history of ALD, but with a VUS in *ABCD1* were sent to our laboratory for diagnostic testing of VLCFA metabolism from different (inter)national laboratories. Two of the *ABCD1* VUS in this cohort were eventually reported as "likely pathogenic" [23,24]. In this paper we name all (inter)national received fibroblasts 'VUS', as they were all initially reported as a VUS at the time of diagnostic testing. For all individuals, clinical information, family history and follow-up biochemical results were obtained.

Biochemical and functional tests of VLCFA metabolism

Fibroblasts were cultured in parallel in Ham's F-10 Medium supplemented with 10% fetal bovine serum (Invitrogen, Carlsbad, CA), 25 mM HEPES, 100 U/mL penicillin, 100 µg/mL streptomycin and 250 µg/mL amphotericin in a humidified atmosphere of 5% CO2 at 37°C.

Total levels of VLCFA (C22:0, C24:0 and C26:0) in fibroblast homogenates were measured using gas chromatography-mass spectrometry essentially as described for plasma [25], but with sample preparation described in Dacremont et al [26].

The D_3-C22:0 loading test was performed essentially as described in van de Beek et al [19]. In short, cultured skin fibroblasts were incubated for three days with 30 µM D_3-C22:0 followed by fatty acid analysis using electrospray ionization mass spectrometry [27]. The D_3-C16:0/D_3-C22:0 ratio, which is a measure for peroxisomal ß-oxidation capacity, and D_3-C26:0 levels, which reflects de novo C26:0 synthesis, were calculated. In addition, the peroxisomal ß-oxidation activity is expressed as a percentage of the mean activity in the control cells analyzed in the same experiment. All cell lines were analyzed in two independent experiments (experimental replicates) and the measurements within the experiment were performed in duplicate (technical duplicates). The mean value of the measurements was used for analysis.

For immunoblotting of ALDP cells were harvested by trypsinization and homogenized by sonication in phosphate buffered saline. Homogenates were diluted in sample buffer before 10-20 µg of total protein was loaded on to an SDS/10% polyacrylamide gel. Proteins were transferred on to nitrocellulose by semi-dry blotting, blocked with 4% normal goat serum/PBS/0.1% Tween and probed with the primary monoclonal antibody against human ALDP (ALD-1D6-As, Euromedex or 197013, Abcam). IRDYE 800CW (LICOR Biosciences) goat anti-mouse IgG or IRDYE 800CW (LICOR Biosciences) goat anti-rabbit IgG were used as a secondary antibody. Visualization of the signal was done with the Odyssey IR imaging system (LI-COR Biosciences) [28].

Statistical analysis

Data were summarized as means ± standard deviations (SD) or medians with ranges, depending on distribution of the data. Scatter dot plots were used for visualization of results for the three different groups: control cell lines, VUS cases and ALD patients. Additionally, we described the ranges for ALD patients and control subjects, defined as the minimum and maximum value per group. The grey zone was defined as the area between the upper/lower limit of the ALD values and the upper/lower limit of the control cell lines. Correlations between clinical measures and laboratory results were calculated with Spearmans' Rho correlation coefficient. P-values lower than 0.05 were considered statistically significant. GraphPad Prism 8.3.0 and IBM SPSS Statistics Version 26 were used for data analysis.

RESULTS

Patient characteristics

Thirty-six ALD patients were included for analysis. The patient characteristics are described in **Table 1**. Clinical characteristics are described in **Table 2**. In summary, scores on clinical measures indicated moderate disease severity. Mean age of the patients was 41.8 ± 17.2 years.

Table 2. Clinical characteristics of ALD patients.

Clinical characteristics	ALD patients (n=36)
Age (yr)	41.8 ± 17.2
Body weight (kg)	80.4 ± 12.2
Adrenal insufficiency, n (%)	23 (64)
EDSS	3.0 (0.0-6.5)
SSPROM	89 (61.5-100)
TUG (s)	6.1 (2.9-18.6)

Values are displayed as median (range) or mean ± SD. EDSS, Expanded Disability Status Scale; SSPROM, Severity Scoring system for Progressive Myelopathy; 6MWT, 6-minute walk test; TUG, Timed Up-and-Go

We included 17 individuals with a VUS (labeled VUS01 – VUS17) in *ABCD1* from 5 different centers. VUS01 and VUS09 have the same variant (p.Lys533Gln), but came from different centers. VUS03 and VUS08 are two siblings. All VUS were detected via newborn/family screening or WES, except for one individual who presented with a decline in cognitive and behavioral function. None of the individuals had symptoms of ALD and none had a family history of ALD. Median age of the VUS group was 1.0 years (range 2 months – 34 years) (**Table 3**).

Table 3. Characteristics of individuals with a VUS in ABCD1.

ID	ABCD1 Variant	Consequence	Method of detection	Age	ALD symptoms
VUS01	c.1597A>C	p.Lys533Gln[b]	NBS	11 months	None
VUS02	c.1448C>T	p.Thr483Met	NBS	12 months	None
VUS03[a]	c.1828A>G	p.Lys610Glu	NBS	24 months	None
VUS04	c.1696A>G	p.Met566Val	NBS	5 months	None
VUS05	c.2134C>T	p.Arg712Cys	NBS	6 months	None
VUS06	c.566G>A	p.Arg189Gln	NBS	5 months	None
VUS07	c.895C>T	p.His299Tyr	NBS	2 years	None
VUS08[a]	c.1828A>G	p.Lys610Glu	Extended family screening	4 years	None
VUS09	c.1597A>C	p.Lys533Gln[b]	NBS	2 months	None
VUS10	c.1000C>T	p.Leu334Phe	NBS	3 years	None
VUS11	c.1979G>A	p.Arg660Gln[b]	WES	5 years	None
VUS12	c.896A>G	p.His299Arg	Decline in cognitive function	13 years	None
VUS13	c.1966_1967dup	p.Ile657Profs*35[c]	NBS	2 months	None
VUS14	c.970C>T	p.Arg324Cys	NBS	2 months	None
VUS15	c.1900G>A	p.Ala643Thr	Family screening	34 years	None
VUS16	c.1438C>A	p.Pro480Thr	Family screening	9 years	None
VUS17	c.574A>G	p.Asn192Asp	NBS	2 months	None

a Siblings
b Mutation reported as likely pathogenic
c Atypical zygosity
NBS, Newborn Screening; WES, Whole Exome Sequencing

VLCFA levels in fibroblasts

All ALD patient fibroblasts showed elevated levels of C26:0 (mean ± SD 1.25 ± 0.36 versus 0.29 ± 0.06 nmol/mg protein) when compared to the control cells (**Figure 1A**). In addition, the C26:0/C22:0 ratios were elevated in fibroblasts of all ALD patients compared to the control cells (**Fig. 1B**).

For the VUS cases, C26:0 levels were within reference range (0.18 – 0.39 nmol/mg protein) in 3 VUS (VUS 05,12,13) and elevated within the grey zone or ALD range in the remaining 14 (**Figure 1A** and **Table 4**). In addition, C26:0/C22:0 ratios were within reference range (0.03 – 0.10) in 2 VUS (VUS 05, 07) and elevated in all other 15 (**Figure 1B** and **Table 4**).

D_3-C22:0 loading test

With the D_3-C22:0 loading test the metabolism of D_3-C22:0 in living cells can be followed, which is either elongated to D_3-C26:0 or ß-oxidized to D_3-C16:0. Hence, the ratio D_3-C16:0/ D_3-C22:0 is a measure for peroxisomal ß-oxidation capacity. In all ALD patient fibroblasts the ratio of D_3-C16:0/ D_3-C22:0 was reduced compared to the ratio in control cells: the mean (± SD) ratio in control cells was 1.55 ± 0.29 (range 0.88 – 2.00) and in ALD cells

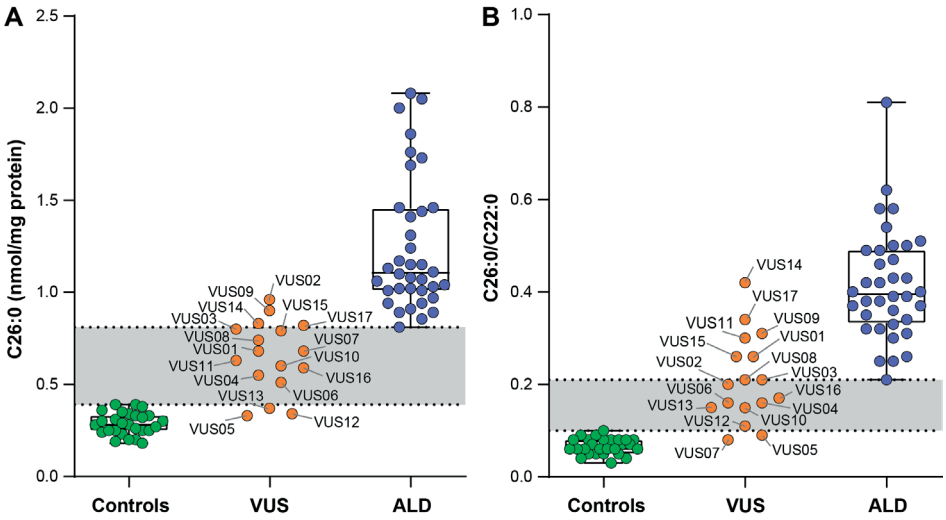

Figure 1. C26:0 levels (A) and C26:0/C22:0 ratios (B) analyzed using gas chromatography. Scatter dot plots show values for fibroblasts of control subjects (green circles); fibroblasts of individuals with a VUS in ABCD1 (orange circles) and fibroblasts of ALD patients (blue circles). The VUS fibroblasts are labelled by ID. Both C26:0 levels and C26:0/C22:0 ratios are elevated in ALD fibroblasts compared to control cells.

0.28 ± 0.06 (range 0.15 – 0.46) (**Figure 2A**). ALD fibroblasts had a median peroxisomal ß-oxidation activity of 17% of controls measured in the same experiment (range 12 – 26%) (**Table 4**). Furthermore, chain elongation from D_3-C22:0 to D_3-C26:0 was increased in ALD fibroblasts: mean (± SD) D_3-C26:0 in control cells was 0.27 ± 0.09 (range 0.15 – 0.51) and in ALD fibroblasts 2.19 ± 0.67 (range 1.00 – 3.69) (**Figure 2B** and **Table 4**).

In the VUS fibroblasts the D_3-C16:0/ D_3-C22:0 ratio was reduced and within ALD range (0.15 – 0.46) in 7 (VUS 01,02,03,04,05,15,17), reduced but in the grey zone (0.47 – 0.87) in 4 (VUS 06,08,09,14) and within reference range (0.88 – 2.00) in 6 (VUS 07,10,11,12,13,16) (**Figure 2A** and **Table 4**). Peroxisomal ß-oxidation activity expressed as % of controls within the same experiments was reduced and within ALD range (12 - 26%) in 7 (VUS 01,02,03,04,14,15,17), reduced but in the grey zone (26% - 56%) in 4 (VUS 05,06,08,09) and within reference range in 6 (VUS 07,10,11,12,13,16) (**Table 4**). Chain elongation to D_3-C26:0 was increased and within ALD range (1.00 – 3.69) in 11 (VUS 01,02,03,04,05,06, 08,09,14,15,17), increased but in the grey zone (0.52 – 0.99) in 5 (VUS 07,10,11,12,13) and within reference range (0.15 – 0.51) in 1 (VUS16) (**Figure 2B** and **Table 4**). The ALD and reference ranges for VLCFA metabolites and D_3-C22:0 loading test in fibroblasts of this cohort are described in **Table 4**.

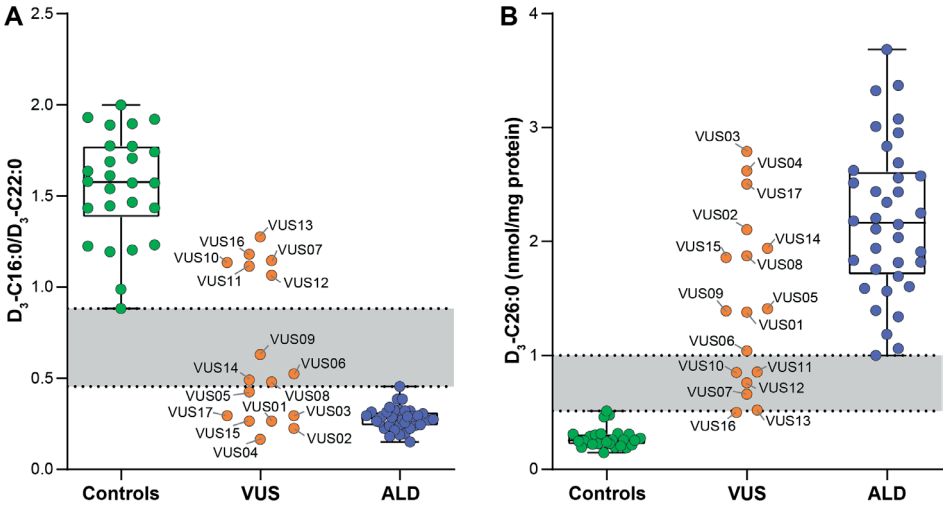

Figure 2. Results of the D3-C22:0 loading tests in fibroblasts of control subjects (green circles); fibroblasts of individuals with a VUS in ABCD1 (orange circles) and fibroblasts of ALD patients (blue circles). The VUS fibroblasts are labelled by ID. A) D3-C16:0/D3-C22:0 ratios, a measure of peroxisomal ß-oxidation capacity, are reduced in ALD fibroblasts compared to control cells. B) D3-C26:0 levels, reflecting chain-elongation, are elevated in ALD fibroblasts compared to the control cells.

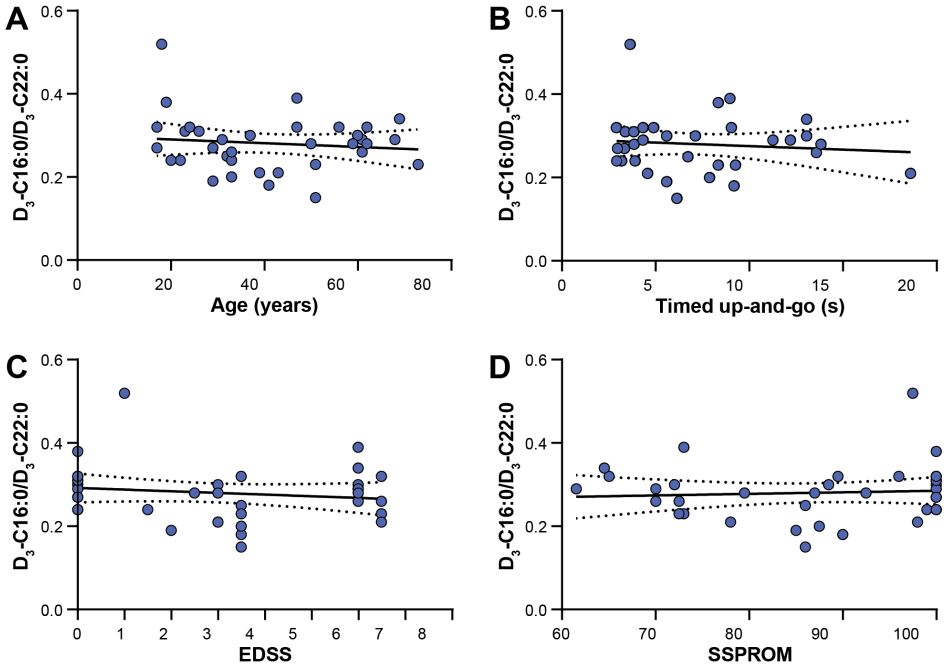

Figure 3. Scatter dot plots show the absence of correlations between clinical characteristics and residual peroxisomal ß-oxidation capacity (D3-C16:0/D3-C22:0 ratio). Lines represent simple linear regression lines with the 95% confidence interval. A) Age, correlation coefficient -0.125, p=0.467; B) Timed Up-and-Go, correlation coefficient -0.092, p=0.61; C) EDSS (Expanded Disability Status Scale), correlation coefficient -0.173, p=0.314; D) SSPROM (Severity Score system for Progressive Myelopathy), correlation coefficient 0.197, p=0.249.

Table 4: VLCFA levels and D3-C22:0 loading test results of VUS individuals compared to ALD patients and control subjects

Test		Reference range	Grey zone	ALD range
VLCFA levels	C26:0 (nmol/mg protein)	0.18 - 0.39	0.40 - 0.80	0.81 - 2.08
	C26:0/C22:0	0.03 - 0.10	0.11 - 0.20	0.21 - 0.81
D_3-C22:0 loading test	D_3-C16:0 (nmol/mg protein)	15.9 - 31.7	12.6 - 15.8	5.9 - 12.5
	D_3-C26:0 (nmol/mg protein)	0.15 - 0.51	0.52 - 0.99	1.00 - 3.69
	D_3-C16:0/D_3-C22:0	0.88 - 2.00	0.47 - 0.87	0.15 - 0.46
	% of control cells	>57	27 - 56	12 - 26

	VUS17	VUS14	VUS02	VUS03°	VUS01*	VUS04	VUS15	VUS09*	VUS08°	VUS05	VUS06	VUS07	VUS10	VUS11	VUS12	VUS13	VUS16
C26:0	0.82	0.83	0.96	0.80	0.68	0.55	0.79	0.9	0.74	0.33	0.51	0.68	0.60	0.63	0.34	0.37	0.56
C26:0/C22:0	0.34	0.42	0.20	0.21	0.26	0.16	0.26	0.31	0.21	0.09	0.17	0.08	0.16	0.30	0.11	0.15	0.18
D_3-C16:0	5.5	7.1	6.2	5.6	4.8	3.2	7.4	12.8	9.5	9.8	9.3	14.3	17.0	17.0	20.8	23.0	19.1
D_3-C26:0	2.51	1.94	2.11	2.79	1.38	2.62	1.86	1.39	1.88	1.41	1.04	0.66	0.85	0.86	0.76	0.52	0.50
D_3-C16:0/D_3-C22:0	0.29	0.49	0.23	0.30	0.27	0.17	0.27	0.63	0.48	0.43	0.53	1.15	1.14	1.12	1.07	1.28	1.18
% of control cells	13	25	17	19	23	14	18	34	34	32	43	67	57	59	107	72	61
Immunoblot	positive	positive	reduced	positive	negative	reduced	positive	negative	positive	positive	positive	positive	positive	positive	positive	positive	ND
VLCFA elevated at follow-up	Yes	Yes	Yes	Yes	ND	Yes	Yes	Yes	No	No	No	No	No	No	No	No	No

Within ALD range
Within reference range
Grey zone

* Same variant

° Siblings

ND = no data

ALDP Immunoblot

In 27 out of 36 ALD patients (75%) immunoblotting for the ALD protein was negative, indicating that the variant in *ABCD1* resulted in no detectable ALD protein (**Table 1**). In the VUS group immunoblotting was negative in two out of 17 (12%): VUS01 and VUS09, which have the same variant: p.Lys533Gln. In all other cases, ALDP protein was detectable, although the amount was reduced compared to control levels in two (VUS 02,04) (**Table 4**).

Clinical correlations

For the 36 ALD patients, there were no associations (correlation coefficient ≤ 0.3 and p-value > 0.05) between measures for disease severity (Expanded Disability Status Scale (EDSS), Severity Score system for Progressive Myelopathy (SSPROM), and Timed Up-and-Go (TUG)) or age and residual peroxisomal ß-oxidation capacity (D_3-C16:0/ D_3-C22:0 ratio) (**Figure 3**).

DISCUSSION

This study shows that biochemical and functional studies in fibroblasts provide a clear defined range of VLCFA levels and metabolism in cell lines from ALD patients and control subjects. This helps to classify variants in the *ABCD1* gene as (likely) pathogenic or benign. A combination of all included tests (VLCFA measurement, D_3-C22:0 loading test and immunoblotting for ALDP) and follow-up measurements, enabled us to make ALD diagnosis unlikely or likely in 15/17 VUS (88%) (see **Table 4**).

In six out of 17 VUS (VUS 07,10,11,12,13,16) we concluded that the *ABCD1* variant is likely benign and an ALD diagnosis is unlikely. From these six VUS three (VUS 07,12,13) had C26:0 levels or C26:0/C22:0 ratios within the reference range, the other three VUS had results within the grey zone. Furthermore, the D_3-C26:0 levels were only mildly elevated (within the grey zone for all but one (VUS16, with normal levels)) and the D_3-C16:0/ D_3-C22:0 ratios were within reference range for all. The peroxisomal ß-oxidation activity as percentage of control cells was ≥57% (range 57 – 107%) and ALDP was present on immunoblot in all VUS individuals (and not performed in one: VUS16). Hence, we can conclude that these six *ABCD1* variants cause only very minor impairment of VLCFA metabolism. In all six VUS, VLCFA levels were normalized at follow-up, with exception of VUS13 who only had a slightly elevated C26:0/C22:0 ratio. This strengthens our conclusion that these individuals are unlikely to develop clinical manifestations of ALD. However, one *ABCD1* variant (VUS11; c.1979G>A, p.Arg660Gln) has been previously reported as pathogenic in two patients with cerebral ALD with clearly elevated plasma VLCFA levels [24] and Western blotting showed absence of ALDP in peripheral blood mononuclear cells from these

patients [29]. In our cohort the p.Arg660Gln was an incidental finding in a 5-year old boy with another unrelated genetic condition. Because p.Arg660Gln was previously reported as pathogenic in the medical literature, there was uncertainty regarding the clinical diagnosis. In this boy (VUS11), however, repeat measurements consistently showed normal plasma VLCFA levels. In order to help clarify this puzzling finding we were asked to perform functional studies in the patients' fibroblasts. Interestingly, our results are not in line with the earlier reports as immunoblotting for ALDP in this individual (VUS11) was positive. Moreover, peroxisomal ß-oxidation was 59% of control cells, and the D_3-C16:0/ D_3-C22:0 ratio was 1.12 which is within reference range (0.88 – 2.00). We have no definitive explanation for the discrepancy between our findings and the earlier reports and it is puzzling why p.Arg660Gln results in non-detectable ALDP in one study and normal ALDP expression in our study. Interestingly, the 2 ALD patients reported by Shukla et al [24] both had additional synonymous variants in exon 9 (c.1899C>T (p.Ser633Ser) and c.1950G>A (p.Ala650Ala)). Synonymous variants in protein-coding regions are considered neutral for protein function, as they synonymously exchange only codons, but not the encoded amino acids. The "ALD Mutation Database" lists 120 synonymous variants in *ABCD1* (https://adrenoleukodystrophy.info/mutations-and-variants-in-abcd1). Although the effect of synonymous variants in *ABCD1* has not been investigated we cannot rule out that they may affect mRNA stability and ALDP expression as has been described for other proteins [30]. It cannot be excluded that c.1899C>T (p.Ser633Ser) and/or c.1950G>A (p.Ala650Ala) aggravate the deleterious effect of p.Arg660Gln on ALDP expression or stability. Therefore, the presence or absence of such a functional synonymous variant may determine the pathogenic outcome of a missense variant. Based on our extensive functional analyses we conclude this p.Arg660Gln variant as likely benign.

In nine out of 17 VUS (VUS 01,02,03,04,08,09,14,15,17) representing 7 different *ABCD1* variants (VUS03-VUS08 and VUS01-VUS09 carry the same variant), we concluded that the *ABCD1* variant is likely pathogenic and an ALD diagnosis is likely. All of these VUS had elevated C26:0 levels and C26:0/C22:0 ratios (within ALD range or grey zone). Results of the D_3-C22:0 loading test were all within or very near the ALD range, with peroxisomal ß-oxidation activity as percentage of control cells ≤34% (range 13 – 34%). Immunoblotting for ALDP was negative in two (VUS 01,09), reduced in two (VUS 02,04) and positive in the remaining five VUS. These combined functional and ALDP expression data indicate that p.Lys533Gln (VUS 01,09), p.Thr483Met (VUS02) and p.Met566Val (VUS04) affect protein folding and stability resulting in no detectable or reduced levels of ALDP, whereas p.Lys610Glu (VUS 03,08), p.Arg324Cys (VUS14), p.Ala643Thr (VUS15) and p.Asn192Asp (VUS17) affect amino acid residues that are important for ALDP function. Furthermore, plasma VLCFA levels were still elevated at follow-up in seven out of nine VUS, in one (VUS01) these results were not yet available. For VUS08 and VUS09 results of the D_3-C22:0

loading test were within the grey zone, albeit close to the ALD range (peroxisomal ß-oxidation activity of 34%). However, for VUS01 – with the same *ABCD1* variant as VUS09 – and VUS03 – who is a sibling (with the same *ABCD1* variant) of VUS08 – results were well within ALD range. Based on these combined results, we conclude that peroxisomal ß-oxidation activity as percentage of control cells of 34% or less should be considered as highly suspicious for ALD, even though the established ALD range in the studied cohort was 12 - 26%.

Of the two remaining VUS (05,06) VUS05 had a peroxisomal ß-oxidation activity of 32%. However, VLCFA analysis in fibroblasts was repeatedly normal, ALDP was normally expressed and plasma VLCFA was normal at follow-up. For VUS06 almost all results were within or close to the grey zone. Hence, we were unable to classify the *ABCD1* variants for VUS05 and VUS06 with certainty. As more cell lines are analyzed, and remaining VUS are classified also based on long-term follow-up, the established ranges might need to be adjusted. Currently it is not known if individuals with peroxisomal ß-oxidation activity within the grey zone will remain healthy or develop symptoms late in life. For instance, it is conceivable that an individual with slightly reduced ß-oxidation activity and slightly elevated VLCFA levels develops symptoms, for example a peripheral neuropathy, in (very late) adulthood. Therefore, it can be considered to include these patients in follow-up care, albeit with a low frequency, to monitor if or when symptoms will occur.

The lack of correlation between clinical disability and D_3-C16:0/ D_3-C22:0 ratio in fibroblasts indicates that residual ß-oxidation capacity has no effect on disease severity in ALD patients. Accordingly, one of our most severely affected patients – a 62-year-old male with EDSS of 6.5 – has a D_3-C16:0/ D_3-C22:0 ratio of 0.32, which is relatively high for an ALD patient. These findings agree with previous research, in which a correlation between VLCFA in plasma and disease severity was not found [31,32]. A certain threshold of accumulated VLCFA may need to be crossed in order to cause symptoms of ALD, but variation above this threshold is not of clinical importance. Furthermore, it is conceivable that metabolic studies in skin fibroblasts are very useful for confirming the diagnosis, but that these parameters do not reflect VLCFA metabolism in the central nervous system.

Our results should be interpreted with some caution. First, we defined reference and ALD ranges as the minimum and maximum value per group. We chose these definitions instead of the mean +/- 2SD, because otherwise ranges for the ALD and healthy control group would overlap. Moreover, not all test results followed a normal distribution and we did not have sufficient statistical power to establish the ranges as mean +/- 2SD. However, we think both groups are of sufficient size, considering the rareness of ALD, to determine the ranges as min – max, especially since we show a clear separation between both groups with

sometimes quite large grey zones in between. Furthermore, for the included VUS cases a definite clinical diagnosis may not yet be possible as they are young individuals that could be presymptomatic. Only long term (many years or even decades) follow-up will provide a definitive diagnosis.

We can conclude that in this large cohort of ALD patients and control cell lines we could define clear ranges for VLCFA metabolism in fibroblasts, which helped us classify 88% of the included VUS fibroblasts. We anticipate that expansion of the cohort with additional cell lines from ALD patients will narrow the grey zone and further reduce the number of cases for which a conclusion (likely) pathogenic or (likely) benign cannot be given. The availability of these functional test is of clinical importance as the insecurity of a possible ALD diagnosis is a major burden for patients and their families. With the ongoing expansion of ALD NBS and increase use of whole exome/genome sequencing in the routine diagnostic process additional *ABCD1* variants will be detected. In case this results in the identification of a VUS, the array of functional tests described here will allow the confirmation or rejection of ALD diagnosis with more certainty, and hopefully will result in personalized clinical follow-up.

REFERENCES

1. Mosser, J.; Douar, A.-M.; Sarde, C.-O.; Kioschis, P.; Feil, R.; Moser, H.; Poustka, A.-M.; Mandel, J.-L.; Aubourg, P. Putative X-linked adrenoleukodystrophy gene shares unexpected homology with ABC transporters. Nature 1993, 361, 726–730, doi:10.1038/361726a0.
2. Moser, H.W.; Smith, K.D.; Watkins, P.; Powers, J.; Moser, A.B. X-linked adrenoleukodystrophy. In The metabolic and molecular bases of inherited disease. McGraw Hill. New York 2001, 8, 3257–3301.
3. Mosser, J.; Lutz, Y.; Stoeckel, M.E.; Sarde, C.O.; Kretz, C.; Douar, A.M.; Lopez, J.; Aubourg, P.; Mandel, J.L. The gene responsible for adrenoleukodystrophy encodes a peroxisomal membrane protein. Hum. Mol. Genet. 1994, 3, 265–271, doi:10.1093/hmg/3.2.265.
4. Singh, I.; Moser, A.B.; Moser, H.W.; Kishimoto, Y. Adrenoleukodystrophy: Impaired oxidation of very long chain fatty acids in white blood cells, cultured skin fibroblasts, and amniocytes. Pediatr. Res. 1984, 18, 286–290, doi:10.1203/00006450-198403000-00016.
5. Igarashi, M.; Schaumburg, H.H.; Powers, J.; Kishimoto, Y.; Koilodny, E.; Suzuki, K. Fatty acid abnormality in adrenoleukodystrophy. J. Neurochem. 1976, 26, 851–860, doi:https://doi.org/10.1111/j.1471-4159.1976.tb04461.x-i1.
6. Kemp, S.; Huffnagel, I.C.; Linthorst, G.E.; Wanders, R.J.A.; Engelen, M. Adrenoleukodystrophy - Neuroendocrine pathogenesis and redefinition of natural history. Nat. Rev. Endocrinol. 2016, 12, doi:10.1038/nrendo.2016.90.
7. Huffnagel, I.C.; van Ballegoij, W.J.C.C.; Van Geel, B.M.; Vos, J.M.B.W.B.W.; Kemp, S.; Engelen, M. Progression of myelopathy in males with adrenoleukodystrophy: towards clinical trial readiness. Brain 2019, 142, 334–343, doi:10.1093/brain/awy299.
8. Huffnagel, I.C.; Dijkgraaf, M.G.W.W.; Janssens, G.E.; van Weeghel, M.; Van Geel, B.M.; Poll-The, B.T.; Kemp, S.; Engelen, M. Disease progression in women with X-linked adrenoleukodystrophy is slow. Orphanet J Rare Dis 2019, 14, 30, doi:10.1186/s13023-019-1008-6.
9. Engelen, M.; Barbier, M.; Dijkstra, I.M.E.; Schür, R.; de Bie, R.M.A.; Verhamme, C.; Dijkgraaf, M.G.W.; Aubourg, P.A.; Wanders, R.J.A.; van Geel, B.M.; et al. X-linked adrenoleukodystrophy in women: a cross-sectional cohort study. Brain 2014, 137, 693–706, doi:10.1093/brain/awt361.
10. Engelen, M.; Kemp, S.; de Visser, M.; van Geel, B.M.; Wanders, R.J.; Aubourg, P.; Poll-The, B. X-linked adrenoleukodystrophy (X-ALD): clinical presentation and guidelines for diagnosis, follow-up and management. Orphanet J Rare Dis 2012, 7, 51, doi:10.1186/1750-1172-7-51.
11. De Beer, M.; Engelen, M.; Van Geel, B.M. Frequent occurrence of cerebral demyelination in adrenomyeloneuropathy. Neurology 2014, 83, 2227–2231, doi:10.1212/WNL.0000000000001074.
12. Huffnagel, I.C.; Laheji, F.K.; Aziz-Bose, R.; Tritos, N.A.; Marino, R.; Linthorst, G.E.; Kemp, S.; Engelen, M.; Eichler, F. The Natural History of Adrenal Insufficiency in X-Linked Adrenoleukodystrophy: An International Collaboration. J. Clin. Endocrinol. Metab. 2019, 104, 118–126, doi:10.1210/jc.2018-01307.
13. Dubey, P.; Raymond, G. V.; Moser, A.B.; Kharkar, S.; Bezman, L.; Moser, H.W. Adrenal insufficiency in asymptomatic adrenoleukodystrophy patients identified by very long-chain fatty acid screening. J. Pediatr. 2005, 146, 528–532, doi:10.1016/J.JPEDS.2004.10.067.
14. Miller, W.P.; Rothman, S.M.; Nascene, D.; Kivisto, T.; DeFor, T.E.; Ziegler, R.S.; Eisengart, J.; Leiser, K.; Raymond, G.; Lund, T.C.; et al. Outcomes after allogeneic hematopoietic cell transplantation for

childhood cerebral adrenoleukodystrophy: the largest single-institution cohort report. Blood 2011, 118, 1971 LP – 1978, doi:10.1182/blood-2011-01-329235.

15. Mallack, E.J.; Turk, B.R.; Yan, H.; Price, C.; Demetres, M.; Moser, A.B.; Becker, C.; Hollandsworth, K.; Adang, L.; Vanderver, A.; et al. MRI surveillance of boys with X-linked adrenoleukodystrophy identified by newborn screening: Meta-analysis and consensus guidelines. J. Inherit. Metab. Dis. 2020, doi:10.1002/jimd.12356.
16. Moser, A.B.; Jones, R.O.; Hubbard, W.C.; Tortorelli, S.; Orsini, J.J.; Caggana, M.; Vogel, B.H.; Raymond, G. V Newborn Screening for X-Linked Adrenoleukodystrophy. Int. J. neonatal Screen. 2016, 2, 15, doi:10.3390/ijns2040015.
17. Barendsen, R.W.; Dijkstra, I.M.E.; Visser, W.F.; Alders, M.; Bliek, J.; Boelen, A.; Bouva, M.J.; van der Crabben, S.N.; Elsinghorst, E.; van Gorp, A.G.M.; et al. Adrenoleukodystrophy Newborn Screening in the Netherlands (SCAN Study): The X-Factor. Front. cell Dev. Biol. 2020, 8, 499, doi:10.3389/fcell.2020.00499.
18. Straus, S.; Paul, G.; Richardson, S.W.; Haynes, B.R. Evidence-Based Medicine; 5th ed.; Elsevier, 2018;
19. van de Beek, M.-C.; Dijkstra, I.M.E.; Kemp, S. Method for Measurement of Peroxisomal Very Long-Chain Fatty Acid Beta-Oxidation and De Novo C26:0 Synthesis Activity in Living Cells Using Stable-Isotope Labeled Docosanoic Acid. Methods Mol. Biol. 2017, 1595, 45–54, doi:10.1007/978-1-4939-6937-1_5.
20. Kurtzke, J.F. Rating neurologic impairment in multiple sclerosis. Neurology 1983, 33, 1444 LP – 1444, doi:10.1212/WNL.33.11.1444.
21. Castilhos, R.M.; Blank, D.; Netto, C.B.O.; Souza, C.F.M.; Fernandes, L.N.T.; Schwartz, I.V.D.; Giugliani, R.; Jardim, L.B. Severity score system for progressive myelopathy: development and validation of a new clinical scale. Brazilian J. Med. Biol. Res. 2012, 45, 565–572, doi:10.1590/S0100-879X2012007500072.
22. Podsiadlo, D.; Richardson, S. The Timed "Up & Go": A Test of Basic Functional Mobility for Frail Elderly Persons. J. Am. Geriatr. Soc. 1991, 39, 142–148, doi:10.1111/j.1532-5415.1991.tb01616.x.
23. Wiens, K.; Berry, S.A.; Choi, H.; Gaviglio, A.; Gupta, A.; Hietala, A.; Kenney-Jung, D.; Lund, T.; Miller, W.; Pierpont, E.I.; et al. A report on state-wide implementation of newborn screening for X-linked Adrenoleukodystrophy. Am. J. Med. Genet. A 2019, 179, 1205–1213, doi:10.1002/ajmg.a.61171.
24. Shukla, P.; Gupta, N.; Gulati, S.; Ghosh, M.; Vasisht, S.; Sharma, R.; Gupta, A.K.; Kalra, V.; Kabra, M. Molecular analysis of ABCD1 gene in Indian patients with X-linked Adrenoleukodystrophy. Clin. Chim. Acta 2011, 412, 2289–2295, doi:10.1016/j.cca.2011.08.026.
25. Vreken, P.; van Lint, A.E.; Bootsma, A.H.; Overmars, H.; Wanders, R.J.; van Gennip, A.H. Rapid stable isotope dilution analysis of very-long-chain fatty acids, pristanic acid and phytanic acid using gas chromatography-electron impact mass spectrometry. J. Chromatogr. B. Biomed. Sci. Appl. 1998, 713, 281–287, doi:10.1016/s0378-4347(98)00186-8.
26. Dacremont, G.; Cocquyt, G.; Vincent, G. Measurement of very long-chain fatty acids, phytanic and pristanic acid in plasma and cultured fibroblasts by gas chromatography. J. Inherit. Metab. Dis. 1995, 18, 76–83, doi:10.1007/BF00711430.
27. Valianpour, F.; Selhorst, J.J.M.; Van Lint, L.E.M.; Van Gennip, A.H.; Wanders, R.J.A.; Kemp, S. Analysis of very long-chain fatty acids using electrospray ionization mass spectrometry. Mol. Genet. Metab. 2003, 79, 189–196, doi:10.1016/S1096-7192(03)00098-2.

28. Kemp, S.; Mooyer, P.A.; Bolhuis, P.A.; van Geel, B.M.; Mandel, J.L.; Barth, P.G.; Aubourg, P.; Wanders, R.J. ALDP expression in fibroblasts of patients with X-linked adrenoleukodystrophy. J Inherit Metab Dis 1996, 19, 667–674.
29. Kumar, N.; Taneja, K.K.; Kalra, V.; Behari, M.; Aneja, S.; Bansal, S.K. Genomic Profiling Identifies Novel Mutations and SNPs in ABCD1 Gene: A Molecular, Biochemical and Clinical Analysis of X-ALD Cases in India. PLoS One 2011, 6, e25094.
30. Simhadri, V.L.; Hamasaki-Katagiri, N.; Lin, B.C.; Hunt, R.; Jha, S.; Tseng, S.C.; Wu, A.; Bentley, A.A.; Zichel, R.; Lu, Q.; et al. Single synonymous mutation in factor IX alters protein properties and underlies haemophilia B. J. Med. Genet. 2017, 54, 338–345, doi:10.1136/jmedgenet-2016-104072.
31. Moser, A.B.; Kreiter, N.; Bezman, L.; Lu, S. en; Raymond, G. V.; Naidu, S.; Moser, H.W. Plasma very long chain fatty acids in 3,000 peroxisome disease patients and 29,000 controls. Ann. Neurol. 1999, 45, 100–110, doi:10.1002/1531-8249(199901)45:1.
32. Boles, D.J.; Craft, D.A.; Padgett, D.A.; Loria, R.M.; Rizzo, W.B. Clinical variation in X-linked adrenoleukodystrophy: fatty acid and lipid metabolism in cultured fibroblasts. Biochem. Med. Metab. Biol. 1991, 45, 74–91, doi:10.1016/0885-4505(91)90010-i.

7 Plasma NfL and GFAP as biomarkers of spinal cord degeneration in adrenoleukodystrophy

Wouter J.C. van Ballegoij
Stephanie I.W. van de Stadt
Irene C. Huffnagel
Stephan Kemp
Eline A.J. Willemse
Charlotte E. Teunissen
Marc Engelen

Annals of Clinical and Translational Neurology 2020; 7(11): 2127–2136

ABSTRACT

Objective: to explore the potential of neurofilament light (NfL) and glial fibrillary acidic protein (GFAP) as biomarkers of spinal cord degeneration in adrenoleukodystrophy, as objective treatment-outcome parameters are needed.

Methods: plasma NfL and GFAP levels were measured in 45 male and 47 female ALD patients and compared to a reference cohort of 73 healthy controls. For male patients, cerebrospinal fluid (CSF) samples (n= 33) and 1-year (n= 39) and 2-year (n= 18) follow-up data were also collected. Severity of myelopathy was assessed with clinical parameters: Expanded Disability Status Scale (EDSS), Severity Scoring system for Progressive Myelopathy (SSPROM) and timed up-and-go.

Results: NfL and GFAP levels were higher in male ($p< 0.001$, effect size (partial η^2) NfL= 0.49, GFAP= 0.13) and female ($p< 0.001$, effect size NfL= 0.19, GFAP= 0.23) patients compared to controls; levels were higher in both symptomatic and asymptomatic patients. In male patients, NfL levels were associated with all three clinical parameters of severity of myelopathy (EDSS, SSPOM and timed up-and go), while GFAP in male and NfL and GFAP in female patients were not. Changes in clinical parameters during follow-up did not correlate with (changes in) NfL or GFAP levels. Plasma and CSF NfL were strongly correlated ($r= 0.60$, $p< 0.001$), but plasma and CSF GFAP were not ($r= 0.005$, $p= 0.98$)

Interpretation: our study illustrates the potential of plasma NfL as biomarker of spinal cord degeneration in adrenoleukodystrophy, which was superior to plasma GFAP in our cohort.

INTRODUCTION

Progressive myelopathy affects all men and over 80% of women with X-linked adrenoleukodystrophy (ALD). ALD is a genetic neurometabolic disorder caused by mutations in the *ABCD1*-gene leading to a defect in the degradation of very long-chain fatty acids (VLCFA).[3, 4] VLCFA accumulate in plasma and tissues, including the spinal cord, adrenal cortex and brain white matter.[5] The pathology of myelopathy in ALD is characterized by axonal degeneration of the long ascending and descending tracts of the spinal cord.[6, 7] Clinically, it presents in adulthood as a progressive gait disorder due to a spastic paraparesis and sensory ataxia; patients also report sphincter disturbance with urinary and fecal urgency and incontinence.[1, 8] Male patients are affected more severely and at a younger age than female patients.[2, 9] In addition to myelopathy, male patients can develop adrenocortical insufficiency and progressive inflammatory white matter lesions (cerebral ALD).[10, 11] Treatment of the myelopathy of ALD is currently supportive only, but disease modifying therapies are under development. Tools to evaluate the efficacy of these treatments in clinical trials are lacking: molecular biomarkers are not available and clinical parameters of disease severity and progression have important limitations.[1] Therefore, objective and easily accessible treatment-outcome parameters for myelopathy in ALD are needed.

Neurofilament light (NfL) and glial fibrillary acidic protein (GFAP) are cytoskeletal proteins of neurons and astrocytes respectively, that are released in the cerebrospinal fluid (CSF) and blood upon damage of these cells. Until recently, these biomarkers could only be measured in CSF because the assays were not sensitive enough for detection of the much lower concentrations in plasma, but the introduction of the single-molecule array (SiMoA) assay has enabled reliable quantification in blood samples as well.[12-15] NfL and GFAP have been shown to serve as biomarkers of nerve tissue damage in a range of neuro-inflammatory and neurodegenerative diseases.[16-18] Among these are diseases with degeneration of the long tracts of the spinal cord, such as hereditary spastic paraplegia (HSP) and amyotrophic lateral sclerosis (ALS).[19, 20] As myelopathy in ALD is characterized by degeneration of the corticospinal tracts and dorsal columns of the spinal cord, we hypothesized that NfL and GFAP could also reflect spinal cord degeneration in ALD. To evaluate this, we measured plasma NfL and GFAP levels in a cohort of male and female ALD patients using SiMoA assay. We compared levels of patients to healthy controls, determined the association with clinical parameters of disease severity and evaluated changes over 2-year follow-up. We hypothesized that NfL would perform better as biomarker than GFAP, because axonal (and not glial) degeneration is the pathological hallmark of myelopathy in ALD.[21] Also, because myelopathy in women with ALD has a milder disease course, we hypothesized that NfL and GFAP levels would be lower and associations with disease severity weaker in female compared to male patients.

METHODS

Study design and participants

This study consists of data from two observational cohort studies performed at the Amsterdam University Medical Centers: a prospective observational cohort study in male ALD patients and a cross-sectional study in female ALD patients. Clinical data of these studies have been previously reported.[1, 2, 9]

Male ALD patients >16 years of age were prospectively recruited between September 2015 and July 2019. Study visits were embedded in routine clinical care, consisting of a yearly hospital visit with neurological examination and cerebral MR imaging. Participation in the study involved a more extensive neurological examination, additional blood sampling and optional CSF sampling (lumbar puncture). Female patients (who are not routinely followed for patient care because of the milder disease course without treatable complications like adrenocortical dysfunction) were previously evaluated for a baseline visit between 2008 and 2010; blood samples of this baseline visit were not available. For the current study, all women were invited for a follow-up visit performed between June 2015 and March 2017. To expand the cohort, women with ALD who were diagnosed at our center after the baseline visit were also recruited. Participation consisted of one hospital visit with venous blood sampling and neurological examination. Patients with active or arrested cerebral ALD (defined as gadolinium-enhancing or non-enhancing cerebral white matter lesions, respectively) or a history of a neurodegenerative or neuro-inflammatory disease (other than ALD) were excluded from participation. The local Institutional Review Board approved the study protocols (METC 2014_302, METC2015_079, METC 2018_310) and all participants provided written informed consent.

Reference values for both NfL and GFAP were obtained from an in-house reference cohort that consisted of healthy volunteers between 18 and 75 years old, who were recruited through public advertising and provided written informed consent. For CSF, only reference values for NfL (and not GFAP) were available.

Assessment of myelopathy

Male and female patients underwent a detailed neurological history and examination to assess myelopathy, as previously described.[1, 9] They were scored as symptomatic if they had both signs and symptoms of myelopathy, otherwise they were scored as asymptomatic. Clinical outcome measures used to quantify myelopathy were the Expanded Disability Status Scale (EDSS), Severity Scoring system for Progressive Myelopathy (SSPROM) and timed up-and-go. The EDSS measures neurological disability ranging from 0 (no disability) to 10 (death).[22] SSPROM measures severity of myelopathy ranging from 0 to 100, with lower

scores indicating a higher degree of impairment.[23, 24] The timed up-and-go is used to assess walking function by recording the time that the patient needs to get up from an armchair, walk 3 meters, turn around, walk back and sit down again.[25, 26]

Sample processing and laboratory methods

Blood was collected in 4 mL EDTA tubes and processed within 2 hours at the biobank of Amsterdam UMC. Samples were centrifuged for 10 min at 2000g and plasma was stored at -80 °C in 0.5 mL volumes until further use. CSF was collected in 10 mL polypropylene tubes and centrifuged for 10 minutes at 1800 g, supernatant was aliquotted in 0.5 mL volumes and stored at -80 °C until further use.

Measurements of NfL and GFAP in plasma and CSF were performed in the Neurochemistry laboratory of the Amsterdam UMC location VUmc using the single molecule array (SiMoA) technology (Quanterix Corp., MA USA). Analyses were performed using the NF-light Kit (Quanterix) and GFAP Discovery Kit (Quanterix), run on the SiMoA HD-1 according to the manufacturer's protocols (www.quanterix.com/products-technology/assays). Measurements were performed in duplicate by certified technicians that were blinded to clinical information. The average variation of duplicate measurements was 4.8% for NfL and 3.3% for GFAP.

Statistical analysis

Baseline characteristics were summarized using descriptive statistics. Normality of the data was assessed by visual inspection of the Q-Q plots and Shapiro-Wilk testing. Data of male and female patients were analyzed separately, as they are known to have a different disease course. To determine whether it was also necessary to subdivide the control group based on gender, we assessed if there were differences in NfL and GFAP levels between male and female controls. Because NfL and GFAP levels are strongly age-dependent (both increasing with age), we corrected for differences in age with analysis of covariance (ANCOVA). We assessed if there were differences in NfL and GFAP levels at baseline between 1) patients compared to controls and 2) symptomatic patients, asymptomatic patients and controls. For comparison of three groups, post hoc testing was performed with Bonferroni correction for multiple comparisons. Although NfL and GFAP levels for the control group were not normally distributed (positively skewed), the standardized residuals were normally distributed, thereby not violating the assumptions of the ANCOVA. For group comparisons in females, controls with age <30 years were excluded to better match the patient group, as there were no female patients represented in this age group. We evaluated the association between severity of myelopathy and NfL/GFAP levels using multiple linear regression analysis with both age and clinical parameters of severity of myelopathy as independent variables.

We compared baseline CSF NfL values of patients and controls with correction for age (ANCOVA). We determined the correlation between plasma and CSF levels of NfL and GFAP with Spearman's correlation test (non-normally distributed data). Because of the relatively low number of available CSF samples, we did not perform comparisons between three groups or correlations with disease severity for CSF data.

For the longitudinal data (male patients only), we calculated mean paired changes in clinical parameters of disease severity and NfL/GFAP levels during follow-up for both the total patient group and the symptomatic subgroup; statistical significance of these differences was assessed using paired t-test (normally distributed data) or Wilcoxon signed rank test (non-normally distributed data). We evaluated the association between changes in disease severity and biomarker levels by correlating delta scores of clinical parameters to (delta scores of) NfL/GFAP levels. In addition, to evaluate the variability of NfL and GFAP levels over time, we determined the correlation between biomarker levels of subsequent visit with Spearman's correlation test.

For all statistical tests a significance level of $\alpha = 0.05$ (2-sided) was chosen. Significance levels after Bonferroni corrections were reported separately. IBM SPSS statistics version 26 (IBM Inc.) was used for all statistical analyses.

RESULTS

In total, 185 samples were analyzed: 105 plasma samples from male patients (45 baseline, 60 follow-up), 47 plasma samples from female patients (all baseline) and 33 CSF samples from male patients (20 baseline, 13 follow-up). Seven male patients were excluded because of cerebral ALD and one female patient was excluded because of a history of Parkinson's disease; otherwise there were no exclusions. Clinical characteristics of both the male and female cohort are described in detail elsewhere and are summarized in **Table 1**.[1, 9]

Table 1. Patient baseline characteristics.

	Males (n=45)	Females (n=47)
Age, years	44.0 ± 16.7	54.0 ± 12.4
Symptomatic	32 (71%)	25 (53%)
EDSS	3.5 (2.0-6.0)	3.5 (2.5-4.0)
SSPROM	87.0 (77.0-99.0)	88.0 (83.0-96.0)
Timed up and go, s	5.1 (3.6-9.6)	5.3 (4.3-7.2)

Values are displayed as mean ± SD for normally distributed data and median (interquartile range) for non-normally distributed data.
EDSS, Expanded Disability Status Scale; SSPROM, Severity Scoring system for Progressive Myelopathy.

The control group consisted of 73 healthy subjects: 36 males (mean age 45.9 ± 11.6 years) and 38 females (mean age 42.3 ± 9.8 years). There was no significant difference in plasma NfL (6.9 versus 5.8 pg/ml, p= 0.25) or GFAP (75.2 versus 68.7 pg/ml, p= 0.97) levels between male and female controls after correcting for age. Therefore, we decided not to subdivide the control group based on gender.

Group comparisons

First, we assessed differences in plasma NfL and GFAP levels between patients and controls (**Fig 1**). Mean age of male patients was very similar to the control group (mean difference 0.1 year, p= 0.978), while female patients were significantly older compared to controls (mean difference 6.3 years, p= 0.002). Age was a significant predictor for NfL levels in both the male (p< 0.001, partial η^2 = 0.42) and female (p< 0.001, partial η^2= 0.41) model. For GFAP, the association with age was less strong than for NfL but still significant (male p< 0.001, partial η^2= 0.13; female p< 0.001, partial η^2= 0.34). After adjustment for age, NfL and GFAP levels were significantly higher in male patients than controls (**Fig 1A** and **B**). Similarly, female patients had significantly higher NfL and GFAP levels than controls (**Fig 1C** and **D**).

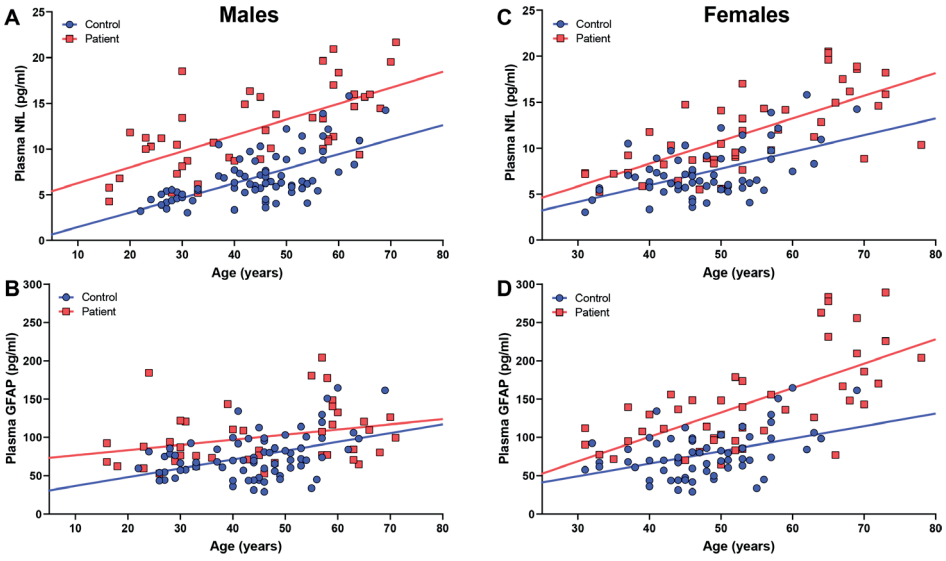

Males	Patient (n=45)	Control (n=74)	p-value	Effect size
Age, years	44.0 ± 16.7	44.1 ± 10.8	0.978	
NfL, pg/ml	11.2 (9.0-15.7)	6.2 (5.2-8.4)	<0.001	0.49
GFAP, pg/ml	87.0 (71.0-120.7)	70.1 (55.6-93.1)	<0.001	0.13

Females	Patient (n=47)	Control (n=61)	p-value	Effect size
Age, years	54.0 ± 12.4	47.7 ± 8.1	0.002	
NfL, pg/ml	10.4 (8.2-14.7)	6.5 (5.6-8.9)	<0.001	0.19
GFAP, pg/ml	136.0 (95.3-173.4)	71.9 (57.4-98.2)	<0.001	0.27

Figure 1. Plasma NfL and GFAP levels in patients versus healthy controls.
Graphs show NfL and GFAP levels plotted against age in male (left panel, A and B) and female (right panel, C and D) patients. Values in the tables below the graphs are the median NfL and GFAP levels per group (IQR); p-values represent the significance level of the difference between groups after correction for age (ANCOVA). Age is displayed as mean ± SD, difference in age were assessed with unpaired t-test. Effect sizes are the partial eta squared values from the ANCOVA models.
GFAP, Glial Fibrillary Acidic Protein; NfL, Neurofilament light.

Second, we compared plasma NfL and GFAP levels between three groups: controls, asymptomatic patients and symptomatic patients (**Table 2**). Asymptomatic patients were significantly younger than symptomatic patients in both the male and female subgroup. For males, after adjustment for age, there was a statistically significant overall difference in NfL ($p< 0.001$, partial $\eta^2= 0.50$) and GFAP ($p= 0.001$, partial $\eta^2= 0.50$) levels between groups. Post hoc comparisons showed that levels were significantly higher in both symptomatic patients (NfL $p< 0.001$, GFAP $p= 0.003$) and asymptomatic patients (NfL $p< 0.001$, GFAP $p= 0.034$) compared to controls, but there was no significant difference between asymptomatic and symptomatic patients. For female patients, there also was a statistically significant overall difference in NfL and GFAP levels between groups (**Table 2**). Similar to male patients, post hoc analysis showed that NfL and GFAP levels were significantly higher in symptomatic (NfL $p< 0.001$, GFAP $p< 0.001$) and asymptomatic (NfL $p= 0.018$, GFAP $p= 0.001$) patients compared to controls, there was no difference between asymptomatic and symptomatic patients.

Table 2. Plasma NfL and GFAP levels in controls, asymptomatic patients and symptomatic patients.

	Control	Asymptomatic	Symptomatic	p-value	Effect size	Post hoc comparisons
Males						
N	74	13	32			
Age, years	44.1 ± 10.8	29.3 ± 13.4	49.9 ± 14.1	<0.001		(C-A, A-S)
NfL, pg/ml	6.2 (5.2-8.4)	8.9 (6.0-11.2)	13.4 (10.2-16.3)	<0.001	0.50	(C-A, C-S)
GFAP, pg/ml	70.1 (55.6-93.1)	76.5 (63.7-93.6)	99.4 (72.7-121.9)	0.001	0.13	(C-A, C-S)
Females						
N	61	22	25			
Age, years	47.7 ± 8.1	45.8 ± 9.7	60.5 ± 10.2	<0.001		(C-S, A-S)
NfL, pg/ml	6.5 (5.6-8.9)	8.9 (7.0-10.3)	14.2 (9.6-17.3)	<0.001	0.22	(C-A, C-S)
GFAP, pg/ml	71.9 (57.4-98.2)	109.6 (84.4-141.7)	148.6 (110.9-217.6)	<0.001	0.28	(C-A, C-S)

Values are displayed as mean ± SD for normally distributed data and median (interquartile range) for non-normally distributed data. Plasma NfL and GFAP levels are the uncorrected medians (not corrected for age). Kruskall-Wallis test was used to assess between-group differences in age. ANCOVA was used to assess between-group differences in NfL and GFAP levels, p-values represent the significance level after correction for age. Post-hoc comparisons indicate which groups significantly differ from each other after Bonferroni correction for multiple comparisons. Effect sizes are the partial eta squared values from the ANCOVA models.
A-S, asymptomatic versus symptomatic; C-A, control versus asymptomatic; C-S, control versus symptomatic; GFAP, Glial Fibrillary Acidic Protein; NfL, neurofilament light.

Association of disease severity with NfL and GFAP levels

We evaluated the association between severity of myelopathy and biomarker levels by performing multiple linear regression analysis with age and 1) EDSS, 2) SSPROM and 3) timed up-and-go as predictors. As expected, age and clinical parameters of severity of myelopathy were correlated (correlation coefficient between 0.48-0.64), but the correlation was below the regularly used cutoff value for collinearity (correlation coefficient >0.8).[27] In male pa-

tients (**Fig 2**), all three models significantly predicted plasma NfL levels. For the first model, both age (B= 0.13, p= 0.001) and EDSS (B= 0.63, p= 0.027) were significant predictors. Similarly, for the second model both age (B= 0.117, p= 0.001) and SSPROM (B= -0.17, p= 0.001) and for the third model both age (B= 0.122, p= 0.002) and Timed up-and-go (B= 0.47, p= 0.009) significantly predicted NfL levels. On the contrary, neither age nor any of the clinical parameters were significant predictors of plasma GFAP levels.

For the female subgroup, age was a significant predictor for NfL and GFAP levels in all three models, but none of the clinical parameters were.

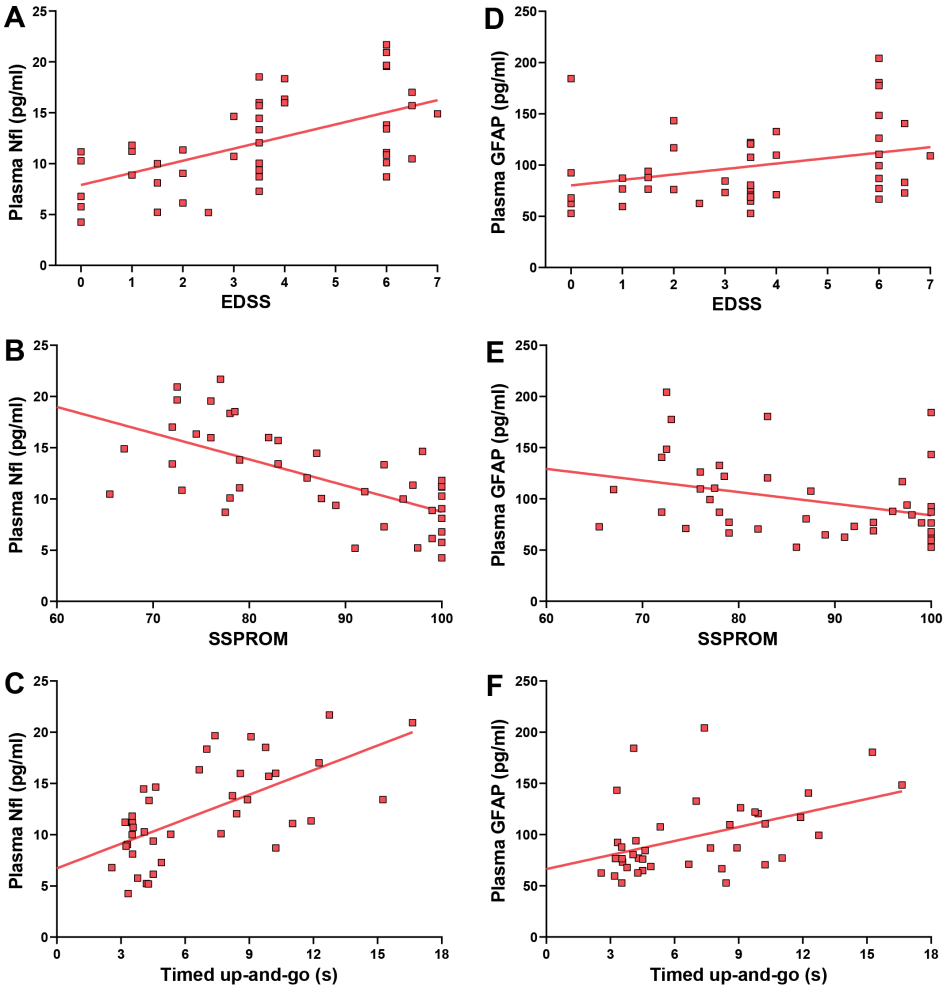

Figure 2. Associations between clinical parameters of severity of myelopathy and plasma NfL levels in male patients. Lines represent simple linear regression lines.
EDSS, Expanded Disability Status Scale; GFAP, Glial Fibrillary Acidic Protein; NfL, Neurofilament light; SSPROM, Severity Scoring system for Progressive Myelopathy

CSF data

Details of CSF data are presented in **Table 3**. CSF NfL levels were significantly higher in patients than controls. There was a strong correlation between CSF and plasma NfL levels (Spearman's rho= 0.60, p< 0.001). Plasma and CSF levels of GFAP were not correlated (Spearman's rho= 0.005, p= 0.98). Unfortunately, CSF GFAP data of healthy controls were not available.

Table 3. Baseline CSF NfL and GFAP levels in patients and controls.

	Patient (n=20)	Control (n=49)	p-value
Age, years	47.5 (30.0-57.0)	54.0 (46.5-60.5)	0.034
Symptomatic	30 (70%)		
EDSS	5.0 (2.0-6.0)		
SSPROM	82.5 (77.6-98.5)		
Timed up and go, s	8.0 (4.3-10.6)		
NfL, pg/ml	752.5 (665.3-1042.1)	642.4 (585.9-743.8)	0.001
GFAP, pg/ml	5156.9 ± 2097.3		

Values are displayed as mean ± SD for normally distributed data and median (interquartile range) for non-normally distributed data. NfL and GFAP levels are the uncorrected medians (not corrected for age). Kruskall-Wallis test was used to assess between-group differences in age. ANCOVA was used to assess between-group differences in NfL levels; the p-values represent the significance level after correction for age. GFAP data for healthy controls were not available.
GFAP, Glial Fibrillary Acidic Protein; CSF, cerebrospinal fluid; EDSS, Expanded Disability Status Scale; NfL, neurofilament light; SSPROM, Severity Scoring system for Progressive Myelopathy.

Longitudinal data

Follow-up samples were available for 39/45 (87%) patients for year 1 and 18/45 (40%) patients for year 2. There was a small increase in the EDSS during follow-up (mean paired change 0.41, p= 0.041), but SSPROM and timed up-and-go did not change (**Supplementary Table 1**). NfL and GFAP levels did not change significantly during follow-up. There were no correlations between changes on clinical parameters and (changes on) NfL/GFAP levels (correlation coefficients <0.3).

Biomarker levels for patients that completed all three visits are represented in **Figure 3**. To evaluate the variability of NfL and GFAP levels over time, we determined the correlation between biomarker levels at subsequent visits. For NfL, levels at baseline and year 1 correlated strongly (Spearman's rho= 0.79, p< 0.001), as did levels at year 1 and year 2 (Spearman's rho= 0.88, p< 0.001). For GFAP, correlations between baseline and year 1 (Spearman's rho=0.75, p< 0.001) and between year 1 and year 2 (Spearman's rho= 0.69, p= 0.002) were also strong, albeit less strong than for NfL.

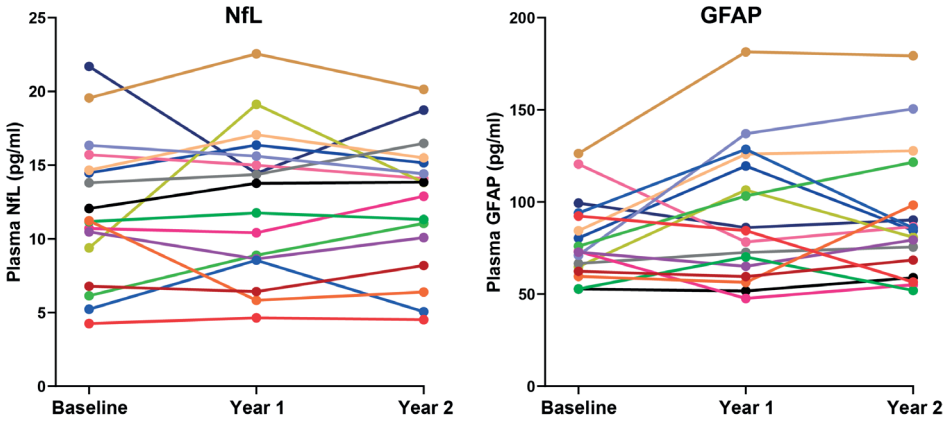

Figure 3. NfL (A) and GFAP (B) levels during follow-up for the 18 male patients that completed all three visits.
GFAP, Glial Fibrillary Acidic Protein; NfL, Neurofilament light.

DISCUSSION

As disease modifying therapies for myelopathy in ALD are under development, there is a need for reliable, observer-independent and easily accessible treatment-outcome parameters. In this explorative study we demonstrate that NfL could serve as a biomarker of spinal cord degeneration in ALD, while GFAP seems less valuable. Both plasma NfL and GFAP levels were significantly elevated in patients compared to healthy controls, but only NfL levels in males were associated with clinical parameters of disease severity. We found no correlations between (changes in) biomarker levels and parameters of disease progression.

We hypothesized that NfL would be a better biomarker for spinal cord degeneration than GFAP, since axonal rather than glial degeneration is the pathological hallmark of myelopathy in ALD.[7] Indeed, data from our study to support NfL as biomarker are much more robust than for GFAP. First, one would expect a biomarker of spinal cord degeneration to be higher in male than female ALD patients, as male patients are more severely affected with an earlier disease onset and faster progression. Group differences in NfL levels were indeed larger for male than female patients (**Fig 1**, **Table 2**). For GFAP, we found exactly the opposite, with larger group differences in female than male patients (**Table 2**). This can be partially explained by the difference in age, as female patients in our study were on average 10 years older than male patients. But even after correction for the difference in age, GFAP levels in female patients were higher, for which we do not have a pathophysiological explanation. Second, NfL levels were associated with each of the three clinical measures of disease severity (with more severely affected patients having higher NfL levels) in males, supporting its role as biomarker of spinal cord degeneration, while these associations were not present for GFAP. Finally, the correlation between CSF and plasma levels of NfL was

strong (correlation coefficient 0.60) and comparable to other studies,[12, 28, 29] while we found no correlation between CSF and plasma levels of GFAP (correlation coefficient 0.005).

There is an important difference between molecular biomarkers such as NfL and GFAP and other (surrogate) outcomes used for myelopathy in ALD. Most outcomes – for example clinical parameters (EDSS, SSPROM, timed walking activities) or imaging biomarkers (spinal cord atrophy, diffusion tensor imaging) – represent disability or accumulated spinal cord damage resulting from years of spinal cord degeneration.[1, 30-32] NfL and GFAP - with an estimated half-life of a number of days and months respectively - reflect current or recent neurodegeneration and are therefore markers of ongoing or recent disease activity.[33, 34] This makes the relationship between NfL and severity of myelopathy not straightforward. For example, a young patient could have severe spinal cord degeneration with elevated NfL levels, while not (yet) having any disability. This theory is supported by our finding that NfL was elevated to a similar degree in asymptomatic patients as in symptomatic patients, suggesting that spinal cord degeneration in the asymptomatic group is already ongoing but has not yet resulted in enough damage to cause symptoms or disability. It is likely that a certain threshold of neurodegeneration has to be reached before symptoms of myelopathy appear. If this hypothesis is true, NfL could be used to monitor disease activity in presymptomatic patients, for whom markers of disability do not apply.

The relationship between NfL and myelopathy in ALD is further complicated by the confounding effect of age. Normal ageing is associated with neurodegenerative processes that cause NfL levels to increase with age.[16] Myelopathy in ALD is also age-dependent: symptoms start on average in early adulthood and slowly progress, with most patients losing unassisted ambulation by the 6th decade.[8] Consequently, the associations between disease severity and NfL levels we found (**Fig. 2**) are partly explained by ageing. However, even after taking this effect of age into account (by multiple regression analysis with both age and severity of myelopathy as predictors), severity of myelopathy was still a significant predictor of NfL levels.

Group differences in NfL levels and correlations with disease severity support the use of NfL as biomarker for ALD. However, in order to prove that NfL is a surrogate marker for spinal cord degeneration, it is necessary to demonstrate that elevated NfL levels lead to (progression of) myelopathy, while low NfL levels do not. In our cohort, we did not find a correlation between NfL levels and clinical disease. Disease progression was probably not substantial enough (with only minimal change on the EDSS and not on the other clinical parameters, **Supplementary Table 1**) to be able to demonstrate such a correlation. This is likely due to the inherent slow progression of myelopathy in ALD, low sensitivity of the clinical parameters in detecting disease progression,[1] and a relatively low number of

patients with complete follow-up. Longer follow-up, which is ongoing in this cohort, might resolve this issue.

NfL has several potential advantages as biomarker in ALD. Being a marker of disease activity, NfL could show an effect of a disease modifying treatment on a short term, while currently available clinical endpoints require very long follow-up. Although phase III trials usually require clinical endpoints, NfL could be particularly useful for phase II-trials to identify drugs that seem promising enough to continue to phase III trials – similar to its application in multiple sclerosis (MS).[16, 35] In addition, it is easily accessible (it can be collected during routine blood sampling), inexpensive, observer-independent, and very reproducible provided that samples are processed in the same laboratory.[12, 13] Main disadvantage is that it is a general biomarker for axonal degeneration, which is not specific for ALD. Other neurological disorders – for example recent stroke, head trauma, Alzheimer or Parkinson's disease – also lead to elevated NfL levels and are an important source of bias.[18, 36] Therefore, if NfL is to be used as treatment outcome parameter, it is important to screen for these conditions and exclude patients if necessary.

In conclusion, our study illustrates the potential of NfL as a biomarker of spinal cord degeneration in male ALD patients, while plasma GFAP seems less valuable. NfL could serve as a surrogate outcome in phase II trials or as secondary outcome in phase III trials. A longitudinal study demonstrating that elevated NfL levels lead to progression of myelopathy is needed to confirm our findings and is currently ongoing in this cohort.

References

1. Huffnagel IC, van Ballegoij WJC, van Geel BM, Vos J, Kemp S, Engelen M. Progression of myelopathy in males with adrenoleukodystrophy: towards clinical trial readiness. Brain. 2019 Feb 1;142(2):334-43.
2. Engelen M, Barbier M, Dijkstra IM, et al. X-linked adrenoleukodystrophy in women: a cross-sectional cohort study. Brain. 2014 Mar;137(Pt 3):693-706.
3. Singh I, Moser AE, Moser HW, Kishimoto Y. Adrenoleukodystrophy: impaired oxidation of very long chain fatty acids in white blood cells, cultured skin fibroblasts, and amniocytes. Pediatr Res. 1984 Mar;18(3):286-90.
4. Moser HW, Smith KD, Watkins PA, Powers JM, Moser AB. X-Linked Adrenoleukodystrophy. In: Scriver CR, Beaudet AL, Sly WS, Valle D, editors. New York: McGraw Hill; 2001. p. 3257-301.
5. Moser HW, Moser AB, Frayer KK, et al. Adrenoleukodystrophy: increased plasma content of saturated very long chain fatty acids. Neurology. 1981 Oct;31(10):1241-9.
6. Engelen M, Kemp S, de Visser M, et al. X-linked adrenoleukodystrophy (X-ALD): clinical presentation and guidelines for diagnosis, follow-up and management. Orphanet J Rare Dis. 2012;7:51.
7. Powers JM, DeCiero DP, Ito M, Moser AB, Moser HW. Adrenomyeloneuropathy: a neuropathologic review featuring its noninflammatory myelopathy. J Neuropathol Exp Neurol. 2000 Feb;59(2):89-102.
8. van Geel BM, Bezman L, Loes DJ, Moser HW, Raymond GV. Evolution of phenotypes in adult male patients with X-linked adrenoleukodystrophy. Ann Neurol. 2001 Feb;49(2):186-94.
9. Huffnagel IC, Dijkgraaf MGW, Janssens GE, et al. Disease progression in women with X-linked adrenoleukodystrophy is slow. Orphanet J Rare Dis. 2019 Feb 7;14(1):30.
10. Kemp S, Huffnagel IC, Linthorst GE, Wanders RJ, Engelen M. Adrenoleukodystrophy - neuroendocrine pathogenesis and redefinition of natural history. Nat Rev Endocrinol. 2016 Oct;12(10):606-15.
11. Huffnagel IC, Laheji FK, Aziz-Bose R, et al. The Natural History of Adrenal Insufficiency in X-Linked Adrenoleukodystrophy: An International Collaboration. J Clin Endocrinol Metab. 2019 Jan 1;104(1):118-26.
12. Gisslén M, Price RW, Andreasson U, et al. Plasma Concentration of the Neurofilament Light Protein (NFL) is a Biomarker of CNS Injury in HIV Infection: A Cross-Sectional Study. EBioMedicine. 2016 Jan;3:135-40.
13. Disanto G, Barro C, Benkert P, et al. Serum Neurofilament light: A biomarker of neuronal damage in multiple sclerosis. Ann Neurol. 2017 Jun;81(6):857-70.
14. Rissin DM, Kan CW, Campbell TG, et al. Single-molecule enzyme-linked immunosorbent assay detects serum proteins at subfemtomolar concentrations. Nat Biotechnol. 2010 Jun;28(6):595-9.
15. Kuhle J, Barro C, Andreasson U, et al. Comparison of three analytical platforms for quantification of the neurofilament light chain in blood samples: ELISA, electrochemiluminescence immunoassay and Simoa. Clin Chem Lab Med. 2016 Oct 1;54(10):1655-61.
16. Khalil M, Teunissen CE, Otto M, et al. Neurofilaments as biomarkers in neurological disorders. Nat Rev Neurol. 2018 Oct;14(10):577-89.
17. Watanabe M, Nakamura Y, Michalak Z, et al. Serum GFAP and neurofilament light as biomarkers of disease activity and disability in NMOSD. Neurology. 2019;93(13):e1299-e311.

18. Bridel C, van Wieringen WN, Zetterberg H, et al. Diagnostic Value of Cerebrospinal Fluid Neurofilament Light Protein in Neurology: A Systematic Review and Meta-analysis. JAMA Neurol. 2019 Jun 17;76(9):1035-48.
19. Wilke C, Rattay TW, Hengel H, et al. Serum neurofilament light chain is increased in hereditary spastic paraplegias. Annals of clinical and translational neurology. 2018;5(7):876-82.
20. Menke RAL, Gray E, Lu C-H, et al. CSF neurofilament light chain reflects corticospinal tract degeneration in ALS. Annals of clinical and translational neurology. 2015;2(7):748-55.
21. Powers JM, DeCiero DP, Cox C, et al. The dorsal root ganglia in adrenomyeloneuropathy: neuronal atrophy and abnormal mitochondria. J Neuropathol Exp Neurol. 2001 May;60(5):493-501.
22. Kurtzke JF. Rating neurologic impairment in multiple sclerosis: an expanded disability status scale (EDSS). Neurology. 1983 Nov;33(11):1444-52.
23. Castilhos RM, Blank D, Netto CB, et al. Severity score system for progressive myelopathy: development and validation of a new clinical scale. Braz J Med Biol Res. 2012 Jul;45(7):565-72.
24. D'Souza M, Yaldizli O, John R, et al. Neurostatus e-Scoring improves consistency of Expanded Disability Status Scale assessments: A proof of concept study. Mult Scler. 2017 Apr;23(4):597-603.
25. Podsiadlo D, Richardson S. The timed "Up & Go": a test of basic functional mobility for frail elderly persons. J Am Geriatr Soc. 1991 Feb;39(2):142-8.
26. van Hedel HJ, Wirz M, Dietz V. Assessing walking ability in subjects with spinal cord injury: validity and reliability of 3 walking tests. Arch Phys Med Rehabil. 2005 Feb;86(2):190-6.
27. Vatcheva KP, Lee M, McCormick JB, Rahbar MH. Multicollinearity in Regression Analyses Conducted in Epidemiologic Studies. Epidemiology (Sunnyvale). 2016;6(2):227.
28. Lu C-H, Macdonald-Wallis C, Gray E, et al. Neurofilament light chain. A prognostic biomarker in amyotrophic lateral sclerosis. 2015;84(22):2247-57.
29. Kuhle J, Barro C, Disanto G, et al. Serum neurofilament light chain in early relapsing remitting MS is increased and correlates with CSF levels and with MRI measures of disease severity. Mult Scler. 2016 Oct;22(12):1550-9.
30. Castellano A, Papinutto N, Cadioli M, et al. Quantitative MRI of the spinal cord and brain in adrenomyeloneuropathy: in vivo assessment of structural changes. Brain. 2016 Jun;139(Pt 6):1735-46.
31. Huffnagel IC, van Ballegoij WJC, Vos J, Kemp S, Caan MWA, Engelen M. Longitudinal diffusion MRI as surrogate outcome measure for myelopathy in adrenoleukodystrophy. Neurology. 2019 Dec 3;93(23):e2133-e43.
32. van de Stadt SIW, van Ballegoij WJC, Labounek R, et al. Spinal cord atrophy as a measure of severity of myelopathy in adrenoleukodystrophy. J Inherit Metab Dis. 2020 Feb 19.
33. Thelin EP, Zeiler FA, Ercole A, et al. Serial Sampling of Serum Protein Biomarkers for Monitoring Human Traumatic Brain Injury Dynamics: A Systematic Review. Front Neurol. 2017;8:300.
34. Barry DM, Millecamps S, Julien JP, Garcia ML. New movements in neurofilament transport, turnover and disease. Exp Cell Res. 2007 Jun 10;313(10):2110-20.
35. Sormani MP, Haering DA, Kropshofer H, et al. Blood neurofilament light as a potential endpoint in Phase 2 studies in MS. Ann Clin Transl Neurol. 2019;6(6):1081-9.

36. Gaetani L, Blennow K, Calabresi P, Di Filippo M, Parnetti L, Zetterberg H. Neurofilament light chain as a biomarker in neurological disorders. Journal of Neurology, Neurosurgery & Psychiatry. 2019;90(8):870-81.

Supplementary Table 1. Changes in Nfl, GFAP and clinical parameters of severity of myelopathy during follow-up.

	Baseline	Year 2	Mean paired change (95%CI)	p-value
All patients				
EDSS	3.5 (1.3-5.0)	3.5 (1.0-6.0)	0.41 (0.01-0.82)	**0.041**
SSPROM	89.0 (78.0-99.5)	87.0 (77.0-100.0)	-0.62 (-2.31-1.08)	0.754
Timed up-and-go, s	4.5 (3.5-8.4)	4.3 (3.4-9.0)	0.24 (-0.33-0.81)	0.569
Nfl, pg/ml	12.0 ± 4.9	12.4 ± 4.5	0.47 (-0.79-1.74)	0.441
GFAP, pg/ml	73.2 (63.6-93.2)	84.5 (63.7-109.9)	11.88 (-4.14-27.92)	0.177
Symptomatic only				
EDSS	3.75 (3.5-6.0)	6.0 (3.5-6.0)	0.55 (-0.13-1.23)	0.109
SSPROM	80.9 ± 8.0	79.8 ± 10.0	-1.15 (-4.11-1.82)	0.404
Timed up-and-go, s	7.5 ± 3.0	8.1 ± 3.5	0.64 (-0.30-1.58)	0.152
Nfl, pg/ml	14.4 ± 4.0	15.0 ± 2.9	0.55 (-1.10-2.20)	0.472
GFAP, pg/ml	73.0 (66.2-104.7)	82.7 (75.5-90.3)	11.31 (-12.35-34.96)	0.445

Values are displayed as mean ± SD for normally distributed data and median (interquartile range) for non-normally distributed data. Changes during follow-up were assessed with paired t-test for normally distributed data and Wilcoxon signed rank test for non-normally distributed data.

EDSS, Expanded Disability Status Scale; GFAP, Glial Fibrillary Acidic Protein; Nfl, neurofilament light, SSPROM, Severity Scoring system for Progressive Myelopathy (SSPROM).

IV MR Imaging studies

8 Spinal cord atrophy as a measure of severity of myelopathy in adrenoleukodystrophy

Stephanie I.W. van de Stadt*
Wouter J.C. van Ballegoij*
René Labounek
Irene C. Huffnagel
Stephan Kemp
Igor Nestrasil°
Marc Engelen°
* equal contributors
° senior authors

Journal of Inherited Metabolic Disease (2020) 43(4): 852-860

ABSTRACT

Background: All men and most women with X-linked adrenoleukodystrophy (ALD) develop myelopathy in adulthood. As clinical trials with new potential disease modifying therapies are emerging, sensitive outcome measures for quantifying myelopathy are needed. This prospective cohort study evaluated spinal cord size (cross-sectional area - CSA) and shape (eccentricity) as potential new quantitative outcome measures for myelopathy in ALD.

Methods: Seventy-four baseline MRI scans, acquired in 42 male ALD patients and 32 age-matched healthy controls, and 26 follow-up scans of ALD patients were included in the study. We used routine T_1-weighted MRI sequences to measure mean CSA, eccentricity, right-left and anteroposterior diameters in the cervical spinal cord. We compared MRI measurements between groups and correlated CSA with clinical outcome measures of disease severity. Longitudinally, we compared MRI measurements between baseline and one year follow-up.

Results: CSA was significantly smaller in patients compared to controls on all measured spinal cord levels ($p<0.001$). The difference was completely explained by the effect of the symptomatic subgroup. Furthermore, the spinal cord showed flattening (higher eccentricity and smaller anteroposterior diameters) in patients. CSA correlated strongly with all clinical measures of severity of myelopathy. There was no detectable change in CSA after one year follow-up.

Conclusions: The cervical spinal cord in symptomatic ALD patients is smaller and flattened compared to controls, possibly due to atrophy of the dorsal columns. CSA is a reliable marker of disease severity and can be a valuable outcome measure in long term follow-up studies in ALD.

INTRODUCTION

X-linked adrenoleukodystrophy (ALD) is a rare inborn error of metabolism, caused by mutations in the *ABCD1*-gene. [1] Pathogenic *ABCD1*-mutations result in defective peroxisomal beta-oxidation causing accumulation of very long chain fatty acids in plasma and tissues. [2] The clinical spectrum in male ALD patients ranges from isolated adrenocortical insufficiency to devastating cerebral demyelination (cerebral ALD). [3,4] Virtually all male and most female patients develop progressive myelopathy and peripheral neuropathy in adulthood. [5–7] Clinical features of this myelopathy include incontinence and a gait disorder due to spastic paraparesis and sensory ataxia. [8,9] Pathologically, there is axonal degeneration of mainly the corticospinal tracts and dorsal columns. [10,11] In men, symptoms usually become apparent in the third decade of life. [1] However, there is variability in age of onset and rate of progression of myelopathy, even within families. [5,12]

Currently no disease modifying treatment is available to halt or slow progression of myelopathy in ALD, but new potential therapies are under development (e.g. NCT03231878, www.clinicaltrials.gov). Clinical trials to determine efficacy are difficult because current measures for the severity of myelopathy are not sensitive to small changes in disease severity (requiring long studies with large numbers of patients) [5,13], are affected by floor and ceiling effects (which means patients at the extreme ends of the disease spectrum cannot be included in trials) and are not disease specific (i.e. walking tests can be influenced by other diseases such as joint arthrosis). Therefore, new surrogate outcome measures are needed.

Spinal cord atrophy measured by conventional Magnetic Resonance Imaging (MRI) has been studied in various neurodegenerative disorders. In diseases such as hereditary spastic paraplegias, multiple sclerosis and amyotrophic lateral sclerosis a significant smaller spinal cord cross-sectional area (CSA) was found in patients compared to healthy controls. [14–16] Furthermore, CSA was associated with disease severity and progression in multiple sclerosis. [17] In addition to CSA, morphometric spinal cord parameters, such as eccentricity, right-left (RL) and anteroposterior (AP) diameters, have been used for a more detailed description of structural changes in the spinal cord in neurological diseases like Friedreich's ataxia and amyotrophic lateral sclerosis. [18–21] Although spinal cord degeneration is the pathological hallmark of ALD and atrophy has been previously described [22,23], only one dedicated study on quantifying spinal cord atrophy has been performed to date. Cervical and thoracic CSA was reduced 26-40% in 13 ALD males compared to 12 healthy controls, but the degree of reduction did not correlate to clinical disability or disease duration. [24] Confirmation of these data in larger cohorts and longitudinal data are lacking.

The main objective of this prospective cohort study was to quantify the degree of spinal cord atrophy in ALD. We measured different spinal cord MRI metrics (i.e. CSA, eccentricity and RL and AP diameters). We correlated spinal cord CSA with conventional clinical outcome measures and evaluated this parameter as a potential surrogate outcome measure for the severity of myelopathy in ALD.

METHODS

Study design and patient selection

This study was part of a prospective cohort study ("the Dutch ALD cohort") performed at the Amsterdam University Medical Centers (location AMC, Amsterdam, The Netherlands), the national referral center for ALD. Patients were recruited at the outpatient neurology clinic between June 2015 and February 2018. For this particular study all men over 16 years of age were eligible to participate. We excluded patients with active cerebral ALD (defined as gadolinium enhancing white matter lesions on cerebral MRI) or other neurological diseases interfering with the assessment of myelopathy. History, neurological examination and outcome measures were assessed at baseline and 1-year follow-up, as described previously [5]. The follow-up protocol of the natural history study was modified to include spinal cord imaging, therefore for 16 of 42 patients only baseline MRI scans were available at the time of analysis. Healthy volunteers were 32 age-matched male individuals without any clinical evidence of neurologic disease. Written informed consent was obtained from all participants. The study protocol was approved by the local Institutional Review Board (METC 2014_347).

Clinical assessment

All patients underwent a structured history, focused on symptoms of myelopathy, and extensive neurological examination as described previously. [5] Based on neurological history and examination, patients were classified as symptomatic or asymptomatic. Symptomatic patients were defined as having signs and symptoms of myelopathy. [5,7] Four outcome measures were used to assess severity of myelopathy: Expanded Disability Status Scale (EDSS), Severity Scoring system for Progressive Myelopathy (SSPROM), timed up-and-go and 6-minute walk test. The EDSS measures neurological disability and ranges from 0 (no disability) to 10 (death). [25] The SSPROM scores symptoms of myelopathy and ranges from 0 to 100 with lower scores indicating higher degree of impairment. [26] The timed up-and-go and 6-minute walk test are timed walking activities. Timed up-and-go measures the time to get up from an armchair, walk 3 meters, turn around, walk back and sit down again. [27] The 6-minute walk test measures the maximum walking distance in 6 minutes. [28] Moreover, semi-quantitative measurements of vibration sense were performed with a Rydel-Seiffer

tuning fork at the hallux and internal malleolus. All examinations, including MRI assessment, were performed on the same day.

Imaging acquisition and measurements

Imaging of the cervical spinal cord was performed on a 3T MR scanner (Philips Ingenia; Philips Medical Systems, Best, Netherlands) with a 20-channel head-neck-spine coil. 3D T_1-weighted fast field-echo sequences were used for analysis. Detailed acquisition parameters included: 189 slices; field of view 256×256×170 mm; voxel size 0.9×0.9×0.9 mm^3; TE (echo time) 4.1 ms; TR (repetition time) 8.9 ms; acquisition time 04:17.3 min. Sagittal image reconstructions with voxel size 0.5×0.5×0.9mm^3 were used for spinal cord metric extraction. Outside body image background was out-thresholded from the region of interest. Then, the scan was bias-field corrected [29], normalized to intensity value range from 0 to 1000, and resampled to isotropic voxel size 0.5×0.5×0.5mm^3 with a cubic spline interpolation method. Automatic axial 2D slice-by-slice spinal cord segmentation was performed with a "deepseg" method [30] followed by semi-automatic vertebral level labeling [31] where SI positions of all present inter-vertebral discs were manually marked. The segmentation, labeling and following quantitative spinal cord anatomy metric extraction were utilized with Spinal Cord Toolbox (SCT, version: 4.0.0). [32] Mean spinal cord CSA (mm^2), mean eccentricity, mean AP diameter (mm) and mean RL diameter (mm) were measured for each separate C1-Th2 level for all participants. Eccentricity is a mathematical measure characterizing the shape of a conic section, such as an ellipse approximating the spinal cord contour. It is defined as the square root of $1 - (d/D)^2$, where D is the largest (RL) diameter and d the smallest (AP) diameter of the ellipse. Values closer to 1 indicate a flatter ellipse, as the eccentricity of a circle is 0.

Statistical analysis

Data were summarized as means with standard deviations or medians with interquartile ranges (IQR), depending on the distribution. Normality of data was assessed by visual inspection and Shapiro-Wilk and Kolmogorov-Smirnov tests for normality. Differences between patients and controls were assessed using Student's t-test (normally distributed data) or Mann-Whitney U test (non-normally distributed data). Differences between controls, asymptomatic and symptomatic patients were assessed with one-way ANOVA with post hoc testing with Tukey correction for multiple comparisons. Spearman's rank order correlation coefficient was used to calculate the correlation between CSA and clinical measures (non-normally distributed data). For longitudinal analysis we used paired t-test or Wilcoxon signed rank test to assess difference in clinical measures and mean CSA between baseline and follow-up. P-values lower than 0.05 were considered statistically significant. IBM SPSS Statistics Version 25 was used for data analysis.

RESULTS

Baseline characteristics

The Dutch ALD cohort consists of 61 male ALD patients. Nineteen were excluded for this study: 15 because of age <16 years, 3 did not give consent and 1 due to poor quality of the spinal cord MRI. Baseline imaging was available for 74 subjects: 42 patients and 32 controls. Mean age of patients 45.9 (±16.1) and healthy controls 43.3 (±16.7) was not statistically significantly different (p=0.551).

Details on the clinical characteristics of this cohort are described in detail elsewhere. [5] In summary, 30 (71%) patients had signs and symptoms of myelopathy and were therefore classified as symptomatic. Median disease duration was 15.0 years (IQR 8-21). Patients had a median EDSS of 3.5 (IQR 2-6) and SSPROM of 84.5 (IQR 77-99), indicating a moderate degree of disability. Median time on the timed up-and-go was 6.9 seconds (IQR 3.5-10.2) and mean distance on the 6-minute walk test was 536.3 meter (±188.6).

Between-group differences

On visual examination, the spinal cord of ALD subjects looked smaller and flattened compared to healthy controls (**Figure 1**). Indeed, spinal cord CSA was significantly smaller in patients compared to controls on all measured levels (**Figure 2**). Absolute reduction was most pronounced at C3 level (mean difference 12.92 mm^2), while relative reduction was most pronounced at thoracic levels (23.5%). When stratifying patients into groups based on their symptomatic status (asymptomatic vs symptomatic), analysis showed that difference in spinal cord CSA between patients and healthy control subjects was determined by the effect of the symptomatic subgroup. There was no difference in CSA between asymptomatic patients and healthy control subjects (**Figure 2**).

In addition, morphometric analysis confirmed that the spinal cord was significantly flatter (reduced AP compared to RL diameter) in patients compared to controls. On all measured levels mean eccentricity and mean AP diameters differed significantly from controls (p<0.001), while RL diameters only differed in high cervical and the first two thoracic levels (**supplementary table 1**).

Correlation with clinical outcome measures

Figure 3 shows the correlations between clinical outcomes and CSA. Spinal cord CSA correlated strongly with EDSS, SSPROM and vibration sense scores (Spearman's rho > 0.7) and moderately with disease duration (Pearson's r = -0.366). There was no correlation between CSA and age of healthy controls (Pearson's r = -0.005).

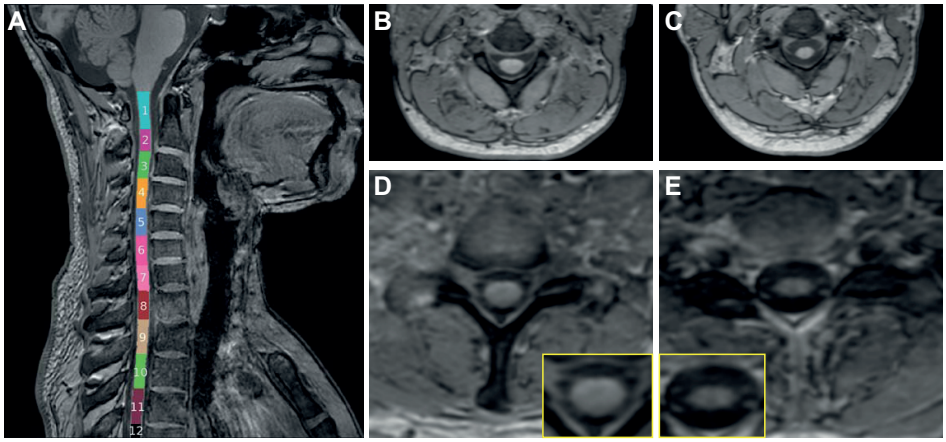

Figure 1: Example of MR images

A: semi-automatic vertebral labelling performed with the Spinal Cord Toolbox and spinal cord anatomy expert.
Upper right: Spinal cord atrophy at C2-C3 level in subjects with similar age: (B) Healthy control and (C) Patient with EDSS 7.0
Lower right: Difference in eccentricity of the spinal cord at the cervicothoracic junction in subjects with similar age: (D) Healthy control, mean eccentricity of 0.82 and (E) patient with EDSS 7.0, mean eccentricity of 0.90.

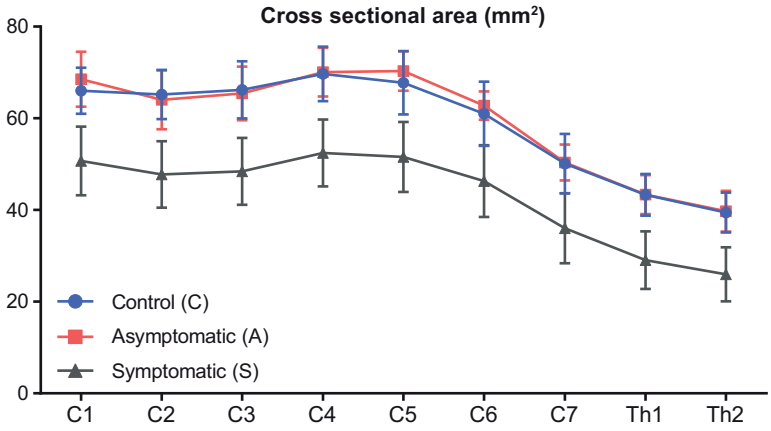

Level	Control (C)	Asymptomatic (A)	Symptomatic (S)		p-values		Mean difference
	(n=32)	(n=12)	(n=30)	C-A	C-S	A-S	C-S
C1	66.00 (5.04)	68.52 (5.98)	50.68 (7.51)	0.469	<0.001*	<0.001*	-15.33
C2	65.19 (5.37)	64.05 (6.44)	47.76 (7.27)	0.858	<0.001*	<0.001*	-17.42
C3	66.21 (6.22)	65.42 (5.85)	48.44 (7.31)	0.934	<0.001*	<0.001*	-17.77
C4	69.69 (5.94)	70.09 (5.32)	52.46 (7.30)	0.981	<0.001*	<0.001*	-17.23
C5	67.73 (6.94)	70.33 (4.32)	51.56 (7.64)	0.510	<0.001*	<0.001*	-16.17
C6	60.97 (7.03)	62.79 (3.12)	46.29 (7.84)	0.722	<0.001*	<0.001*	-14.68
C7	50.14 (6.48)	50.36 (3.93)	36.01 (7.64)	0.995	<0.001*	<0.001*	-14.13
Th1	43.33 (4.55)	43.35 (4.27)	29.07 (6.29)	1.000	<0.001*	<0.001*	-14.26
Th2	39.46 (4.35)	39.75 (4.48)	25.95 (5.90)	0.983	<0.001*	<0.001*	-13.51

Figure 2: Cross-sectional area in patients and controls

Line chart: Mean CSA in healthy controls (blue circle), asymptomatic patients (red square) and symptomatic patients (grey triangle) with standard deviations (error bars).
Table: Differences in mean CSA between healthy controls, asymptomatic and symptomatic patients. Differences between groups are analyzed with one-way ANOVA.
*statistically significant p-value.

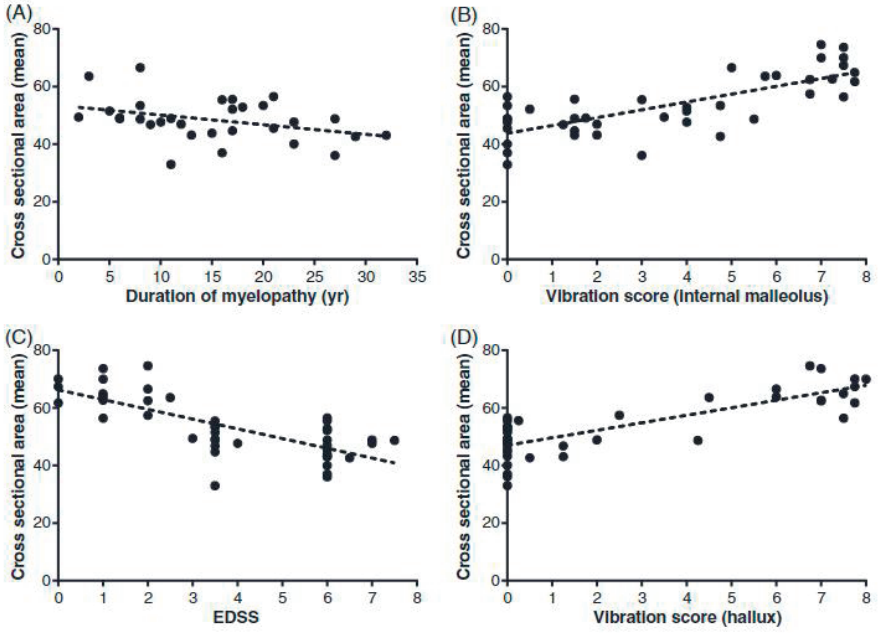

	r	p-value	N
EDSS[1]	-0.75	<0.001*	42
6MWT[1]	0.27	0.112	35
SSPROM[1]	0.70	<0.001*	42
Timed up-and-go[1]	-0.71	<0.001*	37
Vibration score[1] (internal mallelous)	0.71	<0.001*	41
Vibration score[1] (hallux)	0.71	<0.001*	41
Disease duration[2]	-0.37	0.046*	30
Age controls[2]	-0.01	0.980	32

Figure 3: Correlations between clinical outcomes and cross-sectional area
Above: scatterplots of correlation between CSA measured at C3 level and (A) disease duration, (B and D) vibration score measured at the internal malleolus and hallux and (C) EDSS.
Below: correlation coefficients for clinical outcomes and CSA. *statistically significant p-value. [1] Spearman's rank order correlation test. [2] Pearson's correlation test.
Abbreviations: CSA, cross-sectional area; EDSS, Expanded Disability Status Scale; SSPROM, Severity Scoring system for Progressive Myelopathy; 6MWT, 6 Minute Walk Test.

Disease progression

Follow-up imaging was available for 26/42 patients (62%). Median time between baseline and follow-up scans was 11 months (IQR 9-14). Three of the clinical outcome measures were able to detect disease progression: EDSS (mean change 0.21, p=0.042), the timed up-and-go (mean change 0.23, p=0.045) and quantitative vibration score measured at the hallux (mean change -0.30, p=0.007). However, there was no change in spinal cord CSA between baseline and follow-up on any of the measured levels (**Table 1**). When looking at the symptomatic subgroup (n=17), a trend in reduction of CSA measured at C2 was found (-0.39 mm², 95%

CI: -0.04 to 0.83, p=0.073). For the morphometric measures, only a significant decrease of the AP diameter at C2 level was detected (-0.08 mm, Z-value: -2.095, p=0.036). There was no correlation between baseline CSA and disease progression, measured as the change in EDSS and vibration sense score.

Table 1: Disease progression

	Baseline (n=26)	Follow-up (n=26)	Difference (95% CI)	p-value
Clinical outcome measures				
EDSS	3.5 (1.0-6.0)	3.5 (1.8-6.0)	0.21 (0.01-0.42)	0.042*
SSPROM	91.0 (81.0-100)	87.0 (75.8-100)	-2.23 (-4.43--0.03)	0.052
6MWT (n=24)	562.6 (±198.4)	555.3 (±197.0)	-8.73 (-13.0-27.5)	0.464
TUG (n=23)	4.7 (3.5-9.1)	5.2 (3.7-9.0)	0.23 (-0.41-0.86)	0.045*
Quantitative vibration score (internal malleolus)	4.38 (1.06-6.81)	3.75 (0.19-6.56)	-0.24 (-0.57-0.09)	0.199
Quantitative vibration score (hallux)	1.63 (0.00-7.00)	0.75 (0.00-6.50)	-0.30 (-0.50- -0.10)	0.007*
Spinal cord CSA (mm^2)				
C1	56.49 (11.03)	56.16 (10.46)	0.33 (-0.35-1.00)	0.330
C2	53.36 (9.95)	53.29 (10.79)	0.07 (-0.75-0.88)	0.867
C3	54.13 (9.81)	54.04 (10.59)	0.09 (-0.75-0.93)	0.823
C4	58.78 (9.96)	58.43 (10.39)	0.34 (-0.69-1.38)	0.501
C5	58.05 (11.08)	58.18 (11.11)	-0.13 (-0.98-0.73)	0.763
C6	51.54 (10.49)	51.98 (10.25)	-0.44 (-1.57-0.68)	0.426
C7	40.87 (10.10)	41.66 (10.46)	-0.79 (-1.96-0.37)	0.174
Th1	33.88 (8.86)	33.89 (9.38)	-0.01 (-1.03-1.01)	0.981
Th2	30.88 (8.58)	30.85 (8.93)	0.03 (-0.61-0.67	0.917

Values are medians with IQRs or means with standard deviations
Differences between groups are analyzed with Wilcoxon signed rank test or Paired t-test
* p-value statistically significant
Abbreviations: EDSS, Expanded Disability Status Scale; SSPROM, Severity Scoring system for Progressive Myelopathy; 6MWT, 6 Minute Walk Test; TUG, Timed up-and-Go; CSA, Cross-sectional area.

DISCUSSION

In this prospective cohort study we quantitatively assessed spinal cord atrophy as a potential biomarker for severity of myelopathy in ALD. Our findings showed that the spinal cord is smaller and flatter in ALD patients with symptomatic myelopathy compared to controls. The degree of thinning correlated with clinical outcome measures for myelopathy. We did not detect any change after one-year follow-up.

CSA was reduced at all levels in ALD patients compared to controls, and this reduction was explained by the symptomatic subgroup. Relative reduction was most pronounced at

thoracic levels (23.5%) whereas absolute reduction was more prominent at C2-C3 levels (12.92 mm^2). These results are in agreement with previously published data. [24] Moreover, the spinal cord of ALD patients shows anteroposterior flattening, as can be seen by visual assessment of MR images. In the patients' spinal cord relative reduction of AP diameters was greater than reduction of RL diameters and mean eccentricity was closer to 1, indicating a flatter spinal cord as compared to healthy controls. Comparable results were found in other neurodegenerative disorders, such as spinocerebellar ataxia and Friedreich's ataxia. [18,19] These diseases have similar pathological mechanisms as ALD, with predominant degeneration of dorsolateral tracts of the spinal cord. Conversely, in amyotrophic lateral sclerosis where corticospinal tracts are mostly affected, this flattening was not seen and eccentricity values for patients and controls were virtually the same. [20] Spinal cord flattening in ALD is thus likely due to dorsal column degeneration.

Furthermore, CSA correlated significantly with all used clinical outcome measures for myelopathy, with more severely affected patients having a smaller CSA. This implies that spinal cord CSA is a reliable biomarker for disease severity and can be used, for example, in multi-center studies or studies with a longer follow-up period. Since CSA can be derived from routine diagnostic MRI sequences and data processing software libraries are freely accessible, data collection and analysis may be reproducible across sites.

After one-year follow-up there was no significant decrease in CSA. Nevertheless, disease duration and CSA were significantly negatively correlated, confirming the initial hypothesis that CSA decreases over time in ALD patients. A sub-analysis in symptomatic patients showed a trend towards smaller CSA after one year at C2 level (-0.39 mm, p=0.073), but the mean change was small and not found at other levels. Furthermore, AP diameter measured at C2 level decreased significantly (-0.08 mm, p=0.036) but again the mean change was not found at other levels and also, this detected change is below a spatial resolution of the MRI sequence used in our protocol. It is likely that significant changes may be observed after longer follow-up, also considering the large difference in CSA between symptomatic and asymptomatic patients. A new prospective cohort study is ongoing to confirm this hypothesis.

A few limitations apply to our study. First is the relatively low number of available follow-up MRI scans. Nevertheless, this study is one of the largest prospective cohort studies in ALD. Secondly, age can be considered as a confounding factor when looking at clinical outcome measures over time. However, in our control group we did not find a relationship between CSA and age. Therefore it seems unlikely that the difference we detected is explained by aging. Finally, CSA as macrostructural quantitative marker is not sensitive enough to detect changes in a presymptomatic stage. With diffusion MRI protocols, namely DTI, we were able to detect differences between asymptomatic patients and controls. [33] Correlations between

CSA and clinical outcomes were, on the contrary, stronger than correlations between DTI parameters and clinical outcomes. For this reason CSA is still a reliable marker for disease severity. In the future, advanced diffusion MRI protocols, such as high angular resolution diffusion imaging (HARDI) sampled at multiple q-space shells optimized for spinal cord imaging, can increase the outcome sensitivity and also correlation property for the DTI metrics. [34]

In conclusion, our study shows that the spinal cord in male ALD patients is smaller and flatter compared to controls, likely due to atrophy predominantly affecting the dorsolateral columns. Moreover, spinal cord CSA is strongly associated with disease severity and represents a promising biomarker in the myelopathy of ALD. Due to a slowly progressive disease course, there is no detectable change after one-year follow-up. In studies with a longer follow-up period or multi-center studies CSA can be of use since it requires only routine MRI sequences. Our future research is aimed at identifying more sensitive and dynamic outcome measures able to detect change after a shorter follow-up period, such as optical coherence tomography (OCT), body sway measurement, and other quantitative MRI techniques like DTI. These studies will hopefully contribute to clinical trial readiness in ALD.

REFERENCES

1. Kemp S, Huffnagel IC, Linthorst GE, Wanders RJA, Engelen M. Adrenoleukodystrophy - Neuroendocrine pathogenesis and redefinition of natural history. *Nat Rev Endocrinol*. 2016;12. doi:10.1038/nrendo.2016.90
2. Singh I, Moser AB, Moser HW, Kishimoto Y. Adrenoleukodystrophy: Impaired oxidation of very long chain fatty acids in white blood cells, cultured skin fibroblasts, and amniocytes. *Pediatr Res*. 1984;18(3):286-290. doi:10.1203/00006450-198403000-00016
3. Van Geel BM, Assies J, Wanders RJA, Barth PG. X linked adrenoleukodystrophy: Clinical presentation, diagnosis, and therapy. *J Neurol Neurosurg Psychiatry*. 1997;63(1):4-14. doi:10.1136/jnnp.63.1.4
4. De Beer M, Engelen M, Van Geel BM. Frequent occurrence of cerebral demyelination in adrenomyeloneuropathy. *Neurology*. 2014;83(24):2227-2231. doi:10.1212/WNL.0000000000001074
5. Huffnagel IC, van Ballegoij WJ, Van Geel BM, MBW Vos J, Kemp S, Engelen M. Progression of myelopathy in males with adrenoleukodystrophy: towards clinical trial readiness. *Brain*. 2019;142(2):334-343. doi:10.1093/brain/awy299
6. Huffnagel IC, Laheji FK, Aziz-Bose R, et al. The natural history of adrenal insufficiency in X-linked adrenoleukodystrophy: an international collaboration. *J Clin Endocrinol Metab*. 2019;104(1). doi:10.1210/jc.2018-01307
7. Engelen M, Barbier M, Dijkstra IME, et al. X-linked adrenoleukodystrophy in women: A cross-sectional cohort study. *Brain*. 2014;137(3):693-706. doi:10.1093/brain/awt361
8. Budka H, Sluga E, Heiss WD. Spastic paraplegia associated with addison's disease: Adult variant of adreno-leukodystrophy. *J Neurol*. 1976;213(3):237-250. doi:10.1007/BF00312873
9. Griffin JW, Goren E, Schaumburg H, Engel WK, Loriaux L. Adrenomyeloneuropathy: A probable variant of adrenoleukodystrophy. I. Clinical and endocrinologic aspects. *Neurology*. 1977;27(12):1107-1113.
10. Powers JM, DeCiero DP, Cox C, et al. The Dorsal Root Ganglia in Adrenomyeloneuropathy: Neuronal Atrophy and Abnormal Mitochondria. *J Neuropathol Exp Neurol*. 2001;60(5):493-501. doi:10.1093/jnen/60.5.493
11. Powers JM, DeCiero DP, Ito M, Moser AB, Moser HW. Adrenomyeloneuropathy: A neuropathologic review featuring its noninflammatory myelopathy. *J Neuropathol Exp Neurol*. 2000;59:89-102.
12. Berger J, Molzer B, Fae I, Bernheimer H. X-Linked Adrenoleukodystrophy (ALD): A Novel Mutation of the ALD Gene in 6 Members of a Family Presenting with 5 Different Phenotypes. *Biochem Biophys Res Commun*. 1994;205(3):1638-1643. doi:https://doi.org/10.1006/bbrc.1994.2855
13. Huffnagel IC, Dijkgraaf MGW, Janssens GE, et al. Disease progression in women with X-linked adrenoleukodystrophy is slow. *Orphanet J Rare Dis*. 2019;14(30). doi:10.1186/s13023-019-1008-6
14. Querin G, Bede P, El Mendili MM, et al. Presymptomatic spinal cord pathology in c9orf72 mutation carriers: A longitudinal neuroimaging study. *Ann Neurol*. 2019;86(2):158-167. doi:10.1002/ana.25520
15. Hedera P, Eldevik OP, Maly P, Rainier S, Fink JK. Spinal cord magnetic resonance imaging in autosomal dominant hereditary spastic paraplegia. *Neuroradiology*. 2005;47(10):730-734. doi:10.1007/s00234-005-1415-3
16. Zurawski J, Glanz BI, Healy BC, et al. The impact of cervical spinal cord atrophy on quality of life in multiple sclerosis. *J Neurol Sci*. 2019. doi:10.1016/j.jns.2019.04.023

17. Casserly C, Seyman EE, Alcaide-Leon P, et al. Spinal Cord Atrophy in Multiple Sclerosis: A Systematic Review and Meta-Analysis. *Journal of Neuroimaging*. 2018.

18. Chevis CF, Da Silva CB, D'Abreu A, et al. Spinal cord atrophy correlates with disability in Friedreich's ataxia. *Cerebellum*. 2013;12(1):43-47. doi:10.1007/s12311-012-0390-6

19. Martins CR, Martinez ARM, de Rezende TJR, et al. Spinal Cord Damage in Spinocerebellar Ataxia Type 1. *Cerebellum*. 2017;16(4):792-796. doi:10.1007/s12311-017-0854-9

20. Branco LMT, De Albuquerque M, De Andrade HMT, Bergo FPG, Nucci A, França MC. Spinal cord atrophy correlates with disease duration and severity in amyotrophic lateral sclerosis. *Amyotroph Lateral Scler Front Degener*. 2014;15(1-2):93-97. doi:10.3109/21678421.2013.852589

21. de Albuquerque M, Branco LMT, Rezende TJR, De Andrade HMT, Nucci A, França MC. Longitudinal evaluation of cerebral and spinal cord damage in Amyotrophic Lateral Sclerosis. *NeuroImage Clin*. 2017;14:269-276. doi:10.1016/j.nicl.2017.01.024

22. Kumar AJ, Kohler W, Kruse B, et al. MR findings in adult-onset adrenoleukodystrophy. *Am J Neuroradiol*. 1995;16(6):1227-1237.

23. Israel H, Ostendorf F, Stiepani H, Ploner CJ. Spinal Cord Atrophy in Adrenomyeloneuropathy. *Arch Neurol*. 2005;62(7):1157. doi:10.1001/archneur.62.7.1157

24. Castellano A, Papinutto N, Cadioli M, et al. Quantitative MRI of the spinal cord and brain in adrenomyeloneuropathy: In vivo assessment of structural changes. *Brain*. 2016;139(6):1735-1746. doi:10.1093/brain/aww068

25. Kurtzke JF. Rating neurologic impairment in multiple sclerosis. *Neurology*. 1983;33(11):1444 LP - 1444. doi:10.1212/WNL.33.11.1444

26. Castilhos RM, Blank D, Netto CBO, et al. Severity score system for progressive myelopathy: development and validation of a new clinical scale. *Brazilian J Med Biol Res*. 2012;45(7):565-572. doi:10.1590/S0100-879X2012007500072

27. Podsiadlo D, Richardson S. The Timed "Up & Go": A Test of Basic Functional Mobility for Frail Elderly Persons. *J Am Geriatr Soc*. 1991;39(2):142-148. doi:10.1111/j.1532-5415.1991.tb01616.x

28. van Hedel HJ, Wirz M, Dietz V. Assessing walking ability in subjects with spinal cord injury: Validity and reliability of 3 walking tests. *Arch Phys Med Rehabil*. 2005;86(2):190-196. doi:https://doi.org/10.1016/j.apmr.2004.02.010

29. Tustison NJ, Avants BB, Cook PA, et al. N4ITK: Improved N3 Bias Correction. *IEEE Trans Med Imaging*. 2010;29(6):1310-1320. doi:10.1109/TMI.2010.2046908

30. Gros C, De Leener B, Badji A, et al. Automatic segmentation of the spinal cord and intramedullary multiple sclerosis lesions with convolutional neural networks. *Neuroimage*. 2019;184:901-915. doi:https://doi.org/10.1016/j.neuroimage.2018.09.081

31. de Leener B, Cohen-Adad J, Kadoury S. Automatic Segmentation of the Spinal Cord and Spinal Canal Coupled With Vertebral Labeling. *IEEE Trans Med Imaging*. 2015;34(8):1705-1718. doi:10.1109/TMI.2015.2437192

32. De Leener B, Lévy S, Dupont SM, et al. SCT: Spinal Cord Toolbox, an open-source software for processing spinal cord MRI data. *Neuroimage*. 2017;145:24-43. doi:https://doi.org/10.1016/j.neuroimage.2016.10.009

33. Huffnagel IC, van Ballegoij WJ, Vos JM, Kemp S, Caan MW, Engelen M. Longitudinal diffusion MRI as surrogate outcome measure for myelopathy in adrenoleukodystrophy. *Neurology*. 2019;93:1-12. doi:10.1212/WNL.0000000000008572

34. Labounek R, Valosek J, Horak T, et al. Novel HARDI-ZOOMit protocol detects changes in spinal cord microstructure in patients with asymptomatic non-myelopathic degenerative cervical spinal cord compression. 2019;Submitted.

Supplementary Table 1: Anterior-posterior diameter and mean eccentricity in patients and controls

	Control (n=32)	Patient (n=42)	p-value	Control (n=32)	Patient (n=42)	p-value
	AP diameter	**AP diameter**		**Eccentricity**	**Eccentricity**	
C1	7.74 (7.51-8.04)	6.78 (6.15-7.51)	<0.001*	0.70 (0.65-0.73)	0.73 (0.69-0.79)	0.007*
C2	7.41 (7.14-7.72)	6.14 (5.52-7.04)	<0.001*	0.76 (0.70-0.78)	0.80 (0.76-0.83)	0.001*
C3	7.09 (6.77-7.51)	5.94 (5.27-7.02)	<0.001*	0.79 (0.76-0.83)	0.83 (0.78-0.86)	0.004*
C4	6.91 (6.67-7.45)	5.76 (5.21-6.75)	<0.001*	0.83 (0.80-0.86)	0.88 (0.81-0.91)	0.002*
C5	6.78 (6.48-7.19)	5.65 (5.15-6.79)	<0.001*	0.84 (0.81-0.87)	0.88 (0.83-0.91)	0.005*
C6	6.39 (6.01-6.80)	5.37 (4.69-6.42)	<0.001*	0.85 (0.82-0.87)	0.88 (0.84-0.91)	0.001*
C7	5.86 (5.69-6.56)	5.00 (4.15-5.74)	<0.001*	0.81 (0.79-0.83)	0.86 (0.84-0.89)	<0.001*
Th1	5.93 (5.68-6.47)	4.72 (4.09-5.79)	<0.001*	0.75 (0.71-0.78)	0.83 (0.78-0.85)	<0.001*
Th2	5.73 (5.48-6.29)	4.67 (4.09-5.45)	<0.001*	0.73 (0.68-0.76)	0.79 (0.75-0.84)	<0.001*

Values are medians with IQRs

Differences between groups are analyzed with Mann-Whitney U test

*statistically significant p-value

9 Magnetic Resonance Spectroscopy as marker for neurodegeneration in X-linked adrenoleukodystrophy

Stephanie I.W. van de Stadt
Anouk Schrantee
Irene C. Huffnagel
Wouter J.C. van Ballegoij
Matthan W.A. Caan
Petra J.W. Pouwels
Marc Engelen

NeuroImage: Clinical (2021) 32: 102793

ABSTRACT

X-linked adrenoleukodsytrophy (ALD) is a genetic neuro-metabolic disorder, causing a slowly progressive myelopathy in adult male and female patients. New disease modifying therapies for myelopathy are under development. This calls for new (imaging) markers able to measure disease severity and progression in clinical trials. In this prospective cohort study, we measured cerebral metabolite levels with Magnetic Resonance Spectroscopy (MRS), and evaluated their potential as biomarkers for disease severity and neurodegeneration in ALD. We used a comprehensive protocol of 3T Magnetic Resonance Spectroscopic Imaging (MRSI) and 7T Single Voxel Spectroscopy (SVS) in a large cohort of adult ALD males without cerebral demyelination. One hundred seven baseline scans – 59 obtained in ALD patients (42 3T MRSI and 17 7T SVS) and 48 obtained in healthy male controls (32 3T MRSI and 16 7T SVS) – and 82 one and two-year follow-up scans (66 3T MRSI and 16 7T SVS) of ALD patients were included. Both protocols showed significantly lower concentration ratios of N-acetylaspartate/creatine (tNAA/tCr) and Glx (glutamine + glutamate)/tCr in the grey and white matter of patients, compared to controls. A novel finding is the higher level of inositol (Ins)/tCr and choline containing compounds (tCho)/tCr in ALD patients without cerebral demyelination. Furthermore, tNAA/tCr correlated strongly with clinical measures of severity of myelopathy. There was no detectable change in metabolite ratios after one-year or two-year follow-up. Our results imply that cerebral metabolite levels – and more specifically the tNAA/tCr ratio – measured with MRS, have potential value as (imaging) biomarkers in ALD.

INTRODUCTION

Adrenoleukodsytrophy (ALD) is an X-linked metabolic disorder, caused by mutations in the *ABCD1* gene [1,2]. Mutations cause dysfunction of ALD protein, a peroxisomal transmembrane protein, resulting in impaired β-oxidation of very long chain fatty acids (VLCFA) and elevated levels of VLCFAs in plasma and tissues [3,4]. In males, there is a broad spectrum of symptoms, from isolated adrenocortical insufficiency to a rapidly progressive cerebral demyelination (cerebral ALD) [5,6]. Eventually, all men – and most women – will develop a slowly progressive and invalidating myelopathy [7,8]. Currently, treatment for myelopathy is supportive only, but new potential therapies are emerging. There is a great need for identification of surrogate outcome measures or (imaging) biomarkers able to monitor disease severity and progression in clinical trials, as current clinical outcome measures require large numbers of patients and long follow-up [7].

An imaging technique that provides insight in the brain pathology of ALD is Magnetic Resonance Spectroscopy (MRS). MRS is used to measure cerebral metabolite levels, such as N-acetylaspartate (tNAA, including contributions of N-acetyl aspartyl glutamate), choline containing compounds (tCho), inositol (Ins), glutamate (Glu), glutamine (Gln), lactate (Lac) and creatine (tCr). In all ALD patients – including heterozygotes, cerebral ALD and asymptomatic patients – significantly reduced tNAA levels and correspondingly lower tNAA/tCr ratios have been found compared to controls [9–13]. A reduction in tNAA levels is an indicator of axonal damage, which is the pathological hallmark of the myelopathy in ALD [14,15], but occurs in cerebral ALD as well. Additionally, in cerebral ALD, concentrations of tCho, Lac and Ins were elevated, which corresponds to the process of active demyelination [16–18].

MRS can be acquired at varying spatial coverage and field strength. Single-voxel spectroscopy (SVS) may be superior for diseases in which the affected brain region is well defined, as the measured area is smaller and more accessible to analyze. Magnetic Resonance Spectroscopic Imaging (MRSI), in which data from multiple voxels within a whole area or "slab" are obtained, is more suitable for studying diffuse disease processes [19]. With ultra-high magnetic field strengths (7T) sensitivity of metabolite concentration measurements increases due to increased signal-to-noise ratio (SNR) and spectral resolution, which allows for better separation of individual metabolite peaks. However, this increased sensitivity might be attenuated by enhanced susceptibility artefacts. These characteristics make both 3T and 7T MRS of potential interest to include.

The majority of previous ALD studies on MRS focused on patients with cerebral ALD and consisted of small numbers of patients. Furthermore, longitudinal data is often lacking. In this prospective study we evaluated the potential of cerebral metabolite levels, measured

with MRS, as imaging biomarkers for disease severity in ALD. We used a comprehensive protocol of 3T MRSI and 7T SVS in a large cohort of adult ALD males without cerebral involvement, and monitored disease severity over a 2-year follow-up period.

METHODS

Patient selection

This study was part of a prospective cohort study ("the Dutch ALD cohort") performed at Amsterdam University Medical Centers (location AMC, Amsterdam, The Netherlands), the national referral center for ALD, between June 2015 and February 2018. Clinical data of this cohort has been published previously [7]. For this particular study we included all male patients over 16 years of age with confirmed diagnosis of ALD (VLCFA and *ABCD1* analysis). Exclusion criteria were cerebral ALD (defined as gadolinium enhancing and non-enhancing cerebral white matter lesions on MRI), other neurological diseases interfering with the assessment of myelopathy, or contra-indications for MRI examination. Additionally, for 7T MR imaging patients were eligible to participate if they were over 18 years of age and if there were no additional contra-indications for 7T MRI examination (such as devices compatible with 3T but not 7T imaging). The control group consisted of age-matched healthy male individuals without clinical evidence of neurological disease. For 7T MR imaging a subset of the healthy controls were included. Written informed consent was obtained from all participants. The study protocol was approved by the local Institutional Review Board (METC 2014_347).

Clinical assessment

History and neurological examination were assessed at baseline and at one-year and two-year follow-up, as described previously [7]. Based on history and neurological examination, patients were classified as symptomatic or asymptomatic. Symptomatic patients were defined as having signs and symptoms of myelopathy [7,20]. Three outcome measures were used to assess severity of myelopathy: Expanded Disability Status Scale (EDSS), Severity Scoring system for Progressive Myelopathy (SSPROM) and Timed Up-and-Go (TUG). The EDSS measures neurological disability and ranges from 0 (no disability) to 10 (death) [21]. The SSPROM scores symptoms of myelopathy and ranges from 0 to 100, with lower scores indicating a higher degree of impairment [22]. TUG measures the time to get up from a chair, walk 3m, walk back and sit down again [23]. Furthermore, semi-quantitative measurements of vibration sense were performed with a Rydel-Seiffer tuning fork at the hallux and internal malleolus. The mean score of vibration sense at the left and right hallux and internal malleolus (vibration score foot) was used for analysis.

MRI protocols

All 3T MRI examinations were performed on the same day as the clinical examinations. 7T imaging was added to the imaging protocol at a later stage, therefore only two instead of three 7T MRIs were available per patient. 7T imaging was performed on a separate day, as close to the second and third 3T MRI as possible. **(Fig. 1)**

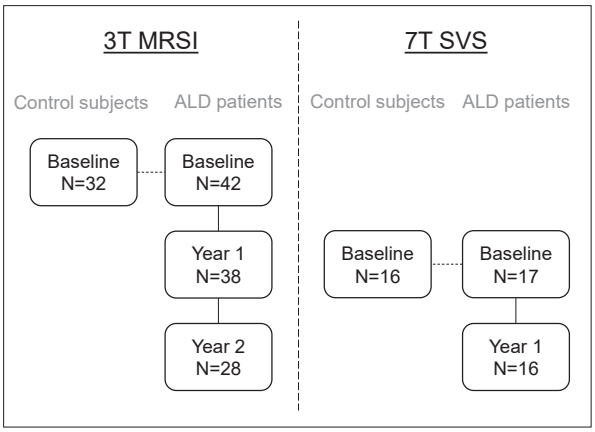

Figure 1. Study overview
An overview showing the timeline of included MRS scans per protocol: on the left 3T magnetic resonance spectroscopic imaging; on the right 7T single voxel spectroscopy, which was added to the imaging protocol one year later.

3T protocol

Conventional MR imaging and MRSI were performed on a 3T MR scanner (Philips Ingenia; Philips Medical Systems, Best, Netherlands) using a 32-channel head coil. Three-dimensional T1-weighted fast field echo images (repetition time/echo time (TR/TE) = 7.6/3.5 ms; voxel size = 1.1x1.1x1.1 mm; field of view = 256x256x170 mm; number of slices = 155) and three-dimensional fluid attenuated inversion recovery (FLAIR) images were acquired (TR/inversion time (TI)/TE) = 4800/1650/356 ms; voxel size = 1.1x1.1x1.1 mm; field of view = 250x250x180 mm; number of slices = 160). MRSI was obtained with point resolved spectroscopy (PRESS) localization on a single axial slab (TR/TE 3000/35 ms; field of view 160×160 mm; volume of interest (VOI) 80x90 mm; 16x16 phase-encodings; BW=1000; 1024 datapoints; NSA = 1; SENSE factor 2(AP)/2(RL), voxel size 10x10x15 mm) centered onto the corpus callosum. Outer volume suppression was performed using 10 circular rest slabs. **(Fig 2A)** First and second order shimming was performed using FASTMAP.[24] Total acquisition time was 04:57 minutes.

7T protocol

Conventional MR imaging and SVS were performed on a 7T MRI scanner (Philips Achieva; Philips Medical Systems, Best, Netherlands) with a volume transmit coil and a 32-channel receive coil (Nova Medical, Burlington, MA, USA). Magnetization-Prepared 2 Rapid Acquisition Gradient Echo (MP2RAGE) images were acquired for planning (TR/TE = 6.2/2.3

ms; voxel size = 0.64x0.64x0.64 mm; field of view = 220x220x164 mm; number of slices = 256). SVS was obtained using a semi-LASER sequence with FOCI pulses [25] (VOI size = 30(AP)x15(RL)x15(FH) mm; TR/TE= 5000/36 ms; BW=4000; 2048 data points; NSA = 32; VAPOR water suppression (NSA = 2)). One VOI was planned in the left and one VOI in the right semioval center. **(Fig 2B)** First and second order shimming was performed using FASTMAP. [24] Acquisition time was 02:50 minutes per voxel.

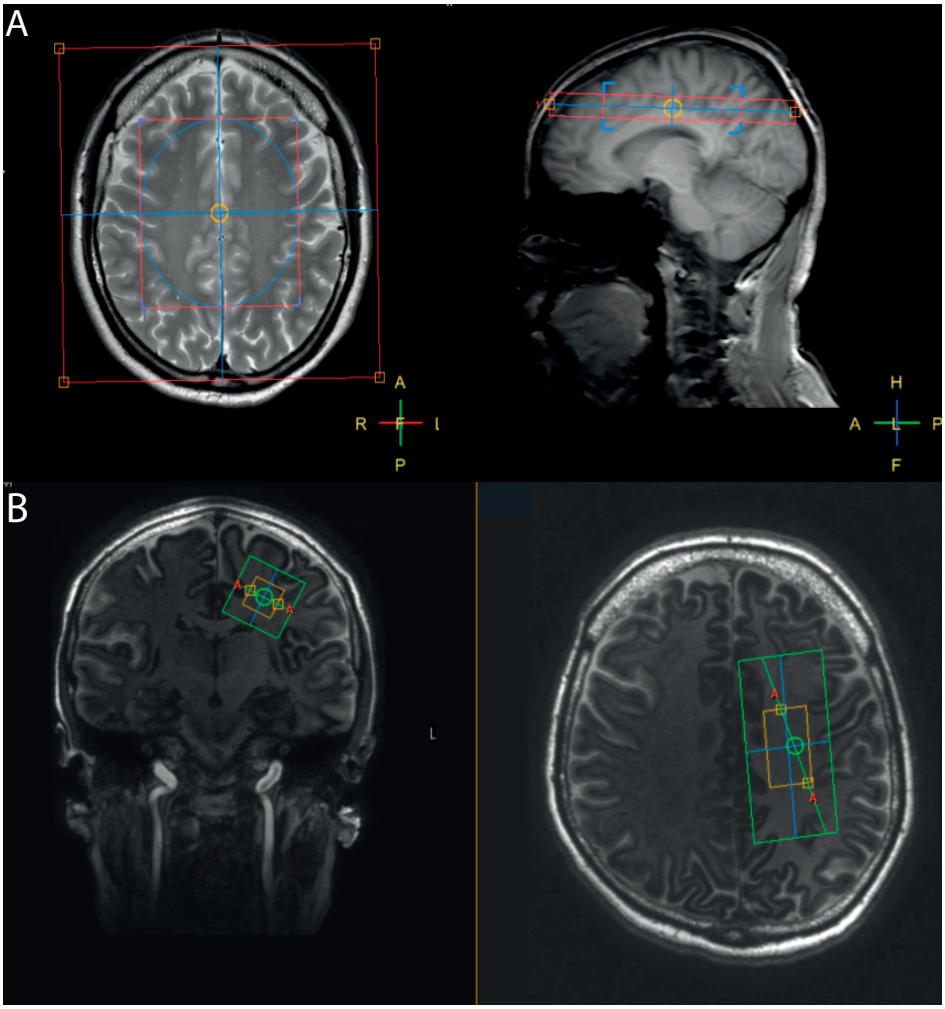

Figure 2. Slice and voxel placement
(A) 3T axial T2-weighted image of a healthy control subject showing placement of the MRSI slab. The VOI (small red rectangle, 80(RL)x90(AP) mm) was centered one slice above the cerebrospinal fluid, onto the corpus callosum. Blue ellipsoid indicates the inner border of the rest slabs. (B) 7T MP2RAGE raw magnitude image of a healthy control subject showing placement of the single voxel (in yellow, 30(AP)x15(RL)x15(FH) mm) in the left and right sided semioval center.
MRSI, magnetic resonance spectroscopic imaging; VOI, volume of interest; MP2RAGE, magnetization-prepared 2 rapid acquisition gradient echo; AP, anterior-posterior; RL, right-left; FH, feet-head.

MRI data processing

3T MRSI

Patients with typical cerebral ALD lesions were excluded, therefore lesion volume on FLAIR images was negligible and lesion segmentation and quantification was not performed. T1-weighted images were segmented into grey matter (GM), white matter (WM) and cerebrospinal fluid (CSF) partial volume estimates using SPM 12. The MRSI slab was registered to the T1 scan and the partial volume estimates using in-house Matlab scripts. Metabolites within the VOI were fitted between 1 and 4.2 ppm using a standard LCModel basis set for PRESS (TE=35ms)[26] including simulated macromolecular contributions, with tCr as a reference metabolite **(Fig 3)**. Voxels were only included if they met the following spectral quality criteria: full width half maximum (FWHM) <0.08 ppm, signal-to-noise ratio (SNR) > 8, Cramèr-Rao lower bounds (CRLB) <20% for the sum of Glu and Gln (Glx). For the included voxels, for each of the estimated metabolites (tNAA, tCho, Ins and Glx), a non-linear least squares fit (Curve Fitting Toolbox, Matlab) was performed to estimate the mean metabolite ratios in GM and WM. In this analysis, metabolite concentrations in CSF were assumed negligible. FWHM and SNR values were extracted from LCModel.

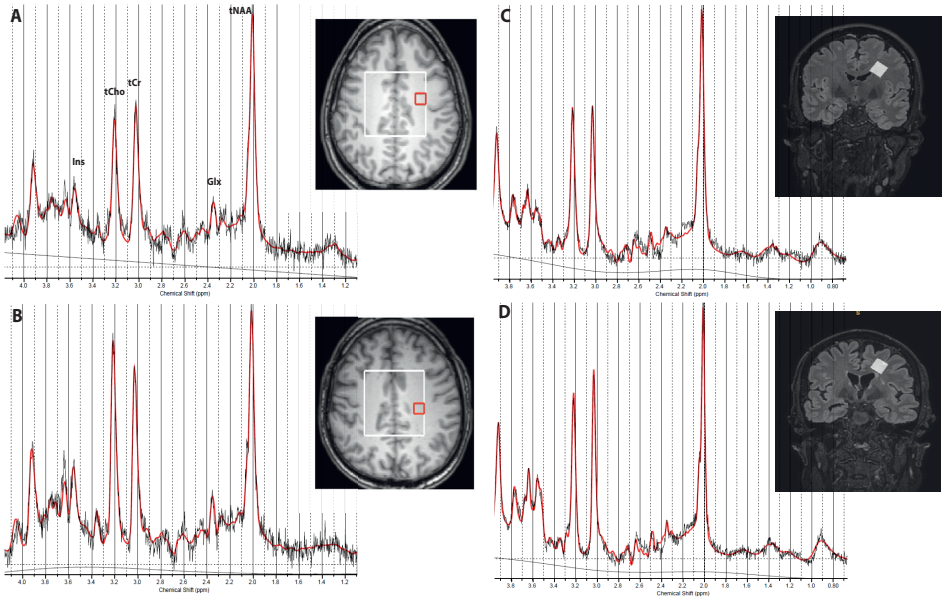

Figure 3. Quantification of spectra with LCModel

Left panel: the T1-weighted image was registered to the 3T MRSI slab; the white grid represents rows 6-11 and columns 6-11 that were considered for analysis. In red is the voxel from which the spectrum is displayed, (A) for a healthy control (FWHM 0.038 ppm, SNR 15) and (B) for a patient with moderate disease severity (FWHM 0.038 ppm, SNR 14). Right panel: the FLAIR image was registered to the 7T single voxel (in white). The spectrum is displayed, (C) for a healthy control (FWHM 0.039 ppm, SNR 24) and (D) for a patient with moderate disease severity (FWHM 0.033 ppm, SNR 25).

MRSI, magnetic resonance spectroscopic imaging; FWHM, full width half maximum; SNR, signal-to-noise ratio

7T SVS

Metabolites were fitted between 0.5 and 4.0 ppm using LCModel with a simulated basis set (based on [27]) for sLASER (TE=34ms) with a measured macromolecular baseline **(Fig 3)**. Spectra were included for analysis if they met the following spectral quality criteria: FWHM < 0.08 ppm, SNR > 7 and CRLB (Glu) < 15%. The same metabolite concentration ratios were calculated as with 3T MRSI (tNAA, tCho, Ins and Glx) with tCr as a reference metabolite. Lac concentrations were too low to measure reliably and therefore excluded.

Statistical analysis

Data were summarized as means with standard deviations (SDs) or medians with interquartile ranges (IQR), depending on the distribution of the data. Normality of the data was assessed by visual inspection and Shapiro-Wilk test for normality.

Baseline differences in metabolite ratios between patients and controls were assessed using Student's *t* test (normally distributed data). Effect sizes were described by measuring Cohen's *d*. For 3T MRSI we also compared metabolite ratios between three groups: controls, asymptomatic patients and symptomatic patients, using one-way ANOVA with post-hoc analysis according to Tukey. Pearson's *R* correlation coefficient (normally distributed data) or Spearman's Rho (non-normally distributed data) was used to calculate the correlation between metabolite ratios and clinical measures. To correct for the influence of age on metabolite ratios, we used multiple linear regression analysis.

For 3T MRSI longitudinal analysis (three time-points) we used longitudinal mixed model analysis to assess differences in metabolite ratios over time and Kruskall Wallis test to assess differences in clinical outcomes between baseline and 2-year follow-up. For 7T SVS longitudinal analysis (two time-points) we used paired t-test to assess differences in clinical parameters and metabolite ratios over time. Differences between metabolite ratios acquired with 3T and 7T were assessed using Bland-Altman method comparison.

For all statistical tests a significance level of α=0.05 (2-sided) was chosen. IBM SPSS Statistics Version 25 was used for statistical analysis.

RESULTS

3T MRSI

Clinical characteristics of patients are described in **Table 1**. In summary, scores on clinical outcome measures indicated moderate disease severity. Thirty-one patients (70%) were scored as symptomatic. The mean age of patients (44.3±16.2) and controls (42.4±17.3) was comparable (p=0.67).

Table 1. Baseline characteristics

Clinical characteristics 3T MRSI	Control (n=32)	Patient (n=44)	Asymptomatic (n=13)	Symptomatic (n=31)
Age, yr	42.4 ± 17.3	44.3 ± 16.2	30.1 ± 13.0	50.2 ± 13.5
EDSS	-	3.5 (1.5-5.5)	1.0 (0.1-1.9)	4.5 (3.3-5.8)
SSPROM	-	86.5 (75.3-97.8)	100 (99-100)	79 (71.5-86.5)
Timed Up-and-Go (s)	-	5.3 (4.1-10.2)	3.7 (3.3-4.2)	8.7 (5.1-10.6)
Vibration score foot	-	2.8 (0.0-5.7)	7.3 (7.0-7.6)	1.8 (1.1-2.4)
Symptomatic myelopathy (%)	-	31 (70%)	-	-

Clinical characteristics 7T SVS	Control (n=17)	Patient (n=18)
Age, yr	45.7 ± 16.4	46.5 ± 15.1
EDSS	-	4.3 (2.9-5.8)
SSPROM	-	85 ± 10.7
Timed Up-and-Go (s)	-	7.8 ± 3.9
Vibration score foot	-	1.1 (0.0-3.8)
Symptomatic myelopathy (%)	-	14 (78%)

Values are displayed as mean ± SD for normally distributed data and median (interquartile range) for non-normally distributed data.
EDSS, Expanded Disability Status Scale; SSPROM, Severity Scoring system for Progressive Myelopathy

Baseline MRI, including MRSI was available for 44 adult patients. Two full MRSI datasets were excluded due to poor quality. The control group consisted of 32 participants, resulting in 32 MRSI datasets, of which none were excluded. Across all included voxels, median FWHM was 0.046 ppm and median SNR was 12.

Between-group differences and clinical correlations

All baseline metabolite ratios measured in the brain WM differed significantly between patients and controls **(Table 2)**. Patients had lower tNAA/tCr and Glx/tCr and higher tCho/tCr and Ins/tCr compared to controls. In the GM, only tNAA/tCr and Glx/tCr differed significantly between groups, and were lower in patients compared to controls. When stratifying patients based on disease severity (asymptomatic versus symptomatic patients), we found that differences in WM metabolite ratios were almost completely explained by the symptomatic subgroup; except for tCho, for which significant differences were found between controls and both patient groups, but not between asymptomatic and symptomatic patients **(Fig 4)**.

All clinical measures showed significant correlations with metabolite ratios **(Fig 5)**. Age was a significant predictor for all metabolite ratios. After correction for age, we found a significant predictive value for SSPROM (B=0.31, p=0.021) and TUG (B=-0.32, p=0.03) on WM tNAA/tCr and for TUG on WM Ins/tCr (B=0.31, p=0.03).

Table 2. Baseline metabolite ratio's

Baseline metabolite ratios 3T MRSI	Control (n=32)	Patient (n=42)	Mean difference (95% CI)	p-value	Effect size (D)
WM tNAA/tCr	1.38 ± 0.10	1.23 ± 0.14	-0.15 (-0.21 to -0.09)	<0.001	1.23
WM tCho/tCr	0.32 ± 0.03	0.35 ± 0.03	0.03 (0.01 to 0.04)	<0.001	1.00
WM Ins/tCr	0.70 ± 0.10	0.81 ± 0.12	0.11 (0.06 to 0.17)	<0.001	0.99
WM Glx/tCr	1.65 ± 0.13	1.51 ± 0.18	-0.13 (-0.21 to -0.06)	0.001	0.89
GM tNAA/tCr	1.01 ± 0.09	0.96 ± 0.10	-0.05 (-0.10 to 0.01)	0.029	0.53
GM tCho/tCr	0.22 ± 0.02	0.21 ± 0.02	-0.01 (-0.02 to 0.00)	0.191	0.50
GM Ins/tCr	0.60 ± 0.08	0.57 ± 0.11	-0.03 (-0.08 to 0.01)	0.150	0.31
GM Glx/tCr	2.19 ± 0.21	2.03 ± 0.21	-0.16 (-0.27 to -0.04)	0.009	0.76
Baseline metabolite ratios 7T SVS	**Control (n=16)**	**Patient (n=18)**	**Mean difference (95% CI)**	**p-value**	**Effect size (D)**
WM tNAA/tCr	1.75 ± 0.16	1.51 ± 0.21	-0.25 (-0.37 to -0.12)	<0.001	1.29
WM tCho/tCr	0.31 ± 0.03	0.34 ± 0.04	0.03 (0.01 to 0.06)	0.006	0.85
WM Ins/tCr	0.78 ± 0.10	0.99 ± 0.17	0.22 (0.11 to 0.32)	<0.001	1.51
WM Glx/tCr	1.00 ± 0.13	0.87 ± 0.12	- 0.13 (-0.22 to -0.05)	0.004	1.03

Values are displayed as mean ± SDs.
Differences between groups are analyzed with Student's t-test.
WM, white matter; GM, grey matter; tNAA, N-acetylaspartate; tCho, choline containing compounds; Ins, inositol; Glx, glutamate+glutamine; tCr, creatine

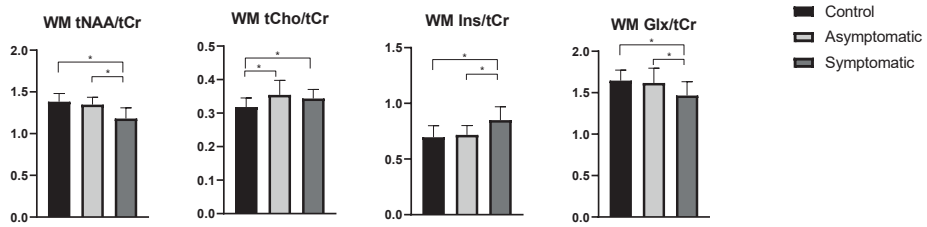

Figure 4. White matter metabolite concentration ratios per group
Bars show WM metabolite ratios measured with 3T MRSI for controls, asymptomatic and symptomatic patients. Differences between groups were analyzed using one-way ANOVA with Tukey's post-hoc analysis. Stars indicate significant differences between groups.
WM, white matter; tNAA, N-acetylaspartate; tCho, choline containing compounds; Ins, inositol; Glx, glutamate and glutamine combined.

Disease progression

Follow-up scans were available for 38 (year 1) and 28 (year 2) patients. The median time between scans was 11 months from baseline to year 1 and from year 1 to year 2. During the entire follow-up only one patient converted from asymptomatic to symptomatic status. All clinical outcome measures, except TUG, could detect disease progression over the 2-year follow-up period. None of the metabolite ratios changed significantly over time. **(Supplementary Table 1)**

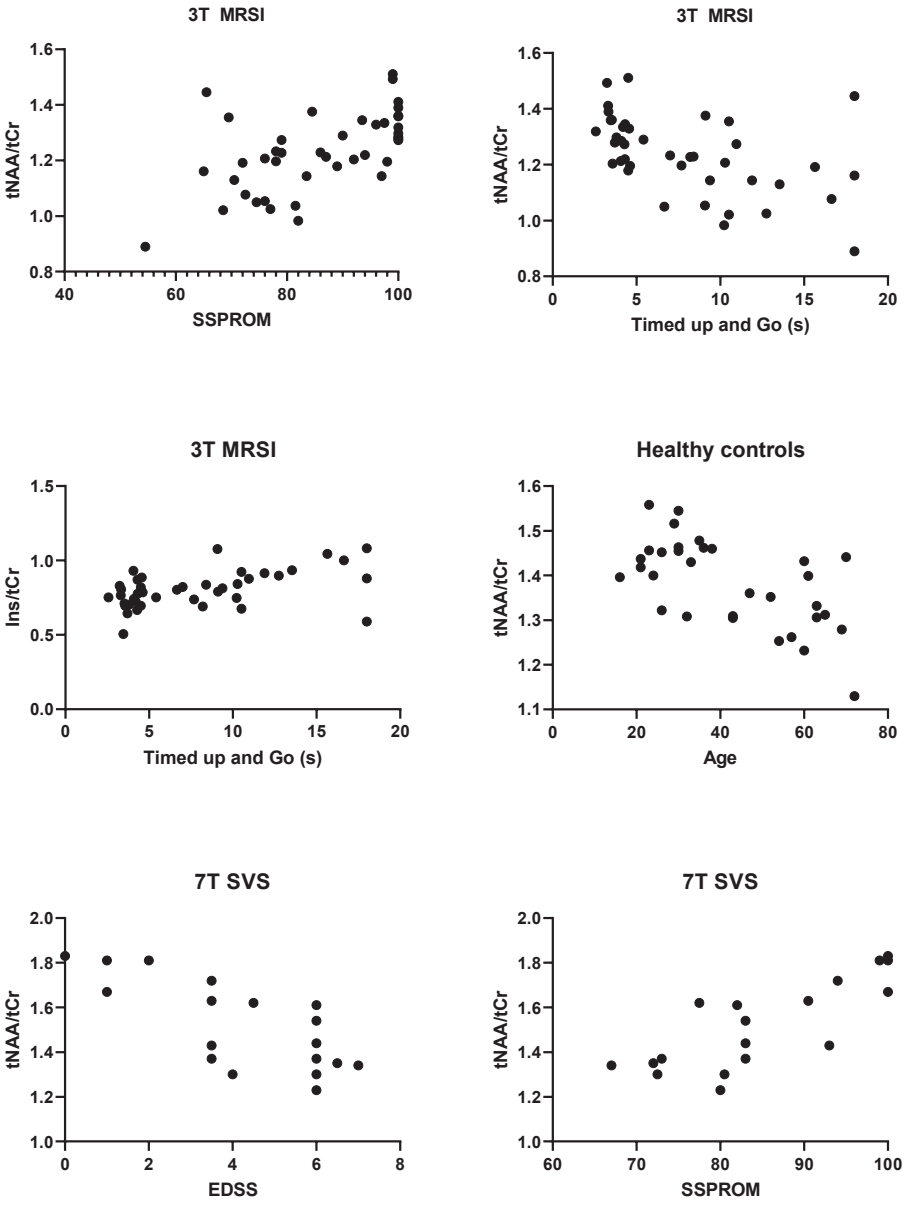

Figure 5. Associations between clinical parameters and metabolite concentration ratios

Scatterplots show associations between clinical outcome measures and 3T MRSI WM metabolite ratios, for (A) SSPROM and tNAA/tCr: r=0.58 p=<0.001; (B) TUG and tNAA/tCr: r=-0.64 p=<0.001; (C) TUG and Ins/tCr: r=0.54 p=0.001 and associations between clinical outcome measures and 7T SVS WM metabolite ratios for (E) EDSS and tNAA/tCr: r=-0.747 p=<0.001; (F) SSPROM and tNAA/tCr: r=0.771 p=<0.001. (D) association between age and WM tNAA/tCr in healthy controls: r=-0.62 p=<0.001.

MRSI, magnetic resonance spectroscopic imaging; WM, white matter; SSPROM, severity scoring system for progressive myelopathy; EDSS, expanded disability status scale; TUG, timed up and go; tNAA, N-acetylaspartate; tCr, creatine; Ins, inositol; SVS, single voxel spectroscopy

7T SVS

Clinical characteristics were similar to the 3T MRSI group **(Table 1)**. The mean age of patients (46.5±15.1) and controls (45.7±16.4) was comparable (p=0.88).

A total of 18 patients underwent 7T imaging twice, resulting in 72 acquired spectra of which 65 were included. Seven spectra were excluded due to poor quality, amongst which three right sided and four left sided spectra. In the control group a total 17 subjects underwent 7T imaging once, resulting in 34 acquired spectra. Three spectra were excluded due to poor quality, of which two spectra belonged to the same subject. For all spectra combined, median FWHM was 0.046 ppm and median SNR was 21. The tissue fraction (GM/WM/CSF) in healthy controls and patients was comparable (0.08/0.91/0.01 versus 0.04/0.96/0.00).

Between-group differences and clinical correlations

All measured baseline metabolite ratios differed significantly between patients and controls. Patients had lower tNAA/tCr and Glx/tCr and higher tCho/tCr and Ins/tCr **(Table 2)**. Due to the small sample size, we were not able to stratify patients into groups based on their symptomatic status.

Significant correlations between metabolite ratios and clinical measures were found between tNAA/tCr and EDSS, SSPROM and vibration score foot and between Ins/tCr and EDSS, SSPROM and vibration score foot **(Fig 5)**. There were no correlations between tCho/tCr or Glx/tCr and clinical outcome measures. Age was a significant predictor for all metabolite ratios. After correction for age, we found a significant predictive value for SSPROM (B= 0.01, p= 0.006) and EDSS (B= -0.05, p= 0.026) on tNAA/tCr and for SSPROM on Ins/tCr (B= -0.01, p= 0.022).

1-year follow-up

Follow-up scans were available for 16 patients. The median time between baseline and follow-up scan was 9 months (IQR 9-10). From the clinical outcome measures only SSPROM was able to detect disease progression after 1 year (mean change -5.2, p=0.004). There was no difference in metabolite ratios between baseline and 1-year follow-up (p>0.05). **(Supplementary Table 2)**

Comparisons between 3T and 7T imaging methods

When comparing metabolite ratios between 3T MRSI and 7T SVS we found a bias of -0.006 ±0.02 (95% limits of agreement from -0.05 to 0.03) for the tCho/tCr levels. The bias for ratio of the difference versus the average was 0.98 ± 0.06 (95% limits of agreement from 0.86 to 1.10) **(Supplementary Figure 1)**. Similar results were found for the other metabolite ratios.

DISCUSSION

In this prospective imaging study, we showed that brain metabolite levels of adult ALD patients without cerebral involvement, measured with 3T MRSI and 7T SVS, have the potential to be utilized as imaging biomarkers in ALD. Metabolite ratios differed between clinically distinct groups and correlate with severity of myelopathy. Although clinical measures demonstrated progression of myelopathy, brain metabolite ratios remained unchanged during the two-year follow-up period.

In adult ALD patients neurodegeneration occurs predominantly in the corticospinal tracts and dorsal columns of the spinal cord and this axonal degeneration is the pathological hallmark of the myelopathy in ALD [14]. Recently, it has been shown that even in cerebral ALD extensive axonal degeneration occurs primarily, followed by a loss of myelin [28]. tNAA and Glu both are markers for axonal damage, and reduced tNAA levels are found in almost all neurodegenerative processes. In the present study, symptomatic patients had significantly lower WM tNAA/tCr and Glx/tCr, compared to controls, corresponding to previous MRS studies in ALD [9,12,13,18]. With the 7T data it was possible to separate Glu and Gln and we observed that the lower Glx/tCr in patients was driven by a decrease in Glu, as Gln was not different between patients and controls (data not shown). Moreover, GM tNAA/tCr and Glx/tCr were also lower compared to controls. Decreased tNAA in the cortex of ALD patients has been described before [18], however, a decrease in cortical Glx/tCr is a novel finding. Our results show that neuronal loss is present throughout the brain – including the GM – of ALD patients and is not confined to the spinal cord and peripheral nerves. Another novel finding is the elevation of Ins/tCr in patients, even in the absence of active inflammation or demyelination. Elevated Ins is generally considered a marker for gliosis [9,19]. In the two previous ALD studies that assessed Ins, significantly increased Ins levels were found only in pediatric and adult patients with active cerebral ALD [9,18], but not in asymptomatic patients or males and females with myelopathy. Our findings suggest that a mild elevation of Ins, as found in this study, is already present in patients without cerebral ALD. In addition to Ins, higher tCho levels are associated with gliosis and indicate processes of active demyelination, inflammation or cell proliferation [29]. In ALD, increased tCho levels have been described in adult and pediatric patients with cerebral ALD [9,18]. In males and females with myelopathy reports are ambiguous, as one study showed no significant elevation of tCho/tCr and another study showed significant elevation only in the frontal white matter [10,12]. In this study, we excluded patients with cerebral ALD and nevertheless found a significant elevation in tCho/tCr in patients. This elevation is probably not a result of demyelination or inflammation as these pathological processes are not ongoing in ALD patients with myelopathy [30,31]. Furthermore, the tCho/tCr ratio was the only metabolite ratio that differed between asymptomatic patients and controls but not between asymptomatic

and symptomatic patients. This suggests that tCho levels are increased in all types of ALD patients, even before symptoms of a myelopathy are present, and may be an early marker for neurodegeneration.

We found the strongest correlations, after adjustment for age, between measures of severity of myelopathy and tNAA/tCr ratios. This confirms that tNAA levels are indeed specific for neuroaxonal damage and are associated with clinical disability. tNAA/tCr ratios may therefore be of potential value as biomarker for severity of myelopathy in ALD. We also found correlations between Ins/tCr and TUG, which has been described before [18]. However, these correlations are measured indirectly, and biomarkers measured directly in the spinal cord – for example magnetization transfer imaging or diffusion tensor imaging [32,33] – may be even more valuable.

Longitudinally, there were no significant changes in metabolite levels. This is probably due to the slow progression of disease in ALD, in which symptoms progress over years to decades.[7] Our findings show that neither 3T MRSI nor 7T SVS was sensitive enough to measure disease progression in ALD in a relatively short follow-up, whereas clinical measures were.

When comparing the two MRS methods, we found that both imaging methods produce similar results **(Supplementary Figure 1)**. In the 7T SVS group we found larger effect sizes for differences between patients and controls for almost all of the metabolite ratios. Additionally, SNR in the 7T SVS group was higher. However, it should be noted that direct comparisons between field strengths are difficult, because of differences in localization methods, timing parameters, field inhomogeneities and relaxation times, and this was not the primary aim of this study.

A limitation of this study is, first, that the follow-up period was relatively short, making it difficult to conclude on the predictive value of MRS on disease progression. Second, the number of available 7T scans was limited as many patients were not eligible or not motivated to participate and we had to exclude a substantial number of spectra in this 7T subgroup, due to poor quality. The quality of the 7T scans may have been compromised due to an accidentally large shim box in some of the scans. Although this may have affected the linewidth of our spectra, the quality of the data was sufficient for metabolite quantification.

We can conclude that, in addition to providing pathophysiological insights into the disease, MRS – and more specifically the tNAA/tCr ratio – is of potential value as imaging biomarker for neurodegeneration in ALD. It should however be noted that the added value to the currently available clinical outcome measures for monitoring disease progression has not been shown. In this homogenous group of ALD males without cerebral involvement we could

not draw conclusions on the value of MRS in predicting disease course. However, MRS may play a promising role in cohorts in which disease course changes, for example in predicting the onset of cerebral ALD or in providing insight into the pathophysiological changes after hematopoietic stem cell transplant. These hypotheses will be evaluated in future studies of our ALD cohort.

REFERENCES

1. Moser HW, Smith KD, Watkins PA, Powers J, Moser AB. X-linked adrenoleukodysotrophy. In: *The Metabolic and Molecular Bases of Inherited Disease*. ; 2001:3257-3302.
2. Kemp S, Huffnagel IC, Linthorst GE, Wanders RJA, Engelen M. Adrenoleukodystrophy - Neuroendocrine pathogenesis and redefinition of natural history. *Nat Rev Endocrinol*. 2016;12. doi:10.1038/nrendo.2016.90
3. Singh I, Moser AB, Moser HW, Kishimoto Y. Adrenoleukodystrophy: Impaired oxidation of very long chain fatty acids in white blood cells, cultured skin fibroblasts, and amniocytes. *Pediatr Res*. 1984;18(3):286-290. doi:10.1203/00006450-198403000-00016
4. Mosser J, Lutz Y, Stoeckel ME, et al. The gene responsible for adrenoleukodystrophy encodes a peroxisomal membrane protein. *Hum Mol Genet*. 1994;3(2):265-271. doi:10.1093/hmg/3.2.265
5. Van Geel BM, Bezman L, Loes DJ, Moser HW, Raymond G V. Evolution of phenotypes in adult male patients with X-linked adrenoleukodystrophy. *Ann Neurol*. 2001;49(2):186-194. doi:10.1002/1531-8249(20010201)49:2<186::AID-ANA38>3.0.CO;2-R
6. Huffnagel IC, Laheji FK, Aziz-Bose R, et al. The natural history of adrenal insufficiency in X-linked adrenoleukodystrophy: an international collaboration. *J Clin Endocrinol Metab*. 2019;104(1). doi:10.1210/jc.2018-01307
7. Huffnagel IC, van Ballegoij WJ, Van Geel BM, MBW Vos J, Kemp S, Engelen M. Progression of myelopathy in males with adrenoleukodystrophy: towards clinical trial readiness. *Brain*. 2019;142(2):334-343. doi:10.1093/brain/awy299
8. Huffnagel IC, Dijkgraaf MGW, Janssens GE, et al. Disease progression in women with X-linked adrenoleukodystrophy is slow. *Orphanet J Rare Dis*. 2019;14(30). doi:10.1186/s13023-019-1008-6
9. Pouwels PJ, Kruse B, Korenke GC, Mao X, Hanefeld FA, Frahm J. Quantitative proton magnetic resonance spectroscopy of childhood adrenoleukodystrophy. *Neuropediatrics*. 1998;29(5):254-264. doi:10.1055/s-2007-973571
10. Fatemi A, Barker PB, Ulug AM, et al. MRI and proton MRSI in women heterozygous for X-linked adrenoleukodystrophy. *Neurology*. 2003;60(8):1301-1307. doi:10.1212/01.wnl.0000059546.15529.cb
11. Rajanayagam V, Grad J, Krivit W, et al. Proton MR spectroscopy of childhood adrenoleukodystrophy. *Am J Neuroradiol*. 1996;17(6):1013-1024.
12. Dubey P, Fatemi A, Barker PB, et al. Spectroscopic evidence of cerebral axonopathy in patients with "pure" adrenomyeloneuropathy. *Neurology*. 2005;64(2):304-310. doi:10.1212/01.WNL.0000149514.13580.84
13. Eichler FS, Itoh R, Barker PB, et al. Proton MR Spectroscopic and Diffusion Tensor Brain MR Imaging in X-linked Adrenoleukodystrophy: Initial Experience. *Radiology*. 2002;225(1):245-252. doi:10.1148/radiol.2251011040
14. Powers JM, DeCiero DP, Ito M, Moser AB, Moser HW. Adrenomyeloneuropathy: A neuropathologic review featuring its noninflammatory myelopathy. *J Neuropathol Exp Neurol*. 2000;59:89-102.
15. Powers JM, DeCiero DP, Cox C, et al. The Dorsal Root Ganglia in Adrenomyeloneuropathy: Neuronal Atrophy and Abnormal Mitochondria. *J Neuropathol Exp Neurol*. 2001;60(5):493-501. doi:10.1093/jnen/60.5.493
16. Eichler FS, Barker PB, Cox C, et al. Proton MR spectroscopic imaging predicts lesion progression on MRI in X-linked adrenoleukodystrophy. *Neurology*. 2002;58(6):901-907. doi:10.1212/WNL.58.6.901

17. Kruse B, Barker PB, van Zijl PCM, Duyn JH, Moonen CTW, Moser HW. Multislice proton magnetic resonance spectroscopic imaging in X-linked adrenoleukodystrophy. *Ann Neurol*. 1994;36(4):595-608. doi:10.1002/ana.410360408

18. Ratai E, Kok T, Wiggins C, et al. Seven-tesla proton magnetic resonance spectroscopic imaging in adult X-linked adrenoleukodystrophy. *Arch Neurol*. 2008;65(11):1488-1494. doi:10.1001/archneur.65.11.1488

19. Öz G, Alger JR, Barker PB, et al. Clinical Proton MR Spectroscopy in Central Nervous System Disorders. *Radiology*. 2014;270(3):658-679. doi:10.1148/radiol.13130531

20. Engelen M, Barbier M, Dijkstra IME, et al. X-linked adrenoleukodystrophy in women: A cross-sectional cohort study. *Brain*. 2014;137(3):693-706. doi:10.1093/brain/awt361

21. Kurtzke JF. Rating neurologic impairment in multiple sclerosis. *Neurology*. 1983;33(11):1444 LP - 1444. doi:10.1212/WNL.33.11.1444

22. Castilhos RM, Blank D, Netto CBO, et al. Severity score system for progressive myelopathy: development and validation of a new clinical scale. *Brazilian J Med Biol Res*. 2012;45(7):565-572. doi:10.1590/S0100-879X2012007500072

23. Podsiadlo D, Richardson S. The Timed "Up & Go": A Test of Basic Functional Mobility for Frail Elderly Persons. *J Am Geriatr Soc*. 1991;39(2):142-148. doi:10.1111/j.1532-5415.1991.tb01616.x

24. Gruetter R. Automatic, localized in vivo adjustment of all first- and second-order shim coils. *Magn Reson Med*. 1993;29(6):804-811. doi:10.1002/mrm.1910290613

25. Arteaga de Castro CS, Boer VO, Andreychenko A, et al. Improved efficiency on editing MRS of lactate and γ-aminobutyric acid by inclusion of frequency offset corrected inversion pulses at high fields. *NMR Biomed*. 2013;26(10):1213-1219. doi:10.1002/nbm.2937

26. Provencher SW. Estimation of metabolite concentrations from localized in vivo proton NMR spectra. *Magn Reson Med*. 1993;30(6):672-679. doi:10.1002/mrm.1910300604

27. Govindaraju V, Young K, Maudsley AA. Proton NMR chemical shifts and coupling constants for brain metabolites. *NMR Biomed*. 2000;13(3):129-153. doi:10.1002/1099-1492(200005)13:3<129::AID-NBM619>3.0.CO;2-V

28. Bergner CG, Genc N, Hametner S, et al. Concurrent axon and myelin destruction differentiates X-linked adrenoleukodystrophy from multiple sclerosis. 2021;(May):1-16. doi:10.1002/glia.24042

29. Mader I, Rauer S, Gall P, Klose U. 1H MR spectroscopy of inflammation, infection and ischemia of the brain. *Eur J Radiol*. 2008;67(2):250-257. doi:https://doi.org/10.1016/j.ejrad.2008.02.033

30. Schaumburg HH, Powers JM, Raine CS, et al. Adrenomyeloneuropathy: a probable variant of adrenoleukodystrophy. II. General pathologic, neuropathologic, and biochemical aspects. *Neurology*. 1977;27(12):1114-1119. doi:10.1212/wnl.27.12.1114

31. Engelen M, Kemp S, Poll-The BT. X-linked adrenoleukodystrophy: Pathogenesis and treatment. *Curr Neurol Neurosci Rep*. 2014;14(486). doi:10.1007/s11910-014-0486-0

32. Huffnagel IC, van Ballegoij WJ, Vos JM, Kemp S, Caan MW, Engelen M. Longitudinal diffusion MRI as surrogate outcome measure for myelopathy in adrenoleukodystrophy. *Neurology*. 2019;93:1-12. doi:10.1212/WNL.0000000000008572

33. Fatemi A, Smith SA, Dubey P, et al. Magnetization transfer MRI demonstrates spinal cord abnormalities in adrenomyeloneuropathy. *Neurology*. 2005;64(10):1739-1745. doi:10.1212/01.WNL.0000164458.02141.06

Supplementary Table 1. Longitudinal 3T MRSI analysis

Metabolite ratios	Baseline (n=42)	Year 1 (n=38)	Year 2 (n=28)	Mean difference (95% CI) Baseline – Year 2	p-value
WM tNAA/tCr	1.23 ± 0.14	1.21 ± 0.25	1.22 ± 0.15	-0.01 (-0.03 to 0.02)	0.823
WM tCho/tCr	0.35 ± 0.03	0.33 ± 0.06	0.33 ± 0.03	-0.01 (-0.02 to -0.01)	0.140
WM Ins/tCr	0.81 ± 0.12	0.78 ± 0.18	0.81 ± 0.13	0.00 (-0.03 to 0.03)	0.625
WM Glx/tCr	1.51 ± 0.18	1.45 ± 0.28	1.54 ± 0.19	0.02 (-0.09 to 0.05)	0.236

Disease progression	Baseline (n=32)	Year 2 (n=32)	Mean difference (95% CI)	p-value
EDSS	3.5 (1.3-5.7)	4.0 (2.1-6.0)	0.33 (0.08 to 0.58)	0.01
SSPROM	85.3 (73.4-97.3)	83.0 (69.1-97.0)	-2.1 (-3.8 to -0.3)	0.024
Timed Up-and-Go (s)	4.5 (1.8-7.2)	5.4 (2.6-8.2)	0.32 (-0.1 to 0.75)	0.182
Vibration score foot	3.8 (0.9-6.6)	3.4 (0.3-6.5)	-0.47 (-0.81 to -0.13)	0.008

Values are displayed as mean ± SD or median (interquartile ranges)
Differences between groups are analyzed with Kruskal Wallis test or longitudinal mixed models

Supplementary Table 2. Longitudinal 7T SVS analysis

Metabolite ratios follow-up	Baseline (n=16)	Year 1 (n=16)	Difference (95% CI)	p-value
WM tNAA/tCr	1.49 ± 0.20	1.46 ± 0.19	-0.03 (-0.07 to 0.01)	0.109
WM Ins/tCr	0.34 ± 0.04	0.34 ± 0.03	0.00 (-0.01 to 0.01)	0.688
WM tCho/tCr	0.98 ± 0.17	1.02 ± 0.19	0.04 (-0.02 to 0.10)	0.161
WM Glx/tCr	0.87 ± 0.12	0.86 ± 0.12	-0.01 (-0.07 to 0.05)	0.740

Disease progression	Baseline (n=18)	Year 1 (n=18)	Difference (95% CI)	p-value
EDSS	4.2 ± 2.1	4.4 ± 2.1	0.19 (-0.1 to 0.5)	0.109
SSPROM	85.0 ± 10.7	79.8 ± 14.7	-5.2 (-8.5 to -1.9)	0.004
Timed Up-and-Go (s)	7.8 ± 3.9	8.0 ± 3.8	0.25 (-0.5 to 1.0)	0.148
Vibration score foot	1.1 (0.0-3.8)	0.9 (0.0-3.4)	-0.12 (-0.47 to 0.22)	0.463

Values are displayed as mean ± SD or median (interquartile ranges)
Differences between groups are analyzed with Paired t-test or Wilcoxon signed rank test

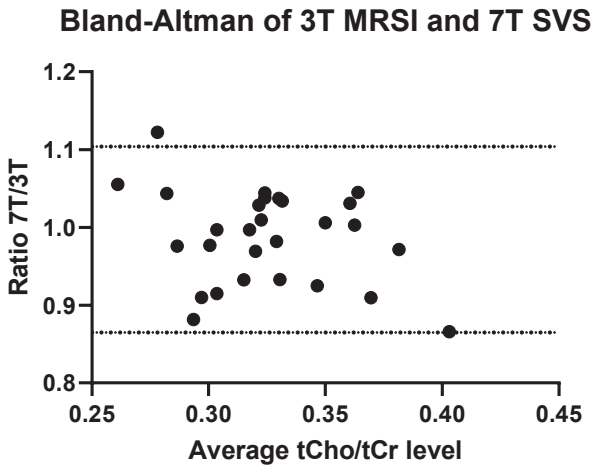

Supplementary Figure 1.
Bland-Altman plot of the 3T MRSI method versus the 7T SVS method showing the average tCho/tCr concentration on the x-axis versus the ratio of 7T/3T acquired tCho/tCr metabolite levels on the y-axis. 95% limits of agreement are shown with dotted lines (0.86 to 1.10).
MRSI, magnetic resonance spectroscopic imaging; SVS, single voxel spectroscopy; tCho, choline; tCr, creatine.

V General discussion and summary

10 General discussion

As described in this thesis and previous research, the clinical spectrum of ALD is broad and the disease is unpredictable in individual cases. A diagnosis of ALD is an immense burden for patients and their families. It means a lifetime of insecurity and hospital visits, not only for individuals with the genetic defect but also for their (unborn) children. Male ALD patients are at risk of developing cerebral ALD, adrenal insufficiency and testicular dysfunction and virtually all patients, male and female, will eventually develop a progressive and invalidating myelopathy.[1–6] For male patients the standard of care now includes yearly – or twice yearly when <12 years of age – hospital visits[7] including brain MRI and consultation by a neurologist and endocrinologist, even though some patients will never develop (all of) these signs. For those patients experiencing signs of a myelopathy, no curative treatment is available yet, although therapeutic options are under development. In order to determine efficacy of these new treatments, better measures for monitoring disease severity are needed. With the studies described in this thesis, we first aimed to gain more insight in disease course of individual patients by describing various clinical, biochemical and MRI aspects of the ALD spectrum. Second, we aimed to develop sensitive (surrogate) outcome measures to be used in clinical trials, by investigating several clinical, biochemical and MRI measures.

Towards more personalized health care

We currently lack biomarkers able to predict disease course for patients with ALD, not only for predicting if certain disease signs will occur (for instance leukodystrophy or adrenal insufficiency) but also for predicting the rate of disease progression. This information would improve patient care (better counseling and follow-up) and clinical trials (stratification of patients in groups with comparable disease progression). To develop these predictive and prognostic biomarkers, 'deep phenotyping' of ALD patients, to better understand disease manifestations and evolution over time, is necessary **(Fig. 1)**. Deep phenotyping can be described as a precise and comprehensive analysis of phenotypic abnormalities, in which the individual components of the phenotype are observed and described.[8] In this way, the studies in **chapters 2, 3, 4 and 6** of this thesis are conducted, where various ALD phenotypes are described for which we can now provide different or more specific advise for follow-up as compared to the standard of care.

First, in **chapter 3** we described a cohort of male patients who developed cerebral ALD, but with spontaneously arrested lesion progression (arrested cerebral ALD). This phenomenon was always considered to be rare[9], but now appears to occur in approximately 12% of all ALD patients – mainly adolescent or adult. This means that for adults with cerebral ALD, follow-up should be different from follow-up in children, because progression of cerebral demyelination in adults is often slower than in children and cerebral abnormalities will more often spontaneously arrest. So instead of immediate referral for bone marrow trans-

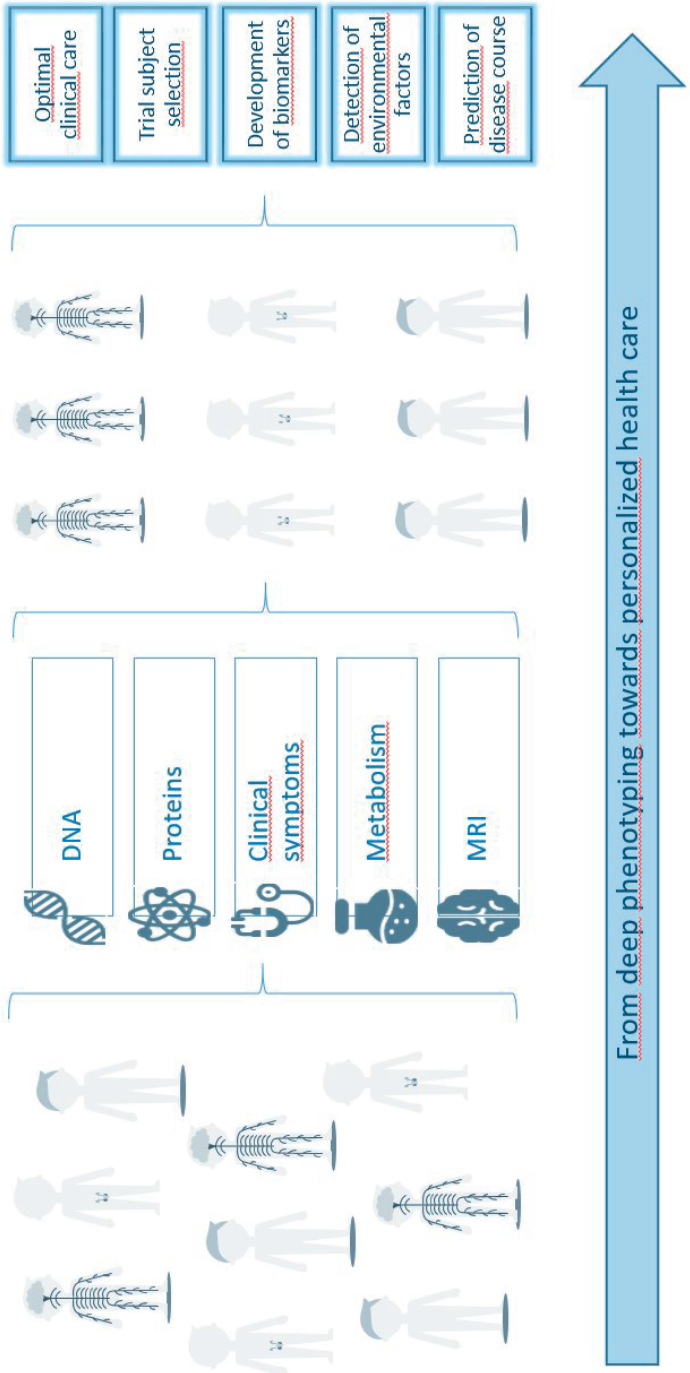

Figure 1: Deep phenotyping in adrenoleukodystrophy. Individual components of various phenotypes are described which leads to comprehensive classification and analysis of the phenotypic abnormalities, providing information for more personalized health care and follow-up

plantation, there may be time to closely monitor lesion progression with frequent MRI-examinations and gadolinium administration in adults. Additionally, in the case of an adult male with cerebral ALD, levels of neurofilament light (NfL) **(Chapter 7)** can be determined in plasma. Based on our own experience (data not published), we hypothesize that if NfL levels are low (i.e. within the range of patients with only a myelopathy), active cerebral ALD is less probable and bone marrow transplantation is not (yet) necessary. This hypothesis has recently been confirmed by a large multi-center study in which elevated levels of NfL were highly associated with activity and progression of cerebral demyelination.[10] Second, in **chapter 4** we showed that screening for hypogonadism should be performed in adult males with sexual dysfunction (such as erectile dysfunction and/or diminished libido). However, no screening is necessary in males without sexual dysfunction, in contrast to screening for adrenal insufficiency which should be performed yearly, even in the absence of symptoms.[2] Based on testosterone and gonadotropin levels, patients can receive targeted therapies, for example, testosterone replacement therapy in case of testosterone deficiency, or sildenafil when testosterone levels are normal and a severe myelopathy is the main cause of the sexual dysfunction. In **chapter 6** we showed that, in case of difficulties in establishing an ALD diagnosis due to a negative family history and a variant of unknown significance (VUS) in *ABCD1*, functional studies in fibroblasts can provide clarification. With the array of tests described, we were able to classify variants as likely pathogenic or benign, making an ALD diagnosis more or less likely. This means that not all individuals with a variant in *ABCD1* automatically have ALD, and individuals unlikely to have ALD do not have to visit the hospital for yearly follow-up. Individuals with slightly abnormal results of these tests can be offered a less frequent follow-up, or, since they may be less likely to develop symptoms of ALD at all, only at the moment of symptom onset.

Linking detailed clinical data from a well-characterized cohort of deep-phenotyped patients with biochemical, genetic and imaging studies will hopefully lead to the detection of useful predictive biomarkers. A useful predictive biomarker enables the identification of patients at risk of developing certain clinical signs and symptoms. These can for example be found in detailed complex lipids analysis (i.e. lipidomics)[11] and quantitative MRI techniques such as neurite orientation dispersion and density imaging and myelin water fraction imaging, as described in **chapter 2** of this thesis.

Development of surrogate outcome measures

There is an unmet need for better outcome measures to monitor disease severity in clinical trials. As stated before, the currently used clinical outcome measures such as EDSS, SSPROM and 6 minute walk test, require trials with large numbers of patients and long follow-up.[1] These clinical outcome measures are susceptible to day-to-day variability (for instance due to factors not related to the disease being studied) and 'floor- and ceiling effects' (meaning

that changes in patients at the extremes of the clinical spectrum cannot be measured, i.e. patients who cannot walk cannot undergo a 6-minute walk test). This means that some patients will not be eligible to participate in clinical trials, which is especially problematic when studying rare diseases. New surrogate outcome measures should overcome these disadvantages. They are more disease specific, if they are able to directly measure the underlying pathology, and they may be more sensitive (i.e. eligible for patients over the whole spectrum of disease severity), which may result in shorter follow-up in clinical trials. However, these surrogate outcome measures may lack clinical relevance for the patient. Our ALD research group has recently shown that optical coherence tomography (OCT – a non-invasive tool for analysis of the retinal and peripapillary nerve fiber layer) and diffusion tensor imaging (DTI – an MRI technique for evaluation of white matter microstructural properties) may be of value for sensitively measuring severity and progression of the myelopathy in ALD.[12–14] We expanded on this work, and described new potential surrogate outcome measures in **chapters 5, 7, 8 and 9** of this thesis, which all meet various aspects of the abovementioned criteria **(see Table 1)**.

Table 1: Surrogate outcome measures and their characteristics

	Clinically relevant	Small or no floor/ceiling effect	Low variability*	Disease specific	Easy to measure
Postural body sway	+	+	+/-	+/-	+/-
NfL	-	+	+	-	+
CSA	-	+/-	+	+	-
MRS	-	+/-	+	-	-

** day-to-day or intra-/ interrater*
NfL: neurofilament light; CSA: cross-sectional area; MRS: magnetic resonance spectroscopy

For instance, a feature of postural body sway measurement **(chapter 5)** is that it may be a clinically relevant outcome measure since balance disturbance is one of the main causes of disability in ALD.[15] However, this also means there is still a 'ceiling effect' as severely affected or wheelchair-bound patients cannot perform the test. On the other hand, with postural body sway measurement it is possible – in contrast to the clinical outcome measures – to detect abnormalities in otherwise asymptomatic patients. This means there is little or no 'floor effect'. On the contrary, NfL **(chapter 7)** may be considered less clinically relevant (because it does not directly reflect any of the ALD symptoms) and is not disease-specific because it may be elevated in case of recent head trauma or other neurodegenerative diseases,[16] but elevated NfL is an important marker of neuroaxonal damage in many neurodegenerative diseases[17] and NfL reflects recent neurodegeneration (the estimated half-life is a number of days).[18] Therefore, NfL has potential to relatively easy measure efficacy of disease modifying treatment on short term (i.e. without long follow-up). A possibly more

disease-specific marker is the spinal cord cross-sectional area (CSA) measured with MRI **(chapter 8)**. CSA correlates with severity of myelopathy and disease duration in ALD and the flattened aspect of the spinal cord in symptomatic ALD patients shows that the atrophy is probably initiated by degeneration of specifically the dorsal columns and corticospinal tracts, which are responsible for the myelopathy in ALD. Asymptomatic patients, however, do not have atrophy yet, so CSA probably only changes after clinical signs become apparent which means that CSA is not valuable in patients without clinical signs of disease (i.e. there is still a 'floor effect'). An important feature of MRI-based outcome measures is that there is less or no intra-/interrater or day-to-day variability in the measurement, which is also true for Magnetic Resonance Spectroscopy (MRS) **(chapter 9)**. The most promising of the MRS acquired metabolites (*N*-acetylaspartate) is, however, decreased in many neurodegenerative diseases[19] and therefore not disease specific. Also, in our study all MRI-based markers did not change over 1- or 2 year follow-up, where clinical measures do.

Unfortunately, none of the above mentioned surrogate outcome measures proves to be superior over the currently used clinical outcomes. Most likely, a combination of a clinically relevant measure and multiple more sensitive surrogate outcome measures may be valuable for assessing treatment efficacy in clinical trials.

The importance of interdisciplinary collaboration

In general, the studies presented in this thesis show that research in patients with ALD involves various disciplines, including (pediatric) neurology, endocrinology, radiology (including MR physics), and biochemistry (including laboratory specialist). Less visible in this thesis, but of great importance, is the pharma industry. At this moment, pharmaceutical companies are very interested in ALD, probably as a result of the comprehensive description of the natural history of the disease and the development and implementation of new outcome measures, meaning they put a lot of effort in the development of new possible treatments. For improvement of clinical trial feasibility and personalized health care, as presented in this thesis, a good collaboration between all the different disciplines is required. This may sometimes seem difficult in a culture where every expert takes care of their own sub specialism. Therefore, it may be of value to deploy (local) ALD specialist units, which can exchange information with (inter)national ALD specialist units. **(Fig. 2)**

A large collaboration between these units may aid in setting up larger international studies, or registries, to create more follow-up data and sufficient patient inclusion in clinical trials, which is challenging in a rare disease like ALD. Such collaborative networks would also improve the development of surrogate outcome measures and clinical trial design, perhaps making even factorial trials possible. First efforts have already been made in this area – including the first international clinical trial in drug development for the ALD myelopa-

thy and the first international observational cohort study. Additionally, an international consortium would improve clinical care in ALD. Some international collaborations have already proven their value, for example the implementation of ALD in the Dutch newborn screening program[20], resulting in pre-symptomatic detection of ALD patients and families facilitating early treatment when necessary. Moreover, the ALD guideline is conducted through different consensus meetings with experts from different countries in Europe and the United States. This guideline will soon be published, which is an important step towards harmonizing care and follow-up worldwide. A significant part of this thesis was conducted via international collaborations and thereby contributed to better understanding of the disease course of ALD and development of new surrogate outcome measures. In the future, we hope these collaborations continue to exists, expand and further provide new insights in ALD.

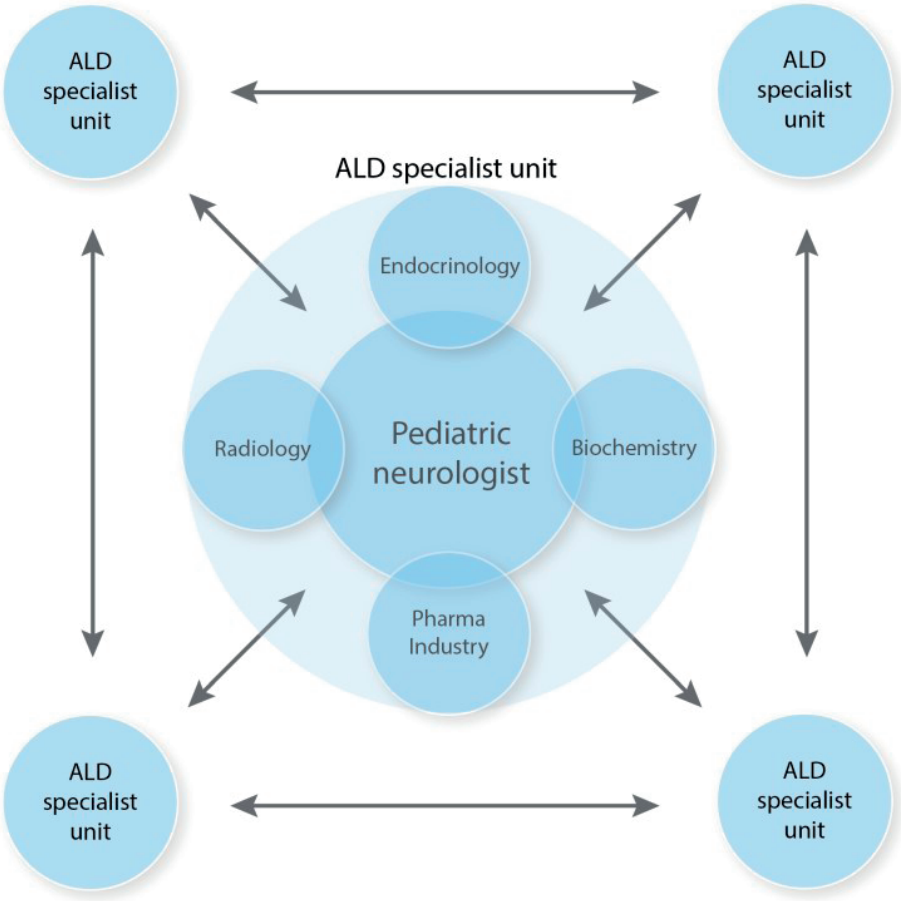

Figure 2: Collaboration between ALD specialist units. These units include various disciplines and experts and should exchange knowledge and information in order to improve ALD research and clinical care.

References

1. Huffnagel IC, van Ballegoij WJ, Van Geel BM, MBW Vos J, Kemp S, Engelen M. Progression of myelopathy in males with adrenoleukodystrophy: towards clinical trial readiness. *Brain*. 2019;142(2):334-343. doi:10.1093/brain/awy299
2. Huffnagel IC, Laheji FK, Aziz-Bose R, et al. The natural history of adrenal insufficiency in X-linked adrenoleukodystrophy: an international collaboration. *J Clin Endocrinol Metab*. 2019;104(1). doi:10.1210/jc.2018-01307
3. Assies J, Gooren LJG, Van Geel B, Barth PG. Signs of testicular insufficiency in andrenomyeloneuropathy and neurologically asymptomatic X-linked adrenoleukodystrophy: A retrospective study. *Int J Androl*. 1997;20(5):315-321. doi:10.1046/j.1365-2605.1997.00066.x
4. De Beer M, Engelen M, Van Geel BM. Frequent occurrence of cerebral demyelination in adrenomyeloneuropathy. *Neurology*. 2014;83(24):2227-2231. doi:10.1212/WNL.0000000000001074
5. Van Geel BM, Bezman L, Loes DJ, Moser HW, Raymond G V. Evolution of phenotypes in adult male patients with X-linked adrenoleukodystrophy. *Ann Neurol*. 2001;49(2):186-194. doi:10.1002/1531-8249(20010201)49:2<186::AID-ANA38>3.0.CO;2-R
6. Huffnagel IC, Dijkgraaf MGW, Janssens GE, et al. Disease progression in women with X-linked adrenoleukodystrophy is slow. *Orphanet J Rare Dis*. 2019;14(30). doi:10.1186/s13023-019-1008-6
7. Engelen M, Kemp S, De Visser M, et al. X-linked adrenoleukodystrophy (X-ALD): clinical presentation and guidelines for diagnosis, follow-up and management. *Orphanet J Rare Dis*. 2012;7(51). http://www.ojrd.com/content/7/1/51.
8. Delude CM. The details of disease (deep phenotyping). *Nature*. 2015;527:14-15.
9. Moser HW, Loes DJ, Melhem ER, et al. X-Linked Adrenoleukodystrophy: Overview and Prognosis as a Function of Age and Brain Magnetic Resonance Imaging Abnormality. A Study Involving 372 Patients. *Neuropediatrics*. 2000;31(5):227-239. doi:10.1055/s-2000-9236
10. Weinhofer I, Rommer P, Zierfuss B, et al. Neurofilament light chain as a potential biomarker for monitoring neurodegeneration in X-linked adrenoleukodystrophy. *Nat Commun*. 2021;12(1). doi:10.1038/s41467-021-22114-2
11. Honey MIJ, Jaspers YRJ, Engelen M, Kemp S, Huffnagel IC. Molecular Biomarkers for Adrenoleukodystrophy: An Unmet Need. *Cells*. 2021;10(12):3427. doi:10.3390/cells10123427
12. van Ballegoij WJC, Kuijpers SC, Huffnagel IC, et al. Optical coherence tomography shows neuroretinal thinning in myelopathy of adrenoleukodystrophy. *J Neurol*. 2019;267(3):679-687. doi:10.1007/s00415-019-09627-z
13. van Ballegoij WJC, Huffnagel IC, van de Stadt SIW, et al. Optical coherence tomography to measure the progression of myelopathy in adrenoleukodystrophy. *Ann Clin Transl Neurol*. 2021;8(5):1064-1072. doi:10.1002/acn3.51349
14. Huffnagel IC, van Ballegoij WJ, Vos JM, Kemp S, Caan MW, Engelen M. Longitudinal diffusion MRI as surrogate outcome measure for myelopathy in adrenoleukodystrophy. *Neurology*. 2019;93:1-12. doi:10.1212/WNL.0000000000008572
15. Powers JM, DeCiero DP, Ito M, Moser AB, Moser HW. Adrenomyeloneuropathy: A neuropathologic review featuring its noninflammatory myelopathy. *J Neuropathol Exp Neurol*. 2000;59:89-102.

16. Bridel C, Van Wieringen WN, Zetterberg H, et al. Diagnostic Value of Cerebrospinal Fluid Neurofilament Light Protein in Neurology: A Systematic Review and Meta-analysis. *JAMA Neurol*. 2019;76(9):1035-1048. doi:10.1001/jamaneurol.2019.1534
17. Khalil M, Teunissen CE, Otto M, et al. Neurofilaments as biomarkers in neurological disorders. *Nat Rev Neurol*. 2018;14(10):577-589. doi:10.1038/s41582-018-0058-z
18. Thelin EP, Zeiler FA, Ercole A, et al. Serial Sampling of Serum Protein Biomarkers for Monitoring Human Traumatic Brain Injury Dynamics: A Systematic Review. *Front Neurol*. 2017;8:300. doi:10.3389/fneur.2017.00300
19. Oz G, Alger JR, Barker PB, et al. Clinical proton MR spectroscopy in central nervous system disorders. *Radiology*. 2014;270(3):658-679. doi:10.1148/radiol.13130531
20. Barendsen RW, Dijkstra IME, Visser WF, et al. Adrenoleukodystrophy Newborn Screening in the Netherlands (SCAN Study): The X-Factor. *Front Cell Dev Biol*. 2020;8(June):1-12. doi:10.3389/fcell.2020.00499

11 Summary

CLINICAL, BIOCHEMICAL AND RADIOLOGICAL INSIGHTS IN ADRENOLEUKODYSTROPHY

Part I – Introduction

X-linked adrenoleukodystrophy (ALD) is an inherited metabolic disorder caused by mutations in the *ABCD1* gene, located on the X-chromosome. Pathologic mutations cause dysfunction of ALD protein (ALDP) resulting in impaired peroxisomal beta-oxidation of very long chain fatty acids (VLCFA), which subsequently results in accumulation of VLCFA in plasma and tissues. Clinically, ALD is characterized by a variation of signs and symptoms, including a slowly progressive and invalidating myelopathy in all male and most female patients, adrenal insufficiency, cerebral leukodystrophy and hypogonadism. Genotype-phenotype correlations are lacking, and environmental factors as well as multiple genetic modifiers are involved in the development of symptoms. Therefore, age of symptom onset and rate of disease progression are highly unpredictable. In order to predict disease course for individual patients it is important to first describe the natural history and individual symptoms of ALD in more detail. Additionally, for patients suffering from a myelopathy, merely supportive treatment is available, as disease modifying therapies are still under development. In order to evaluate potential new therapies in clinical trials, it is of importance to adequately quantify severity of myelopathy. But the currently used clinical outcome measures are not sensitive enough and require many patients and long follow-up, which is challenging in a rare disease like ALD. In this thesis we aimed to provide answers to the abovementioned issues and focused on a twofold objective. First, to gain more insight in the natural history of ALD, with the aim of predicting disease course for individual patients, and second, to develop sensitive (surrogate) outcome measures, able to monitor severity of myelopathy, making clinical trials in ALD feasible.

Imaging in ALD

Approximately 60% of patients with ALD develop a cerebral leukodystrophy (cerebral ALD) during the course of their disease. The largest risk of developing cerebral ALD is <7 years of age but cerebral ALD can also occur in adolescence or adulthood. In **chapter 2** we reviewed the different imaging possibilities for cerebral abnormalities. *In vivo* images of cerebral lesions in ALD patients were first provided in the 1970s via computed tomography (CT) but currently magnetic resonance imaging (MRI) is the gold standard for detection of cerebral lesions. Cerebral ALD lesions often present as T2-hyperintense confluent lesions, predominantly in the splenium of corpus callosum with eventually progression to the entire cerebral white matter when left untreated. Although structural MRI can detect the presence and extent of cerebral lesions, it does not predict if and when cerebral ALD will occur. Possibly quantitative imaging techniques, such as neurite orientation dispersion and density

imaging (NODDI) and myelin water fraction imaging (MWF), may be promising in that respect and should be used for future research purposes.

Part II – Clinical studies

In some cases, cerebral ALD spontaneously stops progressing (arrested cerebral ALD). Until recently this was considered to be rare, however in **chapter 3** we showed that arrested cerebral ALD actually occurs relatively often (12.4% of all ALD cases). Arrested cerebral ALD lesions can occur at various ages (childhood, adolescent and adult) and remain stable in the majority of patients, but can still convert to progressive cerebral ALD in some cases. Therefore, patients with arrested cerebral ALD still need to be monitored closely, clinically and with MRI. Patients with ALD also often experience signs of sexual dysfunction (erectile dysfunction and/or diminished libido). In **chapter 4** we described these signs and symptoms and their relation to myelopathy and hypogonadism. In this study the majority of patients (56%) experienced sexual dysfunction, and most of them had normal testosterone levels. Neurological function on the other hand plays a much more important role in these complaints than previously appreciated. For both causes of sexual dysfunction – hypogonadism and myelopathy – suitable treatment options are available. In order to start early treatment, sexual dysfunction should be discussed regularly and, if present, screening for hypogonadism needs to be performed. In **chapter 5** we discussed a clinically relevant surrogate outcome measure for the myelopathy in ALD: postural body sway. For patients with ALD balance disturbance is one of the main causes of disability, and by measuring postural body sway it is possible to quantify the patients' balance. Body sway was significantly higher in both asymptomatic and symptomatic patients compared to controls, and correlated with clinical measures of disease severity in the symptomatic patients. Therefore, postural body sway can serve as a potentially more sensitive outcome measure in clinical trials for ALD.

Part III – Biochemical studies

In most cases diagnosing ALD is relatively straightforward, but sometimes this can be more challenging. For example in (newborn) cases, with a variant of unknown significance (VUS) in the *ABCD1* gene, where family history of ALD is negative and VLCFA are only mildly elevated. In these cases, functional testing in fibroblasts can provide more certainty. We described these functional tests in **chapter 6** and created ALD and reference ranges, with the aim of diagnosing 17 included VUS cases. By using this information, we could classify 88% of the variants as likely pathogenic or benign, making an ALD diagnosis more or less likely. This is of importance as in the future more VUS cases will be found, for which we can now use these tests to aid in diagnosing ALD. In **chapter 7** we explored the potential of neurofilament light (NfL) and glial fibrillary acidic protein (GFAP) as biomarkers for spinal cord degeneration in ALD. Both NfL and GFAP were significantly elevated in male and female patients compared to healthy controls. Only NfL levels were associated with severity

of myelopathy in male patients, GFAP levels (in both male and female patients) were not. Because of the short half-life of NfL (a couple of days), it is possible to monitor disease activity with NfL, which suggests that plasma NfL could serve as biomarker for monitoring the effect of a disease modifying treatment, with a short follow-up.

Part IV – Imaging studies

In addition to structural MRI – for diagnosing anatomical abnormalities – quantitative MRI can provide more detailed physical or chemical information. In ALD patients structural MRI of the spinal cord usually does not reveal any abnormalities, however, by measuring the spinal cord cross-sectional area (CSA) we have shown that significant differences between patients and controls are present (**chapter 8**). ALD patients have a thinner and flatter (reduced antero-posterior diameter) cervical spinal cord, probably due to degeneration of the corticospinal tracts and dorsal columns. CSA is correlated with clinical measures of disease severity and disease duration, suggesting it could be a potential surrogate outcome measure. Another surrogate outcome measure, Magnetic Resonance Spectroscopy (MRS), was explored in **chapter 9**. In this large longitudinal study we measured cerebral metabolite levels in ALD patients without cerebral demyelination, with two MRS protocols (7T single voxel spectroscopy and 3T magnetic resonance spectroscopic imaging) over a period of three years. Both protocols showed decreased concentrations of N-acetylaspartate (tNAA) and glutamine + glutamate (Glx) and increased concentrations of Choline containing compounds (Cho) and Creatine (tCr) in ALD patients compared to controls. Only tNAA/tCr ratios correlated with clinical measures of disease severity and may be of potential value as surrogate outcome measure in clinical trials.

Part V – Discussion

Currently, we still lack biomarkers that aid in predicting disease course for individual ALD patients. In order to develop these predictive and prognostic biomarkers 'deep phenotyping' of ALD patients is necessary. Deep phenotyping can be described as a precise and comprehensive analysis of phenotypic abnormalities. With this method we conducted the first chapters of this thesis, which resulted in a different or more specific advise on follow-up in various patient groups as compared to the standard of care. In the future, linking detailed clinical data from a well-characterized cohort of deep-phenotyped patients with biochemical, genetic and imaging studies will hopefully lead to the detection of useful predictive biomarkers.

Furthermore, there is an unmet need for better outcome measures to monitor disease severity in clinical trials. The currently used clinical outcome measures are susceptible for day-to-day variability and floor- and ceiling effects. This means that, by using these outcome measures, clinical trials would require large numbers of patients and long follow-

up, which is problematic in a rare disease like ALD. New surrogate outcome measures should overcome these disadvantages. For example, body sway analysis provides a clinically relevant outcome measure with minimal or no 'floor effect', plasma NfL is easy to measure and reflects recent neurodegeneration which makes it suitable as short term measure of disease activity, and MR based outcome measures (CSA and tNAA) are less susceptible for day-to-day variability. A combination of these surrogate outcome measures can be valuable for assessing treatment efficacy in clinical trials.

The studies presented in this thesis show that research in patients with ALD involves various disciplines. Good communication between different disciplines is required for improvement of personalized health care and clinical trial feasibility. A large collaboration between different (international) ALD specialist centers can aid in setting up larger international studies, creating more follow-up data and sufficient patient inclusion in clinical trials. This would also further improve the development of surrogate outcome measures and subsequently clinical trial designs. Recent collaborations have already shown their value, for example in the implementation of ALD in the Dutch newborn screening program and the development of an international ALD guideline. A large part of this thesis was conducted via international collaborations and thereby aided in better understanding of the disease course of ALD and development of new surrogate outcome measures. We hope these collaborations will continue to exist and expand in the future.

A

Nederlandse samenvatting
List of publications
Contributing authors and affiliations
PhD portfolio
About the author
Dankwoord

NEDERLANDSE SAMENVATTING

KLINISCHE, BIOCHEMISCHE EN RADIOLOGISCHE INZICHTEN IN ADRENOLEUKODYSTROFIE

Deel I – introductie

X-gebonden adrenoleukodystrofie (ALD) is een erfelijke stofwisselingsziekte die wordt veroorzaakt door mutaties in het *ABCD1*-gen, dat zich op het X-chromosoom bevindt. Pathologische mutaties veroorzaken disfunctie van het ALD-eiwit (ALDP), wat een gestoorde peroxisomale bèta-oxidatie van zeer lange keten vetzuren (ZLKV) veroorzaakt, dit resulteert vervolgens in accumulatie van ZLKV in plasma en weefsels. Klinisch wordt ALD gekenmerkt door een variatie van symptomen, waaronder een langzaam progressieve en invaliderende myelopathie bij alle mannelijke en de meeste vrouwelijke patiënten, bijnierinsufficiëntie, cerebrale leukodystrofie en hypogonadisme. Genotype-fenotype correlaties ontbreken, en omgevingsfactoren en meerdere genetische modifiers zijn betrokken bij de ontwikkeling van symptomen. Daarom zijn leeftijd waarop symptomen beginnen en de snelheid van ziekteprogressie zeer onvoorspelbaar. Om het ziekteverloop voor individuele patiënten te voorspellen, is het belangrijk om eerst het natuurlijke beloop en individuele symptomen van ALD nader te beschrijven. Bovendien is er, voor patiënten met een myelopathie, slechts ondersteunende behandeling beschikbaar, aangezien ziektemodificerende therapieën nog in ontwikkeling zijn. Om potentiële nieuwe therapieën in klinisch onderzoek te evalueren, is het van belang om de ernst van de myelopathie adequaat te kwantificeren. Maar de klinische uitkomstmaten die op dit moment worden gebruikt, zijn niet gevoelig genoeg en vereisen veel patiënten en een lange follow-up, wat een uitdaging is bij een zeldzame ziekte als ALD. In dit proefschrift willen we de bovengenoemde uitdagingen beantwoorden en daartoe hebben we ons gefocust op een tweeledig doel. Ten eerste om meer inzicht te krijgen in het natuurlijk beloop van ALD, met als doel het ziektebeloop voor individuele patiënten te voorspellen, en ten tweede, om gevoelige (surrogaat) uitkomstmaten te ontwikkelen, die de ernst van de myelopathie kunnen monitoren, waardoor klinische studies in ALD beter mogelijk worden.

Beeldvorming bij ALD

Ongeveer 60% van de patiënten met ALD ontwikkelt een cerebrale leukodystrofie (cerebrale ALD) in de loop van hun ziekte. Het grootste risico op het ontwikkelen van cerebrale ALD is <7 jaar, maar cerebrale ALD kan ook optreden in de adolescentie of volwassenheid. In **hoofdstuk 2** bespreken we de verschillende beeldvormingsmogelijkheden voor cerebrale afwijkingen. *In vivo* beelden van cerebrale laesies bij ALD-patiënten werden voor het eerst gemaakt in de jaren 1970 via Computed Tomography (CT), maar momenteel is Mag-

netic Resonance Imaging (MRI) de gouden standaard voor detectie van cerebrale laesies. Cerebrale ALD-laesies presenteren zich vaak als T2-hyperintense confluerende laesies, voornamelijk in het splenium van het corpus callosum met uiteindelijk progressie naar de gehele cerebrale witte stof wanneer het niet behandeld wordt. Hoewel structurele MRI de aanwezigheid en omvang van cerebrale laesies kan detecteren, voorspelt het niet of en wanneer cerebrale ALD zal optreden. Mogelijk zijn kwantitatieve beeldvormingstechnieken, zoals Neurite Orientation Dispersion and Density imaging (NODDI) en Myelin Water Fraction imaging (MWF) in dat opzicht veelbelovend en zouden deze voor toekomstige onderzoeksdoeleinden kunnen worden gebruikt.

Deel II – Klinische studies

In sommige gevallen stopt de progressie van cerebrale ALD spontaan (arrested cerebrale ALD). Tot voor kort werd dit als zeldzaam beschouwd, maar in **hoofdstuk 3** lieten we zien dat arrested cerebrale ALD relatief vaak voorkomt (12,4% van alle ALD-gevallen). Arrested cerebrale ALD-laesies kunnen op verschillende leeftijden voorkomen (kindertijd, adolescentie en volwassenheid) en blijven bij de meeste patiënten stabiel, maar kunnen in sommige gevallen nog steeds overgaan in progressieve cerebrale ALD. Daarom moeten patiënten met arrested cerebrale ALD nog steeds nauwlettend, klinisch en met MRI worden gevolgd over tijd. Daarnaast ervaren patiënten met ALD ook vaak tekenen van seksuele disfunctie (erectiestoornissen en/of een verminderd libido). In **hoofdstuk 4** beschreven we deze symptomen en hun relatie met een myelopathie en hypogonadisme. In deze studie ervoer de meerderheid van de patiënten (56%) seksuele disfunctie, waarbij de meeste van hen normale testosteronniveaus hadden. De neurologische functie speelt daarentegen een veel belangrijkere rol in deze klachten dan tot nu toe werd aangenomen. Voor beide oorzaken van seksuele disfunctie - hypogonadisme en myelopathie - zijn geschikte behandelopties beschikbaar. Om vroegtijdige behandeling te starten, moet seksuele disfunctie regelmatig worden besproken en, indien aanwezig, moet worden gescreend op hypogonadisme. In **hoofdstuk 5** bespraken we een klinisch relevante surrogaat uitkomstmaat voor de myelopathie bij ALD: postural body sway. Voor patiënten met ALD is een evenwichtsstoornis een van de belangrijkste oorzaken van invaliditeit, en door de body sway te meten is het mogelijk om het evenwicht van de patiënt te kwantificeren. Body sway was significant hoger bij zowel asymptomatische als symptomatische patiënten in vergelijking met controles, en correleerde bij de symptomatische patiënten met klinische maten voor de ernst van de ziekte. Daarom kan body sway dienen als een potentieel gevoeligere uitkomstmaat in klinische onderzoeken voor ALD.

Deel III – Biochemische studies

In de meeste gevallen is het diagnosticeren van ALD relatief eenvoudig, maar soms kan dit een grotere uitdaging zijn. Bijvoorbeeld bij (pasgeboren) gevallen, met een variant of

unknown significance (VUS) in het *ABCD1*-gen, waarbij de familie anamnese voor ALD negatief is en de ZLKV slechts mild verhoogd zijn. In deze gevallen kunnen functionele testen in fibroblasten meer zekerheid bieden. We beschreven deze functionele testen in **hoofdstuk 6** en creëerden ALD- en referentiebereiken, met als doel de 17 geïncludeerde VUSsen te diagnosticeren. Door deze informatie te gebruiken, konden we 88% van de varianten classificeren als waarschijnlijk pathogeen of benigne, waardoor een ALD-diagnose meer of minder waarschijnlijk werd. Dit is van belang omdat er in de toekomst meer VUS-gevallen zullen worden gevonden, waarvoor we nu deze tests kunnen gebruiken om de diagnose van ALD makkelijker te stellen. In **hoofdstuk 7** hebben we de potentie van neurofilament light (NfL) en glial fibrillary acidic protein (GFAP) als biomarkers voor neurodegeneratie bij ALD onderzocht. Zowel NfL als GFAP waren significant verhoogd bij mannelijke en vrouwelijke patiënten in vergelijking met gezonde controles. Alleen NfL-spiegels waren geassocieerd met de ernst van myelopathie bij mannelijke patiënten, GFAP-spiegels (bij zowel mannelijke als vrouwelijke patiënten) waren dat niet. Vanwege de korte halfwaardetijd van NfL (een paar dagen), is het mogelijk om hiermee de ziekteactiviteit te volgen, wat suggereert dat plasma-NfL zou kunnen dienen als biomarker voor het vervolgen van het effect van een ziektemodificerende behandeling, met een relatief korte follow-up duur.

Deel IV – Radiologische studies

Naast structurele MRI – voor het diagnosticeren van anatomische afwijkingen – kan kwantitatieve MRI meer gedetailleerde fysische of chemische informatie geven. Bij ALD-patiënten laat structurele MRI van het ruggenmerg meestal geen afwijkingen zien, maar door het meten van de cross-sectional area (CSA) van het ruggenmerg hebben we aangetoond dat er significante verschillen zijn tussen patiënten en controles (**hoofdstuk 8**). ALD-patiënten hebben een dunner en platter (verkleinde antero-posterieure diameter) cervicaal ruggenmerg, waarschijnlijk als gevolg van degeneratie van de corticospinale en dorsale banen. CSA is gecorreleerd met klinische uitkomstmaten voor de ernst en de duur van de myelopathie, wat suggereert dat het een mogelijke surrogaat uitkomstmaat zou kunnen zijn. Een andere surrogaat uitkomstmaat, Magnetic Resonance Spectroscopy (MRS), werd onderzocht in **hoofdstuk 9**. In deze grootschalige longitudinale studie hebben we cerebrale metaboliet levels gemeten bij ALD patiënten zonder cerebrale demyelinisatie, met twee verschillende MRS protocollen (7T single voxel spectroscopy en 3T magnetic resonance spectroscopic imaging) over een periode van drie jaar. Beide protocollen toonden verlaagde concentraties van N-acetylaspartaat (tNAA) en glutamine + glutamaat (Glx) en verhoogde concentraties van choline-bevattende verbindingen (Cho) en creatine (tCr) bij ALD-patiënten in vergelijking met controles. Alleen tNAA/tCr-ratio's correleerden met klinische maten voor ziekte-ernst en kunnen van mogelijke waarde zijn als surrogaat uitkomstmaat in klinische onderzoeken.

Deel V – Discussie

Momenteel missen we nog steeds biomarkers die helpen bij het voorspellen van het ziektebeloop van individuele ALD-patiënten. Om deze voorspellende en prognostische biomarkers te ontwikkelen is 'deep phenotyping' van ALD-patiënten noodzakelijk. Deep phenotyping kan worden omschreven als een nauwkeurige en uitgebreide analyse van verschillende fenotypische afwijkingen. Deze methode hebben we in de eerste hoofdstukken van dit proefschrift uitgevoerd, wat resulteerde in een ander of specifieker advies over de follow-up bij verschillende patiëntengroepen in vergelijking met de standaard zorg. In de toekomst zal het linken van gedetailleerde klinische informatie van een goed gekarakteriseerd cohort van 'deep-phenotyped' patiënten met biochemische, genetische en beeldvormende studies hopelijk leiden tot de detectie van bruikbare voorspellende biomarkers.

Hiernaast is er een onvervulde behoefte aan betere uitkomstmaten om ziekte-ernst in klinische onderzoeken te monitoren. De momenteel gebruikte klinische uitkomstmaten zijn gevoelig voor dagelijkse variabiliteit en 'floor and ceiling' -effecten. Dit betekent dat, door gebruik te maken van deze uitkomstmaten, klinische onderzoeken grote aantallen patiënten en een lange follow-up zouden vergen, wat problematisch is bij een zeldzame ziekte als ALD. Nieuwe surrogaat uitkomstmaten zouden deze nadelen moeten kunnen ondervangen. Body sway analyse biedt bijvoorbeeld een klinisch relevante uitkomstmaat met minimaal of geen 'floor effect', plasma-NfL is gemakkelijk te meten en weerspiegelt recente neurodegeneratie, waardoor het geschikt is als korte termijn meting van ziekteactiviteit, en MR-gebaseerde uitkomstmaten (CSA en tNAA) zijn minder vatbaar voor dagelijkse variabiliteit. Een combinatie van deze surrogaat uitkomstmaten kan waardevol zijn bij het beoordelen van de werkzaamheid van mogelijke behandeling in klinisch onderzoek.

De studies in dit proefschrift laten zien dat bij onderzoek bij patiënten met ALD verschillende disciplines betrokken zijn. Goede communicatie tussen de verschillende disciplines is vereist voor verbetering van gepersonaliseerde gezondheidszorg en de haalbaarheid van klinische studies. Een grote samenwerking tussen verschillende (internationale) ALD-gespecialiseerde centra kan helpen bij het opzetten van grotere internationale onderzoeken, het creëren van meer follow-up gegevens en voldoende patiënten voor inclusie in klinische onderzoeken. Dit zou ook de ontwikkeling van surrogaat uitkomstmaten en daarbij het ontwerp van klinische studies verder verbeteren. Recente samenwerkingen hebben hun waarde al bewezen, bijvoorbeeld bij de implementatie van ALD in het Nederlandse hielprikscreeningsprogramma en de ontwikkeling van een internationale ALD-richtlijn. Een groot deel van dit proefschrift is tot stand gekomen via internationale samenwerkingsverbanden en heeft daardoor bijgedragen aan een beter begrip van het ziekteverloop van ALD en de ontwikkeling van nieuwe surrogaat uitkomstmaten. We hopen dat deze samenwerkingen in de toekomst zullen blijven bestaan en verder uitbreiden.

LIST OF PUBLICATIONS

A randomised, double-blind, placebo-controlled trial to assess the effect of leriglitazone on clinical, imaging, and biochemical markers of disease progression in men with X-linked adrenomyeloneuropathy (ADVANCE)
Submitted to Lancet Neurology 2022

The prevalence of sexual dysfunction and its relationship with hypogonadism and myelopathy in adrenoleukodystrophy
Manuscript in preparation

Presymptomatic lesion in childhood cerebral adrenoleukodystrophy: timing and management
Neurology 2022; ePub DOI: 10.1212/WNL.0000000000200571

Optical Coherence Tomography to measure the progression of myelopathy in adrenoleukodystrophy
Annals of Clinical and Translational Neurology, 2021, 8(5), pp. 1064–1072

A Longitudinal Analysis of Early Lesion Growth in Presymptomatic Patients with Cerebral Adrenoleukodystrophy
American Journal of Neuroradiology 2021, 42(10), pp. 1904–1911

Biochemical studies in fibroblasts to interpret variants of unknown significance in the *ABCD1* gene
Genes 2021;12:1930

Magnetic Resonance Spectroscopy as neurodegenerative marker in adrenoleukodystrophy
NeuroImage: Clinical 2021;32:102793

Imaging in X-linked adrenoleukodystrophy
Neuropediatrics 2021;52:252-260

Plasma neurofilament light and glial fibrillary acidic protein as biomarkers of spinal cord degeneration in adrenoleukodystrophy
Annals of Clinical and Translational Neurology 2020;7(11):2127-2136

Postural body sway as surrogate outcome for myelopathy in adrenoleukodystrophy
Frontiers in physiology 2020;11:786

Clinical and radiographic course of arrested cerebral adrenoleukodystrophy
Neurology 2020;94(24):e2499-e2507

Spinal cord atrophy as a measure of severity of myelopathy in adrenoleukodystrophy
Journal of Inherited Metabolic Disease 2020;43(4):852-860

Thrombolysis related intracranial hemorrhage in estimated versus measured bodyweight
International Journal of stroke 2020 Feb;15(2):159-166

Accurate gewicht schatting voor een veilige dosering
Nederlands Tijdschrift voor de Geneeskunde 2015;159(31):A8909

AUTHOR CONTRIBUTIONS PER PAPER

Imaging in X-linked adrenoleukodystrophy.

Neuropediatrics 2021;52:252-260

Stephanie I.W. van de Stadt	drafting and revision of manuscript
Irene C. Huffnagel	supervision and revision of manuscript
Bela R. Turk	supervision and revision of manuscript
Marjo S. van der Knaap	supervision and revision of manuscript
Marc Engelen	supervision and revision of manuscript

Clinical and radiographic course of arrested cerebral adrenoleukodystrophy.

Neurology 2020;94(24):e2499-e2507

Eric J. Mallack	study design, data acquisition, data analysis, drafting and revision of manuscript
Stephanie I.W. van de Stadt	data acquisition, data analysis, revision of manuscript
Paul A. Caruso	data analysis, supervision and revision of manuscript
Patricia L. Musolino	data analysis, supervision and revision of manuscript
Reza Sadjadi	supervision and revision of manuscript
Marc Engelen	data analysis, supervision and revision of manuscript
Florian S. Eichler	study design, drafting and revision of manuscript

The prevalence of sexual dysfunction and its relationship with hypogonadism and myelopathy in adrenoleukodystrophy.

manuscript in preparation

Stephanie I.W. van de Stadt	study design, data acquisition, data analysis, drafting and revision of manuscript
Aimy M.A. Wessel	data acquisition, data analysis, drafting and revision of manuscript
Mirjam Langeveld	study design, data acquisition, revision of manuscript
Marc Engelen	study design, supervision and revision of manuscript
Barbara Sjouke	study design, data acquisition, data analysis, revision of manuscript

Postural body sway as surrogate outcome for myelopathy in adrenoleukodystrophy.

Frontiers in physiology 2020;11:786

Wouter J.C. van Ballegoij	study design, data acquisition, data anlysis, drafting and revision of manuscript
Stephanie I.W. van de Stadt	data acquisition, revision of manuscript
Irene C. Huffnagel	data acquisition, revision of manuscript
Stephan Kemp	drafting and revision of manuscript
Marjo S. van der Knaap	revision of manuscript
Marc Engelen	study design, data acquisition, revision of manuscript

Biochemical studies in fibroblasts to interpret variants of unknown significance in the *ABCD1* gene.

Genes 2021;12:1930

Stephanie I.W. van de Stadt	data acquisition, data analysis, drafting and revision of manuscript
Petra A.W. Mooyer	data analysis, revision of manuscript
Inge M.E. Dijkstra	data analysis, revision of manuscript
Conny J.M. Dekker	data analysis, revision of manuscript
Divya Vats	data acquisition, revision of manuscript
Moin Vera	data acquisition, revision of manuscript
Maura R. Z. Ruzhnikov	data acquisition, revision of manuscript
Keith van Haren	data acquisition, revision of manuscript
Nelson Tang	data acquisition, revision of manuscript
Klaas Koop	data acquisition, revision of manuscript
Michel A. Willemsen	data acquisition, revision of manuscript
Joannie Hui	data acquisition, revision of manuscript
Frédéric M. Vaz	data analysis, supervision and revision of manuscript
Merel S. Ebberink	data analysis, revision of manuscript
Marc Engelen	study design, data acquisition, supervision and revision of manuscript
Stephan Kemp	study design, data analysis, supervision and revision of manuscript
Sacha Ferdinandusse	study design, data analysis, supervision and revision of manuscript

Plasma neurofilament light and glial fibrillary acidic protein as biomarkers of spinal cord degeneration in adrenoleukodystrophy.

Annals of Clinical and Translational Neurology 2020;7(11):2127-2136

Wouter J.C. van Ballegoij	data acquisition, data analysis, drafting and revision of manuscript
Stephanie I.W. van de Stadt	data acquisition, revision of manuscript
Irene C. Huffnagel	study design, data acquisition, revision of manuscript
Stephan Kemp	drafting and revision of manuscript
Eline A.J. Willemse	data analysis, drafting and revision of manuscript
Charlotte E. Teunissen	drafting and revision of manuscript
Marc Engelen	study design, data acquisition, revision of manuscript

Spinal cord atrophy as a measure of severity of myelopathy in adrenoleukodystrophy.

Journal of Inherited Metabolic Disease 2020;43(4):852-860

Stephanie I.W. van de Stadt	data analysis, drafting and revision of manuscript
Wouter J.C. van Ballegoij	data acquisition, revision of manuscript
René Labounek	data analysis, revision of manuscript
Irene C. Huffnagel	study design, data acquisition, revision of manuscript
Stephan Kemp	revision of manuscript
Igor Nestrasil	data analysis, revision of manuscript
Marc Engelen	study design, data acquisition, revision of manuscript

Magnetic Resonance Spectroscopy as neurodegenerative marker in adrenoleukodystrophy.

NeuroImage: Clinical 2021;32:102793

Stephanie I.W. van de Stadt	study design, data analysis, drafting and revision of manuscript
Anouk Schrantee	data analysis, revision of manuscript
Irene C. Huffnagel	study design, data acquisition, revision of manuscript
Wouter J.C. van Ballegoij	data acquisition, revision of manuscript
Matthan W.A. Caan	study design, revision of manuscript
Petra J.W. Pouwels	data analysis, revision of manuscript
Marc Engelen	study design, revision of manuscript

CONTRIBUTING AUTHORS AND AFFILIATIONS

Aimy M.A. Wessel - Department of Pediatric Neurology, Emma Children's Hospital, Amsterdam University Medical Centers, Amsterdam, The Netherlands

Anouk Schrantee - Department of Radiology and Nuclear Medicine, Amsterdam University Medical Centers, Amsterdam, The Netherlands

Barbara Sjouke - Department of Endocrinology and Metabolism, Amsterdam University Medical Centers, Amsterdam, The Netherlands

Bela R. Turk - Moser Center for Leukodystrophies, Kennedy Krieger Institute, Johns Hopkins University, Baltimore Maryland

Charlotte E. Teunissen - Neurochemistry lab and Biobank, Department of Clinical Chemistry, Amsterdam Neuroscience, Amsterdam University Medical Centers, VU University, Amsterdam, The Netherlands

Conny J.M. Dekker - Laboratory Genetic Metabolic Diseases, Department of Clinical Chemistry, Amsterdam University Medical Centers, Amsterdam Gastroenterology Endocrinology Metabolism, University of Amsterdam, Amsterdam, The Netherlands

Divya Vats - Regional Metabolic Clinic, Department of Medical Genetics, Southern California Permanente Medical Group, Los Angeles, California, United States of America

Eline A.J. Willemse - Neurochemistry lab and Biobank, Department of Clinical Chemistry, Amsterdam Neuroscience, Amsterdam University Medical Centers, VU University, Amsterdam, The Netherlands

Eric J. Mallack - Department of Pediatrics, Division of Child Neurology, Weill Cornell Medical College, NewYork-Presbyterian Hospital, New York, NY, USA. Department of Neurology, Harvard Medical School, Massachusetts General Hospital, Boston, MA, USA

Florian S. Eichler - Department of Neurology, Harvard Medical School, Massachusetts General Hospital, Boston, MA, USA

Frédéric M. Vaz - Laboratory Genetic Metabolic Diseases, Department of Clinical Chemistry, Amsterdam University Medical Centers, Amsterdam Gastroenterology Endocrinology Metabolism, University of Amsterdam, Amsterdam, The Netherlands

Igor Nestrasil - Division of Clinical Behavioral Neuroscience, Department of Pediatrics, University of Minnesota, Minneapolis, MN, USA. Center for Magnetic Resonance Research, Department of Radiology, University of Minnesota, Minneapolis, MN, USA

Inge M.E. Dijkstra - Laboratory Genetic Metabolic Diseases, Department of Clinical Chemistry, Amsterdam University Medical Centers, Amsterdam Gastroenterology Endocrinology Metabolism, University of Amsterdam, Amsterdam, The Netherlands

Irene C. Huffnagel - Department of Pediatric Neurology, Emma Children's Hospital, Amsterdam University Medical Centers, Amsterdam, The Netherlands

Joannie Hui - Department of Pediatrics & Adolescent Medicine, Hong Kong Children's Hospital, Hong Kong SAR, China

Keith van Haren - Departments of Neurology and Neurological Sciences and Pediatrics, Stanford, California, United States of America

Klaas Koop - Department of Metabolic Diseases, Wilhelmina Children's Hospital, University Medical Center Utrecht, Utrecht, the Netherlands

Marc Engelen - Department of Pediatric Neurology, Emma Children's Hospital, Amsterdam University Medical Centers, Amsterdam, The Netherlands

Marjo S. van der Knaap - Department of Pediatric Neurology, Amsterdam Leukodystrophy Center, Emma Children's Hospital, Amsterdam University Medical Centers, Amsterdam, The Netherlands

Matthan W.A. Caan - Department of Biomedical Engineering & Physics, Amsterdam University Medical Centers, University of Amsterdam, Amsterdam, The Netherlands

Maura R. Z. Ruzhnikov - Departments of Neurology and Neurological Sciences and Pediatrics, Stanford, California, United States of America

Merel S. Ebberink - Laboratory Genetic Metabolic Diseases, Department of Clinical Chemistry, Amsterdam University Medical Centers, Amsterdam Gastroenterology Endocrinology Metabolism, University of Amsterdam, Amsterdam, The Netherlands

Michel A. Willemsen - Department of Pediatric Neurology, Amalia Children's Hospital, Radboud University Medical Center, Nijmegen, the Netherlands

Mirjam Langeveld - Department of Endocrinology and Metabolism, Amsterdam University Medical Centers, Amsterdam, The Netherlands

Moin Vera - Regional Metabolic Clinic, Department of Medical Genetics, Southern California Permanente Medical Group, Los Angeles, California, United States of America

Nelson Tang - Department of Chemical Pathology and Li Ka Shing Institute of Health Sciences, The Chinese University of Hong Kong, Hong Kong SAR, China

Patricia L. Musolino - Department of Neurology, Harvard Medical School, Massachusetts General Hospital, Boston, MA, USA

Paul A. Caruso - Department of Radiology, Division of Neuroradiology, Harvard Medical School, Massachusetts General Hospital, Boston, MA, USA

Petra A.W. Mooyer - Laboratory Genetic Metabolic Diseases, Department of Clinical Chemistry, Amsterdam University Medical Centers, Amsterdam Gastroenterology Endocrinology Metabolism, University of Amsterdam, Amsterdam, The Netherlands

Petra J.W. Pouwels - Department of Radiology and Nuclear Medicine, Amsterdam University Medical Centers, Amsterdam, The Netherlands

René Labounek - Division of Clinical Behavioral Neuroscience, Department of Pediatrics, University of Minnesota, Minneapolis, MN, USA

Reza Sadjadi - Department of Neurology, Harvard Medical School, Massachusetts General Hospital, Boston, MA, USA

Sacha Ferdinandusse - Laboratory Genetic Metabolic Diseases, Department of Clinical Chemistry, Amsterdam University Medical Centers, Amsterdam Gastroenterology Endocrinology Metabolism, University of Amsterdam, Amsterdam, The Netherlands

Stephan Kemp - Laboratory Genetic Metabolic Diseases, Department of Clinical Chemistry, Amsterdam University Medical Centers, Amsterdam Gastroenterology & Metabolism, University of Amsterdam, Amsterdam, The Netherlands

Wouter J.C. van Ballegoij - Department of Pediatric Neurology, Emma Children's Hospital, Amsterdam University Medical Centers, Amsterdam, The Netherlands

PHD PORTFOLIO

	Year	ECTs
General courses		
AMC World of Science	2018	0.7
Basic Legislation in Science (BROK)	2018	1.0
Practical biostatistics	2019	1.4
Scientific writing in English	2020	1.5
Specific courses		
MRI basics for (bio)medical researchers	2019	1.0
Unix	2020	1.4
From Pixel to publication	2020	1.0
Seminars, workshops and master classes		
Medical Business Masterclass	2019	0.8
Presentations		
Advanced MR imaging in adrenoleukodystrophy. United Leukodystrophy Foundation annual meeting, Chicago, USA (oral)	2019	0.5
ALD research in the Netherlands. United Leukodystrophy Foundation annual meeting (for patients), Chicago, USA (oral)	2019	0.5
Biochemical studies in fibroblasts to interpret variants of unknown significance in the *ABCD1* gene. European Paediatric Neurology Society, Glasgow (poster)	2022	0.5
(inter)national conferences		
United Leukodystrophy Foundation annual meeting, Chicago, USA	2019	0.8
Minoryx Expert meeting, Paris	2019	0.5
Amsterdam Kindersymposium, Amsterdam	2019	0.5
United Leukodystrophy Foundation, annual meeting, Chicago (online)	2020	0.5
ALD connect annual meeting (online)	2021	0.5
Minoryx Expert meeting, Paris	2021	0.5
European Paediatric Neurology Society, Glasgow (online)	2022	0.5
Other		
Medical Business Projects, Amsterdam	2021	4.7
Teaching		
Supervising bachelor thesis student (Aimy)	2021	2.0

ABOUT THE AUTHOR

Stephanie van de Stadt was born on July 5th 1991 in Blaricum, the Netherlands. She is the eldest of three children. After graduating high school (Willem de Zwijger College, Bussum) in 2009, she started medical school at the Vrije Universiteit Amsterdam in 2010. Before and during her study she also did volunteer work and internships abroad. After graduating medical school in 2017 she started her first job as a resident (not in training) in neurology at the Flevoziekenhuis and later the Onze Lieve Vrouwe Gasthuis. In 2018 she started her PhD training at the department of pediatric neurology at the Amsterdam University Medical Centers, under supervision of prof. dr. Marjo van der Knaap, dr. Marc Engelen en dr. Stephan Kemp. She performed a three-year prospective cohort study in X-linked adrenoleukodystrophy ("the Dutch ALD cohort") which led to the production of this thesis. Currently, she has left Amsterdam and moved to Rotterdam where she is about to start her residency in neurology at the Erasmus Medical Center.

Besides her work she enjoys the (sunny) outdoor life, to go sailing, cycling, ice-skating or to have dinner/drinks with friends.

DANKWOORD

Dit promotietraject is voor mij een onvergetelijke periode geweest. Ik had een aantal jaar geleden nooit verwacht hier ooit te zullen staan. Hoogstwaarschijnlijk was dit proefschrift dan ook niet tot stand gekomen zonder de bijdrage van een aantal mensen die mij hebben gemotiveerd en geïnspireerd.

Allereerst wil ik alle **ALD-patiënten** bedanken**.** Jullie leven staat in het teken van deze onvoorspelbare ziekte. Vrijwel allemaal zijn jullie ook al jaren betrokken bij dit onderzoek. Wat jullie al wisten, en wat ik inmiddels ook heb geleerd, is dat onderzoek naar zo'n zeldzaam ziektebeeld maar langzaam vordert. Desondanks blijven jullie altijd gemotiveerd om weer met het volgende onderzoek mee te doen. Ik heb zelfs meerdere keren de vraag gekregen of er nog iets nieuws was waar jullie aan mee konden doen, in plaats van dat ik jullie moest vragen. Ik ben blij dat ik jullie allemaal zo persoonlijk heb mogen leren kennen en waardeer jullie inzet en doorzettingsvermogen enorm.

Prof. dr. van Goudoever. Hans, op het moment dat jij bij mijn onderzoek betrokken raakte, waren we allebei al aan het voorbereiden op een nieuwe baan, zoals jij het passend omschreef. Desondanks heb jij tijd vrijgemaakt om mij in deze laatste fase nog te begeleiden, dat heb ik heel erg gewaardeerd. **Prof dr. van der Knaap.** Marjo, wat was het een feest om onderdeel te zijn van de wekelijkse ALC (Amsterdam Leukodystrophy Center) werkbespreking en aan te sluiten bij de kinder-neuro-radiologie besprekingen. Ik heb enorm veel van je geleerd en jouw enthousiasme voor leukodystrofieën heeft op mij zeker aanstekelijk gewerkt. **Dr. Engelen.** Marc, tijdens mijn keuze co-schap kinderneurologie in het VUmc 6 jaar geleden viel het mij al op dat jij veel voor het ALD-onderzoek en de patiënten over hebt. Jij staat altijd klaar om te bellen, te mailen, een kaartje te sturen of zelfs even langs te gaan. Later merkte ik dat ook terug in mijn begeleiding. Jij liet mij mijn eigen gang gaan en mijn eigen weg zoeken maar was altijd beschikbaar als ik er niet uit kwam. Hierbij stelde je vrijwel altijd mijn belangen voorop, in plaats van die van anderen. Daarnaast heb ik natuurlijk ook veel van je geleerd over (speciaal)bier, en wat het doet op je balans. Heel veel dank voor de fijne, laagdrempelige en betrokken begeleiding. Wie weet worden we ooit weer collega's. **Dr. Kemp.** Stephan, jouw eindeloze enthousiasme over alles wat met ALD te maken heeft, vind ik prachtig. Zo werden de figuren in mijn artikelen en proefschrift dankzij jou nog altijd net iets mooier en blijft de ALD-kerstkaart een terugkerend succes. Dankzij jouw enthousiasme gingen er altijd zoveel mogelijk mensen mee naar congres en werd er ook voldoende aandacht besteed aan (sportieve) activiteiten buiten het congres (helaas door corona wel wat minder dan gepland).

De leden van de **promotiecommissie**: prof. dr. I.N. van Schaik, dr. J.J.F.M. Smolders, prof. dr. A.M. Bosch, dr. S.D. Roosendaal, dr. F.M. Vaz, prof. dr. N.I. Wolf en prof. dr. C.E.M. Hollak, hartelijk bedankt voor jullie interesse in mijn proefschrift en de bereidheid om het kritisch te beoordelen.

Collega's van de ALD-onderzoeksgroep, te beginnen met **Marije**. Jij hebt mijn PhD leven zó ongelofelijk veel makkelijker gemaakt. Na een jaartje oefenen liep alles als een geoliede machine en heb je mij enorm veel werk uit handen genomen. Ondanks dat we zelfstandig MRI's konden maken, deden we dit relatief vaak toch nog samen en werd het meestal een combinatie van werkbespreking en kletsuurtje waarbij ook veel werd gelachen. De expert-meetings in Parijs waren een stuk leuker als we daarvoor of daarna nog even samen de stad gingen verkennen. **Irene**, we hebben jammer genoeg geen overlap gehad in het AMC, maar dankzij jouw zeer gedetailleerde overdracht (in elke map vond ik wel een document met uitleg) voelde het alsof je er gewoon nog was. Jij liet mij altijd beseffen dat elke prestatie (hoe klein ook) gevierd of in elk geval erkent moest worden. **Wouter**, dankzij jou ben ik natuurlijk hier terecht gekomen. Ook jij hebt mij goed ingewerkt en een hele berg aan data achtergelaten waar ik mee aan de slag kon. Ik heb geprobeerd het net zo snel af te ronden als jij, maar dat was vrijwel onmogelijk. **Hemmo,** ik hoop dat ik het net zo mooi heb achtergelaten als mijn voorgangers en dat je minstens net zoveel MRI's hebt om te beoordelen. Veel plezier en succes de komende tijd, ik ben erg benieuwd naar de resultaten! **Yorrick en Inge,** de wekelijkse bijeenkomsten gingen mij soms weleens de pet te boven als het over mass spectrometry of de hielprik diagnostiek en logistiek ging. Maar het was absoluut interessant en leerzaam en laat zien dat ons ALD-onderzoek in de volle breedte wordt verricht.

Anouk, Sandra en Raschel, bedankt voor jullie hulp en geduld bij het leren scannen en het uitleggen van de achtergrond van MRI. Dat was vast niet makkelijk bij iemand zonder al te veel fysische en programmeer vaardigheden. Maar het heeft toch geresulteerd in een aantal mooie MRI-artikelen.

Alle co-auteurs die hebben bijgedragen aan dit proefschrift, van over de hele wereld. And especially our fellow ALD researchers and clinicians in the USA, thank you for the fruitful collaborations and nice meetings in Amsterdam, Chicago and Paris.

Rosalie. Lieve Roos (vriendin/collega/paranimf), bedankt voor onze bijzondere en al behoorlijk langdurige vriendschap. We hebben de afgelopen jaren een vrij vergelijkbaar pad bewandelend met bijbehorende ups en downs en jij stond (staat) altijd klaar, in of buiten het AMC, voor koffie of iets sterkers als dat nodig was. Ik ben heel blij dat we deze periode, inclusief de promotie ceremonie, samen hebben kunnen doen. En dan wil ik ook maar met-

een je hele neuro-familie bedanken die al sinds de middelbare school hebben bijgedragen aan mijn neuro-enthousiasme.

Collega-onderzoekers van H8-253: Jorn, Floor, Sander, Rosalie, Ella, Thijs, Ilja, Martijn, Fabienne, Anne-Fleur, Lisa en Diana. Ons fantastische, motiverende rommelkantoor zonder ramen stond gelukkig niet in de weg dat we het toch best wel gezellig met elkaar hebben gehad. Zelfs een pandemie kon daar niet tegenop. De borrels, etentjes en dansjes na werk maar ook de vele koffietjes en (buiten) lunch uurtjes tijdens werk gaven genoeg gezelligheid, en mogelijkheid tot ventilatie, om de dagen in dat rommelhok aangenaam te maken.

Neurologie collega's van het EMC, bedankt voor het warme welkom in Rotterdam. Ik ben mij vrij snel op mijn plek gaan voelen bij jullie, en kijk er daardoor enorm naar uit om de komende jaren met jullie te blijven werken en borrelen!

VVVs, jullie gaan al een behoorlijke tijd mee en onze hechte vriendschap is heel erg belangrijk voor mij. De ontstane 'splitsing' tussen medici en niet-medici zorgt voor vermakelijke en interessante discussies die mij altijd weer scherp houden. Ookal heeft een groot deel van ons Amsterdam inmiddels achter zich gelaten, ik verwacht nog steeds dat wij tot en met onze oude dagen bij elkaar blijven!

Vivian (of eigenlijk 'Mac'), bijzonder veel dank voor het prachtige ontwerp van de cover van dit proefschrift. Mijn hersenen zullen er nooit meer zo goed uit zien. Je hebt zelf misschien een haat-liefde verhouding met het menselijk lichaam, ik hoop toch dat het je blijft inspireren en dat je inmiddels weet dat je niet alleen maar mijn (ex)huisgenoot bent.

Chris & Cecile. Lieve broer en zus, jullie zijn dan wel jonger (en niet gepromoveerd…) en we doen alle drie iets compleet anders, ik kijk soms best wel een beetje tegen jullie op. Jullie hadden natuurlijk een goed voorbeeld om te volgen, maar toch werd ik op het gebied van school- en sportprestaties vaak overtroffen. Desalniettemin laten jullie mij altijd wel inzien dat ik trots mag zijn op wat ik doe. Ik vind het heerlijk om te sparren met jullie over van alles en nog wat en ben blij dat ik jullie tijdens mijn promotie naast mij heb!

Lieve papa en mama, Jullie onvoorwaardelijke liefde en steun zijn het allerbelangrijkste voor mij. Van jullie heb ik geleerd om mijn hart te volgen en mezelf te zijn en dat, wanneer ik dat doe, alles goed komt. Mama, dankjewel voor je luisterend oor, het kritisch meedenken of mijn pad nog wel mijn pad is en, ondanks dat je er zelf zo hard voor werkt, dat je mij ook liet inzien dat de h-index heus niet alles is. Papa, bedankt voor je grenzeloze vertrouwen in mijn kunnen, en dat je alles altijd van de positieve kant ziet, of zoals jij het samenvat: "Plan for succes!". Ik zal dat altijd blijven meenemen.

Lieve Floris, met jou aan mijn zijde is het leven altijd nóg een stukje leuker. Misschien liet ik dat tijdens dit traject niet altijd even goed zien. Maar gelukkig bleef je altijd meedenken aan oplossingen, vooral als ik stress kreeg van grote hoeveelheden data, met het motto "veel werk, komt goed". Jouw verrassende ideeën, en je eindeloze enthousiasme en energie bewonder ik enorm. Samen gaan we hopelijk nog veel avonturen tegemoet!